Insights into the Interactions between Replication Protein A and the Ubiquitin Ligase Rad18 from *Saccharomyces cerevisiae*

Diana Huttner

DNA Damage Tolerance Laboratory
Clare Hall Laboratories
Cancer Research UK
London Research Institute
London

A thesis submitted for the degree of
Doctor of Philosophy
at the University of London
2008

ProQuest LLC
789 East Eisenhower Parkway
P.O. Box 1346
Ann Arbor, MI 48106-1346

I, Diana Huttner, confirm that the work presented in this thesis is my own. Where information has been derived from other sources, I confirm that this has been indicated in the thesis.

Abstract

DNA damage may lead to mutations and loss of genome integrity. Lesions encountered during replication cause the replication machinery to stall and, unless repaired or bypassed, can result in lethality of the cell. The DNA polymerase processivity clamp, PCNA (proliferating cell nuclear antigen), mediates either mutagenic damage bypass or error-free damage avoidance through its post-translational modification states. Mono-ubiquitylated PCNA stimulates the activity of translesion DNA polymerases, while poly-ubiquitylation of PCNA is a pre-requisite for error-free damage avoidance by a yet unknown mechanism. Recent findings in the laboratory suggested that Replication Protein A (RPA), an essential single-stranded (ss) DNA-binding protein, is required for induction of PCNA ubiquitylation upon DNA damage. Consequently, the aim of my thesis was to gain further insight into the mechanism by which RPA is involved in the up-stream signals that activate PCNA modification.

The Rad18 protein from *Saccharomyces cerevisiae* (*S. cerevisiae*) is the ubiquitin ligase (E3) responsible for PCNA mono-ubiquitylation. The interactions of Rad18 with DNA and RPA, and the effects of this interaction on Rad18 binding to ssDNA, were studied in detail.

Recombinant Rad18 was purified as a complex with its ubiquitin-conjugating enzyme, Rad6. Their stable association and ubiquitin conjugation activity was verified. Furthermore, basal levels of PCNA ubiquitylation were reconstituted *in vitro*. Yeast Rad18 was reported by others to bind preferentially to ssDNA over dsDNA. The intrinsic ssDNA-binding activity of the recombinant Rad18 protein was confirmed by pull-down assays using biotinylated oligonucleotides. Importantly, Rad18 is able to bind to ssDNA and to other ssDNA-containing structures, but also to forked-DNA consisting entirely of double-stranded (ds) DNA regions. Rad18 binding to DNA was demonstrated to be dependent on the ionic strength of the buffer. At low salt concentrations Rad18 was found to stably associate with ssDNA. At moderate to high salt concentrations, including in ionic strength conditions that could be considered

physiological, Rad18 did not bind to ssDNA. Interestingly, binding to ssDNA at low ionic strength confers a stable association of Rad18 with the DNA for subsequent high ionic strength conditions. Taken together, these findings suggest that Rad18 binds to ssDNA at low salt concentrations with low affinity. Thereafter, a slow conformational change leads to an increased binding affinity that renders the ssDNA-bound Rad18 stable association with the ssDNA in high salt concentrations. Furthermore, these findings argue against the speculation that Rad18 can bind to sites of DNA damage *in vivo* by itself.

In vitro experiments further demonstrated that the yeast Rad18-Rad6 complex interacts physically with RPA. The findings in this work support a mechanism through which both proteins bind directly to RPA. Further analysis of recombinant RPA subunits revealed that both Rfa2 and the DNA-binding domain of Rfa1 contribute independently to the specific interactions with the complex. Interestingly, the association between the Rad18-Rad6 complex and the DNA-binding domain of Rfa1 is stimulated by the presence of ssDNA. Furthermore, at physiological ionic strength, RPA recruits the Rad18-Rad6 complex to ssDNA. These findings support a model by which RPA-coated ssDNA recruits Rad18 to sites of DNA damage. Thus, ssDNA-bound RPA may provide the up-stream signal for the activation of the DNA damage tolerance pathway and for PCNA ubiquitylation. Although this has yet to be clarified, most likely the interactions of Rad18 with both RPA and DNA contribute to its localisation to stalled replication forks *in vivo*.

Although the SAP domain of human Rad18 was reported to be both necessary and sufficient for its interactions with DNA, the results obtained in this work suggest that this function may not be conserved in yeast. Nevertheless, this domain is essential for the *in vivo* function of yeast Rad18. Although its effect may be indirect, the SAP domain appears to contribute to the correct conformation of the Rad18 protein and to facilitate the interaction of the E3 with PCNA, thereby allowing the ubiquitylation of the clamp.

Acknowledgements

First and foremost, I would like to thank my supervisor, Dr. Helle Ulrich, who took me on a long PhD journey, allowing me to experience two different countries and cultures and two superb scientific institutes. Thank you, Helle, for your guidance, ideas and support. I would also like to thank my second supervisor Dr. John Diffley and my thesis committee member Dr. Dale Wigley for their support and guidance. Thank you as well to Dr. Svend Petersen-Mahrt for invaluable guidance and discussions.

I would like to thank past members of my lab: Kristine Schmidt, Anke Schuerer, Shuhua Chen, Andrea Neiss and Marie Anders for their friendship and scientific discussions in Marburg. Ola Bielen, Efterpi Papouli, Hanna Windecker and Andrea Bucceri for many enjoyable laughs and coffees in Clare Hall. Thank you Efterpi for being such good and wise friend. Thank you Hanna for the long hours we spent side by side at the bench and for your dear friendship. Many thanks go to the existing members of my lab: Nicola Zilio, Kai Zhao, Sue Jacobs, Yasu Daigaku, Irene Saugar Gomez, Jo parker and Addie Davies, for their friendship and support throughout my PhD. Special thanks to Addie for lots of technical and personal guidance and advice. Thank you, Jo, for teaching me how to do good biochemistry and for your many helpful scientific advices. Many thanks, Irene, for your laughter and invaluable insights regarding science and life in general. Thanks, Yasu, for sharing the bench, your philosophical views and Japanese snacks. Thank you, Sue, for your spirit and knowledge.

Big thanks to all of my friends at Clare Hall and LIF throughout the years. Thanks especially to Alessia Balestrini, Jordan Ward, Eloise Smith, Feng Li, Nicola Brown and Katherina Willmann. An immense thanks goes to Tom Ben-Shahar for her friendship, support and advice. Thanks are owed to the Cancer Research UK LRI central cell services and to the mass-spectrometry service. Many thanks also to Erin Fortin, Sally Leevers and Ava Yeo for making life as a grad student so much easier. A huge thank you to Jackie Martinez, Mary Nicolaou and Kath Ames, whom I enjoyed sharing St. Antolins with, and who together with Matt Miller and Mark Johnson make sure that everything runs smoothly in Clare Hall. The Boehringer Ingelheim Fonds, the Overseas Research Student Awards and Cancer Research UK are greatly acknowledged for the funding.

Many thanks to my beloved family and friends at home, whose love, guidance and support made me the person I am today. A very special thanks goes to my best friend and husband, Eli, who took me on the greatest adventure of our lives. Thank you, my love, for sharing with me the ups and downs and whatever was between. Thank you for your constant encouragement, support and love. And last, but not least, I have to thank my dog, Fliz, for constantly reminding me to enjoy the small things in life, and for not eating my thesis.

Table of Contents

Title Page....1
Declaration....2
Abstract....3
Acknowledgements....5
Table of Contents....6
List of Figures....15
List of Tables....18
List of Abbreviations....19

1 Chapter One: Introduction....25
1.1 Parameters Affecting DNA-Protein Interactions....25
1.1.1 Chemical Bonds Participating in DNA-Protein Interactions....25
1.1.2 Buffer Conditions Can Affect DNA-Protein Interactions....26
1.1.2.1 The Effects of the Solvent....26
1.1.2.2 The Effects of Ions....26
1.1.3 Structural Aspects Affecting DNA-Protein Interactions....27
1.2 DNA-Binding Domains....28
1.2.1 The OB Fold....29
1.2.2 The Zinc Fingers....31
1.2.2.1 C2H2-like Finger (Fold Group 1, see Table 1-1)....32
1.2.2.2 Treble Clef Finger (Fold Group 3 – see Table 1-1)....34
1.2.3 The SAP Domain....34
1.3 Single-stranded DNA-Binding Proteins....38
1.3.1 The Single-Stranded Binding Protein....39
1.3.2 Replication Protein A....40
1.3.2.1 Rfa1....41
1.3.2.2 Rfa2....42
1.3.2.3 Rfa3....43
1.3.2.4 Interactions of RPA with DNA....43
1.3.2.5 Interactions of RPA with Proteins....45
1.4 The DNA Damage Response....49

1.4.1 DNA Damage and Its Sources 49
1.4.1.1 Endogenous Damage 49
1.4.1.2 Physical Sources of DNA Damage 49
1.4.1.3 Chemical Sources of DNA Damage 50
1.4.2 The DNA Damage Response throughout the Cell Cycle 50
1.4.2.1 Direct Damage Reversal 51
1.4.2.2 Single-Strand Damage Repair (BER, NER, MMR) 51
1.4.2.3 Double-Strand Break Repair (HRR, NHEJ) 53
1.4.2.4 DNA Damage Bypass 54
1.4.2.5 Interstrand Cross-Link (ICL) Repair 54
1.5 Maintenance of Genomic Stability during Replication 55
1.5.1 Sensing DNA Damage during Replication 56
1.5.2 Mechanisms of Replication Fork Stalling and Collapse 57
1.5.3 Stabilisation of Stalled Forks by the Replication Checkpoint 60
1.5.4 Mechanisms of Replication Fork Restart 61
1.5.4.1 Recombination-Mediated Replication Restart 61
1.5.4.2 DNA Damage Tolerance Mechanisms 62
1.6 The Ubiquitin System 62
1.6.1 The Mechanism of Ubiquitin Conjugation 63
1.6.2 Different Types of Ubiquitin Modifications 64
1.6.3 Consequences of Ubiquitin Modifications 64
1.7 The *RAD6* Pathway 65
1.7.1 Consequences of PCNA Modifications 68
1.7.2 The Rad6 Protein 71
1.7.3 The Rad18 Protein 71
1.7.4 The Rad5 Protein 75
1.7.5 The Ubc13 and Mms2 Proteins 76
1.7.6 DNA Translesion Synthesis 76
1.7.7 DNA Damage Avoidance 79
1.7.8 The Timing of the DNA Damage Tolerance Mechanisms 80
1.8 Aims of this Thesis 81
2 Chapter Two: Materials and Methods 82
2.1 Enzymes and Reagents 82
2.1.1 Enzymes and Proteins 82

2.1.2 Antibodies....82
2.1.3 Chemicals and Reagents....83
2.2 Media and Solutions....85
2.2.1 Media for Bacterial Cells....85
2.2.2 Media for Yeast Cells....85
2.2.3 Media for Insect Cells....87
2.2.4 Buffers and Solutions....87
2.2.4.1 Buffers for Molecular Biology Methods for *E. coli*....87
2.2.4.2 Buffers for Molecular Biology Methods for Yeast Cells....87
2.2.4.3 Buffers for General Manipulation of DNA....88
2.2.4.4 Buffers for General Manipulation of Proteins....88
2.2.4.5 Buffers for Protein Purifications....89
2.2.4.6 Buffers for Interaction Studies and Enzymatic Assays....90
2.3 Plasmids....91
2.4 DNA Oligonucleotides....94
2.5 Strains....95
2.5.1 *Escherichia coli* Strains....95
2.5.2 Yeast Strains....97
2.6 Molecular Biology Methods for *E. coli*....100
2.6.1 Preparation of *E. coli* Competent Cells....100
2.6.1.1 Electro-competent Cells....100
2.6.1.2 Chemically Competent Cells....100
2.6.2 Transformation of *E. coli*....101
2.6.2.1 Electroporation Method....101
2.6.2.2 Heat-shock Method....101
2.6.3 Isolation of Plasmid DNA....101
2.7 Molecular Biology Methods for Yeast Cells....102
2.7.1 Transformation of Yeast Cells by the LiOAc/PEG Method....102
2.7.2 Colony PCR....102
2.7.3 Preparation of Total Cell Extracts from Yeast Cells....103
2.8 Molecular Biology Methods of Baculovirus and Insect Cells....103
2.8.1 Baculovirus Production....103
2.8.2 Transfection of Insect Cells....104
2.8.3 Amplification of Baculovirus....105

2.9 General Methods for DNA Manipulation 105
2.9.1 Determination of DNA Concentration 105
2.9.2 DNA Standards 106
2.9.3 Agarose Gel Electrophoresis 106
2.9.4 Visualization of DNA by Ethidium Bromide Staining 106
2.9.5 Native PAGE 106
2.9.6 Autoradiography 107
2.9.7 Phosphorimager Analysis 107
2.10 General Methods of Protein Manipulation 107
2.10.1 Determination of Protein Concentration 107
2.10.1.1 Absorbance at 280 nm 107
2.10.1.2 Comparison by Coomassie Staining 107
2.10.1.3 Bradford Method 108
2.10.2 Molecular Weight Standards 108
2.10.3 SDS-PAGE 108
2.10.4 Coomassie Blue Staining 109
2.10.5 Western Blotting 109
2.11 Generation of Antibodies against Rad18 110
2.11.1.1 Anti-Rad18 Mouse Polyclonal Serum 110
2.11.1.2 Anti-Rad18 Rabbit Polyclonal Serum 111
2.12 Protein Purification 111
2.12.1 Purification of Yeast Replication Protein A (RPA) 111
2.12.2 Purification of ^{GST}Rfa1 (DNA-Binding Domain) 113
2.12.3 Purification of ^{GST}Rfa2 114
2.12.4 Purification of Rad6 115
2.12.5 Purification of ^{His}PCNA *WT* and ^{His}PCNA Mutants 116
2.12.6 Purification of Yeast ^{HisVSV}Rad18-Rad6 from Insect Cells 118
2.12.6.1 Purification under Native Conditions 118
2.12.6.2 Purification under Denaturing Conditions 119
2.13 Yeast Genetics 120
2.13.1 UV Sensitivity Streak Assay 120
2.13.2 Sensitivity Spot Assay 120
2.13.3 Induction of *RAD18* Over-Expression 121
2.13.4 Two-Hybrid Analysis 121

2.14 Enzymatic Assays 122
2.14.1 *In vitro* Ubiquitylation Assays 122
2.14.2 Radiolabelling of Oligonucleotides 122
2.14.2.1 5'-^{32}P-End Labelling of Oligonucleotides 122
2.14.2.2 3'-^{32}P-End Labelling of Oligonucleotides 122
2.15 Preparation of DNA Substrates and Protein - DNA Interaction Assays 123
2.15.1 Removal of Unincorporated Nucleotides 123
2.15.2 Preparation of DNA Substrates 123
2.15.3 Gel Purification of Oligonucleotides and DNA Substrates 123
2.15.4 Protein - DNA Interaction Assays 124
2.15.4.1 Gel Shift Assays 124
2.15.4.2 Pull-Down Assays with Biotinylated DNA 124
2.15.4.2.1 Binding DNA Structures to Streptavidin Beads 124
2.15.4.2.2 Binding ssDNA to Streptavidin Beads 124
2.15.4.2.3 DNA-Bound Streptavidin Pull-Down Assays 125
2.16 Protein - Protein Interaction Assays 125
2.16.1 Co-immunoprecipitation of Rad6 with ^{HisVSV}Rad18 125
2.16.2 Glutathione Pull-Down Assays 126
2.16.2.1 In the Absence of ssDNA 126
2.16.2.2 In the Presence of ssDNA 126
2.16.3 Protein-Derivatised Sepharose Pull-down Assays 126
2.16.3.1 Coupling Proteins to CH-Sepharose Beads 126
2.16.3.2 Protein-Derivatised Sepharose Pull-Down Assays 127
2.17 Analysis of Post-Translational Modifications of Proteins 127
2.17.1 Ni-NTA Pull-Down Assays from Yeast Extracts under Denaturing Conditions 127
3 Chapter Three: Results I - Purification and Catalytic Activity of Rad18 129
3.1 Introduction 129
3.2 Results 130
3.2.1 Co-infection with ^{HisVSV}*RAD18* and *RAD6* Baculoviruses Improves Solubility of Rad18 130
3.2.2 Purification of the ^{HisVSV}Rad18-Rad6 Complex from Baculovirus-Infected Insect Cells 131

3.2.3 Rad6 Co-purifies with ^{HisVSV}Rad18 132
3.2.3.1 Gel Filtration 132
3.2.3.2 Co-Immunoprecipitation 134
3.2.4 Attempts to Improve the Purity of the ^{HisVSV}Rad18-Rad6 Complex... 134
3.2.4.1 Cation Exchange Column 134
3.2.4.2 Hydrophobic Phenyl Sepharose Chromatography 134
3.2.4.3 Heparin Column 135
3.2.5 Rad18 is Auto-ubiquitylated 138
3.2.5.1 Yeast ^{HisVSV}Rad18 is Ubiquitylated in Insect Cells 138
3.2.5.2 Rad18 is Ubiquitylated in Yeast Cells 139
3.2.5.3 ^{HisVSV}Rad18 is Auto-ubiquitylated *In vitro* 140
3.2.6 The ^{HisVSV}Rad18-Rad6 Complex Mono-ubiquitylates PCNA *In vitro*... 143
3.2.6.1 Specificity of PCNA Mono-ubiquitylation 143
3.2.6.2 Optimisation of PCNA Mono-ubiquitylation 143
3.3 Discussion 146
3.3.1 Purification of Rad18 146
3.3.2 The Catalytic Activity of Rad18 147
3.3.2.1 Rad18 Auto-ubiquitylation 147
3.3.2.2 PCNA Mono-ubiquitylation 149
4 Chapter Four: Results II - Interactions of the Rad18-Rad6 Complex and DNA 151
4.1 Introduction 151
4.2 Results 152
4.2.1 Rad18 Binding to ssDNA is Affected by NaCl 152
4.2.2 Rad18 Binds Directly to ssDNA 154
4.2.3 Kinetics of the interaction between the Rad18-Rad6 complex and ssDNA 156
4.2.4 The Effect of Salt Type on Rad18's Binding to ssDNA 156
4.2.5 Rad18 Binds to Different Lengths of ssDNA 158
4.2.6 The Rad18-Rad6 complex binds to different DNA structures 158
4.3 Discussion 159
4.3.1 Advantages and Disadvantage of the Experimental Methods ... 159

4.3.2 Experimental Conditions and Specificity of Binding....162
4.3.3 DNA-Binding Properties of Rad18....162
4.3.3.1 Binding Affinity....162
4.3.3.2 Binding Kinetics....163
4.3.3.3 Minimal Binding Site....164
4.3.3.4 Structure Preference....165
5 Chapter Five: Results III - Interactions of the Rad18-Rad6 Complex and RPA....166
5.1 Introduction....166
5.2 Results....167
5.2.1 Rad18 Interacts Directly with RPA....167
5.2.2 Mapping of Rad18-RPA Interaction....170
5.3 Discussion....173
6 Chapter Six: Results IV - Interactions of the Rad18-Rad6 Complex, RPA and ssDNA....175
6.1 Introduction....175
6.2 Results....175
6.2.1.1 ssDNA Stimulates the Interaction between Rad18 and the DNA-Binding Domain of Rfa1....175
6.2.2 Salt Concentration Defines Two Modes of Interaction....180
6.2.2.1 Interactions of Rad18 with ssDNA and RPA at High Salt Concentrations....180
6.2.2.2 Interactions of Rad18 with ssDNA and RPA at Low Salt Concentrations....181
6.2.2.3 Interactions of Rad18 with ssDNA and RPA under a Range of Salt Concentrations....181
6.3 Discussion....184
6.3.1 Ionic Strength Modulates the Interactions between Rad18, RPA and ssDNA....184
6.3.1.1 ssDNA-Binding Properties of RPA and SSB....184
6.3.1.2 RPA Recruits Rad18 to ssDNA at High Ionic Strength....187
6.3.1.3 RPA Competes with Rad18 for ssDNA-Binding at Low Ionic Strength....189

6.3.2 Varying Affinities of RPA, ^{GST}Rfa1 (182-421) and ^{GST}Rfa2 for ssDNA....191
6.3.3 ssDNA Stimulates the Interaction between Rad18 and Rfa1 DNA-Binding Domain....192
7 Chapter Seven: Results V - Contribution of the SAP Domain to Rad18 Interactions and Activity....193
7.1 Introduction....193
7.2 Results....196
7.2.1 *rad18* (*SAP*Δ) and *rad18* (*SAP**) Alleles Fail to Complement the Damage Sensitivity of the *rad18* Deletion Strain....196
7.2.2 Purification of the ^{HisVSV}Rad18 (SAPΔ)-Rad6 Complex....200
7.2.3 The SAP Domain is Dispensable for ssDNA-Binding....200
7.2.4 The Importance of the SAP Domain for Rad18's Interactions with RPA....202
7.2.4.1 Rad18 (SAPΔ)-RPA Interaction....202
7.2.4.2 Rad18 (SAPΔ)-Rfa1 DNA-Binding Domain Interaction....202
7.2.5 ^{HisVSV}Rad18 (SAPΔ) is Recruited to ssDNA by RPA....204
7.2.6 The SAP Domain Contributes to the Interaction between Rad18 and PCNA....204
7.2.7 The Catalytic Activity of the ^{HisVSV}Rad18 (SAPΔ)-Rad6 Complex....205
7.3 Discussion....209
7.3.1 Comparison between the hRad18 and the yRad18 SAP Domains....209
7.3.2 The SAP Domain is Essential for Rad18's Activity *In vivo*....209
7.3.3 Dissecting the Role of the SAP Domain *In vitro*....210
7.3.3.1 ssDNA-Rad18 (SAPΔ) Interactions....210
7.3.3.2 Rad18 (SAPΔ)-RPA Interactions....211
7.3.3.3 ssDNA-Rad18 (SAPΔ)-RPA Interactions....212
7.3.3.4 Rad18 (SAPΔ)-PCNA Interactions....212
7.3.3.5 The Catalytic Activity of Rad18 (SAPΔ)....213
7.3.3.6 Additional Putative Roles of the SAP Domain....214
7.3.3.6.1 Regulation of Localisation by the SAP Domain....214

7.3.3.6.2 Regulation of Substrate Selectivity....215
8 Chapter Eight: Discussion and Outlook....217
8.1 The Catalytic Activity of Rad18....218
8.2 Interactions between Rad18 and DNA....220
8.3 Interactions between Rad18 and RPA....222
8.4 Interactions between Rad18, RPA and ssDNA....223
8.5 The Role of the SAP Domain....230
8.6 Outlook....232
9 References....234
10 Appendix....257

List of Figures

Figure 1.1 – The canonical OB-fold domain....30
Figure 1.2 – Sequence alignment of SAP motives from different genes and organisms....36
Figure 1.3 – Schematic representation of yRPA subunits and their OB domains....47
Figure 1.4 – The crystal structure of hRPA70 DNA-binding domain bound to ssDNA....48
Figure 1.5 – Stalling of replication forks....59
Figure 1.6 – The *RAD6* pathway in *S. cerevisiae*....66
Figure 1.7 – Coordination of replication and DNA damage tolerance by PCNA modifications....70
Figure 1.8 – Schematic representation of yRad18 structural domains....73
Figure 3.1 – Solubility of ^{HisVSV}*RAD18* produced in baculovirus-infected insect cells....133
Figure 3.2 – Partial purification of the yeast ^{HisVSV}Rad18-Rad6 complex from baculovirus-infected insect cells....136
Figure 3.3 – Rad6 associates with ^{HisVSV}Rad18 in a complex....137
Figure 3.4 – Rad18 is ubiquitylated *in vivo*....141
Figure 3.5 – ^{HisVSV}Rad18 is auto-ubiquitylated *in vitro*....142
Figure 3.6 – PCNA mono-ubiquitylation can be reconstituted *in vitro* by the ^{HisVSV}Rad18-Rad6 complex....145
Figure 4.1 – Rad18 binding to ssDNA is affected by NaCl....153
Figure 4.2 – Rad18 binding to ssDNA is stable even after stringent washing....153
Figure 4.3 – Rad18 but not Rad6 binds directly to ssDNA....155
Figure 4.4 – Kinetics of the interaction between the Rad18-Rad6 complex and ssDNA....155
Figure 4.5 – Rad18 binding to ssDNA is less sensitive to glutamate or to acetate than to chloride anion....157
Figure 4.6 – The Rad18-Rad6 complex binds to different oligo dT lengths 160

Figure 4.7 – The Rad18-Rad6 complex binds to different DNA structures 160
Figure 5.1 – Purified proteins used for interaction studies 168
Figure 5.2 – ^{HisVSV}Rad18 and RPA interact directly with each other via protein-protein interactions. 168
Figure 5.3 – Rad6 interacts with RPA in the presence or in the absence of Rad18 169
Figure 5.4 – ^{GST}Rfa1 (182-421) is sufficient for Rad18 interaction 171
Figure 5.5 – ^{GST}Rfa2 is sufficient for Rad18 interaction 172
Figure 6.1 – ^{GST}Rfa1 (182-421) binds to short oligos with various affinities 177
Figure 6.2 – ssDNA stimulates the interaction between ^{GST}Rfa1 and ^{HisVSV}Rad18 178
Figure 6.3 – ^{GST}Rfa2 has lower affinity for ssDNA than ^{GST}Rfa1 (182-421) 179
Figure 6.4 – RPA can recruit Rad18 to ssDNA *in vitro* 182
Figure 6.5 – Low salt concentration results in competition between Rad18 and RPA for binding to ssDNA 183
Figure 6.6 – Interactions of Rad18 with RPA and ssDNA under a range of salt concentrations 185
Figure 6.7 – RPA and SSB have higher affinity for ssDNA than Rad18 186
Figure 7.1 – Possible mechanisms for the interactions between Rad18, RPA and ssDNA 195
Figure 7.2 – *rad18* (*SAP*Δ) and *rad18* (*SAP**) alleles cannot complement *rad18* sensitivity to DNA damage 198
Figure 7.3 – Over-expression of *RAD18* mutant alleles does not rescue *rad18* sensitivity to DNA damage 199
Figure 7.4 – Purified ^{HIsVSV}Rad18 (SAPΔ)-Rad6 complex 201
Figure 7.5 – ^{HisVSV}Rad18 (SAPΔ) can still bind to ssDNA at low ionic strength 201
Figure 7.6 – ^{HisVSV}Rad18 (SAPΔ) can still bind to Rfa1 via its DNA-binding domain but not to the RPA complex 203

Figure 7.7 - ^{HisVSV}Rad18 (SAPΔ) is recruited to ssDNA by RPA 206
Figure 7.8 – Protein-protein interactions between Rad18 SAP mutant proteins, Rfa1 and PCNA.....207
Figure 7.9 – The ^{HisVSV}Rad18 (SAPΔ)-Rad6 complex retains its E3 ligase activity but cannot ubiquitylate PCNA 208
Figure 8.1 – The interactions between Rad18-Rad6, RPA and DNA....226
Figure 8.2 – Model for the activation of the DNA damage tolerance pathway through Rad18-Rad6 recruitment by RPA 228

List of Tables

Table 1-1: Eight ZnF fold groups based on the structural properties around the zinc-binding site 33
Table 1-2: Members of the *RAD6* pathway in *S. cerevisiae* 67
Table 2-1: A list of the enzymes that were used. 82
Table 2-2: A list of the primary monoclonal antibodies that were used. ..82
Table 2-3: A list of the primary polyclonal antibodies that were used..... 83
Table 2-4: A list of the secondary antibodies that were used. 83
Table 2-5: A list of the additional chemicals and reagents that were used. 84
Table 2-6: A list of the antibiotic stock solutions..... 85
Table 2-7: A list of all plasmids used in this thesis that were constructed by others or commercially available. 91
Table 2-8: A list of all plasmids that were constructed for this thesis. 93
Table 2-9: A schematic representation of the DNA structures that were used. 94
Table 2-10: A list of all *E. coli* strains that were used and their genotypes. 95
Table 2-11: A list of all yeast strains that were used and their genotypes. 96
Table 10-1: The sequences of all the oligonucleotides that were used..... 257

List of Abbreviations

2D-gels	two-dimensional gels
4NQO	4-nitroquinoline 1-oxide
A_{260}	absorbance at 260 nm
aa	amino acids
ADP	adenosine 5'-diphosphate
AP	apurinic / apyrimidinic
APE1	AP endonuclease 1
APS	ammonium persulfate
Asp-tRNA	aspartic transfer RNA
ATM	ataxia-telangiectasia mutated
ATP	adenosine 5'-triphosphate
ATR	ataxia-telangiectasia mutated- and Rad3-related
AT-rich	adenine & thymine rich
ATRIP	ATR-interacting protein
β-ME	beta mercaptoethanol
BER	base excision repair
BIR	break-induced replication
bp	base pair
BRCT	breast cancer susceptibility protein (BRCA1) C-terminus
Bre1	brefeldin A sensitivity 1
BSA	bovine serum albumin
Cdc7	cell division cycle 7
Cdk	cyclin dependent kinase
CPDs	cis, syn cyclobutane pyrimidine dimers
Csm3	chromosome segregation in meiosis 3
Cys	cysteine
Da	dalton
DA	damage avoidance
Dbf4	dumbbell forming 4
dC	deoxycytosine
Ddc2	DNA damage checkpoint 2

DDR	DNA damage response
DMSO	dimethyl sulfoxide
DNA	deoxyribonucleic acid
DNA-PK	DNA-dependent protein kinase
DNA-PKcs	DNA-dependent protein kinase catalytic subunit
DSB	double-strand break
DSBs	double-strand breaks
dsDNA	double-stranded DNA
DTT	dithiothreitol
E. coli	*Escherichia coli*
EBNA1	Epstein-Barr nuclear antigen-1
ECL	enhanced chemiluminescence
EDTA	ethylenediaminetetraacetic acid
ERCC1/XPF	excision repair cross-complementation group 1 / xeroderma pigmentosa group F
EST	E26 transformation specific
FACT	facilitates chromatin transcription
FANCD2	Fanconi Anemia protein D2
Fli1	friend leukemia integration-1
G	glycine
GAL	galactose
GST	glutathione S-transferase
H	histidine
h	human
HAP	hydroxyapatite
HECT	homologous to E6-associated protein C-terminus
HHR6A	human homologue Rad6 protein A
HHR6B	human homologue Rad6 protein B
HIRAN	HIP116 & Rad5 protein N-terminal
His	six histidines epitope
HLTF	helicase-like transcription factor
HO endonuclease	homing endonuclease

HRR	homologous recombination repair
HR23B	human homologue of yeast *RAD23* B
HRP	horse radish peroxidase
HU	hydroxyurea
i.e.	id est
ICLs	interstrand cross-links
IDLs	insertion & deletion loops
IPTG	isopropyl-1-thio-β-D-galactopyranoside
IR	ionising radiation
K	lysine
kb	kilo base
kDa	kilo dalton
L	leucine
LB	luria broth
LRI	London Research Institute
MBP	maltose binding protein
MCM	minichromosome maintenance
Mec1	mitosis entry checkpoint 1
MMR	mismatch repair
MMS	methyl-methane sulfonate
MOPS	3-(N-Morpholino)propanesulfonic acid
Mrc1	mediator of the replication checkpoint 1
Mre11	meiotic recombination 11
MRX	Mre11, Rad50 and Xrs2 complex
Myc	myelocytomatosis (epitope derived from the Myc protein)
NEB	New England Biolabs
NER	nucleotide excision repair
NHEJ	non-homologous end joining
NP-40	nonylphenyl-polyethylene glycol (nonidet P-40)
nt	nucleotides
$O.D._{600}$	optical density at 600 nm

OB	oligonucleotide / oligosaccharide binding
PAD	polymerase-associated domain
PAGE	polyacrylamide gel electrophoresis
PBSA	phosphate buffer saline A
PBST	phosphate buffer saline & Tween 20
PCNA	proliferating cell nuclear antigen
PCR	polymerase chain reaction
PEG	polyethylene glycol
pfu	plaque forming units
PGK	yeast 3-phosphoglycerate kinase
PHD	plant homeo domain
PIAS	protein inhibitor of activated signal transducer and activator of transcription 1
PIP	PCNA interacting peptide
PMSF	phenylmethanesulfonyl fluoride
PNK	polynucleotide kinase
Polδ	DNA polymerase δ
Polε	DNA polymerase ε
Polκ	DNA polymerase κ
Polι	DNA polymerase ι
Polη	DNA polymerase η
Polζ	DNA Polymerase ζ
PP	photoproducts
RAD	radiation sensitive
REV	reversionless
RFA	replication factor A
RFC	replication factor C
RING	really interesting new gene
RNA	ribonucleic acid
RPA	replication protein A
RPM	rotations per minute
S. cerevisiae	*Saccharomyces cerevisiae*

SAF-A/B	scaffold attachment factor A or B
SAP	SAF-A/B, Acinus and PIAS
SAR	scaffold attachment regions
SDS	sodium dodecyl sulfate
Sf9	*Spodoptera frugiperda*
SHPRH	SNF2, (linker-) Histone, PHD finger, RING domain and Helicase domain
Siz1	SAP and miz-finger domain 1
SOC	super optimal catobolite repression
Srs2	suppressor of radiation-sensitive
ss	single-stranded
SSB	single-stranded DNA-binding (protein)
SSBs	single-stranded DNA-binding proteins
ssDNA	single-stranded DNA
SUMO	small ubiquitin-related modifier
SV40	simian virus 40
SWI2 / SNF2	swItch / sucrose nonfermenting 2
TAE	Tris acetate EDTA
TB	teriffic broth
TBE	Tris borate EDTA
TCA	trichloroacetic acid
TE	Tris-EDTA
Tel1	telomere maintenance 1
TEMED	N,N,N',N'-(tetramethylethylenediamine)
TLS	translesion synthesis
Tof1	topoisomerase 1-associated factor 1
Tris	Tris (hydroxymethyl) aminomethane
tRNA	transfer-RNA
u	units
Ubc9	ubiquitin-conjugating 9
UBZ	ubiquitin-binding domain type Z
Usp1	ubiquitin-specific protease 1

UV	ultraviolet
v/v	volume per volume
VP16	virion phosphoprotein 16
VSV	vesicular stomatitis virus (epitope derived from the VSV glycoprotein)
W	tryptophane
w/v	weight per volume
WT	wild type
X-Gal	5-bromo-4-chloro-3-indolyl-β-D-galactopyranoside
XPA	xeroderma pigmentosa group A
XPB	xeroderma pigmentosa group B
XPD	xeroderma pigmentosa group D
XPG	xeroderma pigmentosa group G
XPV	xeroderma pigmentosum variant
Xrs2	x-ray sensitive 2
y	yeast (*S. cerevisiae*)
YP	yeast peptone
YPD	yeast peptone glucose
ZnF	Zinc Finger
ZnFs	Zinc Fingers

1 Introduction

The first aim of this introduction is to describe general concepts regarding DNA-binding proteins. The parameters affecting the binding of proteins to DNA and relevant DNA-binding domains will be presented. Special attention will be given to RPA and to the ssDNA-binding protein family to which it belongs. Next, the problem of DNA damage will be introduced together with the mechanisms through which cells sense and deal with it. Emphasis will be placed on the mechanisms operating during DNA replication. In addition, the involvement of RPA and Rad18 in the different DNA repair and damage bypass pathways will be delineated. As Rad18 belongs to the ubiquitin system, the mechanisms of ubiquitin conjugation and the biological importance of post-translational modification of proteins by ubiquitin will be presented. Finally, the *RAD6* pathway to which the *RAD18* gene belongs will be described in detail.

1.1 Parameters Affecting DNA-Protein Interactions

DNA, the carrier of the genetic information of the cell, is a highly reactive molecule (Friedberg *et al.*, 1995). All biological processes involving the DNA require the activity of DNA-binding proteins. Through their binding, these proteins execute essential manipulations upon the DNA, facilitating DNA replication, transcription, repair and recombination (Lilley, 1995).

1.1.1 Chemical Bonds Participating in DNA-Protein Interactions

The binding of a protein to DNA involves a network of electrostatic and hydrophobic interactions that create a stable DNA-protein interface (Lilley, 1995). The most important electrostatic interactions are the hydrogen bonds, in which nitrogen or oxygen atoms of one binding partner contact a hydrogen atom of another. These are mediated via direct contacts between the side-chains of the protein's amino acids (aa) or its amide groups and the DNA sugar-phosphate backbone. Many DNA-binding proteins form hydrogen bonds with the donor and acceptor atoms along the edges of the minor and the major

grooves of the DNA (Dickerson and Chiu, 1997). Importantly, the DNA base sequence influences its curvature as well as the specific spatial localisation of these donor and acceptor atoms. Thus, some proteins are able to recognise specific DNA sequences through their interactions (Dickerson and Chiu, 1997). Hydrophobic interactions between proteins and DNA include the base stacking interactions, in which aromatic side-chain residues of the proteins and the aromatic ring(s) of the DNA bases participate in van der Waals interactions (Seeman *et al.*, 1976).

1.1.2 Buffer Conditions Can Affect DNA-Protein Interactions

1.1.2.1 The Effects of the Solvent

Naturally, DNA-protein complexes exist in aqueous solutions. Ordered water molecules, which exist at their binding interface and are isolated from the bulk of the solvent, can often mediate the hydrogen bonds between the protein and the DNA (Lilley, 1995). In addition, these water molecules may fill gaps between the surfaces of the two binding partners, contributing to their compatibility. Buried surfaces within DNA-protein complexes may also contribute to their stability (Lilley, 1995). On the one hand, such buried surfaces can form between hydrophilic faces of the protein and the DNA. In this case, dissociation of water molecules could be entropically favourable and the electrostatic contacts between the molecules will be enhanced. On the other hand, non-polar residues of the protein could intercalate between the DNA bases, forming a hydrophobic buried surface while excluding the solvent molecules, and thus enhancing the interactions within the complex (Seeman *et al.*, 1976; Lilley, 1995).

1.1.2.2 The Effects of Ions

The ionic environment can significantly affect DNA-protein interactions. When the two macromolecules bind, new electrostatic bonds are established (Record *et al.*, 1985). Electrolyte ions, previously required for the structural stability of

the individual macromolecules, are often displaced or redistributed in favour of the new interactions. In theory, a release of cations or anions from the interface of the DNA or the protein, respectively, can promote the association of the complex (Leirmo *et al.*, 1987). Thus, even small changes to an *in vitro* ionic environment might result in significant effects to the interactions between DNA and proteins (Record *et al.*, 1985). Correspondingly, the thermodynamics and the kinetics of enzymatic reactions involving DNA-protein interactions are often highly dependent on the salt concentrations in the buffer (Leirmo *et al.*, 1987).

The effects of ions on DNA-protein interactions can be divided into specific or non-specific effects. Specific ion effects are derived from binding sites for a specific ion on one or both of the macromolecules (Griep and McHenry, 1989). These ions can have a direct effect on the function of the protein. In contrast, non-specific ion effects can be regarded as the effects of the buffer ionic strength on the complex formation. However, empirical experiments have revealed that the identity and the charge of ions can specifically promote or disrupt DNA-protein interactions. The Hofmeister series is a useful ranking of anions reflecting their effects on protein solubility, which is in accordance with their ability to be displaced from the protein's interface (Griep and McHenry, 1989). Similarly, recent studies provided an empirical ranking of anions that contributed to DNA-protein interactions. The order of these anions was as follows: glutamate > fluoride > acetate > chloride > bromide = nitrate > iodide > hypochloride (Griep and McHenry, 1989).

1.1.3 Structural Aspects Affecting DNA-Protein Interactions

Conformational changes of both the DNA and the protein are often important for the complex formation (Lilley, 1995). Double-helical DNA is flexible and can have, in principle, two types of movement. One is a twisting motion, in which a base pair rotates around its local helical axis relative to its neighbouring bases. The other is a bending movement, which results in a deviation from the straight helical axis of the DNA backbone. Perhaps the most striking conformational change that dsDNA undergoes is the packaging into chromatin by histones as

approximately 2 m of dsDNA is contained within a nucleus of 20 μm diameter (Rocha and Verreault, 2008). This is achieved through several layers of DNA coiling, with the first one being the wrapping of 147 base pairs (bp) of DNA around a nucleosome. ssDNA can also undergo significant conformational changes. For example, in the case of *Escherichia coli* (*E.coli*) single-stranded DNA-binding protein (SSB), ssDNA can be wrapped around a SSB oligomer, resulting in a compacted filament structure (Krauss *et al.*, 1981).

Conformational changes of a protein, induced by its binding to DNA, may involve a significant rearrangement of the protein structure. These structural alterations confer improved stability and reduce the free-energy state of the protein by enhancing the interactions between the two macromolecules (Lilley, 1995). In addition, these conformational changes can regulate the catalytic activity and the specificity of the DNA-binding protein. For example, conformational changes may facilitate an enzymatic modification of the DNA, if during the transition state of the reaction specific DNA bases are brought into the catalytic centre of the protein. Alternatively, if reactive atoms within the protein re-orientate upon its binding to the DNA, its catalytic activity toward a third molecule can be enhanced (Lilley, 1995). Conformational changes following DNA-protein binding may also result in a cooperative behaviour. For example, DNA binding by one protein monomer may enhance the binding of a second monomer through favourable protein-protein interactions (Lilley, 1995). Examples for cooperative binding can be found during ssDNA-protein filament formation of several single-stranded DNA-binding proteins (Lohman *et al.*, 1986) (see 1.3).

1.2 DNA-Binding Domains

In most cases, DNA-binding proteins interact with the DNA via conserved structural domains. These domains modulate the protein's binding specificity and selectivity toward different DNA structures (Lilley, 1995). In addition, conformational changes within these domains can regulate the protein's affinity for the DNA. Often, a single domain is sufficient and necessary for the DNA-binding activity of a protein, but sometimes multiple DNA-binding domains may

act together (Lilley, 1995). Three DNA-binding domains relevant to this thesis are introduced below.

1.2.1 The OB Fold

The OB (oligonucleotide / oligosaccharide binding) fold, first described in 1993, was identified in five different proteins able to bind either to oligonucleotides or to oligosaccharides (Murzin, 1993). These proteins, a tRNA synthetase from yeast, a nuclease from staphylococcus and three bacterial cytotoxins, did not share sequence homology or similar functions. However, common structural determinants and key residues that contribute to the formation of the fold were found. The OB fold consists of five β-strands that coil together to form a closed β-barrel (Theobald *et al.*, 2003). This barrel is often capped by an α–helix located between the third and fourth β-strands. The conserved ligand-binding interface is centred on β-strands β2 and β3, with additional contributions from the C-terminal regions of strands β1 and β5 (see Figure 1.1). Further important binding residues are located in the loops sticking outwards from the β-barrel axis. These loops, marked as L in Figure 1.1, are variable in sequence, length and conformation. As a consequence, they contribute to significantly different ligand-binding sites and to variations in the fold length, ranging between 70 and 150 amino acids. A representative of the canonical structure of an OB fold, derived from the yeast Asp-tRNA synthetase, is shown in Figure 1.1 (Murzin, 1993; Theobald *et al.*, 2003).

The type and the positioning of the ligand depend on the architecture and the topology of the OB fold rather than on its sequence. Therefore, the OB fold is considered a structure-related binding site (Murzin, 1993). The nucleic acid-binding super-family is the largest within the OB folds and representatives containing this motif participate in almost any process involving the manipulation of either ssDNA or RNA (Theobald *et al.*, 2003). According to the current understanding, OB-fold-containing proteins can be divided into three categories with respect to their functional recognition: (a) proteins that bind nucleic acids without apparent specificity; (b) proteins that bind to sequence-specific single-stranded regions of nucleic acids; and (c) proteins that interact

with non-helical structured nucleic acids. Different OB-fold-containing proteins may undergo either a dramatic conformational change or only subtle shifts upon binding to nucleic acids. In addition, the OB fold is a modular domain, often involved in the protein's oligomerisation on the DNA (Theobald *et al.*, 2003). Since its identification, the OB fold was also found to be involved in protein-protein interactions, and it is now referred to as an oligo-binding fold (Bochkareva *et al.*, 2001).

An OB-fold-containing protein, which is relevant to this thesis, is the hetero-trimeric Replication Protein A from *S. cerevisiae*, hence referred to as yRPA. This protein contains six OB folds, some of which are involved in ssDNA-binding, protein-protein interactions or both. As RPA binds with little or no sequence specificity to ssDNA, it belongs to the first category of nucleic acid-binding OB-fold-containing proteins described above. RPA and its OB folds are described in detail in paragraph 1.3.2 below. Chapters 5 and 6 of this thesis present the importance of the OB folds of RPA in its interaction with Rad18, in the absence and in the presence of ssDNA, respectively.

Figure 1.1 – The canonical OB-fold domain
The OB-fold from Asp-tRNA synthetase is shown as a representative of the ideal OB-fold domain. From the N-terminus to the C-terminus, strand β1 is shown in red, β2 in orange, β3 in yellow, the helix between β3 and β4 in green, β4 in blue, and β5 in violet. The conserved ligand-binding interface is centred on β-strands β2 and β3, with additional contributions from the C-terminal regions of strands β1 and β5. An α-helix, which is found in some, but not in all OB-fold containing proteins, is shown in white at the top of the figure, just N-terminal to strand β1. Variable loops (L) between strands are indicated in black text. This figure was adapted from Theobald *et al.* (2003).

1.2.2 The Zinc Fingers

Zinc-binding repeats were first identified in the *Xenopus laevis* transcription factor IIIA (Miller *et al.*, 1985). This motif was found to be extremely abundant in eukaryotic proteins and is now regarded as a 'classical' Zinc Finger (ZnF). Since then, additional types of zinc binding domains were identified in many proteins, and they are all regarded as Zinc Fingers (ZnFs) (Rubin *et al.*, 2000). The yeast genome is estimated to encode 500 proteins containing ZnFs. These proteins are diverse with regard to their sequences, structures and functions. Reducing conditions in the environment, which favoured protein folding around a zinc atom, could be evolutionary accountable for the versatility and abundance of ZnF-containing proteins (Mackay and Crossley, 1998).

Proteins bind to zinc as a cofactor for their catalytic activity or as a structural component important for their stability. The latter is characteristic for ZnFs, as the zinc atom does not normally participate directly in the function of the protein (Krishna *et al.*, 2003; Gamsjaeger *et al.*, 2007). Although at first ZnFs were thought to only bind to nucleic acids (DNA or RNA), today they are implicated in binding of lipids, in protein-protein interactions and in ubiquitin conjugation. Hence, ZnF-containing proteins participate in a range of cellular processes: DNA replication and repair, protein translation and programmed cell death (Krishna *et al.*, 2003; Gamsjaeger *et al.*, 2007).

Different protein families in a particular ZnF fold group (see below) may have distinct protein / DNA interaction modes, contributing even more to the diversity among the ZnF-containing proteins. However, some common features can be found (Gamsjaeger *et al.*, 2007). First, ZnFs undergo very little, if any conformational changes upon recognition of their binding partners. This could be due to the stability of the domain structure, maintained by coordinative bonds with the zinc atom. Second, ZnFs tend to mediate modular protein-protein interactions. They can either promote oligomerisation of their respective proteins or tandem ZnFs participate in the binding of the same substrate. Third, although ZnFs mediate moderate to weak protein-protein interactions, these

have been proven to be highly specific and their importance in regulation of cellular process is evident (Gamsjaeger *et al.*, 2007).

Structural analysis of ZnF-containing proteins revealed eight distinct classes of ZnF folds (see Table 1-1), comprising of total of 32 protein families (Krishna *et al.*, 2003). Two of them, fold group 1 (C2H2-like Finger) and fold group 3 (Treble Clef Finger), which are relevant to this thesis, are described below.

1.2.2.1 C2H2-like Finger (Fold Group 1, see Table 1-1)

This fold group contains ZnFs in which a left-handed ββα-unit is formed by a β-hairpin followed by an α-helix (Krishna *et al.*, 2003). Two zinc ligands are donated by a conserved turn at the end of the β-hairpin (zinc kunckle) and the other two originate from the C-terminal end of the α-helix. The C2H2-like finger structure is stabilised by the coordinated binding of a single zinc atom. This fold group consists of two families, of which one, the C2H2 finger family (also known as the 'classical' ZnF), has relevance to this thesis. This fold consists of 28 to 30 amino acids with two conserved cysteine residues followed by two conserved histidine residues at a specific spacing (Krishna *et al.*, 2003). However, substitutions of one or both histidines to cysteines can also occur. Usually, members of the C2H2 finger family interact with the major groove of the DNA via their α-helix. Some were reported to be involved in a simultaneous binding to both a specific DNA sequence and a protein, but these interactions occur via different recognition surfaces (Gamsjaeger *et al.*, 2007). Others were found to participate solely in protein-protein interactions.

A C2H2-like finger-containing protein with relevance to this thesis is the Rad18 protein from *S. cerevisiae*, hence referred to as yRad18. It contains a ZnF of the C2H2-like finger family with a C2HC pattern between amino acids 188 and 210. This motif was suggested to participate in DNA-protein or protein-protein interactions of yRad18 (see paragraph 1.7.3 for more details). In addition, yRPA contains a ZnF of the C2H2-like finger family with a C4 pattern (Cys4-type) between amino acids 486 and 508 of its largest subunit, Rfa1. This motif seems to be important for ssDNA-binding and recognition of damaged DNA (see paragraph 1.3.2 for more details).

Table 1-1

Table 1-1: Eight ZnF fold groups based on the structural properties around the zinc-binding site

The ligands that chelate zinc (coloured orange) are shown as ball-and-stick. The helices are coloured cyan. The zinc knuckle connecting the two strands of the β-hairpin is shown in red. The primary β-strands adjacent to the knuckle are coloured in purple and other strands in yellow. Loops are shown in light green. Other parts of the structure, which do not belong to the zinc-binding region of the structure, are shown in grey. A brief description of the ligand placement within each fold group is given. This table was adapted from Krishna *et al.* (2003).

1.2.2.2 Treble Clef Finger (Fold Group 3 – see Table 1-1)

Proteins that contain treble clef fingers are diverse and often do not have any sequence homology nor functional similarity (Krishna *et al.*, 2003). The core structure of the treble clef motif consists of a β-hairpin at the N-terminus and an α-helix at the C-terminus. The zinc knuckle donates two ligands whereas the N-terminal turn of the helix contribute the other two. In most cases, a loop and a β-hairpin are present between the N-terminal β-hairpin and the C-terminal α-helix. Sometimes, a helix or a pair of helices is present instead. These secondary structural elements vary in length and in conformation, contributing to the diversity of the core motif (Krishna *et al.*, 2003). Hence, this group can be divided into ten protein families of which the RING finger-like family is relevant to this thesis. Typically, the RING (really interesting new gene) finger is 40 to 60 amino acids long and consists of a set of histidine and cysteine residues with a characteristics spacing, allowing the coordination of two zinc ions in a cross-brace structure (Pickart, 2001). This domain was found to be involved in protein-protein interactions in the context of ubiquitin ligase activity, bringing together an E2 ubiquitin-conjugating enzyme and a specific substrate (Gamsjaeger *et al.*, 2007).

The yRad18 protein contains a RING domain, of a C3HC4 pattern, between amino acids 28 and 62, which is essential for its ubiquitin ligase activity (see paragraph 1.7.3 for more details). Chapter 3 of this thesis deals with the catalytic activity of yRad18 *in vitro*.

1.2.3 The SAP Domain

Using bioinformatics tools Aravind and Koonin (2000) identified a novel and statistically significant conserved putative DNA-binding motif, consisting of 35 amino acids. They named this motif SAP, after three proteins that contained it: SAF-A/B (scaffold attachment factor A or B), Acinus and PIAS1 (protein inhibitor of activated signal transducer and activator of transcription 1). The identified consensus sequence was predicted to have a helix-extended loop-helix structure, as shown in Figure 1.2. Independently, biochemical studies of human SAF-A protein revealed a 45 amino acid region, which was necessary and

sufficient for binding to scaffold attachment regions (SAR), AT-rich DNA elements found in eukaryotes (Kipp *et al.*, 2000). The authors described a 31 amino acid motif within this region, which they found by database search to be conserved in additional eukaryotic but not prokaryotic proteins, and termed it a SAF-Box. As it turned out, this was the same domain described by Aravind and Koonin (2000). The three early-identified SAP-containing proteins, mentioned previously, have been reported to play different roles involving DNA. Both SAF-A and Acinus are implicated in apoptosis (Gohring *et al.*, 1997; Sahara *et al.*, 1999). The SAF-A protein is cleaved at its SAP domain during apoptosis and, as a result, loses its SAR-binding ability, which is important for the proper nuclear architecture of the cell (Gohring *et al.*, 1997). In contrast, Acinus is activated by caspase-3 cleavage and its SAP domain is required for chromatin condensation during apoptosis (Sahara *et al.*, 1999). The third SAP-containing protein, PIAS1, is implicated in regulation of the tumour suppressor protein, p53 (Okubo *et al.*, 2004). It belongs to a family of proteins, all containing the SAP domain, which are E3 small ubiquitin-related modifier (SUMO) ligases. The mammalian members of this family, encoded by four genes, include the *PIAS1*, *PIASx* (*PIAS2*), *PIAS3* and *PIASy* (*PIAS4*) genes whereas in *S. cerevisiae* there are only two PIAS family members, encoded by *SIZ1* and *SIZ2*. Although the PIAS proteins were first identified as interacting partners of transcription factors, it is now clear that their activity extends to modulation of other cellular processes via their SUMO ligase activity (Palvimo, 2007).

The number of eukaryotic proteins identified to contain a SAP domain is increasing. Among them, there are proteins involved in DNA repair. One example is Ku70, which is important for DNA double-strand break (DSB) recognition and repair via the non-homologous end joining pathway (Walker *et al.*, 2001). In addition, and most relevant for this thesis, Rad18, the ubiquitin ligase involved in the DNA damage tolerance pathways, also contains a SAP domain (Nakajima *et al.*, 2006). Furthermore, this domain is found in all *RAD18* sequences cloned thus far from various eukaryotic organisms (Notenboom *et al.*, 2007), suggesting an important role for this domain in the function of Rad18.

Figure 1.2 – Sequence alignment of SAP motives from different genes and organisms

The alignment is shown along with a schematic representation of the predicted secondary structure (two amphipatic helices). The colouring is according to the 90% consensus that includes h (hydrophobic) or l (aliphatic) residues shaded yellow (YFWLIVMA); s (small) residues coloured green (SAGTVPNHD); p (polar) residues coloured purple (STQNEDRKH); and b (bulky) residues shaded grey (KREQWFYLMI). The species abbreviations are: At, *Arabidopsis thaliana*; Ce, *Caenorhabditis elegans*; Dm, *Drosophila melanogaster*; Gg, *Gallus gallus*; Hs, *Homo sapiens*; Sc, *Saccharomyces cerevisiae*; Sp, *Schizosaccharomyces pombe*; and Zm, *Zea mays*. This figure was taken from Aravind and Koonin (2000).

Some of the SAP-containing proteins harbour this motif as their sole DNA-binding element, while others have additional DNA-binding determinants. In most of these proteins, the SAP domain is believed to be involved directly in DNA-binding. Although Aravind and Koonin (2000) have suggested a few common features for the SAP motif, the variability among the SAP-containing proteins imply that it might have different binding specificities toward DNA depending on the protein. According to Kipp *et al.* (2000), the SAP domain of human SAF-A protein preferentially binds to SAR DNA over non-SAR DNA. Similarly, the SAP domain of the SUMO ligase PIAS1 was found to bind to AT-rich dsDNA sequences (Okubo *et al.*, 2004). In contrast, the Ku70 protein recognises dsDNA ends and binds to them with high affinity independent of the DNA sequence (Lehman *et al.*, 2008), whereas the SAP domain found in the human Rad18 (hRad18) ubiquitin ligase preferentially binds to ssDNA or to forked-DNA structures (Notenboom *et al.*, 2007; Tsuji *et al.*, 2008).

Since its first identification as a putative DNA-binding motif, additional or alternative roles are emerging for the SAP domain. According to Okubo *et al.* (2004), the SAP domain of the PIAS1 protein plays a dual role in binding to DNA and to its substrate, p53. Another example for a dual role of the SAP domain was found in PIASxα, an isoform of the PIASx protein. Its SAP domain was identified to be important for binding to AT-rich DNA elements but also to Fli1 (Friend leukaemia integration-1), an EST (E26 transformation specific) transcription factor (van den Akker *et al.*, 2005). Their interaction results in sequestering Fli1 into a transcriptional inactivated complex and preventing its activity. In addition, the SAP domain of the yeast E3 SUMO ligase Siz1 was suggested to contribute to its selectivity toward some of its substrates as well as to its nuclear localisation (Reindle *et al.*, 2006). Nonetheless, it was not formally shown whether the latter is due to its interaction with the DNA or due to structural overlap of the SAP domain with its nuclear localisation signal. Recent findings in my lab suggest that Siz1 binds to dsDNA via its SAP domain (Parker *et al.*, *in revision*).

As discussed above, the SAP domains from different proteins have diverse DNA-binding specificities. Therefore, it is not surprising that structural

information, obtained for various SAP-containing proteins, reveals differing DNA-binding modes as well as variations in the proposed domain size (Devany *et al.*, 2008). With regard to the SAP domain of hRad18, a few important residues in the extended loop were identified by mutational analysis (Notenboom *et al.*, 2007). As these residues were similar to the residues in the PIAS1's SAP domain that were implicated in DNA-binding (Okubo *et al.*, 2004), the authors suggested that these two proteins might have a similar DNA-binding mode (Notenboom *et al.*, 2007).

The yRad18 protein contains a putative SAP domain between amino acids 278 and 312. Insights regarding the contribution of yRad18's SAP domain to its interactions and catalytic activity and its homology to the hRad18 SAP domain are presented in Chapter 7 of this thesis.

1.3 Single-stranded DNA-Binding Proteins

Among the various DNA-binding proteins that exist, of particular relevance to this thesis is the single-stranded DNA-binding protein (SSB) family, to which RPA belongs. Single-stranded DNA-binding proteins (SSBs) are present in all organisms and they are essential for viability (Kur *et al.*, 2005). These proteins bind to ssDNA with high affinity, most of them with little or no sequence specificity. In addition, they are implicated in all biological processes involving DNA in the cell: replication, repair and recombination (Kur *et al.*, 2005). During these processes, the DNA undergoes multiple conversions between double-stranded and single-stranded forms. Under physiological condition, ssDNA is energetically unfavourable. Therefore, SSBs are required for maintaining its conformation and for preventing interstrand and intrastrand re-annealing (Bochkarev and Bochkareva, 2004). Furthermore, through their binding, SSBs protect ssDNA against nuclease attack or undesired chemical modification and prevent the formation of secondary structures (Kur *et al.*, 2005). Moreover, their binding and activity can facilitate the recognition of ssDNA by other enzymes, whose activity may be essential.

The proteins within the SSB family have high sequence variability and can be found in different oligomeric states (Kur *et al.*, 2005). Depending on the organism, SSBs are homo-dimers, hetero-trimers or homo-tetramers. For example, *Deinococcus Thermus* SSB is a homo-dimer, the eukaryotic Replication Protein A is a hetero-trimer and the *Escherichia coli* (*E. coli*) SSB is a homo-tetramer. In addition, the same protein might change its oligomeric state upon ssDNA-binding, as is the case of the *E. coli* SSB protein. Alterations to its ssDNA-binding mode result in changes to its oligomeric state (Lohman and Ferrari, 1994) (see 1.3.1 below). Nevertheless, SSBs share biochemical and structural characteristics, and there is evidence for their evolutionary conservation (Kur *et al.*, 2005). One common element is a conserved domain, the OB fold, which was discussed in detail in paragraph 1.2.1. Another common trait is an obligatory oligomerisation upon ssDNA-binding, when four DNA-binding OB folds are brought together (Kur *et al.*, 2005). The ssDNA-binding properties of SSBs are defined by several parameters. The length of the ssDNA that directly interacts with a protein is known as the **interaction site**, whereas the length of the ssDNA that is covered when the protein is bound is considered to be the **occluded binding site** (Wold, 1997). The equilibrium binding constant for a single protein molecule binding to the interaction site is termed the **intrinsic binding constant**, while **cooperativity** is a unitless parameter representing the affinity differences between a protein binding in isolation versus in proximity to a previously bound protein. Each set of these parameters represents a **binding mode** under specific conditions.

Two SSBs that were used in this thesis, the *E. coli* SSB protein and yRPA, are described below.

1.3.1 The Single-Stranded Binding Protein

The *E. coli* single-stranded binding (SSB) protein forms a stable homo-tetramer in solution, consisting of four 18.8 kDa monomers (Weiner *et al.*, 1975). It binds to ssDNA with high affinity through its four OB folds (one per monomer), and it is essential for DNA metabolism in bacteria (Lohman and Ferrari, 1994).

In the presence of ssDNA SSB has two binding modes, which result in different occluded binding sites. The first one involves only two subunits out of four contacting the ssDNA, with an occluded site size of ~ 35 nucleotides and high binding cooperativity (also referred to as an "unlimited" cooperativity) (Lohman and Overman, 1985; Lohman and Ferrari, 1994). The second binding mode involves all four subunits contacting the ssDNA, with an occluded site size of ~ 65 nucleotides and low binding cooperativity (limited to formation of octamers). These binding modes are affected principally by salt concentration but also by other factors, such as salt type, temperature, pH and concentration of the SSB protein (Bujalowski *et al.*, 1988). As mentioned earlier, various studies based on electron microscopy, nuclease digestion and oligonucleotide-binding stiochiometry revealed that, at least in the high site-size binding mode, the ssDNA can be wrapped around the SSB tetramer (Krauss *et al.*, 1981; Lohman and Ferrari, 1994). The effects of salt on ssDNA-SSB interactions are complex, even in a single binding mode. This complexity is due to the uptake and release of both cations and anions during the binding reaction (Overman *et al.*, 1988), and these, in turn, are also affected by pH and temperature.

1.3.2 Replication Protein A

Replication protein A (RPA) is an abundant SSB protein, conserved in all eukaryotes (Wold, 1997). It binds to ssDNA with very high affinity and to dsDNA and RNA to a much lesser extent (Kim *et al.*, 1992; Wold, 1997; Sibenaller *et al.*, 1998). Initially, it was isolated from human cell extracts as an essential component for DNA replication *in vitro* by the large T antigen simian virus 40 (SV40) (Fairman and Stillman, 1988; Wold and Kelly, 1988). Later, RPA was discovered in yeast as an essential protein for cell survival, and was suggested to play important roles in DNA recombination and repair (Heyer *et al.*, 1990; Brill and Stillman, 1991).

As mentioned earlier, RPA exists as a hetero-trimeric complex. Human RPA, referred to as hRPA, consists of subunits RPA70, RPA32 and RPA14, according to their molecular weights (Wold, 1997). RPA from *S. cerevisiae* consists of subunits Rfa1, Rfa2 and Rfa3 according to the genes that encode

them, *RFA1*, *RFA2* and *RFA3*. The molecular weight of the RPA subunits slightly varies across species and yRPA subunits are 69, 36 and 13 kDa, respectively (Brill and Stillman, 1989). The yRPA and the hRPA are highly homologous to each other, the overall structure of yRPA was found to be very similar to that of hRPA, and the proteins have similar ssDNA-binding affinities (Kim *et al.*, 1992; Park *et al.*, 2005). Nevertheless, there are some structural differences that may account for differences in protein-protein interactions found between the two species (Park *et al.*, 2005). For example, yRPA cannot support SV40 DNA replication *in vitro* due to its lack of interaction with the large T antigen.

The assembly of the RPA complex is mediated by direct interactions between Rfa1 and Rfa2 and between Rfa2 and Rfa3 (Lin *et al.*, 1996), and the RPA complex appears to be very stable *in vitro*. Current knowledge indicates that RPA is not tightly bound to chromatin throughout the cell cycle, and that a large portion of the RPA molecules can be also found in the cytoplasm (Wold, 1997). The findings in Davies *et al.* (2008) support this notion. Nevertheless, RPA was shown to associate with replication origins following treatment with hydroxyurea (HU) (Tanaka and Nasmyth, 1998) and (Daigaku and Ulrich – unpublished data) and to localise to DNA replication (Adachi and Laemmli, 1992) and repair foci (Sakamoto *et al.*, 2001).

1.3.2.1 Rfa1

Rfa1 can be divided into three functional domains: an N-terminal domain (approximately aa 1 – 170), a central DNA-binding domain (approximately aa 170 – 450) and a C-terminal domain (approximately aa 450 – 621) (Wold, 1997) (see Figure 1.3).

The N-terminal part of yRfa1 contains an OB fold (OB-F). This region was shown to be important for replication and recombination, as point mutations in this domain are either lethal or result in defects in these processes (Longhese *et al.*, 1994; Firmenich *et al.*, 1995). In addition, the N-terminal domain of hRpa70 was reported to bind to p53 (Dutta *et al.*, 1993), to the nucleosome

remodelling complex FACT (facilitates chromatin transcription) (VanDemark *et al.*, 2006) and to the N-terminal region of ATRIP (ATR-interacting protein) (Ball *et al.*, 2007). Hence, it is mainly considered to be important for protein-protein interactions (Braun *et al.*, 1997).

In the centre of Rfa1 lie tandem OB folds (OB-A and OB-B) that bind to ssDNA with high affinity (Gomes and Wold, 1996) and thus are considered to be the principal ssDNA-binding domain of RPA. This is consistent with the finding that mutations in OB-A or -B either reduce or abolish the *in vitro* replication activity of RPA (Wold, 1997). Additionally, there are a few reports on the importance of this region in RPA interactions with other proteins (i.e. transcription factors, Bloom and Werner helicases, SV40 T antigen, XPA (xeroderma pigmentosa group A) protein and Rad51 recombinase), reviewed in Wold (1997) and in Fanning *et al.* (2006).

The C-terminal part of Rfa1 contains an OB fold (OB-C), harbouring a conserved putative Cys4-type ZnF. This ZnF is important for ssDNA-binding (Brill and Bastin-Shanower, 1998) and it was implicated in recognition of DNA damage (Lao *et al.*, 2000). In addition, the C-terminal part of Rfa1 was demonstrated to be both necessary and sufficient for formation of the RPA complex via its interaction with Rfa2 (Lin *et al.*, 1996).

1.3.2.2 Rfa2

Rfa2 consists of three functional domains: a small N-terminal domain (aa 1 – 40), which undergoes a cell-cycle and DNA damage dependent phosphorylation, a central domain (aa 40 – 170) important for interactions with Rfa3 as well as with ssDNA, and a C-terminal domain (aa 170 – 273), which is required for interactions of Rfa2 with other proteins (Wold, 1997) (see Figure 1.3).

There are at least seven possible phosphorylated sites within the N-terminal domain of Rfa2, and a number of different kinases were proposed to modify it (Fanning *et al.*, 2006). Cyclin-dependent kinases (Cdk) phosphorylate Rfa2 in

mitotic cells, thereby reducing its interaction with DNA polymerase α-primase. DNA-PK (DNA-dependent protein kinase), ATM (ataxia-telangiectasia mutated) and ATR (ataxia-telangiectasia mutated- and Rad3-related) kinases were suggested to be involved in Rfa2 phosphorylation in response to DNA damage, but the phosphorylation sites as well as the *in vivo* kinetics of Rfa2 modification differ depending on the type of damage. So far, the consequences of Rfa2 phosphorylation are not entirely understood.

The middle part of Rfa2 consists of an OB fold (OB-D), which was demonstrated to bind ssDNA with weak-affinity in the context of the full complex (Bastin-Shanower and Brill, 2001). Rfa2 was reported to interact with XPA protein, Rad52 and uracil-DNA glycosylase reviewed in Wold (1997). All of these interactions are weak but specific and occur via a common surface of Rfa2 C-terminus (Fanning *et al.*, 2006).

1.3.2.3 Rfa3

Rfa3 contains a single OB fold (OB-E), spanning its entire 122 amino acids (see Figure 1.3). This domain was suggested to be important for the trimerisation and the conformational stability of the RPA complex (Fanning *et al.*, 2006). According to (Bastin-Shanower and Brill, 2001), so far there is no evidence supporting a role of Rfa3 in ssDNA-binding.

1.3.2.4 Interactions of RPA with DNA

As mentioned earlier, RPA interacts preferentially with ssDNA, with an intrinsic binding constant between 10^9 and 10^{11} M^{-1}, depending on the experimental conditions (Kim *et al.*, 1992; Wold, 1997; Sibenaller *et al.*, 1998). In addition, it binds to ssDNA with a defined 5' to 3' polarity (Wold, 1997). It has a slight binding preference towards pyrimidine-rich sequences compared to purine-rich DNA sequences (Kim *et al.*, 1992). These findings hold true for both the yeast and human RPA proteins (Kim *et al.*, 1992). RPA was found to have different ssDNA-binding modes depending on the salt concentration with variation to the occluded binding site (Kumaran *et al.*, 2006). Under physiological conditions,

hRPA bound to 30 nucleotides (nt), whereas under other conditions an occluded site of 8 to 10 nt was evident (Kim *et al.*, 1992; Blackwell and Borowiec, 1994). The latter was confirmed by the crystal structure of the hRPA70 DNA-binding domain bound to ssDNA (Bochkarev *et al.*, 1997) (see Figure 1.4). The findings regarding yRPA were at first ambiguous (Alani *et al.*, 1992), but it appears that its occluded binding site ranges between 18 to 28 depending on the salt concentration (Sugiyama *et al.*, 1997; Kumaran *et al.*, 2006). The binding cooperativity of hRPA was found to be low compared to other SSBs (Kim *et al.*, 1992). Initially, yRPA was reported to have very high binding cooperativity by one publication (Alani *et al.*, 1992), but a few others discovered only low or moderate cooperativity (Sugiyama *et al.*, 1997; Kumaran *et al.*, 2006).

Upon binding to ssDNA, both hRPA and yRPA undergo significant conformational changes (Bochkareva *et al.*, 2001; Park *et al.*, 2005). These involve both RPA70 and RPA32 and result in modulation of RPA activity. This regulation affects RPA as a substrate, i.e. ssDNA-bound RPA becomes a better substrate for phosphorylation (Blackwell *et al.*, 1996), but this can also affect its interactions with other proteins (Bochkareva *et al.*, 2001; Davies *et al.*, 2008). As mentioned previously, although there are six OB folds in the RPA complex, only four of them seem to be directly involved in binding to ssDNA. The current accepted model suggests that these folds act in a sequential mode. OB-A and OB-B contact the ssDNA first, then OB-C is engaged in the binding, and finally OB-D comes into play (Philipova *et al.*, 1996). This sequential binding results in different ssDNA-binding modes of RPA, with different lengths of occluded binding site.

In addition to its high affinity for ssDNA, RPA can bind to dsDNA and promote unwinding of the duplex strands (Lao *et al.*, 1999). The suggested model is that the disruption of the duplex is followed by RPA binding to the exposed ssDNA, thus driving the unwinding reaction forward by enhanced ssDNA stability. In addition, RPA can recognise and bind to damaged DNA and consequently has an important role in DNA repair (Lao *et al.*, 2000). This will be further discussed in paragraph 1.4.2.

1.3.2.5 Interactions of RPA with Proteins

To date, RPA has been found to interact with many proteins. These can be divided into three main groups: proteins involved in DNA replication, proteins involved in DNA repair and recombination and a third miscellaneous group (Wold, 1997). The data from various RPA-protein interaction studies indicate that RPA70 and RPA32 subunits are the major contributors to these interactions (and accordingly Rfa1 and Rfa2 in yeast) (Wold, 1997).

One example from the first group is the primase subunit of DNA polymerase alpha, which interacts with hRPA (Dornreiter *et al.*, 1992). This interaction was suggested to be important for the initiation and the elongation steps of DNA replication, and is conserved in *S. cerevisiae* (Smith *et al.*, 2000).

Other examples within this group are viral proteins, such as the large T antigen from SV40 (Dornreiter *et al.*, 1992), the viral initiator from Epstein-Barr virus EBNA1 (Epstein-Barr nuclear antigen-1) protein (Zhang *et al.*, 1998) and the E1 protein (Loo and Melendy, 2004) from bovine papilloma virus, which interact with hRPA. However, these interactions might be species-specific, suggesting a functional difference between human and yeast RPA (Park *et al.*, 2005).

Examples from the second group extend to proteins from the nucleotide excision repair, XPA protein (He *et al.*, 1995; Matsuda *et al.*, 1995), XPG (xeroderma pigmentosa group G) protein (He *et al.*, 1995; Matsunaga *et al.*, 1996), and ERCC1/XPF (excision repair cross-complementation group 1 / xeroderma pigmentosa group F) nuclease (Matsunaga *et al.*, 1996) as well as with the DSB repair proteins, Rad52 (Hays *et al.*, 1998) and Rad51 (Stauffer and Chazin, 2004). In addition, RPA was found to be involved in the activation of the replication checkpoint through the recruitment of the ATR-ATRIP (ATR-interacting protein) complex (Zou and Elledge, 2003). In the same publication, this role was also confirmed in yeast as ssDNA-bound yRPA recruited the equivalent Mec1-Ddc2 complex. Similarly, the clamp loader Rad17-Rfc2-5 interacted with RPA, thereby recruiting the DNA repair clamp Rad9 complex (also known as the 9-1-1 complex) and activating the checkpoint response (Zou *et al.*, 2003). The function of RPA in DNA repair and recombination as well as in

the activation of the replication checkpoint will be further discussed in paragraphs 1.4 and 1.5.

The third group of proteins that interact with RPA includes transcriptional activators such as Gal4 (He *et al.*, 1993), VP16 (virion phosphoprotein 16) (He *et al.*, 1993; Li and Botchan, 1993) as well as the tumour suppressor p53 (Dutta *et al.*, 1993; Li and Botchan, 1993). The latter interaction was shown to mediate ATR-dependent p53 phosphorylation (Tibbetts *et al.*, 1999), and was suggested to coordinate between DNA repair and the p53-dependent checkpoint control in response to DNA damage (Abramova *et al.*, 1997).

The mechanistic aspects of the interactions of RPA with proteins and ssDNA are complex and diverse. On the one hand, RPA may 'trade places' on the DNA with other proteins (Fanning *et al.*, 2006). This applies, for example, to Rad51 recombinase filament formation during DSB repair via homologous recombination. In addition, this is suggested to occur in DNA replication, repair and recombination pathways when several RPA binding partners may compete for their association with ssDNA-bound RPA, in a hand-off mechanism. This successive exchange of binding partners could rely on a gradual increase in the affinities of the incoming proteins. Alternatively, it could depend on the ability of the incoming proteins to modulate RPA binding to the ssDNA. On the other hand, ssDNA-bound RPA may stimulate the binding of other proteins to the DNA, such as in the cases of ATRIP-ATR or Rad17, mentioned previously (Zou and Elledge, 2003; Zou *et al.*, 2003). Similarly, also the function of other proteins may stimulate RPA binding to ssDNA, as in the case of the Werner and Bloom helicases (Fanning *et al.*, 2006). In turn, RPA binding to the newly exposed ssDNA enhances the unwinding activity of these helicases.

Figure 1.3 – Schematic representation of yRPA subunits and their OB domains
The RPA complex from *S. cerevisiae* consists of three subunits, Rfa1, Rfa2 and Rfa3. Rfa1 contains the principal ssDNA-binding domain (OB-A and OB-B). In addition, OB-C harbours the ZnF motif and contributes to ssDNA and to RPA trimerisation. The N-terminal part of Rfa1 contains OB-F, which is important for protein-protein interactions. Rfa2 can be phosphorylated on its N-terminus. The central OB-D domain can bind weakly to ssDNA and is important for the trimerisation of RPA. The C-terminal part of Rfa2 participates in protein-protein interactions. Rfa3 consists of OB-E, which was shown to be important for the trimerisation of the RPA complex. This figure was adapted from Phillipova *et al.* (1996).

Figure 1.4 – The crystal structure of hRPA70 DNA-binding domain bound to ssDNA

The DNA-binding domain of hRPA70 (aa 181 – 422), shown in green, was crystalized with a 8 bp long ssDNA (the backbone is shown in brown and the bases are marked in blue). Three nucleotides are contained within each OB fold and the space between them is bridged by two nucleotides. The position of these nucleotides is maintained by an extensive network of hydrogen bonds with RPA as well as stacking interactions between phenylalanine residues of RPA and the DNA bases. Although the structure of the tri-nucleotide bound by each fold is almost identical and the overall structure of the two folds is very similar, the protein / DNA contacts for each fold are considerably different, and the OB fold-A makes much more extensive contact with the DNA than OB fold-B. This figure was taken from Bochkarev *et al.* (1997).

1.4 The DNA Damage Response

1.4.1 DNA Damage and Its Sources

Throughout evolution, DNA was chosen over RNA to carry the genetic information and to pass it on to the next generation most likely due to its relative stability. However, this does not mean that it is at all inert. On the contrary, the DNA is constantly exposed to damage either by spontaneous sources occurring during DNA metabolism or by exogenous sources originating from the environment (Friedberg *et al.*, 1995; Hoeijmakers, 2001). The DNA damaging agents that were used in this thesis to test the sensitivity of different yeast strains will be described in detail, whereas others will be only briefly mentioned.

1.4.1.1 Endogenous Damage

Endogenous DNA damage originates from the inner environment within cells as well as from the cellular metabolic processes (Friedberg *et al.*, 1995; Jackson and Loeb, 2001). The DNA can be depurinated by water, resulting in the formation of abasic sites, also know as apurinic / apyrimidinic (AP) sites, due to base loss (Jackson and Loeb, 2001). Deamination of DNA bases, and particularly deamination of cytosines, is an example for a spontaneous loss of functional groups. This can result in base transversion during replication (Jackson and Loeb, 2001). In addition, cellular metabolism of oxygen can give rise to reactive oxygen species, leading to oxidative base damage (Friedberg *et al.*, 1995). Also, base misincorporation by DNA polymerases during replication may lead to mutations (Jackson and Loeb, 2001).

1.4.1.2 Physical Sources of DNA Damage

Physical sources of DNA damage are ultraviolet (UV) light or ionising radiation (IR). UV is a component of the sunlight and can lead to the formation of covalent bonds between two adjacent pyrimidine bases, also known as *cis*, *syn* cyclobutane pyrimidine dimers (CPDs), or pyrimidine (6-4) pyrimidone photoproducts (PP), bulky lesions occurring on cytosine 3' to a pyrimidine base (Setlow, 1966; van Hoffen *et al.*, 1995). These lesions result in the distortion of

the dsDNA helix. The most commonly used form of UV light in biological research is the UVC wavelength (254 nm) (Friedberg *et al.*, 1995). Ionising radiation originating from either natural or man-made sources can cause various type of base damage. In addition, it can cause single-strand or double-strand breaks in the DNA (Veatch and Okada, 1969), which may be the most dangerous types of damage as potentially they can lead to discontinuity in the DNA (Branzei and Foiani, 2005).

1.4.1.3 Chemical Sources of DNA Damage

Exposure to DNA damaging agents can result in chemical alteration of the DNA. Alkylating agents, such as methyl-methane sulfonate (MMS), can covalently insert alkyl groups into DNA bases (Ludlum *et al.*, 1964). Unless repaired, this modification may interfere with DNA replication, as the pairing of the alkylated nucleotide with the correct nucleotide on the complementary strand is compromised (Hakem, 2008). Consequently, this may result in base misincorporation and DNA point mutations. Alternatively, alkylating agents, such as nitrogen mustards, but also other types of cross-linking agents, can catalyse protein-DNA cross-links, introduce monoadducts or cross-links into the same DNA strand (intrastrand cross-links) or covalently link two DNA strands (interstrand cross-links or ICLs) (Lawley *et al.*, 1969; McHugh *et al.*, 2001). The latter may prevent DNA unwinding necessary for replication and transcription. Other chemical agents, such as 4-nitroquinoline 1-oxide (4NQO), lead to bulky adducts in the DNA, inducing predominantly base substitutions or frame shift mutations during DNA replication (Ong *et al.*, 1975).

1.4.2 The DNA Damage Response throughout the Cell Cycle

DNA damage can interfere with the basic processes of DNA metabolism, such as DNA replication and transcription. Hence, DNA damage may have detrimental effects on cell proliferation and survival (Friedberg, 2003; Branzei and Foiani, 2008). In order to reverse or remove DNA damage and maintain their genomic stability, living organisms have developed an array of DNA repair mechanisms (Friedberg, 2003). In response to DNA damage, an orchested

action of sensors, transducers and effectors, employ the appropriate DNA repair pathway and coordinate this with ongoing cellular physiology (Harper and Elledge, 2007). These coordinated processes are termed the DNA damage response (DDR). Many forms of cancer are linked to defects in the DDR, delineating its importance in maintenance of genomic stability. Below, the different DNA repair mechanisms are briefly outlined and the contribution of RPA activity in each pathway is highlighted. The DNA damage response during DNA replication is the most relevant to this thesis. Therefore, a dedicated paragraph follows below (1.5).

The different mechanisms of DNA repair can be regarded as a set of tools, which cells can employ to deal with DNA damage. Which tool is used and when, depends on the type of the DNA lesion and on the cell cycle phase it is encountered (Branzei and Foiani, 2008).

1.4.2.1 Direct Damage Reversal

The direct reversal of DNA damage by lesion-specific enzymes is thought to be active throughout the cell cycle (Branzei and Foiani, 2008). Some types of base alkylation, such as the O^6 alkyl-adduct of guanine or methylation of adenine and cytosine (1-methyladenine and 3-methylcytosine) can be directly reversed by methyltransferases or DNA dioxygenases, respectively (Sedgwick *et al.*, 2007). In many organisms, excluding humans, CPDs or pyrimidine (6-4) pyrimidone PP, the major lesions produced by UV irradiation, can be reversed by photolyases, enzymes activated by blue light (de Lima-Bessa *et al.*, 2008; Goosen and Moolenaar, 2008).

1.4.2.2 Single-Strand Damage Repair (BER, NER, MMR)

Repair of single-strand damage can occur by the base excision repair (BER) or by the nucleotide excision repair (NER) pathways while the mismatch repair (MMR) pathway removes DNA mismatches. BER can replace single DNA bases that were damaged by oxidation, alkylation or deamination. In addition, it processes AP sites and single-stranded breaks (Wilson and Bohr, 2007). NER can replace several damaged bases and is responsible to deal with a large

variety of backbone distorting DNA lesions, induced by UV or mutagenic chemicals, including intrastrand or interstrand cross-links and bulky adducts (Prakash and Prakash, 2000). Both pathways proceed by recognition and excision of the damaged base(s) followed by DNA synthesis to fill in the ssDNA gaps (Prakash and Prakash, 2000; Wilson and Bohr, 2007). *In vitro* reconstitution of eukaryotic BER requires a minimum of four core enzymes (Wilson and Bohr, 2007), whereas for NER, more than 30 proteins are needed (Prakash and Prakash, 2000). Although both repair pathways operate throughout the cell cycle, NER is especially important during G1 phase when it contributes to the repair of lesions prior to DNA replication (Branzei and Foiani, 2008).

In BER, RPA was reported to interact with several DNA glycosylases, enzymes that initiate damaged-base recognition and cleavage (Fan and Wilson, 2005). This interaction is thought to mainly contribute to the long-patch BER sub-pathway, in which a longer repair tract is generated (2-13 bases) (Fortini *et al.*, 2003). In addition, RPA appears to be a negative regulator for the undesired cleavage of single-stranded AP sites by APE1 (apurinic / apyrimidinic endonuclease 1) (Fan *et al.*, 2006), the central AP endonuclease in mammalian cells, which coordinates most of the BER reactions (Fortini *et al.*, 2003). Both in yeast and mammalian cells, RPA plays a central role in the global genome NER sub-pathway. It contributes to lesion recognition via its ZnF (Stigger *et al.*, 1998) and through its association with Rad14 (or XPA in mammalian cells) (He *et al.*, 1995; Matsuda *et al.*, 1995). Following the bidirectional unwinding of the dsDNA at the site of the lesion by Rad3 and Rad25 helicases (or their respective human homologues, XPD and XPB) (Sung *et al.*, 1996), RPA stabilises the bubble structure that is formed. Human RPA is thought to recruit XPG (He *et al.*, 1995) and ERCC1/XPF nucleases (Matsunaga *et al.*, 1996) for the subsequent incisions (Davies *et al.*, 1995; Habraken *et al.*, 1995; Park *et al.*, 1995). Finally, RPA is required for the gap-filling step in coordination with RFC (replication factor C), PCNA (proliferating cell nuclear antigen) and DNA polymerase ε (or δ) (Aboussekhra *et al.*, 1995).

As previously mentioned, mismatch repair (MMR) does not deal with DNA damage per se, but rather recognises base substitutions or small insertions and deletions (IDLs). These mismatches are removed by excision and the ssDNA gaps are filled (Harfe and Jinks-Robertson, 2000; Kunkel and Erie, 2005). MMR acts predominantly during S phase to replace base mispairing during replication (Branzei and Foiani, 2008). In addition, MMR plays important roles in homologous recombination (Harfe and Jinks-Robertson, 2000) and in other DNA metabolic pathways (Li, 2008). RPA seems to be involved in all steps of MMR: it enhances the strand-specific excision, stabilises the ssDNA gap that is formed and facilitates re-synthesis of DNA (Ramilo *et al.*, 2002; Dzantiev *et al.*, 2004; Zhang *et al.*, 2005b). In addition, RPA phosphorylation may regulate the contribution of RPA to MMR (Guo *et al.*, 2006b). Unphosphorylated RPA stimulates the strand-specific cleavage more efficiently, whereas phosphorylated RPA facilitates MMR-associated DNA re-synthesis more effectively (Guo *et al.*, 2006b).

1.4.2.3 Double-Strand Break Repair (HRR, NHEJ)

The common feature of the BER, NER and MMR pathways is that, after removing the damage, they all use the genetic information from the undamaged DNA strand to complete the repair. However, what happens if both DNA strands are damaged? Double strand breaks result in the discontinuity of the DNA helix and thus are often regarded as the most cytotoxic types of DNA damage (Branzei and Foiani, 2008). They can be repaired by the homologous recombination repair (HRR) or by the non-homologous end joining (NHEJ) pathways (Barzel and Kupiec, 2008). While the former uses the genetic information of the homologous sister chromatids to repair the break and avoid mutations, the latter ligates the DNA ends in an error-prone manner. Non-homologous end joining is used mainly during G1 phase, whereas homologous recombination is principally important during S phase to mediate replication fork restart or during G2-M phase when sister chromatids are in close proximity and held by cohesion (Branzei and Foiani, 2008).

Processing of DSBs by homologous recombination involves the resection of the DNA ends exposing 3' ssDNA ends (Barzel and Kupiec, 2008). RPA is required for their protection and stabilisation preceding the binding of the Rad51 recombinase, which is needed for the strand invasion step. In yeast, Rad52 mediates the exchange between RPA and Rad51 on ssDNA, and both proteins have been reported to bind to RPA (Hays *et al.*, 1998; Stauffer and Chazin, 2004). *In vitro*, both yeast and human RPA have been reported to stimulate the yeast or human Rad52 protein, respectively, during the strand-annealing step (Sugiyama *et al.*, 1998; McIlwraith and West, 2008).

1.4.2.4 DNA Damage Bypass

In addition to DNA repair pathways, cells have DNA damage bypass mechanisms, which operate during S phase to ensure the completion of DNA replication, even in the presence of DNA damage (Branzei and Foiani, 2008). These include the break-induced replication (BIR) and the DNA damage tolerance pathways, which are described in detail below (see paragraphs 1.5.4 and 1.7). In brief, both pathways bypass DNA damage encountered during replication. The BIR pathway deals specifically with single-strand breaks while the DNA damage tolerance pathway can bypass various types of single-stranded lesions. The latter pathway can occur via one of two mechanisms: bypass of lesions via translesion synthesis (TLS), mediated by specialised DNA polymerases, or via damage avoidance (1.5.4.2 and 1.7).

1.4.2.5 Interstrand Cross-Link (ICL) Repair

If both DNA strands are cross-linked together, cells have to employ several pathways in a coordinated manner to repair the lesion and restore the ability to separate the DNA strands (McHugh *et al.*, 2001). Studies in yeast have revealed that the mechanism, by which ICLs are repaired, is cell cycle dependent. For example, if a replication fork meets an ICL during S phase, it may collapse (see 1.5.2), leading to the formation of a DSB. The DSBs that arise from such an encounter may be produced by the NER endonucleases or by additional overlapping endonucleases (McHugh *et al.*, 2000). The source of the DSBs can be either dual strand incisions or single-strand breaks that are

converted to DSBs during replication. The homologous recombination repair pathway can, in principle, repair these DSB intermediates. However, in stationary phase haploid yeast cells lacking homologous chromosomes, the processing of ICLs is different. Initial incisions on one strand by the NER proteins allow the cross-link region to become 'unhooked'. Polζ, a specialised lesion bypass (translesion) DNA polymerase (see 1.7.6), is suggested to fill in the exposed ssDNA gap (McHugh *et al.*, 2000). Subsequently, a second NER-mediated incision on the other strand can remove the cross-link, and the remaining nick is sealed. The evidence obtained from yeast cells in G1 phase is consistent with this model (Sarkar *et al.*, 2006). In addition, Polδ was suggested to act up-stream to Polζ, probably in attempt to fill in the gap. Subsequent PCNA mono-ubiquitylation was demonstrated to be required for Polζ recruitment for lesion bypass and repair of the ICLs (Sarkar *et al.*, 2006). In human cells, the repair pathways for ICLs are less understood, but it appears that they mainly occur in S phase (McHugh *et al.*, 2001) and involve a combination of NER, HRR and TLS (Wang, 2007). Consistently, studies with plasmids, either containing site-specific ICL or treated with cross-linking agents, suggest that ICLs repair and homologous recombination repair may be localised to the nuclear matrix in human cells (Atanassov *et al.*, 2005; Mladenov *et al.*, 2006).

1.5 Maintenance of Genomic Stability during Replication

DNA replication, the process by which the cell duplicates its genetic code, has to be accurate and highly processive, and occur only once per cell cycle (Branzei and Foiani, 2007). It is carried out by the replisome, a multi-enzyme-DNA complex (McGlynn and Lloyd, 2002). In brief, the core of the replisome contains two replicative DNA polymerases, ε and δ, which are responsible for the synthesis of the leading and the lagging strand, respectively (Baker and Bell, 1998). Together with accessory proteins, the sliding clamp PCNA and RFC, the sliding clamp-loader, they maintain their processivity (Baker and Bell, 1998). Ahead of the advancing polymerases, a hexameric helicase, MCM2-7 (minichromosome maintenance), unwinds the parental dsDNA. For the

discontinuous lagging strand synthesis, the DNA polymerase α-primase complex is responsible to synthesize the Okazaki fragments (Baker and Bell, 1998). In addition, replication fork progression is controlled by many other proteins that contribute to the stability of the forks and to problem solving, in case that they encounter roadblocks, such as DNA damage (Branzei and Foiani, 2005). The intimate link between DNA replication and repair can be derived from the crucial involvement of RPA and PCNA in both processes (Andreassen *et al.*, 2006).

1.5.1 Sensing DNA Damage during Replication

In order to sense DNA damage or replication stress, cells have evolved sensor proteins. These can activate checkpoint signalling networks that are responsible to decide whether to permit progression of the cell cycle or to arrest it, allowing DNA repair or apoptosis to take place (Shechter *et al.*, 2004). Activation of the checkpoint response by DNA damage leads to a cascade of phosphorylation events, mediated by two major kinases, ATM and ATR. These two proteins regulate two distinct but interconnected pathways, which consist of many feedback loops, and thus are not linear signalling pathways (Petrini and Stracker, 2003; Shechter *et al.*, 2004). The ATM kinase is mainly activated by DSBs, either generated by exogenous sources, such as IR or by intrinsic sources, such as recombination during meiosis (Kurz and Lees-Miller, 2004). The ATR kinase can be activated by a range of DNA damaging agents, UV, and also upon DNA replication stress caused by HU or aphidicolin. Additionally, ATR plays a role in maintaining the activation of the ATM pathway (Shechter *et al.*, 2004). *S. cerevisiae* has two genes *MEC1* and *TEL1* that encode proteins with homology to ATM. However, complementation studies indicated that ATR is the functional homologue of Mec1 protein whereas ATM seems to be functionally more similar to Tel1 protein (Bentley *et al.*, 1996), although the latter was found to be more restricted to functions related to telomere metabolism (Craven *et al.*, 2002). How is DNA damage sensed by the ATR pathway? One of the leading hypotheses suggests that a common DNA intermediate generated either directly by DNA damage or as a result of initial DNA damage processing, results in the activation of the ATR pathway

(Cimprich, 2007). This activation could be mediated through the binding of ATR itself or other component(s) of the pathway to that aberrant DNA structure. Recent studies proposed a common mechanism for checkpoint activation during S phase. Apparently, various types of DNA damaging agents cause the functional uncoupling of the DNA polymerase from the MCM helicase thus exposing ssDNA stretch which is quickly coated by RPA (Byun *et al.*, 2005). As ssDNA-bound RPA was shown to stimulate the recruitment of ATRIP-ATR *in vitro* (Zou and Elledge, 2003), this could provide, in principle, a mechanistic explanation for the activation of the kinase. In addition, the same authors have shown that this recruitment is conserved in yeast. Similarly, RPA and ATRIP are also required for the Rad17-dependent loading of the 9-1-1 complex onto a DNA template (Zou *et al.*, 2003). This complex, composed of the Rad9, Rad1 and Hus1 proteins, is a ring shape protein that resembles PCNA (the homologues in *S. cerevisiae* are named Rad9, Rad17 and Mec3, respectively). The clamp loader Rad17-Rfc2-5 (termed Rad24-Rfc2-5 in *S. cerevisiae*) actively loads it to sites of DNA damage, thereby facilitating ATR-mediated phosphorylation and the activation of the checkpoint (Parrilla-Castellar *et al.*, 2004). In addition, the 9-1-1 complex is suggested to play roles in DSB repair, translesion synthesis and up-regulation of gene expression in response to damage (Fu *et al.*, 2008).

1.5.2 Mechanisms of Replication Fork Stalling and Collapse

DNA replication is the moment in which the cell is most vulnerable to DNA damage as it might challenge the progression, stability or restart of replication forks through several mechanisms, as shown in Figure 1.5 (Branzei and Foiani, 2005; Lambert *et al.*, 2007). Firstly, certain types of DNA lesions encountered during S phase might lead to the uncoupling of the replisome and the helicase (Branzei and Foiani, 2005). Such lesions could be, for example, abasic sites, alkylated bases or bulky intrastrand adducts, which prevent the base pairing within the DNA polymerase, but allow the movement of the helicase (Byun *et al.*, 2005; Lambert and Carr, 2005). Furthermore, exposure to aphidicolin, an inhibitor of DNA polymerases, or to hydroxyurea, which causes nucleotides depletion by inhibition of ribonucleotide reductase, will lead to replication stress

by a similar uncoupling mechanism (Tercero and Diffley, 2001; Shechter *et al.*, 2004). As a consequence, ssDNA regions will be exposed, thereby activating the replication checkpoint via the ATR kinase (1.5.1).

Secondly, DNA damage on the leading strand can result in the uncoupling of its synthesis from that of the lagging strand (Branzei and Foiani, 2005). This may happen, for example, in case of ssDNA nick on the leading strand. During replication, this nick will be converted to a one-ended DSB, resulting in a discontinuity in the nascent strand (McHugh *et al.*, 2000; Aguilera and Gomez-Gonzalez, 2008). Uncoupling of strand synthesis will result in ssDNA exposure of the leading strand, and thus to the activation of the replication checkpoint (Branzei and Foiani, 2005). A nick, located on the lagging strand, may result in a similar but parallel scenario in which the uncoupling between the strands leads to ssDNA exposure on the lagging strand. Alternatively, uncoupling of strand synthesis may be avoided by re-priming of the replication fork downstream of the block (Aguilera and Gomez-Gonzalez, 2008).

Thirdly, interstrand or protein-DNA cross-links can block the helicase movement and inhibit DNA unwinding, thus preventing the progression of the replication fork (Branzei and Foiani, 2005). In this case, the whole replisome will be stalled, and the replication checkpoint will not be activated. However, ICLs do cause a cell cycle arrest, suggesting that fork processing is required for checkpoint activation.

By definition, a stalled fork is regarded as one where the replisome is still bound, whereas in a collapsed fork the replisome has already dissociated and no longer protects the nascent ends of the DNA (Lambert and Carr, 2005). Resumption of DNA replication from a stabilised stalled replication fork is termed fork restart. By a similar notion, re-association of the replisome with a collapsed fork is referred to as fork restart. The contribution of the replication checkpoint to replication fork stabilisation will be delineated in the next paragraph.

Figure 1.5 – Stalling of replication forks
(a) Replication forks encountering genomic pausing sites or lesions on the template may stall, accumulating checkpoint signals represented by long stretches of ssDNA coated by RPA that result from (b) uncoupling between the replisome and the replicative helicase or (c) uncoupling of leading and lagging strand synthesis; (d) checkpoint activation does not occur when the replication block prevents helicase progression. The red and blue circles indicate the leading and the lagging strand DNA polymerases, respectively; the green circle, the RPA complex; and the triangle, the helicase. This figure was taken from Branzei and Foiani (2005).

1.5.3 Stabilisation of Stalled Forks by the Replication Checkpoint

There are several lines of evidence implicating the ATR kinase in the regulation of DNA replication, some reviewed in Shechter *et al.* (2004). Firstly, in response to DNA damage or replication stress, ATR specifically inhibits late origin firing via modulations of the S phase kinases, Cdk2/Cyclin E and Cdc7/Dbf4. Secondly, ATR activation leads to p53 phosphorylation and thereby to inhibition of Cdk and PCNA functions via $p21^{waf1/cip1}$. Thirdly, the ATR kinase was suggested to phosphorylate the MCM helicase subunits, thereby inhibiting replication fork progression directly. Fourthly, activation of the ATR pathway outside of S phase is not robust (Ward *et al.*, 2004). And finally, as convincingly demonstrated in *S. cerevisiae*, under replication stress or damage conditions, Mec1 kinase phosphorylates its downstream target, Rad53 protein, and thereby protects replication forks from collapse (Lopes *et al.*, 2001; Tercero and Diffley, 2001). Additional phosphorylation targets in *S. cerevisiae* that were suggested to contribute to fork stabilisation are Mrc1, Csm3 and Tof1 proteins, which under normal conditions are considered to be non-essential components of the replisome (Branzei and Foiani, 2007; Lambert *et al.*, 2007). These processes are referred to as the DNA replication checkpoint.

Taken together, the replication checkpoint plays an important role in stabilisation of stalled replication forks by preventing the dissociation of the replisome (Lambert *et al.*, 2007). Hence, DNA replication can efficiently restart after the problem is resolved. However, under some circumstances the replisome may dissociate, leading to the collapse of the replication fork (Lambert *et al.*, 2007). In the latter case, forks converging from adjacent replicons may complete the replication (McGlynn and Lloyd, 2002). However, if the fork collapses in regions lacking converging forks, or if it is converted to a DSB, then recombination mechanisms may be needed to either protect the DNA ends or to actively restore replication (McGlynn and Lloyd, 2002; Lambert *et al.*, 2007).

1.5.4 Mechanisms of Replication Fork Restart

As explained in the previous paragraphs, both DNA damage and replication stress may cause stalling or collapsing of the replication fork, thus leading to DNA replication arrest (Shechter *et al.*, 2004). Unless this arrest is overcome and DNA replication is restarted and completed, the cell may die (McGlynn and Lloyd, 2002). As mentioned in paragraph 1.4.2.4, cells use DNA recombination as well as DNA damage tolerance mechanisms to coordinate the progression of DNA replication in the presence of damage (Branzei and Foiani, 2007). The Rad18 protein, which is the focus of this thesis, mediates the DNA damage tolerance mechanisms. These are briefly covered here (paragraph 1.5.4.2) and also described in depth in paragraph 1.7.

1.5.4.1 Recombination-Mediated Replication Restart

Replication-associated DNA breaks pose a significant challenge to the progression of replication forks and may result in fork collapse (Lambert *et al.*, 2007). As previously mentioned, if the replication fork encounters a single-strand break, it is converted to a one-ended DSB (McHugh *et al.*, 2000; Aguilera and Gomez-Gonzalez, 2008). Subsequently, DNA synthesis can be restarted by homologous recombination or by break-induced replication (BIR) (McEachern and Haber, 2006). It appears that there are at least two BIR sub-pathways in *S. cerevisiae*: one is Rad51-dependent and requires about 100 bp of homology whereas the other is Rad52- and Rad50-dependent and can occur with shorter regions of homology (McEachern and Haber, 2006). To date, three possible models were suggested for the mechanism of BIR. The common initiation of all three models involves a strand invasion step that creates a D-loop intermediate, which consists of a joint hetero-duplex DNA molecule. The first model suggests that DNA synthesis occurs via primer extension in parallel to the migration of the D-loop down the template. Subsequently, the newly synthesised single-strand can be filled in. The second model hypothesised that the D-loop is converted into a complete unidirectional replication fork that migrates until the end of the template chromosome. As a result, a single Holliday junction is formed which can be resolved by cleavage and re-ligation events resulting in a crossover dsDNA product. According to the third model, branch migration

enzymes act on the D-loop so that both leading and lagging strands are displaced at the same time, resulting in conservative DNA synthesis.

In general, recombination seems to predominantly act at collapsed forks rather than at stalled forks (Lambert *et al.*, 2007), although this observation may not apply to every organism. The rationale for this may be that it is preferential for the cell to overcome replication-associated damage by DNA damage tolerance mechanisms instead of by recombination.

1.5.4.2 DNA Damage Tolerance Mechanisms

DNA damage tolerance mechanisms, do not remove DNA lesions, but enable the restart of stalled replication forks and the completion of replication by damage bypass (Ulrich, 2005). As mentioned earlier, damage bypass can occur in two distinct ways. Specialised DNA translesion synthesis (TLS) polymerases, can replace the replicative polymerases to allow bypass of DNA lesions. Due to low fidelity of these polymerases, this process may be error-prone (Prakash *et al.*, 2005; Ulrich, 2005). Hence, although TLS promotes cell survival, it can lead to undesirable mutations. Alternatively, DNA damage can be avoided during replication in an error-free bypass as the newly synthesised sister chromatid serves as the new template for the continuation of replication (Ulrich, 2007; Yang and Woodgate, 2007). In eukaryotes, the *RAD6* pathway to which *RAD18* belongs, mediates both of the DNA damage tolerance mechanisms via protein ubiquitylation. Thus, before presenting the *RAD6* pathway in detail (1.7), a brief introduction of the ubiquitin system is provided (1.6).

1.6 The Ubiquitin System

Ubiquitin is a 76 amino acid protein, conserved in all eukaryotes, which serves as a post-translational modifier of proteins. Through its conjugation, the function, localisation and destiny of the target protein may be modulated or altered. The Rad18 protein is an E3 ubiquitin ligase, and Chapters 3 and 7 of my thesis deal with its catalytic activity. Therefore, the mechanism of ubiquitin conjugation, the different types of poly-ubiquitin chains and the consequences that protein ubiquitylation may have, are introduced below.

1.6.1 The Mechanism of Ubiquitin Conjugation

Ubiquitin conjugation occurs between the C-terminus of ubiquitin (glycine 76) and an ε-amino group of a lysine residue of a substrate via a sequential three-step mechanism (Pickart, 2001; Passmore and Barford, 2004). First, the ubiquitin is activated in an ATP-dependent manner by an E1 ubiquitin-activating enzyme. A cysteine in the catalytic domain of this enzyme forms a thioester bond with G76 of ubiquitin. Second, the thioester bond is transferred onto the active-site cysteine residue of an E2 ubiquitin-conjugating enzyme. Third, by the assistance of an E3 ubiquitin ligase enzyme, an isopeptide bond is formed between ubiquitin and a substrate lysine residue. If this cascade of events is repeated, a poly-ubiquitin chain can be formed, where the ubiquitn moieties are covalently linked to each other via one of the lysine residues of ubiquitin. In some occasions, this requires the activity of yet another enzyme, termed E4 (Hoppe, 2005).

Most organisms have only one E1 enzyme, which initiates all ubiquitylation reactions (Pickart, 2001). In its fully loaded state it carries two activated ubiquitin molecules, one as a thioester and the second as an adenylate intermediate. Usually, there are a few different E2 enzymes, which each cooperates with multiple E3s. The catalytic core of the E2 enzymes contains a conserved cysteine residue essential for their activity. The many E3 enzymes in each organism provide the specificity for the substrates. Currently, two principal types of E3s were identified, according to the nature of their catalytic domain: the HECT (homologous to E6-associated protein C-terminus) domain E3s and the RING domain E3s (Pickart, 2001; Passmore and Barford, 2004). As the Rad18 protein belongs to the latter class, the RING domain is the most relevant to this thesis. Its structure and characteristics were already described in detailed in paragraph 1.2.2.2. In short, the RING domain coordinates the binding of two zinc atoms forming a stable scaffold. The RING E3s are believed to bridge between the specific substrate and the E2 enzyme for subsequent ubiquitylation (Pickart, 2001).

1.6.2 Different Types of Ubiquitin Modifications

There are various types of ubiquitin modifications. If only one ubiquitin moiety is conjugated onto a specific lysine of a substrate, the substrate has become mono-ubiquitylated. Alternatively, a few lysines of the same substrate may be mono-ubiquitylated, and this is often regarded in the literature as multi-ubiquitylation. Importantly, ubiquitin has seven different lysine residues. Through them, it can also form poly-ubiquitin chains of variable length and linkage, resulting in protein poly-ubiquitylation (Passmore and Barford, 2004). The specificity of the poly-ubiquitin chain linkage is important as it confers a specific structure, and thereby can result in different outcomes for the modified protein (Passmore and Barford, 2004; Pickart and Fushman, 2004; Harper and Schulman, 2006).

1.6.3 Consequences of Ubiquitin Modifications

In accordance with the variety of ubiquitin modifications, their consequences can be very diverse. Moreover, the knowledge regarding their contribution to the regulation of cellular processes is continuously growing (Pickart and Fushman, 2004). Mono-ubiquitylation of proteins was reported to have different outcomes. For example, mono-ubiquitylation of some plasma membrane proteins has been implicated in their intracellular vesicle trafficking and re-localisation, while for others endocytosis is followed by their degradation in the lysosome (Pickart and Fushman, 2004; Ulrich, 2005). In addition, mono-ubiquitylation of histones was shown to regulate chromatin structure and influence transcription locally, whereas mono-ubiquitylation of DNA repair factors such as the Fanconi anemia FANCD2 protein or PCNA was found to modulate their protein-protein interactions and thereby their function (Wang, 2007) (see also 1.7.6).

Poly-ubiquitylation of proteins via lysine 48 of ubiquitin is largely involved in targeting proteins to degradation via the 26S proteasome (Ulrich, 2002; Pickart and Fushman, 2004). The implications of protein degradation range from the regulation of protein levels to the recycling of misfolded proteins (Ulrich, 2002). More relevant to this thesis are the K63-poly-ubiquitin chains, which were

reported to have a more extended structure compared to the K48-linked poly-ubiquitin chains (Varadan *et al.*, 2004). These non-canonical chains were shown to be involved in intracellular trafficking, in the inflammatory response, in ribosome biogenesis and in DNA damage bypass (Ulrich, 2005) (see also 1.7.7). Additional linkages of ubiquitin-ubiquitin chains exist, however their consequences are less understood (Pickart and Fushman, 2004). In addition to the structurally diverse ubiquitin chains that can be formed, each ubiquitin moiety has multiple protein-interaction surfaces (Harper and Schulman, 2006). These can be recognised by distinct downstream components that contain ubiquitin-binding domains, hence regulating protein-protein interactions and protein functions (see 1.7.6).

In addition to ubiquitin, there are ubiquitin-like modifiers, which have similar conjugation machineries but confer other consequences. The small ubiquitin-like modifier (SUMO) shares similar three-dimensional structure with ubiquitin (Geiss-Friedlander and Melchior, 2007). Protein sumoylation is thought to mainly modulate protein-protein interactions, and there is increasing evidence suggesting that the roles of sumoylation may be as diverse as ubiquitylation.

1.7 The *RAD6* Pathway

Historically, genetic screens for yeast strains sensitive toward UV irradiation resulted in the isolation of several mutants (Cox and Parry, 1968). Subsequently, these mutants were placed into three separate epistasis groups (Friedberg *et al.*, 1995). The *RAD3* group, which consists of genes responsible for the nucleotide excision repair; the *RAD52* group, whose members are involved in repair of DSBs by homologous recombination; and the *RAD6* group (Lawrence and Christensen, 1976) that consists of genes, which when mutated conferred also sensitivity to various chemical agents (Prakash, 1975).

In *S. cerevisiae*, the *RAD6* pathway was sub-divided into three epistasis groups according to their sensitivity and damage-induced mutagenesis (Ulrich, 2005). Both *RAD6* and *RAD18* genes control all three sub-pathways. The *RAD6* gene encodes a ubiquitin-conjugating enzyme (E2) and the *RAD18* gene encodes a

ubiquitin ligase enzyme (E3) (Jentsch *et al.*, 1987; Hoege *et al.*, 2002; Garg and Burgers, 2005). Two of the three sub-pathways contain genes encoding TLS polymerases. The first sub-pathway is an error-prone pathway involving *REV3*, *REV7* and *REV1* genes, encoding two subunits of DNA polymerase ζ (Polζ) and Rev1, respectively (Ulrich, 2005). When these genes are mutated, DNA damage-induced mutation rates are reduced. The second sub-pathway is an error-free pathway involving *RAD30*, which encodes DNA polymerase η (Polη), a fairly accurate polymerase for bypass of CPD lesions induced by UV (Johnson *et al.*, 1999; Washington *et al.*, 2000). The third sub-pathway is damage avoidance (DA), which bypasses DNA damage in an error-free mechanism. It contains the *RAD5*, *UBC13* and *MMS2* genes, encoding a ubiquitin ligase enzyme (E3) and two ubiquitin conjugating enzymes (E2s), which act together as a hetero-dimer (Ulrich and Jentsch, 2000; Torres-Ramos *et al.*, 2002; Ulrich, 2005). The epistatic hierarchy of the *RAD6* pathway is illustrated in Figure 1.6, and a summary of the biochemical activities of the proteins, involved in this pathway, is shown in Table 1-2.

In 2002, the proliferating cell nuclear antigen (PCNA) from *S. cerevisiae*, an essential processivity factor for DNA polymerases, was identified as a substrate for the *RAD6* pathway (Hoege *et al.*, 2002). In response to DNA damage, members of the *RAD6* pathway attach either mono-ubiquitin or poly-ubiquitin chain on PCNA (Hoege *et al.*, 2002; Stelter and Ulrich, 2003; Kannouche *et al.*, 2004). These modifications were found to serve as a molecular switch to decide between the TLS or DA sub-pathways.

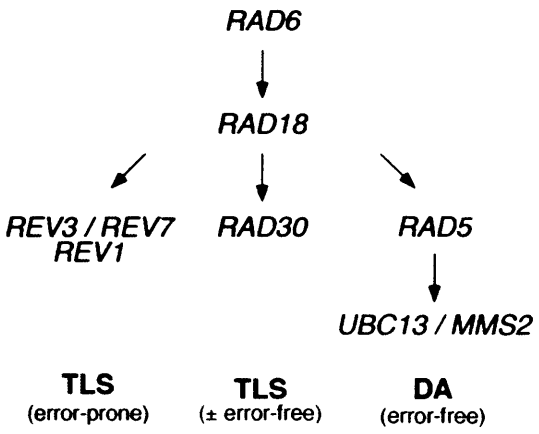

Figure 1.6 – The *RAD6* pathway in *S. cerevisiae*
Arrows indicate the genetic relationships between the members of the *RAD6* pathway, as determined from the sensitivities of the respective mutants towards DNA-damaging agents. Two pathways of translesion synthesis (TLS), mediated by different damage-tolerant DNA polymerases, act independently of the error-free damage-avoidance (DA) system. This figure was taken from Ulrich (2005).

Table 1-2

Table 1-2: Members of the *RAD6* pathway in *S. cerevisiae*
Abbreviations used: TLS – translesion synthesis (error-prone); DA – damage avoidance (error-free); PCNA – proliferating cell nuclear antigen. This table was taken from Ulrich (2005).

1.7.1 Consequences of PCNA Modifications

In *S. cerevisiae*, the *POL30* gene encodes PCNA (Moldovan *et al.*, 2007). PCNA belongs to the DNA sliding clamp family and is essential for DNA replication. It is a homo-trimer with a ring-like structure, which encircles the DNA and is able to slide on it freely. Each PCNA monomer consists of two globular domains linked by an interdomain connecting loop. The three monomers bind to each other in a head-to-tail arrangement, with an inner surface composed of positively charged α-helices and an outer surface composed of β-sheets. Thus, the PCNA ring has a pseudo-hexameric symmetry. Its stable association with the DNA requires an ATP-dependent loading by the clamp loader, RFC, which specifically loads PCNA onto 3' ssDNA-dsDNA junctions. Until now, more than 50 proteins were reported to interact with PCNA. Most of them do so via a conserved motif, termed PCNA interacting peptide (PIP), which contacts the interdomain loop on PCNA. Although this implies a competition between many PCNA interacting partners, it is theoretically possible that different proteins can bind to PCNA simultaneously, via its three identical monomers

In *S. cerevisiae*, PCNA is either mono-ubiquitylated or poly-ubiquitylated in response to DNA damage by the *RAD6* pathway (Hoege *et al.*, 2002). These modifications occur on a specific lysine, K164, which is conserved in all eukaryotes. The latter modification was shown to be K63-linked poly-ubiquitin chain, and according to genetic analysis it is implicated in rescue from damage sensitivity via the error-free *RAD6* sub-pathway (Hoege *et al.*, 2002). The former modification was demonstrated to be physiologically relevant and to mediate the translesion synthesis sub-pathways (Stelter and Ulrich, 2003). This was also confirmed biochemically, when mono-ubiquitylated PCNA was reported to stimulate both Polη and Rev1 bypass of abasic sites (Garg and Burgers, 2005). PCNA ubiquitylation is conserved in higher eukaryotes and mammalian Polη was discovered to have enhanced affinity toward mono-ubiquitylated PCNA (Kannouche *et al.*, 2004; Watanabe *et al.*, 2004). In mammalian cells, PCNA mono-ubiquitylation can be reversed by the de-conjugating activity of Usp1 (Huang *et al.*, 2006). In yeast, although de-ubiquitylation of PCNA is clearly observed (Papouli *et al.*, 2005), no specific

isopeptidase has been identified up to date. Although mono-ubiquitylation of PCNA seems to be the predominant modification in mammalian cells, poly-ubiquitylated PCNA was recently detected as well (Motegi *et al.*, 2006; Unk *et al.*, 2008). It has yet to be determined what are the up-stream signals that choose which PCNA modification will occur, and hence which DNA damage tolerance pathway will be activated. Nevertheless, PCNA ubiquitylation provide a tight regulation to limit the DNA damage tolerance mechanisms to situations when they are needed, such as the restart of a stalled replication fork, and to maintain the correct balance between cell survival and genomic stability (Ulrich, 2007).

In *S. cerevisiae*, PCNA was found to be sumoylated in an S phase dependent manner by the E2 SUMO-conjugating enzyme, Ubc9, and its E3 SUMO ligase partner Siz1 (Hoege *et al.*, 2002; Stelter and Ulrich, 2003). Interestingly, the same residue that was targeted for ubiquitylation, K164, was shown to be sumoylated (Hoege *et al.*, 2002). Additionally, another residue K127, which is located on the interdomain loop of PCNA within a sumoylation conserved motif, was demonstrated to be sumoylated, but to a lesser extent. In contrast to initial beliefs, conjugation of SUMO-SUMO chains was also observed on PCNA (Windecker and Ulrich, 2008). Furthermore, although both SUMO and ubiquitin target the same residue on PCNA, no competition between these modifications was observed (Papouli *et al.*, 2005). PCNA sumoylation was shown to recruit the DNA helicase Srs2 to replication forks during S phase (Papouli *et al.*, 2005; Pfander *et al.*, 2005). This helicase was demonstrated to inhibit Rad51 filament formation *in vitro* (Krejci *et al.*, 2003). Therefore, Srs2 recruitment is suggested to inhibit unscheduled Rad51-dependent recombination events, thereby allowing the DNA damage tolerance mechanisms to take place instead. These findings provided an explanation for the genetic interaction between Srs2 and members of the *RAD6* pathway, as deletion of the *SRS2* gene suppressed the DNA damage sensitivity of the *RAD6* pathway mutants in a *RAD52*-/RAD51-dependent manner (Papouli *et al.*, 2005; Pfander *et al.*, 2005). So far, PCNA sumoylation seems to be limited to budding yeast and frog (Leach and Michael, 2005). In Figure 1.7 the different modification of yeast PCNA and their consequences for DNA damage tolerance and recombination are shown.

Figure 1.7 – Coordination of replication and DNA damage tolerance by PCNA modifications
The scheme shows how the modified forms of PCNA elicit distinct transactions at a replication fork. Whereas unmodified PCNA (ring symbol) acts as a processivity factor for replicative polymerases (Polδ), DNA-damaging agents cause lesions (red star symbols) that block the progression of DNA replication. In response to replication fork stalling, PCNA is mono-ubiquitylated and poly-ubiquitylated at K164. Mono-ubiquitylation activates translesion synthesis by a damage-tolerant polymerase (Polη), whereas poly-ubiquitylation, involving K63 linkage, is a pre-requisite for an error-free damage avoidance pathway. Independent of DNA damage, PCNA is sumoylated during S phase at K164 and to a minor extent at K127, leading to the recruitment of the helicase Srs2 to the site of replication. Srs2 inhibits the formation of the recombinogenic Rad51 filament, thereby facilitating ubiquitin-dependent DNA damage tolerance upon replication fork stalling. This figure was taken from Ulrich (2005b).

1.7.2 The Rad6 Protein

The *RAD6* gene from *S. cerevisiae* encodes yRad6, an E2 ubiquitin-conjugating enzyme of 19.7 kDa (Jentsch *et al.*, 1987). It contains a catalytically conserved cysteine residue, cysteine 88, which when mutated to alanine, results in a *rad6* deletion phenotype (Sung *et al.*, 1990). This phenotype includes sensitivity to UV irradiation (Cox and Parry, 1968) as well as to other DNA damaging agents (Prakash, 1975), an increase in spontaneous mutagenesis rates and loss of UV-induced mutagenesis (Lawrence and Christensen, 1976; Lawrence, 2007). The yRad6 protein was found to interact genetically and biochemically with yRad18, an E3 ubiquitin ligase, and together mediate the DNA damage tolerance mechanisms via PCNA ubiquitylation (Cassier-Chauvat and Fabre, 1991; Bailly *et al.*, 1997a; Bailly *et al.*, 1997b; Hoege *et al.*, 2002). Their interaction is mediated via two amphipathic α-helices on yRad6 (Bailly *et al.*, 1997b). Based on sequence conservation, two human homologues of the yeast *RAD6* gene have been identified, *HHR6A* and *HHR6B* (Koken *et al.*, 1991). Both were able to complement the DNA damage sensitivity of the *rad6* deletion yeast strain, suggesting that they may be functionally redundant to each other (Koken *et al.*, 1991). In addition, their activity with regard to hRad18 binding and to the activation of the DNA damage tolerance mechanisms was found to be conserved (Xin *et al.*, 2000).

The yRad6 protein interacts with two more E3 ubiquitin ligase enzymes, Bre1 and Ubr1, with which it is involved in a number of other processes unrelated to DNA damage tolerance. These include histone H2B ubiquitylation, sporulation, telomere silencing, and protein degradation via the N-end rule (Broomfield *et al.*, 2001).

1.7.3 The Rad18 Protein

The *RAD18* gene from *S. cerevisiae* was isolated by complementation of the UV sensitivity of *rad18* mutants, and was reported to encode a protein of 55.2 kDa (Jones *et al.*, 1988; Fabre *et al.*, 1989). The *rad18* deletion strain was found to have a similar defect in UV-induced mutagenesis as the *rad6* mutant (Cassier-Chauvat and Fabre, 1991), suggesting that *RAD18* and *RAD6* genes

are epistatic to each other. Later on, their physical interaction was demonstrated by co-immunoprecipitation experiments (Bailly *et al.*, 1994) and by biochemical analysis of truncated constructs (Bailly *et al.*, 1997b). A region between amino acid 371 and 410 of yRad18 was found to be sufficient for its interaction with the E2 (Bailly *et al.*, 1997b). In 1997, the yRad18 protein was purified as a hetero-dimer with yRad6 from yeast cells harbouring an over-expression cassette for both genes (Bailly *et al.*, 1997a). The complex was found to have ubiquitin conjugating and ATP hydrolytic activities. The latter activity was thought to originate from a Walker type A motif 'GKS' found in yRad18. However, it was considerably weaker in comparison to other known ATPases and may not be an intrinsic activity of yRad18 (Parker and Ulrich – unpublished results). In addition, the complex was able to bind to DNA with preference to ssDNA over dsDNA. As the Rad6 protein does not contain any DNA-binding domains and cannot bind DNA on its own (Bailly *et al.*, 1994), the authors hypothesised that the DNA-binding activity originates from the Rad18 protein. Furthermore, they speculated that Rad18 recruits Rad6 to DNA damage sites, and thereby mediate DNA damage tolerance. Consistently, yRad18 contains three putative DNA-binding domains: a RING domain, which is essential for its ubiquitin ligase activity (aa 28 – 65), a classical ZnF motif (aa 188 – 210) with homology to the UBZ domain of Polη (Bienko *et al.*, 2005), and a SAP domain (aa 278 – 312). A schematic representation of the structural domains of yRad18 is shown in Figure 1.8.

In accordance with genetic evidence, yRad18 and yRad5 proteins were found to interact with each other and to self-associate (Ulrich and Jentsch, 2000). A few years later, PCNA was identified as the substrate for yRad18-yRad6 – mediated ubiquitylation by genetic analysis and immunoprecipitation assays from MMS treated yeast cells (Hoege *et al.*, 2002). Consistently, yRad18 and PCNA have been shown to interact by two-hybrid analysis. In addition, yRad18 was found to interact with yUbc9, the E2-like enzyme responsible for PCNA sumoylation, suggesting crosstalk between PCNA modifications in yeast.

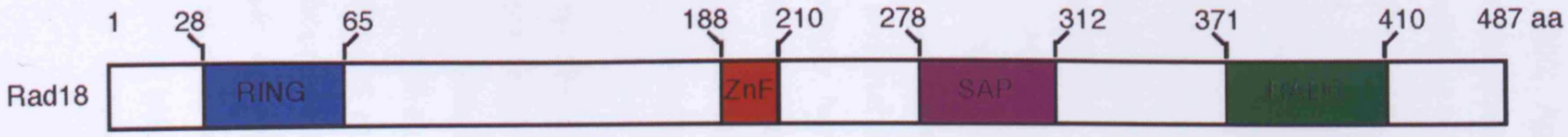

Figure 1.8 – Schematic representation of yRad18 structural domains
Rad18 from *S. cerevisiae* harbours a RING domain (aa 28-65), with C3HC4 structure, a ZnF (aa 188-210), with C2H2 structure, a SAP domain (aa 278-312) and a region sufficient for Rad6 binding (aa 371-410).

Based on sequence homology, the human *RAD18* gene was cloned (Tateishi *et al.*, 2000; Xin *et al.*, 2000). Apart from lacking the Walker type A motif, it was found to harbour homologous structural domains to its yeast counterpart. It bound to either hRad6A or hRad6B proteins (Tateishi *et al.*, 2000; Xin *et al.*, 2000) and together they were able to ubiquitylate PCNA *in vitro* (Watanabe *et al.*, 2004). However, hRad18 did not complement the *rad18* deletion yeast strain with regard to its sensitivity toward DNA damage.

Recently, two publications have provided evidence regarding its DNA-binding properties. According to Notenboom *et al.* (2007), hRad18 showed preference toward ssDNA over dsDNA, but still could bind to both DNA structures. Moreover, the SAP domain of hRad18 was found to be sufficient for these interactions. Consistently, Tsuji *et al.* (2008) found that long ssDNA oligonucleotides, but also forked DNA structures, were the preferred substrate for hRad18 binding, and that the SAP domain was essential for its interaction with the DNA. Accordingly, human Rad18 was suggested to be able to bind to stalled replication forks. In agreement with these *in vitro* results, Nakajima *et al.* (2006) demonstrated that in human cells, the SAP domain of Rad18 contributes to its localisation to stalled replication forks along with Polη.

The contribution of the classical ZnF motif of hRad18 for DNA-binding is still controversial. Nakajima *et al.* (2006) found this domain is important for the formation of replication-independent damage-induced foci in human cells, suggesting that it may contribute to DNA-binding. However, Notenboom *et al.* (2007) reported that the ZnF domain of hRad18 was not able to bind to DNA by itself, but instead it bound to ubiquitin. Hence, the authours suggested that it functions as an ubiquitin-binding domain rather than a DNA-binding domain. In agreement with this latter publication, Bish and Myers (2007) showed that a ZnF construct of human Rad18 binds to K48-linked-poly-ubiquitin chains *in vitro* and reported its homology to ubiquitin-binding domains (type UBZ) from other proteins.

1.7.4 The Rad5 Protein

The *RAD5* gene encodes yRad5, a 134 kDa protein, with homology to helicases and chromatin remodelling factors of the SWI2 / SNF2 family (Johnson *et al.*, 1992). In addition to the seven helicase-like domains it contains a Walker B type ATPase motif, a C3HC4 RING domain and a leucine zipper motif (Johnson *et al.*, 1992; Ulrich and Jentsch, 2000). Furthermore, its N-terminus consists of an HIRAN (HIP116 & Rad5 protein N-terminal) domain, predicted to be a DNA-binding domain (Iyer *et al.*, 2006).

The yRad5 protein was shown to physically interact with yRad18 and yUbc13 proteins (Ulrich and Jentsch, 2000; Ulrich, 2003). Through these interactions, it was suggested to mediate the association of the yRad18-yRad6 and the yUbc13-yMms2 hetero-dimers on damaged chromatin and coordinate their activity (Ulrich and Jentsch, 2000). Accordingly, yRad5 was found to interact with PCNA and regulate its poly-ubiquitylation in a RING-dependent E3 ligase manner (Hoege *et al.*, 2002). The yRad5 protein has an ssDNA-dependent ATPase activity (Johnson *et al.*, 1994). This was demonstrated to be important for a MRX (Mre11, Rad50 and Xrs2) complex-mediated DSB repair (Chen *et al.*, 2005). In correlation with its *in vitro* ssDNA-binding (Johnson *et al.*, 1994), it was shown to bind to 3'-resected ssDNA ends following a site-directed DSB *in vivo* (Chen *et al.*, 2005). Recently, it was shown that the ATPase activity of yRad5 is stimulated by a range of DNA structures (Blastyak *et al.*, 2007). In addition, yRad5 was able to specifically unwind a replication fork-like structure with homologous arms *in vitro*, suggesting that it could be implicated in replication fork reversal *in vivo*, and thus facilitate the DNA damage avoidance pathway (Blastyak *et al.*, 2007).

Due to lack of sequence homology in higher eukaryotes, it was not clear whether a *RAD5* yeast homologue existed. Recently, two functional homologues were identified in humans, SHPRH (the protein name originates from the initials of the domains it contains: SNF2, (linker-) Histone, PHD finger, RING domain and Helicase domain) and HLTF (helicase-like transcription factor), and their importance in PCNA poly-ubiquitylation was demonstrated (Motegi *et al.*, 2006; Unk *et al.*, 2008).

1.7.5 The Ubc13 and Mms2 Proteins

The *UBC13* gene encodes yUbc13, an E2 ubiquitin-conjugating protein (Brusky *et al.*, 2000). The *MMS2* gene encodes yMms2, an evolutionary related E2 enzyme that lacks an active cysteine residue in its catalytic domain (Broomfield *et al.*, 1998). Both genes were found to be components of the error-free sub-pathway of the *RAD6* pathway (Brusky *et al.*, 2000). Together, yUbc13 and yMms2 form a complex that promotes the assembly of K63-linked ubiquitin chains *in vitro*, which were also shown to be required for the error-free DA sub-pathway (Hofmann and Pickart, 1999). As mentioned before, the yeast Ubc13-Mms2 hetero-dimer associates with chromatin in response to DNA damage and co-localises with yRad5 (Ulrich and Jentsch, 2000). In addition, its ability to form K63-linked ubiquitin chains *in vitro* is stimulated by Rad5 (Parker and Ulrich – unpublished results). Mammalian homologues were identified by sequence similarity and their enzymatic activity was shown to be conserved (Franko *et al.*, 2001; McKenna *et al.*, 2001; Ashley *et al.*, 2002).

1.7.6 DNA Translesion Synthesis

Replication-blocking lesions may be overcome by the DNA synthesis activity of DNA translesion synthesis (TLS) polymerases (Ulrich, 2004). The active site of these specialised polymerases can accommodate damaged bases, as it is more open than the active site of replicative polymerases, which have sterical constraints for the correct structure of a Watson-Crick base pair (Yang and Woodgate, 2007). Therefore, this enables them to replicate over DNA lesions. However, the nature of their active sites, combined with the lack of proofreading activity, results in reduced fidelity of the TLS polymerases. In fact, due to their error-prone activity, the TLS polymerases are considered the major contributors to damage-induced mutagenesis (Ulrich, 2004). Hence, their activity must be highly regulated, and their reduced processivity results in their ability to incorporate only a few nucleotides at a time before dissociating from the DNA (Yang and Woodgate, 2007).

Most of the TLS polymerases, relevant to the *RAD6* pathway, belong to the Y-family of polymerases (Ohmori *et al.*, 2001). They differ from each other in the

accuracy by which they process different lesions (Prakash *et al.*, 2005). In addition to palm, thumb and finger domains found in all classical polymerases, the Y-family have a forth domain termed the 'little finger' or PAD (polymerase-associated domain) (Yang and Woodgate, 2007). In yeast there are two Y-family enzymes, which are also found in humans. Polη, encoded by the *RAD30* gene (or *POLH* in humans), can bypass UV-induced lesions with great accuracy (Johnson *et al.*, 1999; Washington *et al.*, 2000). Mutations in this gene may lead to the Xeroderma Pigmentosum Variant (XPV) syndrome (Lehmann, 2006b). This disease illustrates the importance of Polη in maintenance of genomic stability in humans, as XPV patients suffer from high predisposition to skin cancer. Rev1 protein, encoded by the *REV1* gene (or *REV1L* in humans), is a deoxycytidyl transferase, which incorporates a dC across a lesion (Nelson *et al.*, 1996). Normally Rev1 cooperates with Polζ in lesion bypass (see below). In mammalian cells there are two additional Y-family TLS polymerases: Polκ and Polι. The former is efficient in bypass of benzo[*a*]pyrene-guanine adducts (Ogi *et al.*, 2002). The latter was found to associate with damage induced PCNA foci (Kakar *et al.*, 2008), similar to the other Y-family TLS polymerases (Kannouche *et al.*, 2004; Watanabe *et al.*, 2004; Guo *et al.*, 2006a; Guo *et al.*, 2008).

Both in yeast and humans, Polζ, encoded by the *REV3* and *REV7* genes, belongs to the B-family of polymerases and therefore resembles to the replicative polymerases (Prakash *et al.*, 2005). It is not so efficient in lesion bypass, but instead it harbours the ability to extend the primer termini beyond a DNA lesion. Thus, the current view is that many lesions may require the activity of two TLS polymerases, one to incorporate a nucleotide opposite a lesion, and the second one (Polζ) to perform the subsequent extension step (Prakash *et al.*, 2005).

As mentioned earlier, in response to DNA damage, PCNA is mono-ubiquitylated in a Rad18-Rad6-dependent manner both in yeast and in mammalian cells (Hoege *et al.*, 2002; Kannouche *et al.*, 2004; Watanabe *et al.*, 2004), and this modification was shown to activate translesion DNA synthesis in yeast by genetic analysis (Stelter and Ulrich, 2003). But how can this modification induce the polymerase switch from the replicative polymerases to the translesion

synthesis ones? Human Polη, Polι and Polκ were demonstrated to physically interact with PCNA *in vitro* via their PIP domain, however their interactions may be weak (Lehmann, 2006b). Yeast and mammalian Rev1 was demonstrated to interact with PCNA via its BRCT domains (Guo *et al.*, 2006a). In addition, human Polη was shown to preferentially interact with mono-ubiquitylated PCNA (Kannouche *et al.*, 2004; Watanabe *et al.*, 2004). Interestingly, all of these translesion polymerases contain ubiquitin-binding domains, which can potentially confer enhanced affinity of the polymerase to mono-ubiquitynated PCNA (Bienko *et al.*, 2005; Lehmann, 2006b). This hypothesis was verified with yeast Polη (Parker *et al.*, 2007), yeast and vertebrate Rev1 (Guo *et al.*, 2006a; Wood *et al.*, 2007) and verterbrate Polκ (Guo *et al.*, 2008). Furthermore, as mentioned before, both Polη and Rev1 were stimulated for abasic site bypass by mono-ubiquitylated PCNA *in vitro* (Garg and Burgers, 2005).

Currently, there are different models for the mechanistic aspects of the polymerase switch. On the one hand, mono-ubiquitylated PCNA can actively recruit TLS polymerases by their enhanced interaction (Ulrich, 2004). On the other hand, this modification may disrupt the binding of the replicative polymerases and facilitate the access for the TLS ones in a passive mode (Ulrich, 2004). Alternatively, PCNA modification may just switch between 'on' and 'off' modes of DNA polymerases, which are already associated with PCNA, in a manner referred to as the 'Tool belt' model (Pages and Fuchs, 2002).

In addition to their role in replication restart, which is restricted to S phase, TLS polymerases may have additional roles. As mentioned earlier (1.4.2.5), Polζ activity, induced by PCNA ubiquitylation, was demonstrated to be involved in ICL repair in G1 phase, suggesting a more general role of PCNA modification depending on the lesion encountered (Sarkar *et al.*, 2006). Moreover, Polη was shown to participate in somatic hyper-mutation and / or class switching in the immune system as well as in homologous recombination, while Polκ was shown to be involved in the filling-in steps of NER (Lehmann, 2006a).

1.7.7 DNA Damage Avoidance

As mentioned before, the DNA damage avoidance (DA) is an error-free bypass of DNA damage (Ulrich, 2005). Although the mechanism by which it operates is not entirely understood, it is believed to occur in situations when the synthesis between the leading and the lagging strand is uncoupled (Branzei and Foiani, 2007). As the synthesis on one of the strands continues, the synthesis on the other strand can be resumed as well if a template-switch occurs, and the newly synthesised sister chromatid strand is used for bypassing the lesion (Ulrich, 2005). This is supported by genetic experiments with plasmids containing single-stranded specific lesions, which demonstrated a Rad52-independent gene conversion event (Zhang and Lawrence, 2005a). One of the models suggests that the template switch involves the regression of the replication fork, forming a chicken foot-like structure, in which the two nascent DNA strands are paired (Ulrich, 2007). Recently, *in vitro* evidence was obtained in support of this model. Firstly, yeast Rad5 was shown to have a structure-specific helicase activity toward replication fork-like structure, suggesting that it could be involved in replication fork regression *in vivo* (Blastyak *et al.*, 2007). Secondly, a chicken foot-like structure was observed in checkpoint deficient cells by electron microscopy studies (Sogo *et al.*, 2002). Although, in principle, this observation supports the formation of this DNA structure, Muzi-Falconi *et al.* (2003) argues that it may only occur under pathological conditions.

As previously mentioned, the signal for the activation of the DNA damage avoidance is the conjugation of a K63-linked poly-ubiquitin chain on K164 of PCNA. Apparently, this is a two-step reaction (Parker and Ulrich – unpublished results). First, PCNA is mono-ubiquitylated by Rad6-Rad18 in a rate-limiting step. Subsequently, Rad5 together with Mms2 and Ubc13 mediate PCNA poly-ubiquitylation. However, whether the ubiquitin moieties are added in a sequential mode or an entire pre-formed chain is conjugated, is not entirely clear. The mechanism by which PCNA poly-ubiquitylation promotes DNA damage avoidance has yet to be discovered. However, speculative models suggest that it is either important for the recruitment of essential factors, similar to the way PCNA mono-ubiquitylation promotes TLS, or for the dissociation of others (Moldovan *et al.*, 2007).

1.7.8 The Timing of the DNA Damage Tolerance Mechanisms

Historically, post-replicative repair was defined as the activity that cells use to fill in damage-induced single-stranded gaps without removal of the DNA lesions (Broomfield *et al.*, 2001). This definition originated from the observation that the newly synthesised DNA from UV-irradiated *E. coli* strain deficient in NER had a lower molecular weight than that of the untreated controls (Rupp and Howard-Flanders, 1968). This observation was explained by the existence of ssDNA gaps opposed to UV-induced lesions. As further incubation of the DNA with the irradiated cells resulted eventually in its conversion into a higher molecular weight, the ssDNA gaps seemed to be filled in after the completion of replication. Thus, this model suggested that the damage is repaired 'behind' the replication fork (Lehmann and Fuchs, 2006).

Following the discovery of TLS polymerases, the assumption that such ssDNA gaps could be left within the leading strand was disfavoured. An alternative model suggested that these gaps were bypassed at the replication fork by a polymerase switch model (Lehmann and Fuchs, 2006) (see 1.7.6). In contrast, the possibility that ssDNA could be left on the lagging strand, which in its nature is discontinuous, was accepted. However, recent evidence obtained by electron microscopy experiments with *S. cerevisiae* NER deficient UV-irradiated cells, suggests that ssDNA regions can form behind the replication fork on both strands (Lopes *et al.*, 2006). This finding holds true also in NER and TLS double mutants. In addition, 2D-gels revealed that replication forks are able to progress in the presence of UV-induced lesions, even in the TLS-deficient strains. These findings suggest that the ssDNA gaps are left behind the fork to be dealt with later (Lopes *et al.*, 2006). Consequently, this publication raised the awareness of the initial model, and controversy regarding the tempo-spatial characteristics of the DNA damage tolerance mechanism, still persists in the field (Lehmann and Fuchs, 2006).

1.8 Aims of this Thesis

In this thesis, I present my studies of the Rad18-Rad6 complex from *S. cerevisiae* and the analysis of its activity *in vitro*. Recent findings in my lab revealed the up-stream signals leading to the activation of DNA damage tolerance *in vivo* (Davies *et al.*, 2008). RPA was implicated in PCNA ubiquitylation and Rad18 was found to be a limiting factor for this modification of the clamp. Consequently, my aims were to gain further insights into the molecular mechanism of these up-stream events. To this end, I have investigated the relationships between the Rad18-Rad6 complex, RPA and DNA.

Chapter 3 describes the purification process of the Rad18-Rad6 complex and the analysis of its catalytic activity. PCNA ubiquitylation is reconstituted *in vitro* and Rad18 is found to be auto-ubiquitylated. Rad18 ubiquitylation is observed also *in vivo*, both in yeast cells and in recombinant baculovirus infected insect cells. Chapter 4 describes the interactions between the Rad18-Rad6 complex and DNA. These interactions are mediated directly via Rad18, whereas Rad6 cannot bind to the DNA on its own. The effects of salt concentration, salt type and different DNA structures are analysed. Chapter 5 describes the interactions between the Rad18-Rad6 complex and RPA. The E3-E2 complex binds directly and independently to Rfa2 or to the DNA-binding domain of Rfa1. Chapter 6 describes the interactions between the Rad18-Rad6 complex, RPA and ssDNA. The interaction between the DNA-binding domain of Rfa1 and Rad18 is stimulated in the presence of ssDNA. Under conditions of high ionic strength, RPA recruits the Rad18-Rad6 complex to ssDNA. Finally, in Chapter 7, the role of the SAP domain of yeast Rad18 is analysed *in vivo* and *in vitro*.

2 Materials and Methods

2.1 Enzymes and Reagents

2.1.1 Enzymes and Proteins

Table 2-1

Enzyme	Source
Zymolyase (20T)	**AMS Biotechnology**
Ubiquitin activating enzyme (yeast E1) and ubiquitin mutants	**BostonBiochem**
Restriction enzymes, T4 polynucleotide kinase and Terminal transferase	**New England Biolabs (NEB)**
Benzonase	**Novagen**
Single-stranded DNA-binding protein (SSB)	**Promega**
Recombinant His-tagged ubiquitin (human)	**Sigma**
Recombinant ubiquitin (yeast)	Generated in the lab

Table 2-1: A list of the enzymes that were used.

2.1.2 Antibodies

Table 2-2

Monoclonal Antibody	Source	Dilution used
anti-ubiquitin (P4D1)	**Cell Signalling Technology**	1:5000
anti-yeast 3-phosphoglycerate kinase (PGK)	**Molecular Probes**	1:10,000
anti-VSV-G	**Roche**	1:3000
anti-GST (B-14)	**Santa Cruz Biotechnology**	1:3000
anti-His (clone HIS-1)	**Sigma**	1:3000
anti-PCNA (5E6, 3B9, 4A10)	Generated by CR-UK	1:3000 of each

Table 2-2: A list of the primary monoclonal antibodies that were used.

Table 2-3

Polyclonal Antibody	Source	Dilution used
anti-ubiquitin	**Sigma**	1:5000
anti-PCNA (affinity purified)	Generated in the lab	1:5000
anti-Rad6	Generated in the lab	1:5000
anti-yRfa1	A kind gift from Steve Brill	1:10,000
anti-Rad18 (DH1 and DH2 rabbit terminal bleeds)	See 2.11 for details	
anti-Rad18 (mouse 1,2 and 4 terminal bleeds)	See 2.11 for details	

Table 2-3: A list of the primary polyclonal antibodies that were used.

Table 2-4

Secondary Antibody	Source	Dilution used
HRP-conjugated anti-mouse	**DakoCytomation**	1:5000
HRP-conjugated anti-rabbit	**DakoCytomation**	1:10,000
anti-rabbit γ chain specific peroxidase conjugated (clone RG-96)	**Sigma**	1:2000

Table 2-4: A list of the secondary antibodies that were used.

2.1.3 Chemicals and Reagents

All chemicals (analytical reagent grade) were purchased from **Sigma**, **BDH Chemicals** or **Fisher Scientific** unless stated otherwise. Other materials were obtained as listed below.

Table 2-5

Chemicals and Reagents	Source
Ammonium persulfate (APS), Bromophenol blue, 30% Acrylamide/Bis solution (37.5:1 Acrylamide: N,N'-methylene-bis-acrylamide electrophoresis purity reagent), Affi-Gel Blue Gel, Hydroxyapatite BioGel HTP Gel (HAP) and Standard Mw for gel filtration	**Bio-Rad**
NP-40	**Calbiochem**
Amino acids for yeast media	**Duchefa Biochimie**
Activated CH-sepharose 4B beads, Glutathione sepharose 4 fast flow, HiTrap phenyl HP, HiTrap Q HP, HiTrap Heparin HP column, MonoQ (HR 5/5), Superose 6 PC 3.2/30 and Superdex200 10/300 GL	**GE Healthcare**
Agarose, Cellfectin, M13 reverse primer, 20X MOPS buffer, Pre-cast NuPage 4-12% gels, 10X reducing agent and 4X NuPage sample buffer	**Invitrogen**
Dithiothreitol (DTT)	**Melford**
Isopropyl-β-D-thiogalactopyranoside (IPTG)	**MP Biomedicals**
20% (w/v) sodium dodecyl sulfate (SDS)	**National Diagnostics**
10X T4 polynucleotide kinase buffer, 10X $CoCl_2$, Buffers for restriction enzymes, Lambda DNA, 100 bp DNA Ladder, 1 kb DNA Ladder	**New England Biolabs (NEB)**
X-Gal, peqGOLD protein marker and pre-stained peqGOLD protein marker IV	**peqlab**
Western lightning chemiluminescence reagent plus and radiolabelled reagents	**Perkin Elmer**
Ni-NTA agarose	**QIAGEN**
Complete EDTA-free protease inhibitor, Protein G-agarose	**Roche**
Instant skimmed milk powder	**Sainsbury's basics**
Ethidium Bromide (10 mg/mL)	**Seven Biotech**

Table 2-5: A list of the additional chemicals and reagents that were used.

2.2 Media and Solutions

Unless stated otherwise, ultra-pure Millipore water was used in all media and solutions.

2.2.1 Media for Bacterial Cells

Luria Broth (LB) medium, Terrific Broth (TB) medium and SOC medium as well as LB agar were prepared by Cancer Research UK London Research Institute (LRI) Central Services.

All antibiotics were purchased from **Sigma** with the exception of Gentamicin (**Invitrogen**), prepared as 1000-fold stock solutions and stored at -20°C. The antibiotics were used for resistance selection of bacterial cells in media or agar plates.

Table 2-6

Antibiotic	1000X Stock concentration (mg/mL)	Solvent
Ampicillin	100	Water, sterilized by filtration
Chloramphenicol	34	Ethanol
Kanamycin	50	Water, sterilized by filtration
Tetracyclin	10	Water, sterilized by filtration
Gentamicin	7	Water, sterilized by filtration
Spectinomycin	100	Water, sterilized by filtration

Table 2-6: A list of the antibiotic stock solutions.

2.2.2 Media for Yeast Cells

Yeast Peptone (YP) medium, Yeast Peptone Glucose (YPD) medium, 20% (w/v) glycerol, YPD agar and 4% (w/v) bacto agar were prepared by Cancer Research UK LRI Central Services.

Dropout Powder stock was prepared by overnight mixing of 2 g p-aminobenzoic acid and 20 g of each: alanine, arginine, asparagine, aspartic

acid, cysteine, glutamine, glutamic acid, glycine, inositol, isoleucine, lysine, methionine, phenylalanine, proline, serine, threonine, tyrosine and valine.

Synthetic Complete (SC) powder stocks were prepared by overnight mixing of 36.7 g dropout powder, 4 g leucine, 2 g histidine, 2 g tryptophane, 2 g uracil and 0.5 g adenine. (For each specific stock, the appropriate amino acid was not included).

Synthetic Complete (SC) medium 2.5X stock was prepared as followed: 5 g of Synthetic Complete powder stock, 4.25 g Difco Yeast Nitrogen Base (without amino acids and ammonium sulfate) and 12.5 g ammonium sulfate were dissolved in 1 L water and stirred for 30 min. The medium was divided into 5 aliquots of 200 mL each and autoclaved.

In order to prepare **SC medium for yeast growth**, 200 mL of 2.5X SC stock were mixed with 250 mL sterile distilled water and 50 mL of 20% (w/v) glucose solution (resulting in 2% (w/v) final concentration of glucose).

Selective SC plates, lacking the appropriate amino acids, were prepared by melting 250 mL of 4% (w/v) bacto agar and mixing it with 200 mL 2.5X SC specific stock and 50 mL 20% (w/v) glucose. The mix was poured into Petri dishes and allowed to solidify.

2.5X YP stock: 50 g bacto peptone and 25 g bacto yeast extract were dissolved in 1 L of water and stirred for 30 min. The medium was divided into 5 aliquots of 200 mL each and autoclaved.

20% (w/v) Galactose stock: 20 g of galactose were dissolved in warm water up to a final volume of 100 mL and autoclaved.

20% (v/v) Glycerol stock: 20 mL of glycerol were diluted with water up to a final volume of 100 mL and autoclaved.

In order to prepare **YP medium for yeast growth**, 2.5X YP stock was diluted with sterile distilled water and a carbon source (glucose / glycerol / galactose) was added to a final concentration of 2% (w/v).

YP + Galactose agar plates: 250 mL of 4% (w/v) bacto agar were melted and mixed with 200 mL 2.5X YP stock and 50 mL of 20% (w/v) galactose. The mix was poured into Petri dishes and allowed to solidify.

2.2.3 Media for Insect Cells

Insect Cell medium was prepared by Cancer Research UK LRI Central Services and consisted of Grace's medium (without insect haemolymph) supplemented with 3.3 g/L lactalbumin hydrolysate and 3.3 g/L yeastolate (Invitrogen), 10% (v/v) heat inactivated fetal calf serum (Sigma), 100 μg/mL streptomycin and 100 u/mL penicillin.

2.2.4 Buffers and Solutions

Standard solutions of 0.5 M EDTA, 1 M Tris-HCl (pH 7.5 or 8), Tris-EDTA (TE) pH 8, 1 M $MgCl_2$, 5 M NaCl, Phosphate Buffered Saline (PBS) and Tris Borate EDTA (TBE) were prepared by Cancer Research UK LRI Central Services.

2.2.4.1 Buffers for Molecular Biology Methods for *E. coli*

Tbfl solution: 30 mM potassium acetate, 100 mM rubidium chloride, 10 mM calcium chloride, 50 mM manganese chloride, 15% (v/v) glycerol. The pH of the solution was adjusted to 5.8 with dilute acetic acid. The solution was autoclaved prior to use.

Tbfll solution: 10 mM MOPS, 75 mM calcium chloride, 10 mM rubidium chloride, 15% (v/v) glycerol. The pH of the solution was adjusted to 6.5 with dilute NaOH. The solution was autoclaved prior to use.

X-Gal stock solution: X-Gal was dissolved at 100 mg/mL in DMSO.

IPTG stock solution: IPTG was dissolved at 200 mg/mL in water and sterilized by filtration through a 0.2 μm filter (Millipore).

2.2.4.2 Buffers for Molecular Biology Methods for Yeast Cells

LiT buffer: 100 mM lithium acetate and 10 mM Tris-HCl, pH 7.4. The solution was autoclaved prior to use.

LiT / PEG buffer: 100 g PEG (3350) was dissolved in 100 mL of LiT buffer. The solution was autoclaved prior to use.

ST DNA stock solution: Herring sperm DNA (Sigma D6898) was dissolved in TE buffer at 10 mg/mL and sheared by sonication to obtain homogenous

solution (Branson sonifier). Three subsequent extraction steps with phenol, phenol/chlorophorm and chloroform were used to purify the DNA, followed by a sodium acetate / ethanol precipitation procedure (Sambrook *et al.*, 1989). Prior to use, the solution was incubated at 95°C for 5 min.

Zymolyase solution: 50μL of 20 mg/mL Zymolyase (20T) stock solution and 50 μL of 1 M DTT stock solution were mixed with 900 μL sterile water (The final concentrations were 1 mg/mL Zymolase and 50 mM DTT). The solution was prepared fresh prior to an immediate use.

NaOH / β-ME: 1.85 M NaOH and 7.5% (v/v) β-ME. The solution was prepared fresh prior to an immediate use.

55% (w/v) TCA: 55 g TCA were dissolved in water up to 100 mL final volume.

HU buffer: 8 M urea, 5% (w/v) SDS, 200 mM Tris-HCl, pH 6.8, 1 mM EDTA, 0.1% (w/v) bromophenol blue and 1.5% (w/v) DTT (added fresh).

2.2.4.3 Buffers for General Manipulation of DNA

50X TAE: 2 M Tris base, 2 M glacial acetic acid and 50 mM EDTA.

6X DNA Loading buffer: 50% (w/v) sucrose and 0.1% (w/v) bromophenol blue dissolved in TE and filtered through a 0.45 μm filter (Millipore).

2.2.4.4 Buffers for General Manipulation of Proteins

5X Laemmli Sample buffer: 250 mM Tris-HCl, pH 6.8, 500 mM DTT, 10% (w/v) SDS, 0.1% (w/v) bromophenol blue and 10% (v/v) glycerol.

5X Laemmli Running buffer: 125 mM Tris base, 1.25 M glycine and 0.5% (w/v) SDS.

Coomassie Blue Staining solution: 2.5 g brilliant blue R (Sigma), 45% (v/v) methanol, 45% distilled water and 10% (v/v) glacial acetic acid. The solution was filtered prior to use.

De-staining solution: 45% (v/v) methanol, 45% distilled water and 10% (v/v) glacial acetic acid.

Gel Drying solution: 20% (v/v) methanol and 3% (v/v) glycerol in water.

Tris-HCl, pH 10.4 or pH, 9.4: Tris base was dissolved in water to a final concentration of 1 M. The pH was adjusted using HCl solution.

Blotting buffer I: 300 mM Tris-HCl, pH 10.4 and15% (v/v) methanol.

Blotting buffer II: 30 mM Tris-HCl, pH 10.4 and 15% (v/v) methanol.

Blotting buffer III: 25 mM Tris-HCl, pH 9.4, 40 mM 6-aminocaproic acid and 15% (v/v) methanol.

PBST: 1X PBS + 0.1% (w/v) Tween 20.

Blocking solution: 5% milk powder dissolved in PBST.

Stripping buffer: 100 mM Tris-HCl, pH 7.5, 10 mM EDTA and 0.5% (w/v) SDS. 140 μL of 100% (v/v) β-ME were added fresh to 20 mL stripping buffer per membrane.

2.2.4.5 Buffers for Protein Purifications

HI buffer: 30 mM HEPES-KOH, pH 7.8, 0.25 mM EDTA, 0.25% (w/v) myo-inositol and 0.01% (v/v) NP-40.

GF RPA buffer: 30 mM HEPES-KOH, pH 7.8, 0.25 mM EDTA, 200 mM KCl, 10% (v/v) glycerol and 1 mM DTT (added fresh).

RFA1 Washing buffer: 50 mM Tris-HCl, pH 7.5 and 25 mM NaCl.

RFA1 Elution buffer: 50 mM Tris-HCl, pH 7.5, 25 mM NaCl, 10 mM reduced glutathione and 10% (v/v) glycerol. The solution was freshly prepared prior to use.

RFA Dialysis buffer: 50 mM Tris-HCl, pH 7.5, 25 mM NaCl, 10% (v/v) glycerol and 1 mM DTT (added fresh).

RFA2 Lysis buffer: 25 mM Tris-HCl, pH 7.5, 250 mM NaCl, 1 mM EDTA and 1 mM DTT (added fresh).

RFA2 Washing buffer: 25 mM Tris-HCl, pH 7.5, 500 mM NaCl, 1 mM EDTA and 1 mM DTT (added fresh).

RFA2 Elution buffer: 50 mM Tris-HCl, pH 8, 500 mM NaCl, 1 mM EDTA, 10 mM reduced glutathione, 10% (v/v) glycerol and 1 mM DTT (added fresh).

RAD6 Lysis buffer: 20 mM HEPES-NaOH, pH 8, 500 mM NaCl and 1 mM EDTA, pH 8.

RAD6 Dialysis buffer: 50 mM Tris-HCl, pH 7.5, 150 mM NaCl, 10% glycerol and 0.5 mM DTT (added fresh).

PCNA Lysis buffer: 50 mM sodium phosphate, pH 8, 250 mM NaCl, 10% (w/v) sucrose, 5 mM imidazole and 1 mM β-ME (added fresh).

PCNA Washing buffer I: 50 mM sodium phosphate, pH 8, 500 mM NaCl and 10 mM imidazole.

PCNA Washing buffer II: 50 mM sodium phosphate, pH 8, 500 mM NaCl, 20 mM imidazole and 10% glycerol.

PCNA Dialysis buffer: 25 mM Tris-HCl, pH 7.5, 50 mM NaCl, 1 mM EDTA and 10% (v/v) glycerol.

Buffer A: 6 M guanidine hydrochloride, 100 mM sodium phosphate, pH 8, and 10 mM Tris-HCl, pH 8.

Buffer C: 8 M urea, 100 mM sodium phosphate, pH 6.3, and 10 mM Tris-HCl, pH 6.3.

Hypotonic buffer: 50 mM Tris-HCl, pH 8, 10 mM KCl, 1.5 mM $MgCl_2$ and 20 mM sodium phosphate, pH 8.

RAD18 Washing buffer I: 30 mM HEPES-NaOH, pH 7.4, 0.3 M NaCl, 10 mM imidazole and 1 mM β-ME (added fresh).

RAD18 Washing buffer II: 30 mM HEPES-NaOH, pH 7.4, 0.3 M NaCl, 20 mM imidazole and 1 mM β-ME (added fresh).

RAD18 Washing buffer III: 30 mM HEPES-NaOH, pH 7.4, 0.3 M NaCl, 20 mM imidazole, 100 μM $ZnCl_2$, 10% (v/v) glycerol and 1 mM β-ME (added fresh).

RAD18 Elution buffer: 30 mM HEPES-NaOH, pH 7.4, 0.3 M NaCl, 250 mM imidazole, 100 μM $ZnCl_2$, 10% (v/v) glycerol and 1 mM β-ME (added fresh).

RAD18 Dialysis buffer: 30 mM HEPES-NaOH, pH 7.4, 150 mM NaCl, 100 μM $ZnCl_2$, 10% (v/v) glycerol and 1 mM β-ME (added fresh).

QIAGEN buffer A: 100 mM NaH_2PO_4, 10 mM Tris base and 6 M guanidine hydrochloride. The final pH was adjusted to pH 8 with NaOH. The buffer was prepared fresh prior to use.

QIAGEN buffer C: 100 mM NaH_2PO_4, 10 mM Tris base and 8 M urea. The final pH was adjusted to pH 6.3 with HCl. The buffer was prepared fresh prior to use.

QIAGEN buffer D: 100 mM NaH_2PO_4, 10 mM Tris base and 8 M urea. The final pH was adjusted to pH 5.9 with HCl. The buffer was prepared fresh prior to use.

QIAGEN buffer E: 100 mM NaH_2PO_4, 10 mM Tris base and 8 M urea. The final pH was adjusted to pH 4.5 with HCl. The buffer was prepared fresh prior to use.

2.2.4.6 Buffers for Interaction Studies and Enzymatic Assays

Annealing buffer: 25 mM Tris-HCl, pH 7.5, 50 mM NaCl and 5 mM $MgCl_2$.

PD Low-Salt Binding buffer: 25 mM HEPES-NaOH, pH 7.5, 15 mM KCl, 1 mM EDTA and 0.05% Triton X-100. 0.5 mM DTT and 100 μg/mL BSA were added fresh prior to the experiment.

PD Low-Salt Binding ("- KCl") buffer: 25 mM HEPES-NaOH, pH 7.5, 1 mM EDTA and 0.05% Triton X-100. 0.5 mM DTT and 100 μg/mL BSA were added fresh prior to the experiment.

PD High-Salt Binding buffer: 25 mM HEPES-NaOH, pH 7.5, 15 mM KCl, 1 mM EDTA, 0.05% Triton X-100 and 250 mM NaCl. 0.5 mM DTT and 100 μg/mL BSA were added fresh prior to the experiment.

COIP Binding buffer: 50 mM Tris-HCl, pH 7.5, 250 mM KCl, 20% (v/v) glycerol and 1% (v/v) NP-40.

COIP Washing buffer: 50 mM Tris-HCl, pH 7.5, 250 mM NaCl and 20% (v/v) glycerol.

GST-PD Binding buffer: 50 mM Tris-HCl (pH 7.5), 50 mM NaCl, 1 mM EDTA and 0.05% triton X-100.

Coupled-PD Binding buffer: 50 mM Tris-HCl, pH 7.5, 100 mM NaCl, 5 mM $MgCl_2$ and 0.05 % Triton-X100.

Coupled-PD Washing buffer: 50 mM Tris-HCl, pH 7.5, 250 mM NaCl and 0.05 % Triton-X100.

Ubiquitylation buffer: 50 mM HEPES-NaOH, pH 6, 100 mM NaCl, 10 mM $MgCl_2$, 5 mM ATP and 0.1 mM DTT. 5X stock was prepared, divided to aliquots and kept at -80°C for a few months. Aliquots were thawed and diluted prior to use.

2.3 Plasmids

Table 2-7

Number	Name	Use
81	pAD-1	Two Hybrid
82	pGBT9	Two Hybrid
110	pGBT-*RAD18*	Two Hybrid
111	pGAD-*RAD18*	Two Hybrid
308	YEplac181	Expression in yeast
349	pTYB-*RAD6*	Expression in *E. coli*
386	YIplac211	Expression in yeast

387	YIp211-GAL	Expression in yeast
464	YIp211-GAL-*RAD18*	Expression in yeast
617	pGAD-*POL30*	Two-Hybrid
618	pGBT-*POL30*	Two-Hybrid
637	pQE-*POL30*	Expression in *E. coli*
821	YEp181-*CUP1-*^{His}*UBI*	Expression in yeast
860	pETDuet-1	Expression in *E. coli* (2 target genes)
878	pQE-*POL30(K164R)*	Expression in *E. coli*
879	pQE-*POL30(K127/164R)*	Expression in *E. coli*
1128	p11d-sctRPA	Expression in *E. coli*
1185	pGBT-*RFA1*	Two-hybrid
1190	pGBT-*RFA1*(1-563)	Two-hybrid
1191	pGBT-*RFA1*(1-452)	Two-hybrid
1192	pGBT-*RFA1*(1-317)	Two-hybrid
1193	pGBT-*RFA1*(1-116)	Two-hybrid
1194	pGBD-*RFA1*(79-621)	Two-hybrid
1195	pGBD-*RFA1*(320-621)	Two-hybrid
1196	pGBD-*RFA1*(454-621)	Two-hybrid
1199	pGBD-*RFA1*(167-452)	Two-hybrid
1200	pGBD-*RFA1*(167-407)	Two-hybrid
1201	pGBD-*RFA1*(266-446)	Two-hybrid
1265	pGAD-*RAD18*(1-192)	Two-hybrid
1266	pGBT-*RAD18*(1-192)	Two-hybrid
1269	pGAD-*RAD18-SAPΔ*(279-312Δ)	Two-hybrid
1270	pGAD-*RAD18-SAP**(G299A/R301A/M304A)	Two-hybrid
1271	pGBT-*RAD18-SAPΔ*(279-312Δ)	Two-hybrid
1272	pGBT-*RAD18-SAP**(G299A/R301A/M304A)	Two-hybrid
1273	YIp211-P18-*RAD18-SAPΔ*(279-312Δ)	Expression in yeast
1274	YIp211-P18-*RAD18-SAP**(G299A/R301A/M304A)	Expression in yeast
1275	pFastBac-HTc-*VSV-RAD18- SAPΔ*(279-312Δ)	Bacmid cloning
1276	pFastBac-HTc-*VSV-RAD18-SAP**(G299A/R301A/M304A)	Bacmid cloning
1317	pGEX-y*RFA1*(181-422)	Expression in *E. coli*
1502	pGEX-y*RFA2*	Expression in *E. coli*

Table 2-7: A list of all plasmids used in this thesis that were constructed by others or commercially available.

Table 2-8

No.	Name	Construction	Use
861	pETDuet-*RAD6(2)*	PCR (oHU538/oHU539) from pAS-*RAD6* (#102) cloned BamHI/KpnI into pETDuet-1 (BglII/KpnI)	Expression in *E. coli*
862	pETDuet-*His-RAD18(1)-RAD6(2)*	PCR (oHU536/oHU057) from pGAD-*RAD18* (#111) cloned BamHI/PstI into pETDuet-*RAD6(2)*	Expression in *E. coli*
863	pETDuet-*RAD18(2)*	PCR (oHU536/oHU537) from pGAD-*RAD18* (#111) cloned BglII/KpnI into pETDuet-1 (BamHI/KpnI)	Expression in *E. coli*
864	pETDuet-*His-RAD6(1)-RAD18(2)*	PCR (oHU538/oHU055) from pAS-*RAD6* (#102) cloned BamHI/PstI into pETDuet-*RAD18(2)*	Expression in *E. coli*
865	pUC118-PhoA	"p4xH cassette" (#240, Helle's PhD) cloned EcoRI/BamHI into pUC118 (#001)	Cloning
866	pUC118-PhoA-Duet	Synthetic linker (oHU543/oHU544) was filled in with Klenow; cloned XbaI/HindIII into pUC118-PhoA	Cloning
867	pUC118-PhoA-Duet-*His-RAD6*	*His-RAD6* from pETDuet-*His-RAD6(1)-RAD18(2)* (NcoI/PstI) cloned into pUC118-PhoA-Duet	Expression in *E. coli*
868	pUC118-PhoA-Duet-*His-RAD6-RAD18*	*RAD18* from pETDuet-*His-RAD6(1)-RAD18(2)* (BamHI/PstI) cloned into pUC118-PhoA-Duet-*His-RAD6* (BglII/NsiI)	Expression in *E. coli*
869	pUC118-PhoA-Duet-*His-RAD18*	*His-RAD18* from pETDuet-*His-RAD18(1)-RAD6(2)* (NcoI/PstI) cloned into pUC118-PhoA-Duet	Expression in *E. coli*
870	pUC118-PhoA-Duet-*His-RAD18-RAD6*	*RAD6* from pETDuet-*His-RAD18(1)-RAD6(2)* (BamHI/PstI) cloned into pUC118-PhoA-Duet-*His-RAD18* (BglII/NsiI)	Expression in *E. coli*
871	YEp195-ADH-*His-RAD18*	*His-RAD18* from YIp211-*P18-His6-RAD18* (#505) (BamHI/HindIII) cloned into YEp-*ADH-His-Rad5* (#487) (replacing *His-RAD5*)	Expression in yeast
873	pQE-*POL30(K127R)*	*POL30(K127R)* from YIp128-*P30-POL30(K127R)* (#708) (BamHI/PstI) cloned into pQE-32 (#152)	Expression in *E. coli*
1144	YIp128-ADH-*RAD6*	*RAD6* from YEp195-*ADH-RAD6* (#461) (EcoRI/PstI) cloned into YIplac128 (#66)	Expression in yeast
1146	pFastBac-HTc-*VSV-RAD18*	*VSV-RAD18* from YIp211-*P18-VSV-RAD18* (#403) (BamHI/PstI) cloned into pFastBac-HTc (#476)	Bacmid cloning

Table 2-8: A list of all plasmids that were constructed for this thesis.

2.4 DNA Oligonucleotides

Most oligonucletides were purchased from **SIGMA**. Biotinylated oligonucleotides for DNA-binding assays were purchased from **Operon**. Table 10-1 in the appendix contains the sequences of all the oligonucleotides that were used in this thesis.

Table 2-9

Substrate	Oligonucleotides
ssDNA 	XO1 5' [BiodT]ACGCTGCCGAATTCTACCAGTGCCTTGCTAGGACATCTTTGCCCACCTGCAGGTTCACCC 3'
dsDNA 	XO1 5' [BiodT]ACGCTGCCGAATTCTACCAGTGCCTTGCTAGGACATCTTTGCCCACCTGCAGGTTCACCC 3' XO1c 3' CTGCGACGGCTTAAGATGGTCACGGAACGATCCTGTAGAAACGGGTGGACGTCCAAGTGGG 5'
Splayed Duplex 	XO1 5' [BiodT]ACGCTGCCGAATTCTACCAGTGCCTTGCTAGGACATCTTTGCCCACCTGCAGGTTCACCC 3' XO4 3' TGCGACGGCTTAAGATGGTCACGGAACGATGTACCTCGACAGATCTCCTAGGCTGATAGCTA 5'
5'-Flap 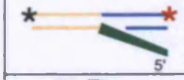	XO1 5' [BiodT]ACGCTGCCGAATTCTACCAGTGCCTTGCTAGGACATCTTTGCCCACCTGCAGGTTCACCC 3' XO2.1/2 3' CCTGTAGAAACGGGTGGACGTCCAAGTGGGT 5' XO4 3' TGCGACGGCTTAAGATGGTCACGGAACGATGTACCTCGACAGATCTCCTAGGCTGATAGCTA 5
3'-Flap 	XO1 5' [BiodT]ACGCTGCCGAATTCTACCAGTGCCTTGCTAGGACATCTTTGCCCACCTGCAGGTTCACCC 3' XO3.1/2 5' CATGGAGCTGTCTAGAGGATCCGACTATCGA 3' XO4 3' TGCGACGGCTTAAGATGGTCACGGAACGATGTACCTCGACAGATCTCCTAGGCTGATAGCTA 5
dsFork 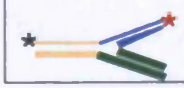	XO1 5' [BiodT]ACGCTGCCGAATTCTACCAGTGCCTTGCTAGGACATCTTTGCCCACCTGCAGGTTCACCC 3' XO2.1/2 3' CCTGTAGAAACGGGTGGACGTCCAAGTGGGT 5' XO3.1/2 5' CATGGAGCTGTCTAGAGGATCCGACTATCGA 3' XO4 3' TGCGACGGCTTAAGATGGTCACGGAACGATGTACCTCGACAGATCTCCTAGGCTGATAGCTA 5

Table 2-9: A schematic representation of the DNA structures that were used.
Complementary DNA strands in the substrates and their corresponding sequences are highlighted with the same colour. Note that all structures share oligonucleotide XO1. Black and red asterisks indicate the biotin and the ^{32}P label, respectively, on each DNA structure. For additional details on each oligonucleotide that was used to generate the structures, refer to Table 10-1.

2.5 Strains

2.5.1 *Escherichia coli* Strains

E. coli Top10 chemically competent cells were used for the propagation of most vectors and for DNA cloning. *E. coli* SURE chemically competent cells were used to propagate the vector harbouring yeast *RFA*1, *RFA*2 and *RFA*3 genes (p11d-sctRPA, number 1128). *E. coli* DH10Bac electro-competent cells were used to generate recombinant baculovirus DNA as described in paragraph 2.8.1. *E. coli* electro-competent or chemically competent cells (see paragraph 2.12 for details): BL21-CodonPlus (DE3)-RIL, ER2655, Rosetta-gami B (DE3) pLysS and Codon^{2+} were used for protein expression.

Table 2-10

Name	Source	Genotype
Top10	Invitrogen	F$^-$ *mcr*A Δ(*mrr-hsd*RMS-*mcr*BC) Φ80*lacZ*ΔM15 Δ*lac*X74 *rec*A1 *ara*Δ139 Δ(*ara-leu*)7697 *gal*U *gal*K *rps*L (Str^R) *end*A1 *nup*G
SURE	Stratagene	*e14- (McrA-)* D*(mcrCB-hsdSMR-mrr)171 endA1 supE44 thi-1 gyrA96 relA1 lac recB recJ sbcC umuC::Tn5* (Kan^r) *uvrC* [F' *proAB lacI^q*ZD*M15 Tn10* (Tet^r)]
DH10Bac	Invitrogen	F$^-$ *mcr*A Δ(*mrr-hsd*RMS-*mcr*BC) Φ80*lacZ*ΔM15 Δ*lac*X74 *rec*A1 *end*A1 *ara*D139 Δ(*ara, leu*)7697 *gal*U *gal*K λ$^-$ *rps*L *nup*G /pMON14272 / pMON7124
BL21-CodonPlus (DE3)-RIL	Stratagene	*E. coli* B F$^-$ *ompT hsdS*(r_B^- m_B^-) *dcm*$^+$ Tet^r *gal* λ(DE3) *endA* Hte [*argU ileY leuW* Cam^r]
ER2655	NEB	*F$^-$ lamda$^-$ fhuA2 [lon] ompT lacZ:: T7 gene1 gal sulA11* D*(mcrC-mrr)114::IS10 R(mcr 73::miniTn10-- TetS)2 R(zgb-210::Tn10) (TetS) endA1 [dcm]*

Rosetta-gami B (DE3) pLysS	Novagen	F^- *ompT* $hsdS_B$ (r_B^- m_B^-) *gal dcm lacY1 ahpC* (DE3) *gor522*::Tn*10 trxB* pLysSRARE (Cam^R, Kan^R, Tet^R)
$Codon^{2+}$	Dale Wigley	The strain was originally obtained from Steve Sandler (Kim *et al.*, 1998), and modified by removing the Chloramphenicol resistance gene allowing selection of helper plasmid by using only Spectinomycin.

Table 2-10: A list of all *E. coli* strains that were used and their genotypes.

2.5.2 Yeast Strains

All yeast strains used in this thesis, except for the strains used in the two-hybrid analysis (2.13.4), were derivatives of the haploid form of the wild-type DF5 strain (*his3-Δ200 leu2-3,112 lys2-801 trp1-1 ura3-52*) (Finley *et al.*, 1987), and were constructed as indicated below. All yeast strains used in the two-hybrid analysis (2.13.4) were derivatives of the yeast strain PJ69-4a (*MATa trp1-901 leu2-3,112 ura3-52 his3-200 gal4Δ gal80Δ LYS2::GAL1-HIS3 GAL2-ADE2 met2::GAL7-lacZ*) (James *et al.*, 1996). These strains were constructed by co-transformation of different vectors harboring the open reading frames of *RFA1*, *RAD18* and *POL30* genes fused either to the *GAL4* activation (AD) or the DNA-binding (BD) domains (see Table 2-7 for detailed plasmid list used in the two-hybrid assays).

Table 2-11

Strain Name	Strain Number	Genotype and Source	Features and Use
DF5 α	2	*MATα, his3- 200, leu2-3,2-112, lys2-801, trp1-1(am), ura3-52* (Finley *et al.*, 1987).	*WT*
DF5 a	3	*MATa, his3- 200, leu2-3,2-112, lys2-801, trp1-1(am), ura3-52* (Finley *et al.*, 1987).	*WT*

rad18::W α	142	*MATα, his3- 200, leu2-3,2-112, lys2-801, trp1-1(am), ura3-52, rad18::TRP1* (Ulrich and Jentsch, 2000)	UV sensitivity; Parental strain for construction
rad18::W a	162	*MATa, his3- 200, leu2-3,2-112, lys2-801, trp1-1(am), ura3-52, rad18::TRP1* (Ulrich and Jentsch, 2000)	UV sensitivity; Parental strain for construction and used as control in 2.13.1 and 2.13.2
PJ69-4A	195	*MATa, trp1-901 leu2-3, 112 ura3-52 his3-200 gal4Δ gal80Δ LYS2::GAL1-HIS3 GAL2-ADE2 met2::GAL7-lacZ)* (James *et al.*, 1996)	Two-hybrid analysis (2.13.4); Parental strain for construction
rad18 + Ylp211-P18	-	*MATα, his3- 200, leu2-3,2-112, lys2-801, trp1-1(am), ura3-52, rad18::TRP1, Ylp211-P18::URA3*	Constructed by integrative vector (no. 386) linearised by StuI; Used in 2.13.1, and 2.13.2.
rad18 + Ylp211-GAL	-	*MATα, his3- 200, leu2-3,2-112, lys2-801, trp1-1(am), ura3-52, rad18::TRP1, Ylp211-GAL::URA3*	Constructed by integrative vector (no. 387) linearised by StuI; Used in 2.13.1, and 2.13.2.
rad18 + Ylp128-ADH-RAD6 + YEp195-ADH-^{His}RAD18	-	*MATα, his3- 200, leu2-3,2-112, lys2-801, trp1-1(am), ura3-52, rad18::TRP1, Ylp128-ADH-RAD6::LEU2, YEp195-ADH-^{His}RAD18*	Constructed by episomal vector (no. 1472); Used for protein purification
RAD18^{TAP}	-	*ATCC 201388: MATa, his3Δ1, leu2Δ0, met15Δ0, ura3Δ0, RAD18^{TAP}::HIS3* (YSC1178-7499523)	Purchased from Open biosystems; Used for protein purification
RAD6^{TAP}	-	*ATCC 201388: MATa, his3Δ1, leu2Δ0, met15Δ0, ura3Δ0, RAD6^{TAP}::HIS3* (YSC1178-7500441)	Purchased from Open biosystems; Used for protein purification
WT + YEp181-CUP1-^{His}UBI	-	*MATa, his3- 200, leu2-3,2-112, lys2-801, trp1-1(am), ura3-52, YEp181-CUP1-^{His}UBI::LEU2*	Constructed by episomal vector (no. 821); Used in 2.17.1
RAD18^{6HA} + YEp181-CUP1-^{His}UBI	-	*MATa, his3- 200, leu2-3,2-112, lys2-801, trp1-1(am), ura3-52, RAD18^{6HA}::TRP1, YEp181-CUP1-^{His}UBI::LEU2*	Constructed by episomal vector (no. 821); Used in 2.17.1

RAD18^{6HA} + YEp181	-	*MATa, his3- 200, leu2-3,2-112, lys2-801, trp1-1(am), ura3-52, RAD18^{6HA}::TRP1, YEplac181::LEU2*	Constructed by episomal vector (no. 308); Used in 2.17.1
rad6 RAD18^{6HA} + YEp181-CUP1-^{His}UBI	-	*MATa, his3- 200, leu2-3,2-112, lys2-801, trp1-1(am), ura3-52, RAD18^{6HA}::TRP1, rad6::HIS3, YEp181-CUP1-^{His}UBI::LEU2*	Constructed by episomal vector (no. 821); Used in 2.17.1
RAD18^{6HA}	205	*MATa, his3- 200, leu2-3,2-112, lys2-801, trp1-1(am), ura3-52, RAD18^{6HA}::TRP1*	Analysis of post-translational modifications of Rad18; Parental strain for construction
rad18 + Ylp128-ADH-RAD6	1472	*MATα, his3- 200, leu2-3,2-112, lys2-801, trp1-1(am), ura3-52, rad18::TRP1, Ylp128-ADH-RAD6::LEU2*	Constructed by integrative vector (no. 1144) linearised by ClaI; Used for strain construction
rad18 + Ylp211-P18-rad18(SAPΔ)	1858	*MATα, his3- 200, leu2-3,2-112, lys2-801, trp1-1(am), ura3-52, rad18::TRP1, Ylp211-P18-RAD18(SAPΔ)::URA3*	Constructed by integrative vector (no. 1273) linearised by StuI; Used in 2.13.1, and 2.13.2.
rad18 + Ylp211-P18-rad18(SAP)*	1859	*MATα, his3- 200, leu2-3,2-112, lys2-801, trp1-1(am), ura3-52, rad18::TRP1, Ylp211-P18-RAD18(SAP*)::URA3*	Constructed by integrative vector (no. 1274) linearised by StuI; Used in 2.13.1, and 2.13.2.
rad6 RAD18^{6HA}	1867	*MATa, his3- 200, leu2-3,2-112, lys2-801, trp1-1(am), ura3-52, RAD18^{6HA}::TRP1, rad6::HIS3*	Analysis of post-translational modifications of Rad18; Parental strain for construction
WT + Ylp211-GAL-RAD18	2058	*MATa, his3- 200, leu2-3,2-112, lys2-801, trp1-1(am), ura3-52, Ylp211-GAL-RAD18::URA3*	*RAD18* over-expression; Used in 2.13.2 and.2.13.3
rad18 + Ylp211-GAL-rad18(SAP)*	2059	*MATa, his3- 200, leu2-3,2-112, lys2-801, trp1-1(am), ura3-52, rad18::TRP1, Ylp211-GAL-RAD18(SAP*)::URA3*	*rad18(SAP*)* over-expression; Used in 2.13.2 and.2.13.3

rad18 + Ylp211-GAL-rad18(SAPΔ)	2060	*MATa, his3- 200, leu2-3,2-112, lys2-801, trp1-1(am), ura3-52, rad18::TRP1, Ylp211-GAL-RAD18(SAPΔ)::URA3*	*rad18(SAPΔ)* over-expression; Used in 2.13.2 and.2.13.3

Table 2-11: A list of all yeast strains that were used and their genotypes.

2.6 Molecular Biology Methods for *E. coli*

2.6.1 Preparation of *E. coli* Competent Cells

2.6.1.1 Electro-competent Cells

A fresh overnight culture was used to inoculate 1 L of LB medium (1/100). The culture was grown at 37°C, with shaking at 250 RPM, up to an $O.D._{600}$ of 0.5 to 0.8. The cells were chilled on ice for 15-30 min and then harvested by centrifugation at 4000g, 4°C, in a SLA-3000 rotor, for 15 min. The supernatant was removed, and the pellet was re-suspended in a total of 1 L of ice-cold sterile water. The cells were harvested by centrifugation at 4000g, 4°C, in SLA-3000 rotor, for 15 min, and the supernatant was removed as before. Then, the pellet was re-suspended in a total of 0.5 L of ice-cold sterile water, and harvested as described before. The pellet was re-suspended again in 20 mL of sterile ice-cold 10% (v/v) glycerol, centrifuged as before and the supernatant was removed as before. Finally, the cells were re-suspended in 2-3 mL of sterile ice-cold 10% (v/v) glycerol to obtain around 1 X 10^{10} cells/mL. The competent cells were then dispensed into 100 µL aliquots on ice and stored at -80°C.

2.6.1.2 Chemically Competent Cells

A fresh overnight culture was used to inoculate 1 L of LB medium (1/100). The culture was grown at 37°C, with shaking at 250 RPM, up to an $O.D._{600}$ of 0.5 to 0.8. The cells were chilled on ice for 15-30 min and then harvested by centrifugation at 4000g, 4°C, in a SLA-3000 rotor, for 15 min. The supernatant was removed, and the cells were re-suspended in 400 mL TfbI solution (0.4 of original volume). The cell suspension was incubated on ice for 15 min, then the cells were harvested and the supernatant was removed as before. The pellet was re-suspended in 40 mL TfbII (0.04 of original volume) and incubated on ice for additional 15 min. Typically, the resulting concentration of cells was ~ 2 X 10^9 cells/mL. Finally, the competent cells were dispensed into 100 µL aliquots on ice and stored at -80°C.

2.6.2 Transformation of *E. coli*

2.6.2.1 Electroporation Method

Aliquots of electro-competent cells were thawed on ice for 10 min (1 aliquot was used per 1 or 2 transformation reactions – see 2.6.1.1). In parallel, a 0.2 cm sterile cuvette (Cell Projects) was placed on ice to cool. The DNA was mixed with the cells and incubated on ice for 30 min. The Pulse Controller (Bio-Rad) was set to 200 Ω and the Gene Pulser apparatus (Bio-Rad) was set to 25 μFD and 2.5 kV. The cells were transferred to the cold cuvette and the cuvette was placed in the safety chamber slide against the electrodes. One pulse was performed to achieve electroporation and the cells were immediately re-suspended in 1 mL of SOC medium. Then, the cells were incubated at 37°C, with shaking at 250 RPM, for 1 h. Finally, about 1/10 of the transformation reaction (if re-transformation) or all of it (if cloning) was plated on LB agar plates with selective antibiotics and incubated overnight at 37°C.

2.6.2.2 Heat-shock Method

Aliquots of chemically competent cells were thawed on ice for 10 min (1 aliquot was used per 1 or 2 transformation reactions – see 2.6.1.2). The DNA was mixed with the cells and incubated on ice for 30 min. Then, the cells were incubated at 42°C for 1.5 min, immediately placed back on ice and re-suspended with 1 mL of SOC medium. If ampicillin was the appropriate selective antibiotic, the cells were spun down, 900 μL of the supernatant was removed and the rest was used to re-suspend the cells and plate them on LB agar plates supplemented with ampicillin. Otherwise, cells were incubated at 37°C, with shaking at 250 RPM, for 1 h. Then, about 1/10 of the transformation reaction (if re-transformation) or all of it (if cloning) was plated on LB agar plates with selective antibiotics and incubated overnight at 37°C.

2.6.3 Isolation of Plasmid DNA

A few isolated *E. coli* colonies were used to inoculate 3 mL of LB medium each, containing the appropriate selection antibiotics. The cultures were grown at 37°C, with shaking at 250 RPM, for 16 h, and subsequently used for plasmid

isolation. The procedure was carried out using the QIAprep Spin Miniprep kit (QIAGEN) according to the manufacturer's instructions. Plasmid concentration was quantified using the Nanodrop (ND-1000 spectrophotometer; Labtech International).

2.7 Molecular Biology Methods for Yeast Cells

2.7.1 Transformation of Yeast Cells by the LiOAc/PEG Method

A yeast culture was grown to logarithmic phase ($O.D._{600}$ =1-2) in YPD or in selective medium at 30°C. The cells were harvested by centrifugation at 3000 RPM, room temperature, for 5 min in rotor A-4-81 (Eppendorf) (~ 1800g). The supernatant was removed; Approximately 9 X 10^7 cells were re-suspended in 100 µL LiT buffer per transformation reaction and transferred to a microcentrifuge tube. ST DNA stock solution was incubated for 5 min at 95°C. 100 µg ST DNA was pre-mixed with approximately 1-2 µg of DNA (either episomal plasmid or linearised integrative plasmid) and then added to the cell suspension. Subsequently, 500 µL of LiT / PEG buffer were added to each transformation reaction, the cells were immediately mixed by vortex for 3-5 s, and incubated for 15-30 min on a rotating wheel at room temperature. Then, 50 µL of DMSO were added per transformation reaction and the cells were incubated at 42°C for 10-15 min followed by centrifugation at 800g for 1 min. The supernatant was quickly removed with a pipette, and the cells were re-suspended in 100 µL sterile water. Finally, the cells were plated on selective media plates lacking the appropriate amino acids and incubated for 2-3 days at 30°C.

2.7.2 Colony PCR

A Zymolyase solution was freshly prepared, and 50 µL were dispensed per PCR tube. Single isolated colonies were picked into each tube (the less material used the better) and incubated at room temperature for 10 min. The lysed cells were pelleted by centrifugation at maximal speed for 2 min in a

butterfly centrifuge (Roth). The supernatant was aspirated using a pump. The tubes were briefly centrifuged again to ensure that all of the supernatant was removed. The pellets were then dried at 95°C for 5 min, re-suspended in a PCR reaction mix and subjected to PCR amplification.

2.7.3 Preparation of Total Cell Extracts from Yeast Cells

A yeast culture was grown to logarithmic phase ($O.D._{600}$ =1-2) in YPD or in selective medium at 30°C. About 2 $O.D._{600}$ of cells were transferred to a 2 mL microcentrifuge tube and harvested by centrifugation at 800g, room temperature, for 3 min. The supernatant was discarded and the cells were either frozen or processed immediately. The pellet was re-suspended in 500 µL of sterile water. Then, 75 µL of freshly made NaOH / β–ME solution was added, the cells were mixed by vortex and incubated on ice for 15 min. Subsequently, 75 µL of 55 % (w/v) TCA solution were added, the cells were mixed by vortex and incubated on ice for additional 10 min. As a result, the protein contents of the cells were precipitated. Total protein was harvested by centrifugation at 16100g, 4°C, for 10 min. The supernatant was removed with a pipette; the pellets were centrifuged again at 16,000g, 4°C, for 2 min and the supernatant was removed as before. Finally, the pellets were re-suspended in 40 µL of HU buffer and incubated at 65°C for 15 min. If necessary, the pH of the samples was adjusted by addition of 1-2 µL Tris-HCl buffer, pH 10.4.

2.8 Molecular Biology Methods of Baculovirus and Insect Cells

2.8.1 Baculovirus Production

DH10Bac electro-competent cells were transformed with ~ 1 ng pFastBac-HTc-*VSV-RAD18*, pFastBac-HTc-*VSV-RAD18-SAP*Δ(279-312Δ) or pFastBac-HTc-*VSV-RAD18-SAP**(G299A/R301A/M304A) plasmid DNA as described in paragraph 2.6.2.1, except that the transformed cells were incubated at 37°C with vigorous shaking for 4 h before plating. Recombinant baculovirus shuttle vectors (bacmid) were generated based on a site-specific transposition of the

expression cassettes (Luckow *et al.*, 1993). The transformation reactions were plated on LB agar plates containing kanamycin, gentamicin and tetracycline as well as 40 μL of X-Gal stock solution and 4 μL of IPTG stock solution that were spread on top of the plates and allowed to dry at 37°C for 4 h (Sambrook *et al.*, 1989). The plates were incubated at 37°C for 48 h. Successful transposition resulted in white colonies (due to the disruption of the *lacZ* gene in the bacmid DNA). The resulting colonies were re-streaked on new plates containing kanamycin, gentamicin, tetracycline, X-Gal and IPTG as described above. After an overnight incubation at 37°C, isolated white colonies were picked, inoculated with shaking in LB medium overnight and the bacmid DNA was extracted according to the method described in the Bac-to-Bac Baculovirus Expression System user manual (Invitrogen). In order to verify the recombination of *VSV-RAD18* gene into the bacmid DNA, PCR amplification was performed using one primer annealing to the bacmid DNA (M13 reverse) and the other to the 5' of the *RAD18* gene (oHU 536). Positive clones gave rise to a PCR product of ~ 1900 bp.

2.8.2 Transfection of Insect Cells

Typically, *Spodoptera frugiperda* Sf9 cells were used for transfection and amplification of the virus, but either High Five of Sf9 cells were used for the protein production.

Sf9 cells were transfected with recombinant bacmid DNA [harbouring ^{HisVSV}*RAD18 WT*, (*SAPΔ*) or (*SAP**)] using the Cellfectin reagent according to the Bac-to-Bac Baculovirus Expression System user manual (Invitrogen) in 6-well plates. The P1 virus stock was harvested after 5 days of incubation at 27°C. Following centrifugation at 1000 RPM for 5 min in rotor TY.JS (J_6B Beckman Centrifuge), the supernatant was collected, dispensed into aliquots and frozen at -80°C (protected from light). The P1 titer was assumed to be ~ 4-7 X 10^6 pfu/mL.

2.8.3 Amplification of Baculovirus

Approximately 2 X 10^7 Sf9 cells were plated per 175 mm flask containing 40 mL of Insect Cell medium (5 X 10^5 cells/mL, >97% viability). The cells were allowed to settle at 27°C for 1 h and then P1 baculovirus stocks, harbouring different constructs, were amplified as described below to obtain P2 stocks. An estimated 0.1 pfu/cell was used per P1 viral stock, but the optimal volumes for virus amplification were tested empirically.

P2 viral stocks of *^{HisVSV}RAD18 WT* or (*SAPΔ*) were obtained by infecting Sf9 cells with 300 μL of the respective P1 stock followed by incubation at 27°C for 7 days.

P2 viral stock of *^{HisVSV}RAD18* (*SAP)** was obtained by infecting Sf9 cells with 500 μL of the P1 stock followed by incubation at 27°C for 7 days.

P3 viral stock of *RAD6* was obtained by 2 subsequent amplifications. A P1 viral stock of *RAD6*, constructed by Dr. Helle Ulrich, was amplified by infecting 1 X 10^6 Sf9 cells (at 1 X 10^6 cells/mL) with 100 μL followed by incubation at 27°C for 4 days. The resulting P2 viral stock had an estimated titer of 4 X 10^8 pfu/mL. 5 μL of it were then used to infect 2 X 10^7 Sf9 cells, followed by incubation at 27°C for 6 days.

All P2 and P3 baculovirus stocks were stored at 4°C, protected from light, and were subsequently used for protein production and purification.

2.9 General Methods for DNA Manipulation

2.9.1 Determination of DNA Concentration

DNA concentrations were determined by measuring the absorbance at 260 nm. Plasmid DNA concentration was usually measured using the Nanodrop (ND-1000 spectrophotometer; Labtech International). Oligonucleotide concentration was measured using a quartz cuvette (GE Healthcare) in an Ultraspec 3100 pro spectophotometer (GE Healthcare). Calculations were based on the estimation

that a solution of 33 μg/mL ssDNA or 50 μg/mL dsDNA results in an absorbance of 1 at 260 nm (A_{260}).

2.9.2 DNA Standards

Lambda DNA was digested with PstI to generate a ladder. Commercial DNA markers, such as 100 bp and 1 kb DNA Ladders, were used as well.

2.9.3 Agarose Gel Electrophoresis

Agarose gels contained 0.8-2% (w/v) agarose in TAE or TBE buffers, depending on the size of the DNA fragment that was analysed. DNA samples were supplemented with 1/5 their volume of 6X DNA Loading buffer and run in TAE or TBE buffer, respectively, at 100 V or at 75 V (6 or 4.5 V/cm) in a Jencons Scientific horizontal gel electrophoresis apparatus.

2.9.4 Visualization of DNA by Ethidium Bromide Staining

0.5 μg/mL ethidium bromide was incorporated into the agarose gel before it was allowed to set. DNA bands were visualized by exposing the gel to UV light at 254 nm in a BioDoc_it UV transilluminator (UVP).

2.9.5 Native PAGE

Native polyacrylamide gels contained 8-12% polyacrylamide, 1X TBE, 0.1% (w/v) APS and 0.1% (v/v) TEMED. Sample buffer consisting of 40% (w/v) sucrose and 0.25% (w/v) bromophenol blue was added in 1/5 volume ratio to the samples. Native gels were either prepared using the Cambridge gel apparatus or the Bio-Rad mini protean gel system and were run at 200 V or at 60 V, respectively, in 1X TBE buffer for a few hours either at room temperature or at 4°C, depending on the experiment. The gels were exposed to an Amersham hyperfilm ECL (GE Healthcare) to allow excision of appropriate ^{32}P-labelled DNA. Alternatively, the gels were dried onto a 3 mm filter paper (Whatman), and ^{32}P-labelled DNA was detected by autoradioagraphy or by phosphorimager analysis (see paragraphs 2.9.6 and 2.9.7).

2.9.6 Autoradiography

Dried polyacrylamide gels were exposed to Amersham hyperfilm ECL (GE Healthcare) for different times (from a few min to a few days), depending on the intensity of the labelling, and developed using an automatic X-Ray film processor (model JP-33; Jungwon Precision Industry).

2.9.7 Phosphorimager Analysis

Dried polyacrylamide gels were exposed to Amersham Bioscience phosphor screens for 5-16 h. The screens were analysed either on a Storm Phosphorimager (model 840) or on a Typhoon Trio (GE Healthcare) using an ImageQuant software.

2.10 General Methods of Protein Manipulation

2.10.1 Determination of Protein Concentration

2.10.1.1 Absorbance at 280 nm

The absorbance at 280 nm was measured either by the Nanodrop (ND-1000 spectrophotometer; Labtech International) or in a quarz cuvette (GE Healthcare) in an Ultraspec 3100 pro spectophotometer (GE Healthcare). The extinction coefficient (ε) was calculated for each protein, using the following formula:

ε [M X cm]$^{-1}$= 5700 X (number of Tryptophane residues) + 1300 X (number of Tyrosine residues)

The protein concentration was calculated using the Beer-Lambert law:

Concentration [M] = Absorbance / ε [M^{-1} X cm^{-1}] X path length [cm]

2.10.1.2 Comparison by Coomassie Staining

Different dilutions of the analysed protein sample were prepared alongside with samples of known BSA concentrations. Then, protein samples were subjected to SDS-PAGE followed by Coomassie staining. The gel was imaged using Fujifilm LAS-3000 and the intensity of the stained bands was evaluated using

the AIDA software (Raytest Isotopenmessgeraete). A BSA standard curve was plotted and further used to estimate the protein concentration.

2.10.1.3 Bradford Method

The Bradford method (Bradford, 1976) was used with the Bio-Rad protein assay according to the manufacturer's instructions. The absorbance at 595 nm was measured in Biophotometer (Eppendorf) using a plastic cuvette and compared to a standard curve obtained with known BSA concentrations.

2.10.2 Molecular Weight Standards

peqGOLD Protein-Marker and peqGOLD Protein-Marker IV (Pre-stained) were used for Coomassie staining and Western blotting.
In order to determine the molecular weights of proteins using gel filtration, a mix of known proteins (Mw standard for gel filtration – Bio-Rad) was used to create a standard curve.

2.10.3 SDS-PAGE

Either pre-cast NuPage 4-12% gels were used or Tris-Glycine-SDS-polyacrylamide gels were prepared according to the Laemmli protocol (Laemmli, 1970) in a Bio-Rad mini protean gel system.
For pre-cast gels, the protein samples were supplemented with NuPage sample buffer containing a reducing agent and incubated at 70°C for 10 min. Gels were run in 1X MOPS buffer at constant 150 V for 1.5 h.
Tris-Glycine-SDS-polyacrylamide resolving gels typically contained 8-15% polyacrylamide whereas stacking gels contained 5% polyacrylamide. Gel solutions and running buffers were prepared according to the protocols described in Sambrook *et al.* (1989). Protein samples were supplemented with sample loading buffer (either Laemmli Sample buffer or HU buffer), followed by incubation at 95°C for 5 min or incubation at 65°C for 15 min, respectively. Gels were run at constant 150 V for 1 h in 1X Laemmli Running buffer.

2.10.4 Coomassie Blue Staining

Following SDS-PAGE, gels were soaked in Coomassie Blue Staining solution for a few hours up to overnight. Stained gels were de-stained with several washes in De-staining solution, briefly washed in distilled water and incubated overnight with Gel Drying solution. Subsequently, gels were dried on 3 mm Whatman paper covered with Saran (Dow) in a GelAir Dryer (Bio-Rad).

2.10.5 Western Blotting

Protein samples were subjected to SDS-PAGE as described in paragraph 2.10.3 and transferred onto a PVDF membrane (Millipore). Prior to transfer, the PVDF membrane was activated with methanol, soaked in water for 2 min and then soaked in Blotting buffer II for at least 20 min. 6 layers of Whatman gel blotting paper (Schleicher and Schuell), cut to membrane size, were used as follows. 2 layers were soaked in Blotting buffer I and placed onto the anode plate of a semi-dry blotter apparatus (Roth). Next, 1 layer, soaked in Blotting buffer II, was overlaid. On top of these 3 layers, the PVDF membrane was placed, followed by the gel, which was briefly washed in buffer II. Finally, 3 layers of Whatman gel blotting paper, soaked in Blotting buffer III, were laid on top, and the whole stack was covered by the cathode plate. The transfer conditions were at constant 40 A (for the Bio-Rad mini protean gels) or at 55 A (for the pre-cast gels (Invitrogen)) for 1.5 h (25 V was set as the maximal voltage allowed). After the transfer, the membranes were incubated in Blocking solution at room temperature for 30 min, followed by an overnight incubation at 4°C with a primary antibody (Table 2-2 and Table 2-3), which was diluted in the Blocking solution. Three consecutive washes with PBST solution, each of 10 min, were carried out. Then, the appropriate secondary antibody (Table 2-4) was diluted in the Blocking solution, and the membranes were incubated at room temperature for 1 h. Three additional consecutive PBST washes were performed as before, followed by the application of the Western lightning chemiluminescence reagent plus according to the manufacturer's instructions. The membranes were exposed to Amersham hyperfilm ECL (GE Healthcare) for 5 s up to 2 h (depending on the intensity of the signal), which was developed

using an automatic X-Ray film processor (model JP-33; Jungwon Precision Industry).

If re-blotting was required, membranes were incubated with Stripping buffer at 50°C for 30 min and then washed three times with PBST for 10 min each. Then, the membranes were blocked and probed with a different primary antibody as described above.

2.11 Generation of Antibodies against Rad18

Recombinant yeast ^{HisVSV}Rad18 was purified under denaturing conditions from High Five insect cells (see paragraph 2.12.6.2). After determination of protein concentration by measuring the absorbance at 280 nm, the denatured protein was dialysed against PBS, resulting in the formation of a white precipitate. This suspension was further used to raise antibodies against yeast Rad18.

2.11.1.1 Anti-Rad18 Mouse Polyclonal Serum

Four ~ 1 mg/mL aliquots (1 mL each) of denatured Rad18 protein were prepared in PBS and used to immunise four mice by the Cancer Research UK - Monoclonal Antibody Facility (project number Ccs 444). Mice test bleeds were analysed by Western blotting on total cell extracts prepared from yeast and on purified ^{HisVSV}Rad18. Spleen tissue was removed from the mice and hybridoma cells were generated from single antibody producing cells. Unfortunately, all positive hybridomas, subjected to scale-up production, proved to lose antibody expression. As a consequence, I diluted the polyclonal serum of each mouse to a final concentration of 50% (v/v) glycerol and used it for Rad18 detection. The terminal bleed of mouse 4 gave the best results in Western blots (used at 1:1500 dilution in blocking solution and could be re-used several times). The terminal bleeds of mice 1 and 2 were somewhat less sensitive (used at 1:1000 dilution in blocking solution) whereas mouse 3 terminal bleed showed a strong non-specific background and therefore was not used.

2.11.1.2 Anti-Rad18 Rabbit Polyclonal Serum

Six aliquots of denatured Rad18 protein were prepared in PBS (200 μg for the first aliquot, 100 μg for 5 aliquots) and used by Harlan Sera-Lab Ltd. to immunise two rabbits. Test bleeds were analysed by Western blotting against total cell extracts prepared from yeast and purified ^{HisVSV}Rad18. The terminal bleeds, designated as DH1 and DH2 from rabbits 1 and 2 respectively, were used as a stock antibody. Aliquots of the bleeds were diluted with glycerol to a final concentration of 50% (v/v) and kept at -20°C. As the DH1 terminal bleed gave slightly better results, it was preferred for Rad18 detection.

Detection of Rad18 in total cell extracts prepared from yeast:
Membranes were first blocked with 3% milk in PBST for 30 min at room temperature. DH1 terminal bleed stock was diluted at 1:10,000 in 0.3% milk in PBST and incubated at 4°C overnight. Following three consecutive washes in PBST, each for 10 min, membranes were incubated with HRP-conjugated anti-rabbit antibody diluted at 1:10,000 in 0.3% milk in PBST at room temperature for 1 h. Membranes were then washed and developed as described in paragraph 2.10.5.

Detection of purified ^{HisVSV}Rad18 in pull-down experiments containing RPA:
Unfortunately, DH1 total bleed was found to cross-react with yeast RPA. To solve this problem, the cross-reactivity activity was depleted from the bleed by incubation of the diluted antibody (1:5000 in 3% milk in PBST) for 4 h at room temperature with a Protran nitrocellulose transfer membrane (Schleicher and Schuell BioScience) onto which purified RPA was spotted (2.3 X 10^{-10} mol RPA per 2.4 μL of DH1 bleed). The depletion procedure was repeated twice and diluted antibodies were stored at -80°C and re-used several times.

2.12 Protein Purification

2.12.1 Purification of Yeast Replication Protein A (RPA)

Yeast *RFA1*, *RFA2* and *RFA3* gene expression was induced and the RPA

complex was purified based on Henricksen *et al.* (1994).

Electro-competent BL21-CodonPlus (DE3)-RIL *E. coli* cells were transformed with an RPA expression vector (no. 1128), harbouring the yeast *RFA1*, *RFA2* and *RFA3* genes, by electroporation and plated on LB agar plates supplemented with ampicillin and chloramphenicol. After an overnight incubation at 37°C, a single colony was used to inoculate 1 L of TB medium containing ampicillin and chloramphenicol. The culture was incubated at 37°C overnight without shaking, and then placed on a shaker at 250 RPM until $O.D._{600}$ reached 0.6. Induction was carried out by adding 0.3 mM IPTG to the culture and subsequently incubating at 37°C for 2 h. Cells were harvested by centrifugation at 4,250g, 4°C, for 20 min in a SLA-3000 rotor, and then re-suspended in cold HI buffer (5 mL of HI buffer per 1 L of culture). The re-suspended cells were quickly frozen in liquid nitrogen and kept at -80°C overnight. Prior to lysis, cells were thawed on ice and supplemented with fresh 1 mM PMSF, 1 mM DTT and 1 tablet of Complete protease inhibitor per 50 mL of buffer. The cells were disrupted by sonication (Branson sonifier) using 5 short bursts of 10 s at 40% output, followed by incubation on ice for 1 min. The lysate was further homogenized by passing through a Stansted homogenizer (model TC5-612W-332) at 70 MPa at 4°C. Soluble lysate was obtained by centrifugation at 45,000g, 4°C, for 20 min in a SS-34 rotor. The supernatant was further cleared by centrifugation at 100,000g, 4°C, for 30 min using a 70Ti rotor (Beckman), then quickly frozen in liquid nitrogen and kept at -80°C overnight. Four chromatographic steps were used to purify RPA: Affi-Gel Blue column (Bio-Rad), HAP column (Bio-Rad), MonoQ column (HR 5/5; GE Healthcare) and gel filtration (Superdex200 10/300 GL; GE Healthcare). The lysate was thawed and the protein concentration was estimated by the Bio-Rad protein assay according to the manufacturer's instructions, using BSA as a standard. Accordingly, the lysate was applied at approximately 8 mg protein per mL of resin by gravity flow to an Affi-Gel Blue column, which was pre-equilibrated in HI buffer containing 50 mM KCl. The column was then connected to a BioLogic pump (Bio-Rad) and sequentially washed at 2 mL/min flow rate with 3 column volumes of each: HI buffer containing either 50 mM KCl, 0.8 M KCl, 0.5 NaSCN or 1.5 M NaSCN. RPA was eluted in the 1.5 M NaSCN wash and the protein concentration was estimated using the Bio-Rad protein assay as described

before. The peak of the protein was pooled and applied directly to a HAP column, pre-equilibrated with HI buffer containing 50 mM KCl. A ratio of 5 mg protein per mL of resin was used and the loading was carried out by gravity flow. The column was connected to a BioLogic pump (Bio-Rad) and washed at a flow rate of 6 mL/min (the fastest flow-rate possible) with 3 column volumes of each: HI buffer, HI buffer containing 80 mM potassium phosphate or HI buffer containing 500 mM potassium phosphate. Wash samples were analysed by SDS-PAGE followed by Coomassie staining. RPA was found to elute mainly in the fractions of the HI buffer containing 80 mM potassium phosphate. Those fractions were combined, and the protein content was determined by the Bio-Rad protein assay as before. The pooled fractions were diluted 2-fold with HI buffer to reduce the ionic strength, and applied to a MonoQ column that was equilibrated with HI buffer containing 50 mM KCl. Up to 8 mg protein was loaded onto this column in one run. The column was washed with HI buffer containing 50 mM KCl followed by a wash with HI buffer containing 100 mM KCl, until a stable UV trace was obtained. Then, a gradient was developed between HI buffer containing 200 mM KCl or 400 mM KCl, with RPA eluting around 300 mM KCl. The flow rate used with this column was 1 mL/min and 500 µL fractions were collected. Elution fractions were supplemented to final 10% (v/v) glycerol concentration and samples were analysed by SDS-PAGE followed by Coomassie staining. Accordingly, peak fractions were pooled and run on a Superdex200 10/300 GL gel filtration column at a flow rate of 0.4 mL/min in GF RPA buffer. The protein purity was assessed to be ~ 91%. The final yield was approximately 3 mg of RPA complex from 12 L of culture.

2.12.2 Purification of ^{GST}Rfa1 (DNA-Binding Domain)

Chemically competent BL21-CodonPlus (DE3)-RIL *E. coli* cells were transformed by heat shock method with a plasmid harbouring the DNA-binding domain of the yeast *RFA1*(182-421) gene fused to GST on its N-terminus (no. 1317). Transformed cells were plated on LB agar plates containing ampicillin. After incubation at 37°C overnight, several colonies were tested for *RFA1*(182-421) expression on a small scale, using 3 mL cultures, inducing expression with addition of IPTG up to 0.5 mM final concentration and incubating the cells at 18°C overnight. A single colony that was identified to show good expression

levels in the small-scale experiment was used to inoculate 400 mL of LB medium containing ampicillin. The culture was incubated at 37°C overnight without shaking. Then, it was incubated with shaking at 250 RPM at 37°C for a few hours, until the absorbance at 600 nm reached 0.6. IPTG was added to the culture to a final concentration of 0.5 mM, and induction of protein expression was carried out at 18°C overnight. Cells were harvested by centrifugation at 4250g, 4°C, in a SLA-3000 rotor and re-suspended in PBS. Prior to lysis, Complete protease inhibitor was added (1 tablet per 50 mL of suspension). Cells were passed through a Stansted homogenizer (model TC5-612W-332) at 70 MPa at 4°C. Then, the lysate was sonicated using 5 short bursts of 10 s at 40% output, followed by incubation for 1 min on ice (Branson sonifier). Crude lysate was centrifuged at 20,000 RPM, 4°C, in a SS-34 rotor. The lysate was further cleared by centrifugation at 40,000 RPM, 4°C, for 30 min, in a 45Ti rotor (Beckman). Glutathione sepharose 4 Fast Flow beads (GE Healthcare) were washed 3 times in PBS (1 mL column bed volume). The supernatant from the ultracentrifugation step was added to those beads and incubated at 4°C for 1 h on a rotating platform. Then, the resin was poured into a 10 mL polypropylene column (Pierce) and allowed to settle. The column was washed by gravity flow with 5 column volumes of PBS followed by 5 column volumes of RFA1 Washing buffer. Then the column was transferred to room temperature for a few min. ^{GST}Rfa1 (182-421) was eluted from the column by re-suspending the beads with RFA1 Elution buffer. Elution fractions were analysed using SDS-PAGE followed by Coomassie staining. Fractions containing ^{GST}Rfa1 (182-421) were pooled and dialysed against RFA Dialysis buffer, using Spectra/Por moleculartporous membrane tubing (Cutoff 3.5 kDa; SpectrumLabs). The protein sample was concentrated by a viva-spin concentrator (Cutoff 3 kDa; Vivascience). The purity of the protein preparation was assessed to be around 70% and the final yield was 0.3 mg.

2.12.3 Purification of ^{GST}Rfa2

Chemically competent Codon^{2+} *E. coli* cells were transformed by heat shock method with a plasmid, harbouring the yeast *RFA2* gene fused to GST on its N-terminus (Table 2-7), and plated on LB agar plates containing ampicillin and spectinomycin. After an overnight incubation at 37°C, a single colony was used

to inoculate 10 mL of LB medium supplemented with ampicillin and spectinomycin and grown at 37°C overnight. This culture was then used to inoculate a 4 L culture that was grown up to an absorbance of 0.6 at 600 nm. Subsequently, GST-*RFA2* expression was induced by addition of IPTG to a final concentration of 0.5 mM and an overnight incubation at 18°C with shaking at 250 RPM. The cells were harvested by centrifugation at 4250g, 4°C, in a SLA-3000 rotor and re-suspended in RFA2 Lysis buffer. Complete protease inhibitor was added (1 tablet per 50 mL of suspension) before the cells were homogenized by passing through a Stansted homogenizer (model TC5-612W-332) at 70 MPa at 4°C. The lysate was cleared by centrifugation at 45,000g, 4°C, for 20 min in a SS-34 rotor. The supernatant was further centrifuged at 100,000g, 4°C, for 30 min using a 45Ti rotor (Beckman). Glutathione sepharose 4 Fast Flow (GE Healthcare) (5 mL bed volume) was packed under pressure and equilibrated with at least 10 column volumes of RFA2 Lysis buffer. The supernatant resulting from the ultracentrifugation step was loaded onto the column by gravity flow. The column was sequentially washed with 3 column volumes of RFA2 Lysis buffer, and then with RFA2 Washing buffer at 2 mL/min until a stable UV absorbance was obtained. The column was transferred to room temperature for a few min. Then, ^{GST}Rfa2 was eluted by re-suspending the beads in a RFA2 Elution buffer. Elution fractions were analysed by SDS-PAGE followed by Coomassie staining, and fractions containing ^{GST}Rfa2 were pooled. The protein was dialysed against RFA Dialysis buffer, using Spectra/Por molecularporous membrane tubing (Cutoff 3.5 kDa; SpectrumLabs). The protein was concentrated using a viva-spin concentrator (Cutoff 10 kDa; Vivascience). The purity of the protein was estimated to be 90% and the final yield was approximately 130 mg.

2.12.4 Purification of Rad6

Chemically competent ER2655 *E. coli* cells were transformed by heat shock method with plasmid pTYB-*RAD6* (no. 349), harbouring the yeast *RAD6* gene fused to a bi-functional tag (intein and chitin binding domain) on its N-terminus, and plated on LB agar plates containing ampicillin. After incubation at 37°C overnight, a single colony was used to inoculate 3 mL of LB medium supplemented with ampicillin and grown at 37°C overnight. This culture was

then used to inoculate a 2 L culture that was grown up to an absorbance of 0.6 at 600 nm. *RAD6* expression was induced by addition of 0.5 mM IPTG followed by incubation at 15°C for 18 h, with shaking at 250 RPM. The cells were harvested by centrifugation at 4250g 4°C in a SLA-3000 rotor and re-suspended in RAD6 Lysis buffer. Prior to lysis, 1 mM PMSF was added. The cells were sonicated by 5 bursts of 10 s each, followed by incubation for 1 min on ice (Branson sonifier). The lysate was cleared by centrifugation at 45,000g, 4°C, for 30 min in a SS-34 rotor. To assess the protein expression levels and its solubility after lysis, samples were taken during various steps, boiled in 1X Laemmli Sample buffer without DTT, and analysed by SDS-PAGE followed by Coomassie staining. The cleared supernatant was added to 15 mL chitin beads (New England Biolabs) that were pre-equilibrated in more than 10 column volumes of RAD6 Lysis buffer. The beads were incubated on a rotating platform at 4°C for 1 h, transferred to a column (Bio-Rad) and allowed to settle. The column was then connected to a BioLogic pump (Bio-Rad). It was washed with 10 column volumes of RAD6 Lysis buffer at 2 mL/min followed by a quick flush with 3 column volumes of RAD6 Lysis buffer containing 50 mM DTT. Subsequently, the column was closed, transferred to room temperature and incubated overnight to promote the self-cleavage reaction of the chitin-bound intein tag. Elution of Rad6 was carried out with RAD6 Lysis buffer and the elution fractions were subjected to SDS-PAGE and analysed by Coomassie staining. Column fractions containing Rad6 were pooled (~ 20 mL) and concentrated by amicon ultra device (Millipore) of 10 kDa cutoff up to 2 mL, according to the manufacturer's instructions. The concentrated sample was dialysed at 4°C against RAD6 Dialysis buffer. The purity of the protein was estimated to be 90% and the final yield was approximately ~ 3.8 mg.

2.12.5 Purification of ^{His}PCNA *WT* and ^{His}PCNA Mutants

The purification procedure was based on Biswas *et al.* (1995).

Electro-competent Rosetta-gami B (DE3) pLysS *E. coli* cells were transformed by electroporation method with a plasmid, harbouring a copy of the yeast *POL*30 gene (either *WT* or point mutation - pQE30-*POL30* (no. 637) / pQE32-*POL30 (K127R)* (no. 873) / pQE32-*POL30 (K164R)* (no. 878) / pQE32-*POL30 (K127/164R)* (no. 879)), and plated on LB agar plates containing ampicillin and

chloramphenicol. After incubation at 37°C overnight, a single colony was used to inoculate 3 mL of LB medium supplemented with ampicillin and chloramphenicol and grown at 37°C overnight. This culture was used to inoculate a 2 L culture that was grown up to an absorbance of 0.6 at 600 nm. Subsequently, *POL30* expression was induced by addition of IPTG to a final concentration of 1 mM, followed by incubation at 37°C for 4 h, with shaking at 250 RPM. The cells were harvested by centrifugation at 4250g, 4°C, in a SLA-3000 rotor and re-suspended in PCNA Lysis buffer. Immediately before lysis, 1 tablet of Complete protease inhibitor was added per 50 mL of suspension. The cells were incubated at 37°C for 5 min and then placed back on ice. The cells were disrupted by passage through a French Press at 750 psi. The crude lysate was centrifuged at 45,000g, 4°C, in a SS-34 rotor for 20 min. The supernatant was collected and kept on ice. The pellet was re-suspended with PCNA Lysis buffer and was further disrupted by 3 bursts of 10 second sonication each followed by incubation for 1 minute on ice (Branson sonifier). Following centrifugation at 30,000g, 4°C, in a SS-34 rotor for 20 min, the supernatants were combined. NaCl and imidazole concentrations were adjusted to 500 mM and 10 mM, respectively, and the supernatant was added to 3 mL column volume of Ni-NTA agarose (QIAGEN) beads that were pre-equilibrated with PCNA Washing buffer I. The beads were incubated on a rotating platform at 4°C for 1 h, then poured into a column (Bio-Rad) and allowed to settle. The column was washed with PCNA Washing buffer I, until the UV absorbance returned to its basal level. Subsequently, the column was washed with 5 column volumes of PCNA Washing buffer II. To elute the protein, a 15 mL gradient was developed up to an imidazole concentration of 250 mM. Column fractions were collected and analysed by SDS-PAGE followed by Coomassie staining. Fractions containing PCNA were pooled and dialysed against PCNA Dialysis buffer. The estimated purity of the proteins was 90-95%. The final yields from a 2 L culture were as follows: ~ 142.8 mg for ^{His}PCNA (*WT*), ~ 37.8 mg for ^{His}PCNA (K164R), ~ 18.3 mg for ^{His}PCNA (K127R) and ~ 32.7 mg for ^{His}PCNA (K127/164R).

2.12.6 Purification of Yeast ^{HisVSV}Rad18-Rad6 from Insect Cells

2.12.6.1 Purification under Native Conditions

The purification procedure was based on Cai *et al.* (1996). Either High Five or Sf9 (Invitrogen) insect cells were used. Cells were plated in Insect Cell medium in 175 mm flasks and allowed to adhere to the surface at 27°C for 1 h. A monolayer (2 X 10^7 cells per flask) of about 80% confluency was infected simultaneously with recombinant viruses that produce either ^{HisVSV}*RAD*18 or *RAD*6 (the optimal ratio of virus stocks was tested empirically each time and was dependent on the respective P2 stocks). The same protocol was used for the purification of ^{HisVSV}Rad18 (SAP*) and ^{HisVSV}Rad18 (SAPΔ) mutants. After infection, cells were incubated at 27°C for 48 h. The cells were collected by gentle tapping and harvested by centrifugation at 1000 RPM, 4°C, in rotor TY.JS (J_6B Beckman Centrifuge) for 20 min. The supernatant was discarded; the cells were washed in cold PBS and harvested as described before. The pellet was re-suspended in two volumes of hypotonic buffer and supplemented with protease inhibitors: 0.5 mM PMSF, 0.2 μg/mL aprotinin, 0.2 μg/mL leupeptin and 1 tablet of Complete protease inhibitor. Subsequently, the cells were lysed with 20 strokes of a Dounce homogenizer (Wheaton) on ice. The lysate was centrifuged at 2400g, 4°C, for 30 min. The supernatant was subjected to ultracentrifugation at 43,500g, 4°C, for 30 min, resulting in a soluble cytoplasmic fraction that was used for subsequent purification steps. In parallel, the nuclear pellet, derived from the low-speed centrifugation step, was re-suspended in two volumes of hypotonic buffer without KCl. The NaCl concentration was adjusted to 0.42 M, protease inhibitors were added as before, and the nuclear mix was incubated on a rotating platform at 4°C for 30 min. Following this incubation, the mix was subjected to ultracentrifugation at 43,500g, 4°C, for 30 min, resulting in a soluble nuclear fraction that was used for subsequent purification steps. Both the soluble cytoplasmic fraction and the soluble nuclear fraction were adjusted to 0.3 M NaCl and 10 mM imidazole, and passed through 0.45 μm filters (Millipore). Each filtrate was incubated separately with Ni-NTA agarose beads (QIAGEN) that were pre-equilibrated in the corresponding buffer (with imidazole) at 4°C for 2 h. Approximately 35 μL of

beads were used per 2 X 10^7 infected insect cells for each fraction. The beads were poured into two separate polypropylene columns (Pierce), allowed to settle and drained by gravity. The columns were washed manually with 5-10 column volumes each of RAD18 Washing buffer I, II and III, subsequently. The columns were incubated with RAD18 Elution buffer for a few min and then eluted. This was repeated several times. Elution fractions were collected and analysed by SDS-PAGE and Coomassie staining. Column fractions containing Rad18 and Rad6 were pooled and dialysed in 3.5 kDa cutoff dialysis tubing (Spectra/Por molecularporous membrane tubing; SpectrumLabs) against RAD18 Dialysis buffer. The sample was concentrated using a 3 kDa cutoff vivaspin concentrator (Vivascience) and the protein concentration was determined by Coomassie staining comparison to a BSA standard curve. Starting from 1.2 X 10^9 Sf9 cells, the typical protein yield was ~ 1 mg for ^{HisVSV}Rad18 purified from cytoplasmic fraction. Using 2 X 10^8 Sf9 cells, the protein yield was approximately 0.1 mg for ^{HisVSV}Rad18 (SAPΔ) and 0.01 mg for ^{HisVSV}Rad18 (SAP*) from the cytoplasmic fraction. The typical purity was around 70-80%. Mock purification was carried out from insect cells infected with baculovirus harbouring only *RAD6*.

2.12.6.2 Purification under Denaturing Conditions

Purification of Rad18 under denaturing conditions was based on the QiAexpressionist handbook (QIAGEN). Pellets obtained from the ultracentrifugation steps described in 2.12.6.1 were combined and re-suspended in QIAGEN buffer A. The suspension was disrupted by 4 bursts of 10 s (Branson sonifier) each followed by incubation for 1 min on ice. Then, the suspension was incubated on a rotating platform for 30 min at room temperature and centrifuged at maximal speed for an additional 30 min in a F-34-6-38 rotor (Eppendorf). The supernatant was filtered through a 0.45 μm filter (Millipore) and added to Ni-NTA beads (QIAGEN) that were pre-washed in QIAGEN buffer A. The beads were incubated for 2 h at room temperature, transferred to a column (Bio-Rad), allowed to settle and the column was drained by gravity. The beads were then washed twice with 8 column volumes of QIAGEN buffer C. Subsequently, the beads were eluted four times with 1 column volume of QIAGEN buffer D and four times with 1 column volume of

QIAGEN buffer E. The elution fractions of the column were subjected to SDS-PAGE and were analysed by Coomassie staining. Column fractions containing Rad18 were pooled and used for antibody production as described in paragraph 2.11.

2.13 Yeast Genetics

2.13.1 UV Sensitivity Streak Assay

The relevant yeast strains were grown in YPD medium to logarithmic phase. Equal numbers of cells (typically 1.5 - 3.5 X 10^5 cells) were streaked out onto YPD plates and subjected to a gradient of UV irradiation (0-3 min, 1.67 $Jm^{-2}s^{-1}$) as described in Ulrich (2001).

2.13.2 Sensitivity Spot Assay

The relevant yeast strains were constructed by transformation of a *rad18* deletion strain with an integrative plasmid harbouring *RAD18* (*WT*), *RAD18* (*SAP**) or *RAD18* (*SAPΔ*) under the control of either the *RAD18* or the *GAL1* promoter (Table 2-7 and Table 2-11). Transformed cells were re-streaked, and the presence of the *RAD18* alleles was confirmed by colony PCR. To ensure protein expression, total cell extracts were prepared and analysed by SDS-PAGE followed by Western blotting. Isolated colonies were inoculated in YPD for overnight incubation at 30°C. Yeast strains harbouring the *GAL1* promoter for *RAD18* over-expression were induced as described in paragraph 2.13.3. Overnight cultures were then diluted in YPD or YP + GAL, as appropriate, and were grown for 2 generations up to a logarithmic phase. The absorbance at 600 nm was measured, and the cells were diluted with sterile water to a final $O.D._{600}$ = 0.2. Additional three 10-fold serial dilutions were prepared, and 3.5 μL of each dilution was spotted onto plates containing DNA damaging agents (approximately 1.4 X 10^4, 1.4 X 10^3, 140 and 14 cells / drop, respectively).

Preparation of plates:

MMS (100% stock) or 4NQO (dissolved in DMSO), both purchased from Sigma, were added to the melted agar at appropriate concentrations. Plates were

poured, allowed to settle on a straight surface and then dried for at least 4 h in a DNA/RNA UV-cleaner cabinet (Alpha laboratories).

2.13.3 Induction of *RAD18* Over-Expression

Yeast strains harbouring *RAD18* (*WT*), *RAD18* (*SAP**) or *RAD18* (*SAP*Δ) under control of the *GAL1* promoter (Table 2-11) were re-streaked onto selective medium plates lacking uracil to ensure the correct integration of the expression cassette and even growth conditions. Single colonies were inoculated in YPD for overnight incubation at 30°C. The $O.D._{600}$ of the cultures was measured and the cells were diluted in YP + 2% glycerol at $O.D._{600}$ = 0.4. The cells were incubated at 30°C for approximately 8 h. The $O.D._{600}$ was measured (~ $O.D._{600}$ = 1-1.5), the cells were diluted into either YPD (for suppression of expression) or YP + 2% galactose (for over-expression), and the cultures were incubated at 30°C overnight. In the morning, overnight cultures were diluted in YPD or YP + GAL, as appropriate, and were grown for 2 generations up to a logarithmic phase. Subsequently, these cultures were used for total cell extract preparations or for sensitivity spot assays.

2.13.4 Two-Hybrid Analysis

Different constructs of the open reading frames of *RFA1*, *RAD18* and *POL30* fused either to the *GAL4* activation (AD) or to the DNA-binding domain (BD) were co-transformed into the yeast strain PJ69-4A (James *et al.*, 1996) (according to 2.7.1, except that 0.3 – 0.5 μg per plasmid DNA were used per transformation). Transformed cells were selected by growth on selective medium lacking leucine and tryptophane (-LW). Five representative colonies per transformation were combined in 500 μL of sterile water, followed by an additional 5-fold dilution in sterile water. 3.5 μL of each dilution was plated on selective medium plates lacking different sets of amino acids. Positive interactions were scored by growth on plates lacking leucine, tryptophane and histidine (-HLW) whereas stronger interactions were detected on plates also lacking adenine (-AHLW). Selective plates lacking leucine and tryptophane (-LW) were used as a positive control for growth.

2.14 Enzymatic Assays

2.14.1 *In vitro* Ubiquitylation Assays

A complete ubiquitylation reaction (8 μL) contained 112.5 nM yeast E1, 65 μM ubiquitin, 3 μM ^{His}PCNA and different concentrations of the purified ^{HisVSV}Rad18-Rad6 complex. The samples were incubated in Ubiquitylation buffer at 30°C for various times (30 min to 4 h). The reactions were stopped by addition of one volume of HU buffer, followed by 15 min incubation at 65°C. The samples were subjected to SDS-PAGE and analysed by Western blotting.

2.14.2 Radiolabelling of Oligonucleotides

Either 5'- or 3'-biotinylated oligonucleotides were purchased from Operon. The dried pellet was re-suspended in TE, pH 8, to a final concentration of 1 mM, and subjected to a radiolabelling reaction as described in 2.14.2.1 or in 2.14.2.2., as appropriate. Non-modified oligonucleotides, typically purchased from SIGMA, were re-suspended in TE, pH 8, to a final concentration of 100 μM, and subjected to a radiolabelling reaction similar to that described in 2.14.2.1.

2.14.2.1 5'-^{32}P-End Labelling of Oligonucleotides

Approximately 3 nmol of each 3'-biotinylated oligo-dT (Table 10-1) were used per labelling reaction. The reaction mix consisted of 1X NEB T4 polynucleotide kinase buffer, 20 μCi of [γ-^{32}P] ATP and 20 units of T4 polynucleotide kinase enzyme, in a final volume of 50 μL. Following incubation at 37°C for 30 min, the reaction was stopped by addition of EDTA to a final concentration of 50 mM and incubation at 65°C for 15 min.

2.14.2.2 3'-^{32}P-End Labelling of Oligonucleotides

Approximately 7 nmol of 5'-biotinylated XO1 oligo (Table 2-9 and Table 10-1) were used in each labelling reaction. The 50 μL reaction mix contained 1X of NEB buffer 4, 0.25 mM of $CoCl_2$, 50 μCi of [α-^{32}P] dATP or dCTP and 40 units of Terminal transferase enzyme. After incubation at 37°C for 30 min, the

reaction was terminated by addition of EDTA to a final concentration of 50 mM and incubation at 70°C for 10 min.

2.15 Preparation of DNA Substrates and Protein - DNA Interaction Assays

2.15.1 Removal of Unincorporated Nucleotides

5'- or 3'-radiolabelled oligonucleotides (from paragraph 2.14.2) were separated from an excess of the radioactive nucleotide using ProbeQuant G-50 micro columns (GE Healthcare) according to the manufacturer's protocol. As the radiolabelling of the oligos was for tracing purposes only, the efficiency of labelling was not assessed.

2.15.2 Preparation of DNA Substrates

Approximately 1 nmol of 3'-radiolabelled XO1 oligonucleotide were used per annealing reaction. Different combinations of unlabelled nucleotides were used in a 3-fold excess to generate the different DNA structures (Table 2-9) in Annealing buffer. Annealing reactions were heated in a water bath at 95°C for 5 min and then allowed to slowly cool overnight.

2.15.3 Gel Purification of Oligonucleotides and DNA Substrates

Radiolabelled oligonucleotides or annealed DNA substrates were purified on 12% native polyacrylamide gels at 200 V, 4°C, for 2-3 h. The gel was exposed to an Amersham hyperfilm ECL (GE Healthcare) for a few min, and the appropriate DNA bands were excised from the gel. The bands were cut to small pieces, and soaked in 900 µL 0.5X TBE overnight. The gel particles were spun down, the supernatant was transferred to a clean tube and the gel particles were further washed with 300 µL 0.5X TBE. To assess the elution efficiency, radioactive counts were measured using the liquid scintillation analyzer (Packard).

2.15.4 Protein - DNA Interaction Assays

2.15.4.1 Gel Shift Assays

Approximately 0.5 pmol of radiolabelled oligonucleotide were used per 10 μL reaction. The DNA was incubated with various concentrations of the respective proteins at 4°C or 30°C for 15 min up to 1 h and then subjected to native gel electrophoresis followed by phosphorimager analysis.

2.15.4.2 Pull-Down Assays with Biotinylated DNA

2.15.4.2.1 Binding DNA Structures to Streptavidin Beads

Streptavidin beads (ImmunoPure, Pierce) were washed 3 times in 0.5X TBE buffer. Equal amounts of radioactive counts per DNA structure were incubated with streptavidin beads. The radioactive counts of the input sample and the unbound DNA were compared to assess how much DNA was bound to the beads. In general, approximately 5-10 pmol DNA were bound per 15 μL aliquots of beads. After washing 3 times in 0.5X TBE beads were either used immediately or stored at 4°C for subsequent pull-down experiments as described in paragraph 2.15.4.2.3.

2.15.4.2.2 Binding ssDNA to Streptavidin Beads

Streptavidin beads (ImmunoPure, Pierce) were washed 3 times in PBS with 1 mM EDTA. Unlabelled biotinylated oligonucleotides were immobilized on the beads for 1 h at room temperature. The absorbance at 260 nm for both the input sample and the unbound DNA was compared to assess how much DNA was bound to the beads. Typically and unless stated otherwise, 5 pmol DNA was bound per 15 μL aliquots of beads. After washing 3 times in PBS with 1 mM EDTA beads were either used immediately or stored at 4°C for subsequent pull-down experiments as described in paragraph 2.15.4.2.3.

2.15.4.2.3 DNA-Bound Streptavidin Pull-Down Assays

DNA-bound streptavidin beads, prepared as described in 2.15.4.2.1 or in 2.15.4.2.2, were washed three times in PD Binding buffer (Low- or High-Salt according to the experiment). 15 µL of beads were incubated with 5 pmol ^{HisVSV}Rad18 for 1 h at 4°C (100 µL). Alternatively, prior to Rad18 addition, increasing amounts of purified yeast RPA or bacterial SSB (Promega) (2.4, 8 and 24 pmol) were incubated with the beads for 30 min at 4°C (300 µL), followed by a brief wash in PD Binding buffer (Low- or High-Salt according to the experiment - 500 µL each wash). After incubation with ^{HisVSV}Rad18, the beads were washed three times with 500 µL of High-Salt Binding buffer and twice with the same buffer without BSA. Bound material was eluted with 20 µL of 2X NuPage sample buffer containing a reducing agent and incubated at 70°C for 10 min. The samples were then analysed by SDS-PAGE (NuPage 4-12% Bis-Tris Gel – Invitrogen) followed by Western blotting.

2.16 Protein - Protein Interaction Assays

2.16.1 Co-immunoprecipitation of Rad6 with ^{HisVSV}Rad18

Approximately 5 pmol of ^{HisVSV}Rad18 were diluted into 100 µL COIP Binding buffer. The input was pre-cleared with 60 µL of protein-G agarose beads (Roche) at 4°C for 1 h. A 1/10 dilution of anti-Rad18 DH1 terminal bleed (from the 50% (v/v) glycerol stock) was prepared in PBS and centrifuged at maximal speed for 2 min. 5 µL of the antibody's supernatant were added to the cleared input and incubated at 4°C for 2.5 h. After centrifugation for 1 min at maximal speed, the supernatant was mixed with 20 µL of washed protein-G agarose beads at 4°C for 1 h. After four washes in COIP Binding buffer, the beads were washed once in COIP Washing buffer. The samples were eluted with 20 µL of 2X NuPage sample buffer containing a reducing agent, incubated at 70°C for 10 min and subjected to SDS-PAGE (NuPage 4-12% Bis-Tris Gel – Invitrogen). Western blotting against Rad18 and Rad6 was carried out as follows: Rad18 was detected by terminal bleed of mouse 4 as described in paragraph 2.11.1.1.

Rad6 was detected by anti-Rad6 antibody (1:3000) followed by incubation with anti-rabbit γ chain specific peroxidase conjugated antibody (1:2000).

2.16.2 Glutathione Pull-Down Assays

2.16.2.1 In the Absence of ssDNA

Approximately 0.5 nmol of GST, ^{GST}Rfa1 (182-421) or ^{GST}Rfa2 were immobilized on 20 μL of glutathione sepharose 4 Fast Flow (GE Healthcare) in GST-PD Binding buffer for 30 min at 4°C. The beads were briefly washed with 500 μL GST-PD Binding buffer. 10 pmol ^{HisVSV}Rad18 were added in the same buffer containing 100 μg/mL BSA and incubated at 4°C for 1 h. Then, the beads were washed 3 times with 500 μL of GST-PD Binding buffer containing BSA and twice more with the same buffer without BSA. Finally, the bound material was eluted with 20 μL of 2X NuPage sample buffer containing a reducing agent, incubated at 70°C for 10 min and subjected to SDS-PAGE (NuPage 4-12% Bis-Tris Gel – Invitrogen) followed by Coomassie staining or Western blotting.

2.16.2.2 In the Presence of ssDNA

Approximately 0.5 nmol of GST or ^{GST}Rfa1 (182-421) were incubated with oligo-dT of different lengths (10, 16, 35) at either 1:1 ratio or 1:5 excess of oligo for 45 min at 4°C in GST-PD Binding buffer. Each sample was then incubated with 20 μL of glutathione sepharose 4 Fast Flow (GE Healthcare) at 4°C for 1.5 h. Subsequently, the beads were washed once with 500 μL GST-PD Binding buffer containing 100 μg/mL BSA. 10 pmol ^{HisVSV}Rad18 were added and the pull-down reactions were carried out as described in paragraph 2.16.2.1.

2.16.3 Protein-Derivatised Sepharose Pull-down Assays

2.16.3.1 Coupling Proteins to CH-Sepharose Beads

Yeast RPA (2.12.1), BSA or SSB were covalently coupled to CH-sepharose 4B beads (GE Healthcare) at 2.5 μg/μL according to the manufacturer's instructions.

2.16.3.2 Protein-Derivatised Sepharose Pull-Down Assays

Protein-derivatised sepharose beads (2.16.3.1) were used for pull-down reactions (15 μL of beads per reaction). Approximately 5 pmol of recombinant Rad6, ^{HisVSV}Rad18 and ^{His}PCNA were added to the beads and incubated in Coupled-PD Binding buffer, supplemented with 2.5 u benzonase (Novagen), at 4°C for 1 h. The beads were washed 5 times with Coupled-PD Washing buffer. Bound material was eluted with 20 μL of 2X NuPage loading buffer containing a reducing agent, incubated at 70°C for 10 min and analysed by SDS-PAGE followed by Western blotting.

2.17 Analysis of Post-Translational Modifications of Proteins

2.17.1 Ni-NTA Pull-Down Assays from Yeast Extracts under Denaturing Conditions

Yeast strains harbouring the gene of interest fused to a His-tag were grown in adequate conditions to allow the expression of the His-tagged protein. Overnight cultures were diluted in adequate medium and subsequently were grown for 2 generations up to $O.D._{600}$ = 1-2. When appropriate, cells were treated with DNA damaging agents for 60-90 min. Approximately 70-100 $O.D._{600}$ of cells were harvested per strain by centrifugation at 1800g for 5 min in 50 mL falcon tubes at room temperature. Cells were re-suspended in 5 mL of ice-cold sterile water. 800 μL of freshly prepared NaOH / β-ME solution were added, the tubes were mixed by vortex and the cells were incubated on ice for 20 min. Then, 800 μL of 55% (w/v) TCA were added, the tubes were mixed by vortex and incubated on ice for additional 20 min. Tubes were centrifuged at 8000 RPM at 4°C for 20 min in a F-34-6-38 rotor (Eppendorf). The supernatant was removed by aspiration and the pellet was centrifuged at the same conditions for additional 2 min, and the supernatant was aspirated as before. The pellet was then re-suspend in 1.5 mL of buffer A and allowed to rotate at room temperature for 1 h (or until the pellet was completely dissolved). Subsequently, the solution was transferred to a microcentrifuge tube and centrifuged at maximal speed for 15 min at room temperature. The supernatant

was then used for the following Ni-NTA pull-down procedure. Ni-NTA agarose beads (QIAGEN) were washed 3 times in 1 mL of buffer A followed by short centrifugations of 5 s at 5000 RPM. 20 μL of beads (40 μL of 50% slurry) were used per pull-down reaction. The cell extract was added to the beads along with 22.5 μL 1M imidazole and 22.5 μL 10% (v/v) Tween 20, resulting in final concentrations of 15 mM and 0.15% (v/v), respectively. The tubes were left to mix overnight on a rotating wheel at room temperature. The beads were harvested by a brief centrifugation of 5 s at 5000 RPM, and most of the supernatant was carefully removed with a pipette. The rest of the supernatant was then removed by a 25 μL Hamilton syringe. The beads were washed twice with buffer A supplemented with 0.05% (v/v) Tween 20. Then, 3 times with buffer C, supplemented with 0.05% (v/v) Tween 20. Finally, the beads were eluted in 20-40 μL of 2X NuPage loading buffer containing a reducing agent, incubated at 70°C for 10 min and analysed by SDS-PAGE followed by Western blotting.

3 Results I: Purification and Catalytic Activity of Rad18

3.1 Introduction

My initial goal was to gain insights into the *in vitro* activity of the Rad18 protein from *S. cerevisiae*, especially with relevance to PCNA mono-ubiquitylation. Based on Bailly *et al.* (1997), I intended to purify yeast Rad18 in a complex with Rad6. My first approach was to purify these proteins recombinantly from *E. coli*. Two different cloning strategies were used. One strategy was based on the pETDuet-1 expression vector that facilitated the cloning of two open reading frames. This vector was used to generate two constructs harbouring both *RAD18* and *RAD6* genes with one or the other fused to an N-terminal His tag. The other strategy was based on a bi-cistronic *RAD6-RAD18* construct where the two genes were connected by a linker with a ribosomal entry site. This insert was cloned into a pUC118 expression vector under the control of the *phoA* promoter. This promoter allows a gradual increase in gene expression following phosphate starvation conditions and was previously used by Ulrich *et al.* (1995) for the successful production of antibodies. Following various optimisation experiments, the best expression conditions were obtained for the *phoA* ^{His}*RAD18-RAD6* construct and the proteins were purified using Ni-NTA affinity chromatography based on Biswas *et al.* (1995). Although the protein preparation exhibited ubiquitin-conjugating activity, this was not specific for PCNA. Moreover, two of the prominent protein bands in the preparation corresponding in size to yRad18, were identified as metabolic bacterial proteins by mass spectrometry analysis. As a result, I recognised the necessity to explore alternative expression systems.

Even though a purification of yeast protein from its native organism would seem the obvious choice, the relatively low expression levels of the *RAD18* gene has posed a significant challenge. In order to obtain constitutive over-expression of the Rad18 and the Rad6 proteins, a yeast strain was constructed to harbour both the *RAD6* and the *RAD18* genes under the control of the *ADH1* promoter. Nonetheless, the Rad18 protein, which was fused to an N-terminal His-tag, was

only detected by Western blot analysis. Following a preliminary attempt to purify Rad18 by Ni-NTA affinity chromatography, which resulted in poor yield, this approach was abandoned.

Another strategy was to use yeast strains harbouring either the *RAD6* or the *RAD18* genes fused to a C-terminus TAP tag (these strains were obtained from Open biosystems). This strategy was shown to be useful for native purification of low abundance protein complexes (Puig *et al.*, 2001). A few purification attempts were carried out. Essentially, Rad6-TAP was isolated and identified by mass-spectrometry. However, none of the prominent bands that co-purified with Rad6 and corresponded in size to the yRad18 protein were identified as such. Subsequently, this approach was not pursued.

In parallel to the trials described above, insect cells were tested as an alternative expression system. Baculovirus harbouring a copy of the yeast ^{HisVSV}*RAD18* gene was constructed and used to infect insect cells. Consequently, high expression levels of *RAD18* were observed in whole cell extracts of baculovirus-infected insect cells, thus providing a promising source for protein production.

3.2 Results

3.2.1 Co-infection with ^{HisVSV}*RAD18* and *RAD6* Baculoviruses Improves Solubility of Rad18

As previously mentioned, insect cells (either High Five or Sf9), infected with a baculovirus harbouring a copy of yeast ^{HisVSV}*RAD18,* proved to express high levels of *RAD18*. However, initial experiments revealed that the protein was mostly insoluble (Figure 3.1A). To overcome this, different methods for cell lysis were analysed. Cell lysis was carried out using either Dounce homogenizer alone, a combination of Dounce homogenizer and sonication, or gentler extraction using a hypo-osmotic buffer followed by addition of a detergent. Moreover, Tris-HCl, HEPES or sodium phosphate buffers were tried combined with detergents (NP-40 or triton X-100) and with osmolytes (sucrose or glycerol).

Bailly *et al.* (1997a) were only able to purify Rad18 from yeast cells when it was associated in a complex with Rad6. This suggests that Rad6 contributes to Rad18's proper conformation. To test if this observation also applied to yeast Rad18 produced in insect cells, the cells were co-infected with a baculovirus harbouring a copy of the yeast *RAD6* gene. As shown in Figure 3.1B, the levels of Rad18 protein in whole cell extracts were similar when the cells were infected either with ^{HisVSV}*RAD18* virus alone or with both ^{HisVSV}*RAD18* and *RAD6* viruses. However, following cell fractionation and ultracentrifugation of the cytoplasmic and nuclear fractions, an increased amount of soluble Rad18 could be detected by Western blot analysis in the extracts of cells that were co-infected.

The optimised protocol for cell lysis and subsequent manipulation prior to Rad18 purification was based on Cai *et al.* (1996) and it is described in detail in paragraph 2.12.6.1. In brief, 48 h co-infected insect cells were lysed with a Dounce homogenizer, and the cellular extract was fractionated into nuclei and cytoplasm by two centrifugation steps: low speed centrifugation followed by an ultracentrifugation. To prevent carry-over of any insoluble Rad18, the cytoplasmic fraction was subjected to an ultracentrifugation step after its isolation. Both fractions were used in subsequent steps separately.

3.2.2 Purification of the ^{HisVSV}Rad18-Rad6 Complex from Baculovirus-Infected Insect Cells

The ^{HisVSV}Rad18-Rad6 complex was partially purified under native conditions by Ni-NTA affinity chromatography as described in paragraph 2.12.6.1. Modifications to the purification protocol, which was based on Cai *et al.* (1996), involved the use of HEPES buffer instead of Tris-HCl. In addition, 100 μM $ZnCl_2$ were included in the RAD18 Washing III, Elution and Dialysis buffers, following a suggestion in Mackereth *et al.* (2000) that including $ZnCl_2$ in the purification steps could improve the conformational stability of zinc binding proteins. Elution fractions that contained both Rad18 and Rad6 were pooled and either subjected to further purification steps as described later in paragraph 3.2.4 or dialysed, concentrated and quantified as described in paragraph 2.12.6.1. As shown in Figure 3.2A and Figure 3.2B, both ^{HisVSV}Rad18 and Rad6 proteins can

be detected by Coomassie staining and by Western blot analysis. In addition, the identity of the prominent band in the protein preparation, which corresponded in size to yeast ^{HisVSV}Rad18, was verified by mass spectrometry, as was the band corresponding in size to yeast Rad6. The purity of the ^{HisVSV}Rad18 protein was estimated to be 80%. For control purposes, the same purification procedure was carried out on insect cells that were only infected with *RAD6* baculovirus. As shown in Figure 3.2C and Figure 3.2D, the mock preparation contained a small amount of Rad6, but no Rad18.

3.2.3 Rad6 Co-purifies with ^{HisVSV}Rad18

3.2.3.1 Gel Filtration

The purified complex from paragraph 3.2.2 was subjected to further qualitative analysis by gel filtration, using a Superdex 6 PC 3.2/30 column (GE Healthcare). The fractions obtained from this column were subjected to SDS-PAGE and analysed by Western blot. As shown in Figure 3.3A, (fractions 27-31), Rad6 was found to co-elute with Rad18, verifying that they form a complex. However, free Rad6 was also found (fractions 34-39), suggesting either that the complex is partially unstable or that an excess of Rad6 had bound non-specifically to the Ni-NTA affinity column during purification. Using a mix of standard proteins, the complex size was estimated to be around 450 kDa. Assuming a stoichiometric ratio of 1:1 between Rad18 and Rad6 obtained from yeast (Bailly *et al.*, 1997a), a complex formation of six Rad18-Rad6 hetero-dimers could theoretically fit to this approximated molecular weight. However, using gel filtration analysis to estimate the size of a complex can be quite inaccurate, as the elution profile is affected by the proteins' shape. Moreover, according to Notenboom *et al.* (2007), mammalian Rad18-Rad6 complex was found to form a dimer of hetero-dimers.

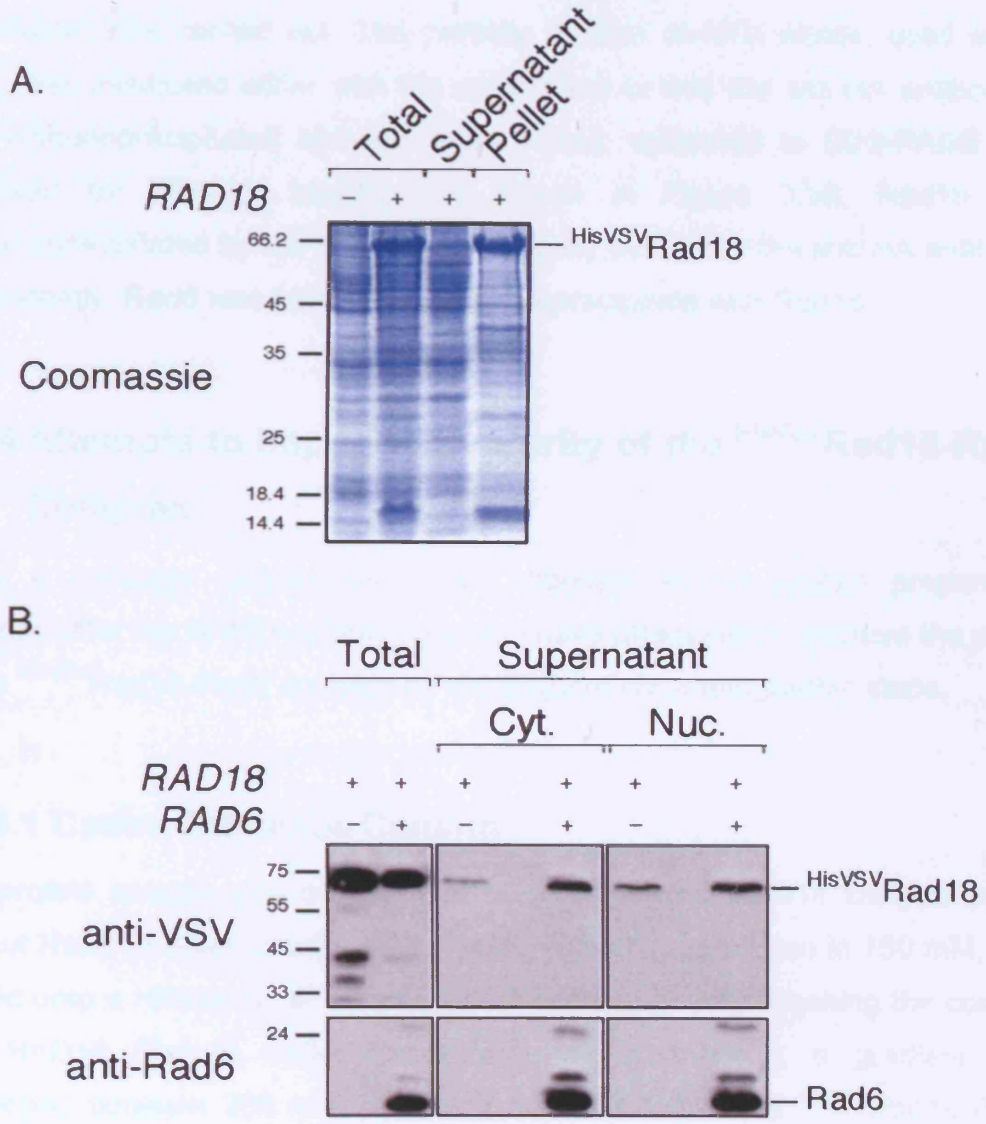

Figure 3.1 – Solubility of ^{HisVSV}*RAD18* produced in baculovirus-infected insect cells

A. A Coomassie-stained gel of total cell extracts obtained from either non-infected or ^{HisVSV}*RAD18* baculovirus-infected High Five insect cells. The cells were lysed by sonication in Tris-HCl buffer containing NP-40 (Total). Note that yeast ^{HisVSV}RAD18 was over-expressed. The cell extracts were subjected to centrifugation; The supernatant and the pellet material were compared.

B. Western blot analysis of total cell extracts derived from High Five insect cells infected either with ^{HisVSV}*RAD18* virus alone or in combination with *RAD6* virus. Cell extracts were prepared using the optimised protocol and the supernatants of cytoplasmic (Cyt.) and nuclear (Nuc.) fractions obtained after an ultracentrifugation step were analysed. Anti-VSV antibody was used for ^{HisVSV}Rad18 detection and anti-Rad6 antibody was used for Rad6 detection.

3.2.3.2 Co-Immunoprecipitation

In order to verify that Rad6, detected in the protein preparation, was indeed associated with Rad18 in a stable complex, a co-immunoprecipitation experiment was carried out. The partially purified Ni-NTA eluate, used as an input, was incubated either with the anti-Rad18 or with the anti-HA antibodies. The immunoprecipitated samples were eluted, subjected to SDS-PAGE and analysed by Western blotting. As shown in Figure 3.3B, Rad18 was immunoprecipitated by the anti-Rad18 antibody but not by the anti-HA antibody. Consistently, Rad6 was found to co-immunoprecipitate with Rad18.

3.2.4 Attempts to Improve the Purity of the ^{HisVSV}Rad18-Rad6 Complex

Since a nuclease contamination was detected in the protein preparation obtained after the Ni-NTA affinity column, I have attempted to improve the purity of the ^{HisVSV}Rad18-Rad6 complex by subsequent chromatographic steps.

3.2.4.1 Cation Exchange Column

The protein sample was diluted at a ratio of 1:1 with RAD18 Dialysis buffer without NaCl, in order to adjust the starting NaCl concentration to 150 mM, and loaded onto a HiTrap Q HP column (GE Healthcare). After washing the column with RAD18 Dialysis buffer (containing 150 mM NaCl), a gradient was developed between 200 mM NaCl and 500 mM NaCl. The ^{HisVsV}Rad18-Rad6 complex was found to elute in a discrete peak around 300 mM NaCl. However, the resulting purified complex still exhibited significant nuclease activity and the overall purity did not seem to be significantly improved.

3.2.4.2 Hydrophobic Phenyl Sepharose Chromatography

Hydrophobic phenyl sepharose chromatography requires the application of a sample in a high ionic strength buffer, to enhance the hydrophobic interactions between the proteins and the column. Consequently, the protein sample was adjusted to 1.5 M NaCl, loaded onto a HiTrap phenyl HP column (GE

Healthcare) and the column was washed with RAD18 Dialysis buffer containing 1.5 M NaCl. Two linear gradients were applied to elute the column. First, the NaCl concentration was gradually reduced to 200 mM NaCl. Thereafter, it was gradually reduced down to 0 mM NaCl. ^{HisVSV}Rad18 was found to elute as a discrete peak around 200 mM NaCl. However, Rad6 did not bind to the column and was detected in the column's flow through. Unfortunately, this resulted in the precipitation of the ^{HisVSV}Rad18 protein in subsequent steps. Similar results were obtained when ammonium sulfate was used instead of NaCl.

3.2.4.3 Heparin Column

Heparin is a naturally occurring glycosaminoglycan. The purification method using Heparin columns is based on the affinity of different proteins for heparin. It is often used for the purification of DNA-binding proteins, as it is negatively charged and can mimic the charge of the DNA. The protein sample was dialysed in RAD18 Dialysis buffer at 4°C overnight as described in 2.12.6.1. The sample was loaded onto the HiTrap Heparin HP column (GE Healthcare) and the column was washed with RAD18 Dialysis buffer. To elute the column, a two-step linear gradient was applied. The gradient was developed between 150 mM NaCl and 500 mM NaCl followed by a second gradient between 500 mM NaCl and 1 M NaCl. The ^{HisVsV}Rad18-Rad6 complex was found to elute in two peaks around 500 mM and 600 mM NaCl. However, the overall purity did not seem to improve much and the nuclease activity still persisted in the protein preparation.

Additional attempts to improve the purity of the ^{HisVSV}Rad18-Rad6 complex were not pursued.

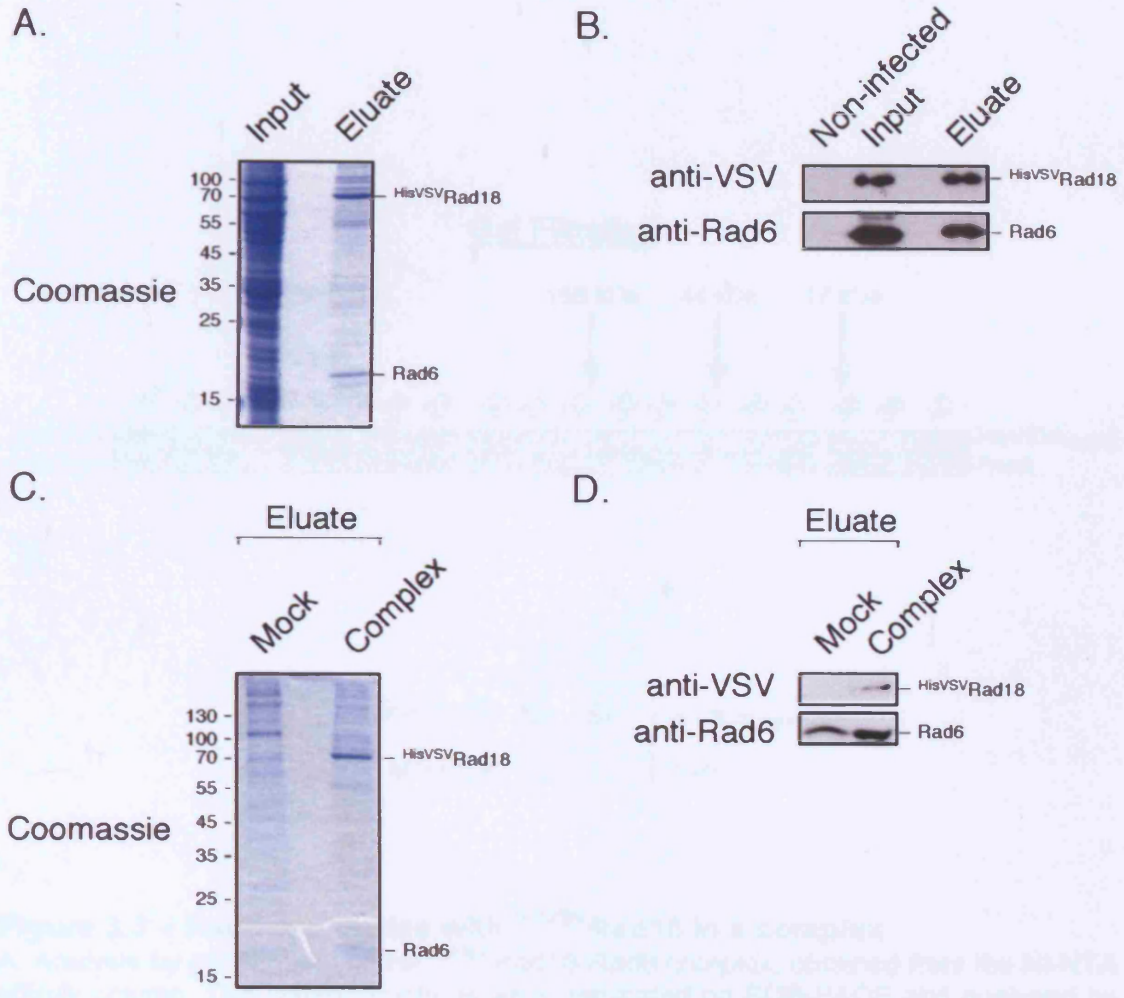

Figure 3.2 – Partial purification of the yeast ^{HisVSV}Rad18-Rad6 complex from baculovirus-infected insect cells

A. Analysis of the input and the eluate obtained after Ni-NTA affinity chromatography by Coomassie staining.

B. Analysis of the input and the eluate obtained after Ni-NTA affinity chromatography by Western blotting. Whole cell extract from non-infected cells was used as a negative control. ^{HisVSV}Rad18 was detected by anti-VSV antibody and Rad6 was detected by anti-Rad6 antibody.

C. Comparison by Coomassie staining between the mock eluate, obtained from *RAD6* baculovirus-infected insect cells, and the purified ^{HisVSV}Rad18-Rad6 complex, obtained from *RAD6* and *^{HisVSV}RAD18* baculoviruses-infected insect cells.

D. Comparison by Western blot analysis between the mock eluate, obtained from *RAD6* baculovirus-infected insect cells, and the purified ^{HisVSV}Rad18-Rad6 complex, obtained from *RAD6* and *^{HisVSV}RAD18* baculoviruses-infected insect cells. ^{HisVSV}Rad18 was detected by anti-VSV antibody and Rad6 was detected by anti-Rad6 antibody.

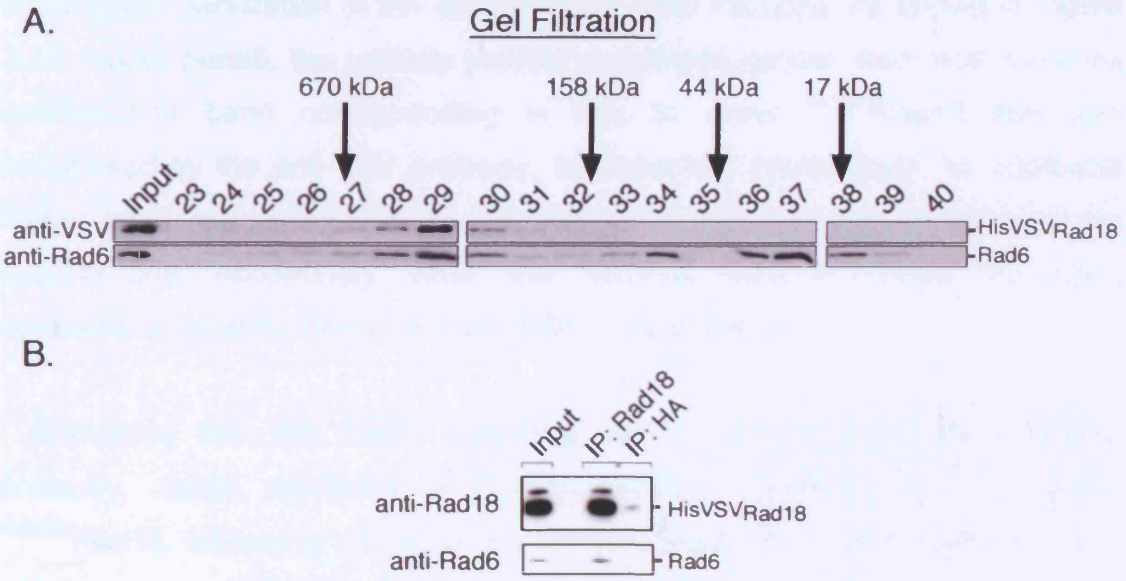

Figure 3.3 – Rad6 associates with ^{HisVSV}Rad18 in a complex
A. Analysis by gel filtration of the ^{HisVSV}Rad18-Rad6 complex, obtained from the Ni-NTA affinity column. The column fractions were separated on SDS-PAGE and analysed by Western blot. ^{HisVSV}Rad18 was detected by anti-VSV antibody and Rad6 was detected by anti-Rad6 antibody. Arrows indicate the molecular weights of the standard proteins used as a control.
B. The ^{HisVSV}Rad18-Rad6 complex, obtained from the Ni-NTA affinity column, was subjected to immunoprecipitation either with anti-Rad18 (polyclonal DH1 rabbit serum) or with anti-HA (polyclonal) antibodies. Western blot analysis was performed using anti-Rad18 antibody (polyclonal mouse 4 serum) for Rad18 detection, and anti-Rad6 antibody followed by anti-rabbit γ chain-specific peroxidase-conjugated antibody, for Rad6 detection.

3.2.5 Rad18 is Auto-ubiquitylated

3.2.5.1 Yeast ^{HisVSV}Rad18 is Ubiquitylated in Insect Cells

As described in paragraph 3.2.1, the purification procedure of yeast ^{HisVSV}Rad18-Rad6 complex from baculovirus-infected insect cells involved the fractionation of the cellular extract into nuclei and cytoplasm followed by subsequent purification of the complex from both fractions. As shown in Figure 3.4A (upper panel), the partially purified complexes derived from both fractions contained a band corresponding in size to yeast ^{HisVSV}Rad18 that was recognised by the anti-VSV antibody, as expected. Interestingly, an additional higher band was detected in the cytoplasmic fraction that was absent from the nuclear one. Accordingly, when the fractions were combined, this band appeared to become diluted (Figure 3.4A – upper panel).

I postulated that this higher migrating band, recognised by the anti-VSV antibody, could represent a post-translational modified form of yeast ^{HisVSV}Rad18. Miyase *et al.* (2005) found that mammalian Rad18 existed in two species, an unmodified and a mono-ubiquitylated form, with the latter predominantly found in the cytoplasm. Accordingly, the size of this band corresponded to the size of a nuclei-derived ^{HisVSV}Rad18 protein conjugated to one ubiquitin moiety *in vitro* (Figure 3.5A and Figure 3.5B). This will be further discussed in paragraph 3.2.5.3 below. Thus, most probably, yeast ^{HisVSV}Rad18 is mono-ubiquitylated in baculovirus-infected insect cells, and its modified form can be found in the cytoplasm.

As shown in Figure 3.4A (lower panel), the partially purified complexes derived from both fractions contained comparable levels of Rad6. Similarly to Rad18, Rad6 was also modified, most probably by ubiquitin. However, differently from Rad18, the higher migrating band, corresponding to mono-ubiquitylated Rad6, could be detected in the complexes derived from both fractions, although it appeared weaker in the nuclei-derived one.

3.2.5.2 Rad18 is Ubiquitylated in Yeast Cells

It was not clear whether ubiquitylation of yeast Rad18 in baculovirus-infected insect cells was an artefact of the expression system or a physiologically relevant post-translational modification. Therefore, it was important to test if Rad18 was also modified in yeast cells. To this end, either *WT*, *RAD18*^{6HA} or *rad6 RAD18*^{6HA} yeast strains were transformed with an episomal plasmid containing a His-tagged *UBI* gene under the control of the *CUP1* promoter (no. 821). As a negative control, the *RAD18*^{6HA} strain was transformed with an empty plasmid (no. 308). Following induction of ^{His}*UBI* over-expression with $CuSO_4$, the post-translational modifications of Rad18 in the different strains were analysed by Ni-NTA pull-down assays under denaturing conditions. As shown in Figure 3.4B (lower panel – anti-His antibody), the presence of ^{His}ubiquitin conjugates was verified in total cell extracts from strains harbouring the *CUP1-*^{His}*UBI* construct. In addition, these conjugates were precipitated as a result of the Ni-NTA pull-down assay, confirming that the experiment was working properly. According to the loading control, equivalent amounts of cells were used from each strain for the preparation of cell extracts (Figure 3.4B – middle panel – anti-PGK antibody). Correspondingly, similar Rad18^{6HA} levels were observed in total cell extracts derived from the *rad6 RAD18*^{6HA} strain, harbouring the *CUP1-*^{His}*UBI* construct, or from the *RAD18*^{6HA} strain, harbouring the empty plasmid (Figure 3.4B – upper panel – anti-HA antibody). In contrast, the cell extract obtained from the *RAD18*^{6HA} strain, harbouring the *CUP1-*^{His}*UBI* construct, appeared to contain somewhat higher Rad18^{6HA} levels as well as another band, probably corresponding to mono-ubiquitylated Rad18^{6HA} (Figure 3.4B – upper panel – anti-HA antibody). The identity of this band as mono-ubiquitylated Rad18^{6HA} was further confirmed as it was precipitated by the Ni-NTA pull-down assay, together with another higher migrating band, probably corresponding to Rad18^{6HA} conjugated to two ubiquitin moieties. The results suggest that this pull-down experiment was useful for the identification of His-tagged ubiquitin-Rad18^{6HA} conjugates, as unmodified Rad18^{6HA} was not precipitated. As mentioned above, the strains harbouring the *CUP1-*^{His}*UBI* construct did not contain equal levels of the Rad18^{6HA} protein. Even though the *rad6 RAD18*^{6HA} strain had less Rad18 compared with the *RAD18*^{6HA} strain, mono-ubiquitylated Rad18^{6HA} could be pulled-down from it, suggesting that

under the tested conditions, the *in vivo* ubiquitylation of Rad18 does not depend on Rad6.

3.2.5.3 ^{HisVSV}Rad18 is Auto-ubiquitylated *In vitro*

The ability of E3 ligases to become auto-ubiquitylated is often regarded as a hallmark of their catalytic activity in the absence of a substrate. Therefore, ^{HisVSV}Rad18-Rad6 complexes derived from the cytoplasmic or the nuclear fractions were assessed for their auto-ubiquitylation activity by *in vitro* ubiquitylation assays with the E1 activating enzyme and ubiquitin, but without PCNA. As shown in Figure 3.5A, the ^{HisVSV}Rad18 protein of both complexes was auto-ubiquitylated in the complete reactions, but not in those lacking the E1 enzyme. These results indicate that the ^{HisVSV}Rad18 protein in both complexes is functional, and that its RING domain is properly folded. After 2 h of incubation at 30°C, the nuclei-derived ^{HisVSV}Rad18-Rad6 complex was conjugated to one ubiquitin moiety. This mono-ubiquitylated ^{HisVSV}Rad18 corresponded in size to the higher migrating band observed in the cytoplasm-derived ^{HisVSV}Rad18 protein preparation. This result is consistent with the suggestion that the latter consists of both an unmodified and a mono-ubiquitylated form of ^{HisVSV}Rad18.

As shown in Figure 3.5B, the levels of ubiquitin-Rad18 conjugates increased with increased incubation time in the reactions containing the cytoplasm-derived ^{HisVSV}Rad18-Rad6 complex (Cyt.), as expected. However, the auto-ubiquitylation activity of the nuclei-derived ^{HisVSV}Rad18-Rad6 complex (Nuc.) was significantly reduced compared to that of the cytoplasm-derived complex (Cyt.). Since the Rad6 content in both complexes was similar (Figure 3.4A – lower panel), it is unlikely that this protein is responsible for the difference observed in the auto-ubiquitylation efficiency. Rather, it is more probable that this difference originates from a variation in Rad18 between the two protein preparations. Possibly, mono-ubiquitylation of ^{HisVSV}Rad18, found in the cytoplasm-derived complex, could enhance its catalytic activity. Alternatively, the nuclei-derived protein preparation might contain a contaminant that limits the efficiency of the auto-ubiquitylation reaction.

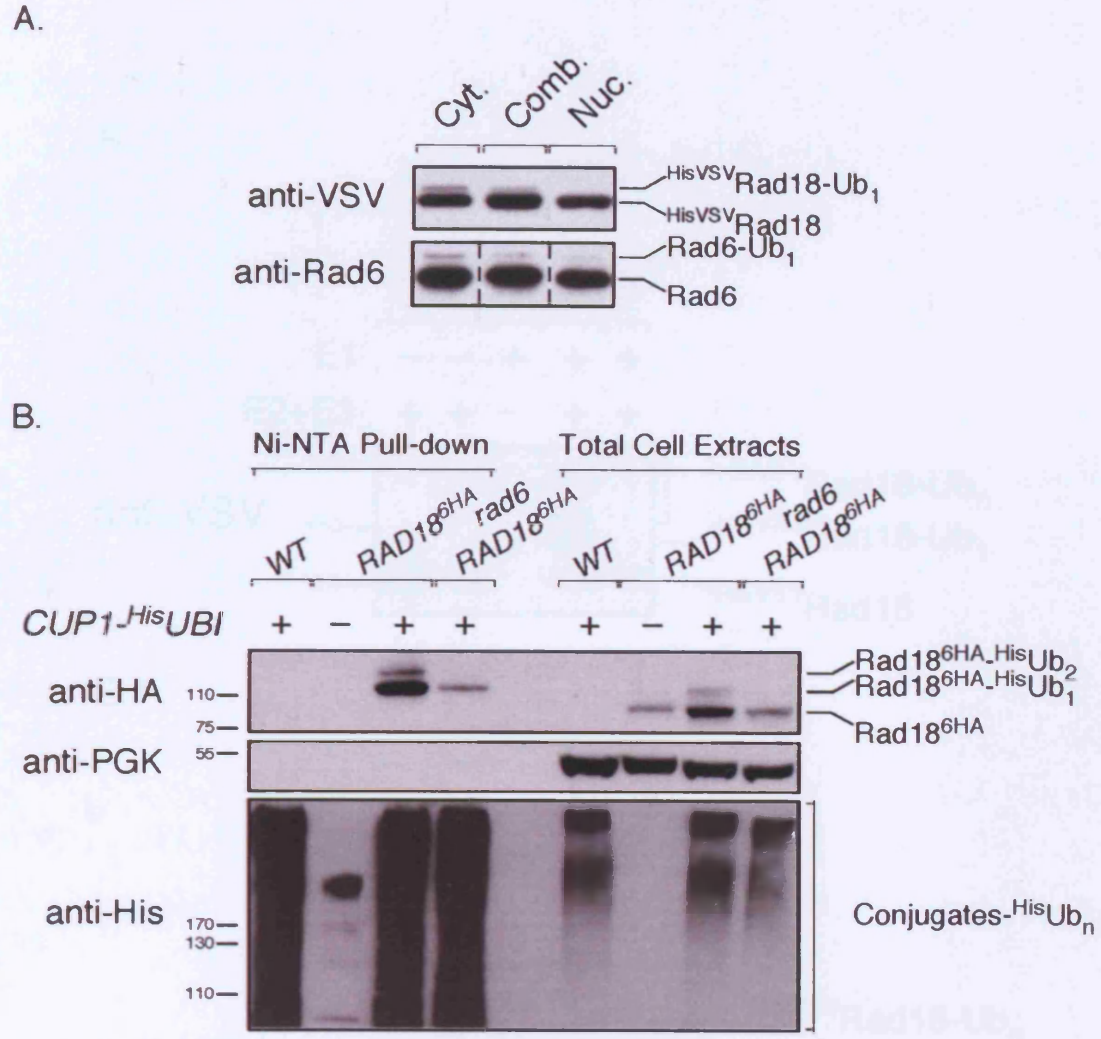

Figure 3.4 – Rad18 is ubiquitylated *in vivo*

A. The yeast ^{HisVSV}Rad18 and Rad6 proteins are post-translationally modified in baculovirus-infected insect cells. Western blot analysis of partially purified ^{HisVSV}Rad18-Rad6 complexes obtained from isolated cytoplasm (Cyt.) or nuclei (Nuc.). A 1:1 ratio mix of both complexes was loaded in the middle lane (Comb.). Rad18 was detected by anti-VSV antibody and Rad6 was detected by anti-Rad6 antibody. Note that for Rad18 analysis, the samples were separated on an 8% SDS-PAGE gel, whereas for Rad6 analysis, the samples were separated on a 12% gel.

B. Rad18 is ubiquitylated in yeast cells. The *WT*, *RAD18^{6HA}* or *rad6 RAD18^{6HA}* yeast strains, harbouring the *CUP1-^{His}UBI* construct, or the *RAD18^{6HA}* strain, harbouring an empty plasmid, were induced for ^{His}*UBI* over-expression with 100 mM $CuSO_4$. ^{His}Ubiquitin conjugates were precipitated from the different strains by Ni-NTA pull-down assays under denaturing conditions. In parallel, total cell extracts were prepared as well. Samples were subjected to SDS-PAGE followed by Western blot analysis. ^{His}Ubiquitin conjugates were detected with anti-ubiquitin antibody. PGK was used as a loading control and detected with anti-PGK antibody. Rad18^{6HA} was detected with anti-HA antibody (polyclonal).

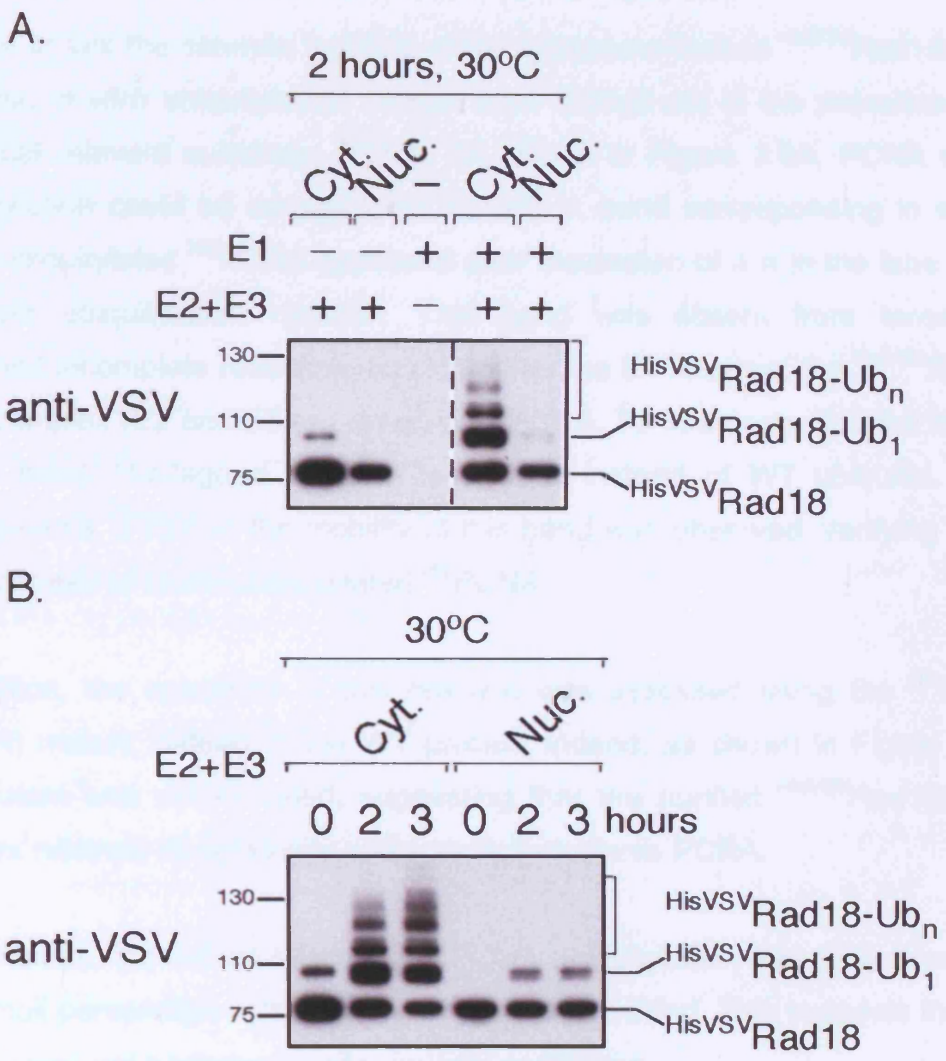

Figure 3.5 – ^{HisVSV}Rad18 is auto-ubiquitylated *in vitro*

A. Approximately 3 μM of ^{HisVSV}Rad18-Rad6 complexes, purified either from the cytoplasmic fraction (Cyt.) or from the nuclear fraction (Nuc.) of baculovirus-infected insect cells, were incubated in buffer containing 25 mM Tris-HCl, pH 7.5, 100 mM NaCl, 10 mM $MgCl_2$, 5 mM DTT and 10 mM ATP at 30°C for 2 h. The complete ubiquitylation reaction contained 190 nM E1 enzyme and 39 μM ubiquitin. Incomplete ubiquitylation reactions, lacking the E1 enzyme, were used as a negative control. The reactions were stopped; samples were subjected to SDS-PAGE and analysed by Western blotting. ^{HisVSV}Rad18 was detected by anti-VSV antibody.

B. Same as in A., but complete ubiquitylation reactions were incubated at 30°C for 0, 2 and 3 h.

3.2.6 The ^{HisVSV}Rad18-Rad6 Complex Mono-ubiquitylates PCNA *In vitro*

3.2.6.1 Specificity of PCNA Mono-ubiquitylation

In order to test the catalytic function of the cytoplasm-derived ^{HisVSV}Rad18-Rad6 complex, *in vitro* ubiquitylation assays were carried out in the presence of its biological relevant substrate, PCNA. As shown in Figure 3.6A, PCNA mono-ubiquitylation could be reconstituted *in vitro*. A band corresponding in size to mono-ubiquitylated ^{His}PCNA appeared after incubation of 4 h in the lane of the complete ubiquitylation reaction. This band was absent from lanes that contained incomplete reactions, lacking either the E1 enzyme, the ^{HisVSV}Rad18-Rad6 complex (E2 and E3 enzymes) or ^{His}PCNA. To further confirm the identity of this band, His-tagged ubiquitin was used instead of WT ubiquitin. As a consequence, a shift in the mobility of this band was observed, verifying that it corresponded to mono-ubiquitylated ^{His}PCNA.

In addition, the specificity of this reaction was assessed using the ^{His}PCNA (K164R) mutant instead of the WT protein. Indeed, as shown in Figure 3.6A, this mutant was not modified, suggesting that the purified ^{HisVSV}Rad18-Rad6 complex retained its selectivity and specificity towards PCNA.

Nevertheless, the overall efficiency of PCNA ubiquitylation was fairly poor as a very small percentage of the substrate became modified. This suggests that the reaction was not performed under optimal conditions.

3.2.6.2 Optimisation of PCNA Mono-ubiquitylation

In order to improve the conditions for PCNA mono-ubiquitylation *in vitro*, various parameters were analysed for their effects on the reaction efficiency. These included variations to buffer composition, buffer pH and incubation times. In short, HEPES buffer was found to be favourable over Tris-HCl. In addition, moderately acidic buffer conditions (pH 6) seemed to enhance PCNA modification over basic conditions (pH 9). Initially, 5 mM of the reducing agent DTT were used in the reaction. Reducing the concentration of this agent to 0.1

mM significantly contributed to PCNA ubiquitylation. Two different E1 enzymes, which were available in the lab, wheat E1 (purified in the lab) and yeast E1 (purchased from Boston Biochem) were tested, and the latter provided better results. Moreover, different concentrations of ubiquitin, PCNA and the modifying enzymes were tested. Comparison of reactions containing either the nuclei-derived ^{HisVSV}Rad18-Rad6 complex or the cytoplasm-derived one revealed that the latter exhibits better PCNA mono-ubiquitylation efficiency. This result correlated with the findings for Rad18 auto-ubiquitylation (Figure 3.5B).

In contrast to parameters that had an effect on the reaction efficiency, addition of 100 μM $ZnCl_2$ to the reaction buffer did not make a significant difference. Furthermore, addition of DNA (ssDNA, dsDNA or dsFork DNA structures) to the reaction did not result in enhanced PCNA modification. As shown in Figure 3.6B, by optimising the reaction parameters as mentioned above, the efficiency of PCNA mono-ubiquitylation by ^{HisVSV}Rad18-Rad6 complex was slightly improved (compare to Figure 3.6A).

However, as it later turned out, the conditions used for this reaction only allowed a basal level of PCNA modification by the Rad18-Rad6 complex. According to Garg and Burgers (2005), PCNA has to be loaded on DNA in order to obtain efficient PCNA mono-ubiquitylation. Nevertheless, under these optimised conditions of the basal reaction, the intensity of the band corresponding in size to mono-ubiquitylated PCNA increased with incubation time and with higher ^{HisVSV}Rad18-Rad6 concentrations (Figure 3.6B). Therefore, the ability of ^{HisVSV}Rad18-Rad6 to perform its catalytic activity towards its biological identified substrate, as established by Hoege *et al.* (2002), was confirmed in our *in vitro* system.

Interestingly, the auto-ubiquitylation levels of cytoplasm-derived ^{HisVSV}Rad18 were not altered in the presence or the absence of PCNA (Figure 3.6B – upper panel), suggesting that these two ubiquitylation reactions are independent of each other.

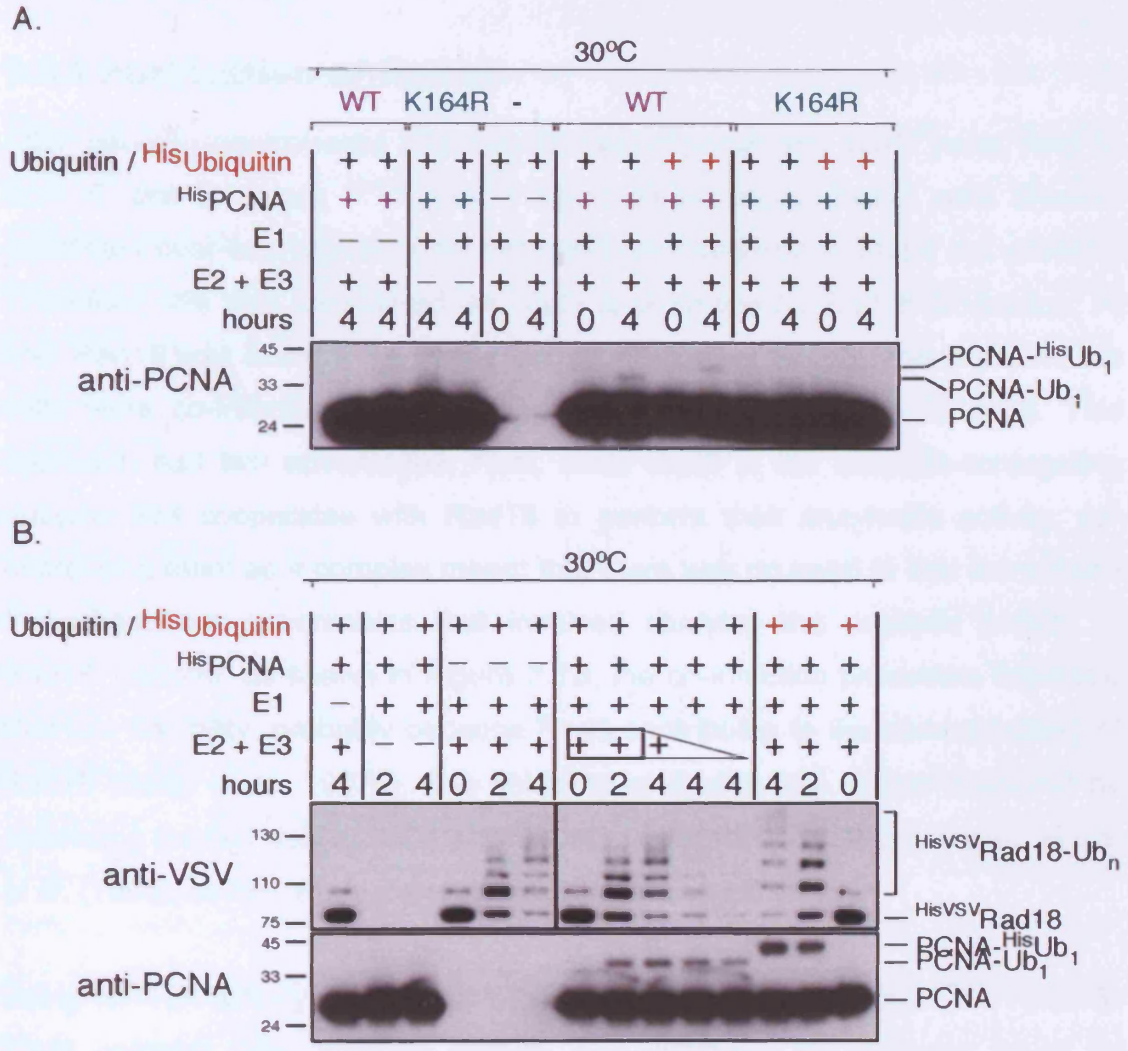

Figure 3.6 – PCNA mono-ubiquitylation can be reconstituted *in vitro* by the ^{HisVSV}Rad18-Rad6 complex

A. PCNA is specifically mono-ubiquitylated on K164 by the ^{HisVSV}Rad18-Rad6 complex *in vitro*. *In vitro* ubiquitylation assays were carried out using either WT or mutant ^{His}PCNA (K164R) as substrate (3 μM). His-tagged ubiquitin replaced WT ubiquitin where indicated (65 μM). Approximately 1.5 μM ^{HisVSV}Rad18-Rad6 complex were used as indicated. E1 was used at 190 nM. Samples were incubated in a buffer containing 25 mM Tris-HCl, pH 7.5, 100 mM NaCl, 10 mM $MgCl_2$, 5 mM DTT and 10 mM ATP at 30°C for 0 or 4 h. The reactions were stopped; samples were subjected to SDS-PAGE followed by Western blot analysis. PCNA was detected by anti-PCNA antibody (polyclonal).

B. PCNA mono-ubiquitylation was improved by modification of the reaction conditions. The complete reaction (8 μL) contained 65 μM ubiquitin, 112.5 nM E1, 3 μM PCNA and increasing concentrations of cytoplasm-derived ^{HisVSV}Rad18-Rad6 complex (0.75, 1.5 or 3 μM). The proteins were incubated in Ubiquitylation buffer at 30°C for 0, 2 or 4 h. Reactions were analysed as in A. ^{HisVSV}Rad18 was detected by anti-VSV antibody. PCNA was detected by anti-PCNA antibody (polyclonal).

3.3 Discussion

3.3.1 Purification of Rad18

After several unsuccessful attempts to over-express and purify yeast *RAD18* from *E. coli* or yeast, ^{HisVSV}*RAD18* bacoluvirus-infected insect cells showed significant over-expression of the recombinant constructs in whole cell extracts. Therefore, this was considered the method of choice for Rad18 production. At first, Rad18 was found to be nearly insoluble. In order to solve this problem, the cells were co-infected with a baculovirus harbouring the *RAD6* gene. This approach had two advantages. First, since Rad6 is the ubiquitin-conjugating enzyme that cooperates with Rad18 to perform their enzymatic activity, co-expressing them as a complex meant that there was no need to add extra Rad6 for subsequent experiments that involved studying the catalytic activity of Rad18. Second, as shown in Figure 3.1B, the co-infection procedure improved Rad18's solubility, probably because Rad6 contributes to the correct folding of Rad18 (Bailly *et al.*, 1997a). The solubility of Rad18 was further improved by optimising the cell lysis and the subsequent purification conditions based on Cai *et al.* (1996), as described in paragraphs 3.2.1 and 3.2.2.

Using Ni-NTA affinity chromatography, a partially purified yeast ^{HisVSV}RAD18-Rad6 complex was obtained (Figure 3.2). Although the complex could be purified either from the cytoplasm or from the nuclei fractions, the protein preparation resulting from the former was found to be more active than the latter (Figure 3.5 and data not shown). Thus, the cytoplasm-derived ^{HisVSV}Rad18-Rad6 complex was used in all subsequent experiments described in Chapters 4-7.

According to the Coomassie staining, it seemed that there was an excess of Rad18 compared to Rad6 in the protein preparation. However, since the Coomassie blue dye does not bind to all proteins with the same efficiency, it could be that the Rad6 protein does not stain as well as the Rad18 protein. Alternatively, Rad6 could have been partially lost during the purification procedure.

The association of Rad18 with Rad6 in a complex was verified by gel filtration (Figure 3.3A) as well as by co-immunoprecipitation (Figure 3.3B). Some of the gel filtration fractions contained free Rad6. As this was not a characteristic of all the protein preparations obtained in separate experiments, and since the mock purification, derived from *RAD6* baculovirus-infected insect cells, contained a residual amount of Rad6 (Figure 3.2C and Figure 3.2D), it is likely that a small percentage of Rad6 had bound non-specifically to the Ni-NTA column. Another possibility is that the complex was partially unstable during the experiment, leading to the dissociation of the Rad18 protein from Rad6 and its subsequent precipitation.

Additional attempts to further purify the ^{HisVSV}Rad18-Rad6 complex were carried out. Nevertheless, the Rad18 protein was found to be sensitive to aggregation if separated from Rad6 during purification, as in the case of the phenyl sepharose column. In addition, although ^{HisVSV}Rad18 and Rad6 were found to co-elute following the cation exchange or the heparin columns, the nuclease contamination still persisted after these procedures. As a consequence, I have settled for the purification protocol described earlier (3.2.2). The nuclease contamination problem was bypassed using EDTA to inhibit the nuclease activity (Viadiu and Aggarwal, 1998) and the DNA-binding activity of Rad18 was studied by pull-down experiments followed by Western blot analysis that allowed the detection of a specific interaction between the Rad18 protein and the DNA.

3.3.2 The Catalytic Activity of Rad18

3.3.2.1 Rad18 Auto-ubiquitylation

As shown in Figure 3.4A, the protein preparation of the yeast ^{HisVSV}Rad18-Rad6 complex, derived from the cytoplasmic fraction of baculovirus-infected insect cells, contains both unmodified and mono-ubiquitylated ^{HisVSV}Rad18. This observation reproduces the findings of Miyase *et al.* (2005) for mammalian Rad18. Furthermore, it suggests that similarly, the pool of yeast ^{HisVSV}Rad18-Rad6 complex in the cytoplasm is different from the pool of this complex in the

nucleus of insect cells. Therefore, the complexes derived from both fractions were used separately.

Although I was able to verify that Rad18 can be ubiquitylated in yeast cells (Figure 3.4B), the significance of this modification is still unclear. In mammalian cells, mono-ubiquitylated Rad18 was predominantly found in the cytoplasm (Miyase *et al.*, 2005). In addition, poly-ubiquitylated Rad18 species were found to accumulate following a treatment with an inhibitor of the 26S proteasome (Miyase *et al.*, 2005). Based on these observations, Miyase *et al.* (2005) concluded that ubiquitylation of mammalian Rad18 regulates its localisation and thereby modulates its levels in the cell. Possibly, this explanation also holds true for the post-translational modification of yeast ^{HisVSV}Rad18 observed in baculovirus-infected insect cells. However, the ubiquitylation of Rad18 in yeast cells may have other physiologically relevant roles.

Indications that the mammalian and the yeast systems may be different from each other were obtained from Figure 3.4B. First, in contrast to mammalian cells, in which Rad18 poly-ubiquitylation was reported to depend on Rad6 (Miyase *et al.*, 2005), deletion of the *RAD6* gene in yeast cells did not completely abolish Rad18 ubiquitylation. Although Rad6 seems to contribute to Rad18 modification to some extent, another E2 may contribute as well. Alternatively, Rad18's E3 ligase activity may be sufficient for its own modification. The finding that ^{HisVSV}Rad18-Rad6 is auto-ubiquitylated *in vitro* (Figure 3.5) supports this last explanation but cannot rule out the involvement of the Rad6 protein in Rad18's modification. Second, although the total cell extracts were prepared from equivalent number of cells for all the tested yeast strains (Figure 3.4B), it appears that over-expression of ^{His}ubiquitin results in enhanced levels of Rad18 compared to the same strain harbouring the empty plasmid. In contrast, deletion of the *rad6 gene* appears to reduce Rad18 levels (Figure 3.4B and data not shown). Although these observations should be confirmed with additional strains, it seems unlikely that Rad18 ubiquitylation in yeast leads to its degradation as was suggested for the mammalian Rad18 protein (Miyase *et al.*, 2005).

A clue for the possible role of mono-ubiquitylation of yeast Rad18 can come from the findings presented in Figure 3.5. Accordingly, the cytoplasm-derived ^{HisVSV}Rad18-Rad6 complex that contains mono-ubiquitylated Rad18 is more active than the one derived form the nuclear fraction, with respect to both Rad18 auto-ubiquitylation and PCNA mono-ubiquitylation. Hence, it is possible that this modification of Rad18 enhances its catalytic activity. Mechanistically, the improved catalytic efficiency observed for mono-ubiquitylated Rad18 could simply imply that conjugation of the first ubiquitin moiety onto Rad18 is a rate-limiting step for the subsequent addition of ubiquitin moieties and the build-up of poly-ubiquitin chains on Rad18. Furthermore, the conjugation of ubiquitin onto Rad18 may be a pre-requisite and a rate-limiting step for subsequent PCNA mono-ubiquitylation. Alternatively, Rad18 ubiquitylation could involve a change of the protein's conformation that results in an improved E3 ligase activity. Accordingly, mono-ubiquitylation of Rad18 in yeast cells might have a regulatory role for its function.

Whether Rad18 auto-ubiquitylation is a side reaction or a relevant step in Rad18's biological activity is yet to be determined. Nevertheless, preliminary experiments suggested that Rad18 ubiquitylation in yeast cells is not dependent on DNA damage (data not shown), whereas PCNA ubiquitylation is specifically induced by DNA damage or replication arrest (Davies *et al.*, 2008). Therefore, it is plausible that these two modifications are independent processes. On one hand, the results presented in Figure 3.6B support this hypothesis, as ^{HisVSV}Rad18-Rad6 auto-ubiquitylation activity was similar in the presence or in the absence of PCNA. On the other hand, this observation does not contradict a model in which Rad18 auto-ubiquitylation is needed prior to PCNA modification.

3.3.2.2 PCNA Mono-ubiquitylation

As shown in Figure 3.6, PCNA mono-ubiquitylation was reconstituted *in vitro* using the partially purified yeast ^{HisVSV}Rad18-Rad6 complex. In addition, the specificity of the *in vitro* reaction for the physiological site of modification was verified using a PCNA mutant, K164R, which lacks the conserved ubiquitin attachment site (Figure 3.6A).

The poor reaction efficiency for PCNA mono-ubiquitylation, observed in Figure 3.6A, was slightly improved by optimisation of various reaction conditions (Figure 3.6B). However, Garg and Burgers (2005) argued that efficient mono-ubiquitylation of PCNA by yeast Rad18 could only be obtained if PCNA was loaded on DNA. These results were different from the observations for the human counterpart, which was shown to readily mono-ubiquitylate PCNA in the absence of DNA (Watanabe *et al.*, 2004). Thus, the results obtained in Figure 3.6 represent only a basal activity of ^{HisVSV}Rad18-Rad6 complex towards PCNA. Nonetheless, taking together the results presented in Figure 3.5 and in Figure 3.6, I can conclude that the purified ^{HisVSV}Rad18-Rad6 complex exhibits an E3 ligase activity, and retains its selectivity and specificity toward PCNA. In addition, these results indicate that the domains essential for the catalytic activity of Rad18 are folded properly.

In 2005, Garg and Burgers (2005) showed that mono-ubiquitylated yeast PCNA was able to stimulate Polη and Rev1 bypass of abasic sites. As a consequence of this publication, the focus of my thesis has shifted. Rather than focusing on the characterisation of PCNA mono-ubiquitylation by the Rad18-Rad6 complex, I decided to study other aspects of Rad18's function *in vitro*. As will be discussed later, those aspects proved to be tightly connected to the up-stream signals that activate the DNA damage tolerance response via PCNA modification.

4 Results II: Interactions of the Rad18-Rad6 Complex and DNA

4.1 Introduction

Originally, the open reading frame of the *RAD18* gene from *S. cerevisiae* was suggested to contain three potential nucleic acid binding domains with homology to ZnFs (Chanet *et al.*, 1988; Jones *et al.*, 1988; Bailly *et al.*, 1997b). Two of these three domains form a RING domain, which nowadays is suggested to be responsible for the ubiquitin ligase activity of Rad18 (Ulrich and Jentsch, 2000), while the third domain is a classical ZnF domain. In addition, yRad18 contains a putative SAP domain that may contribute to its DNA-binding activity.

The ability of the Rad18 protein to bind ssDNA was initially determined by pull-down experiments from yeast cell extracts using an ssDNA-agarose column. In addition, radiolabelled ssDNA was shown to bind to immunopurified Rad18, transferred onto a nitrocellulose membrane (Bailly *et al.*, 1994). Later, this was confirmed by filter binding assays with purified Rad18-Rad6 complex from *S. cerevisiae* (Bailly *et al.*, 1997a). However, these filter binding experiments were performed at low salt concentration of 15 mM KCl using poly(dT) oligonucleotides that were, in average, 221 nt long. Most probably, these conditions do not represent the physiological conditions found inside yeast cells. Nonetheless, these findings led to the hypothesis that yeast Rad18 could recognise and bind to ssDNA stretches resulting from DNA damage sites, thus mediating DNA damage bypass (Bailly *et al.*, 1997a).

In order to gain additional insights regarding the DNA-binding properties of yeast Rad18 and to compare its properties with those of the human protein (Nakajima *et al.*, 2006; Notenboom *et al.*, 2007; Tsuji *et al.*, 2008), further characterisation of the interaction between Rad18 and DNA was carried out.

4.2 Results

4.2.1 Rad18 Binding to ssDNA is Affected by NaCl

In order to test the ssDNA-binding properties of the purified ^{HisVSV}Rad18-Rad6 complex described in Chapter 3, biotinylated oligonucleotides were immobilized onto streptavidin beads and used in pull-down experiments. The retention of the ^{HisVSV}Rad18-Rad6 complex on ssDNA was detected by Western blot analysis.

In Bailly *et al.* (1997a), increasing sodium chloride (NaCl) concentrations were shown to displace Rad18 from ssDNA by filter binding assays. At 100 mM NaCl, about 40% of bound Rad18 was displaced whereas at 250 mM NaCl, more than 95% of bound Rad18 was displaced from the ssDNA. In order to test the effect of NaCl on the interaction between Rad18 and ssDNA in our system, ^{HisVSV}Rad18-Rad6 was incubated at a range of NaCl concentrations with an immobilized oligonucleotide. The ionic strength was kept constant in each of the samples throughout the experiment, including the washing steps. After elution, the samples were subjected to SDS-PAGE and analysed by Western blotting. As shown in Figure 4.1, the Rad18 signal gradually decreased as the NaCl concentration increased. However, some non-specific binding of Rad18 to the DNA-free streptavidin beads was also detected.

To avoid this background signal, the same experiment was repeated incubating the ^{HisVSV}Rad18-Rad6 complex and the ssDNA with the same binding buffers as in Figure 4.1 but using more stringent washing conditions. The PD High-Salt Binding buffer (250 mM NaCl) was used in the washing steps for all of the binding reactions and the samples were analysed as before. As shown in Figure 4.2, the background signal was now abolished, and only specific signals of Rad18 binding to ssDNA-bound streptavidin beads were detected. Surprisingly, even at these stringent washing conditions, a significant Rad18 signal was observed for the samples in which the initial binding buffer contained NaCl concentration equivalent to or lower than 50 mM. As before, the affinity of Rad18 for ssDNA had decreased with the increase of NaCl concentration in the binding buffer (Figure 4.1).

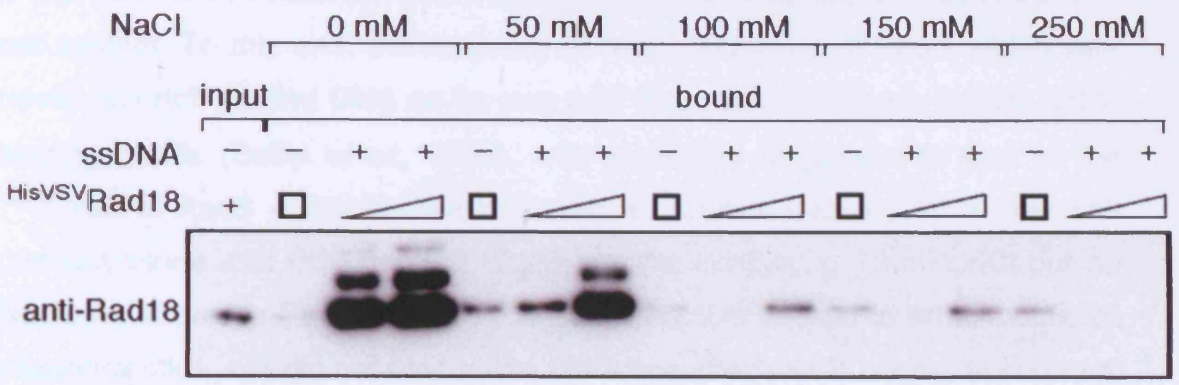

Figure 4.1 – Rad18 binding to ssDNA is affected by NaCl
The ^{HisVSV}Rad18-Rad6 complex (5 or 25 pmol) was incubated with a 75mer of mixed sequence (no. 870; ~ 5 pmol) at 4°C for 1 hour in PD Low-Salt Binding buffer supplemented with different NaCl concentrations (0, 50, 100, 150 and 250 mM NaCl). Then, the beads were washed 3 times in respective binding buffers and twice with respective buffers with no BSA. After elution, the samples were subjected to SDS-PAGE followed by Western blotting. Rad18 was detected with anti-Rad18 antibody (polyclonal mouse 4 serum). The rectangle in the label of the figure refers to the maximal amount of protein used, which in this case was 25 pmol.

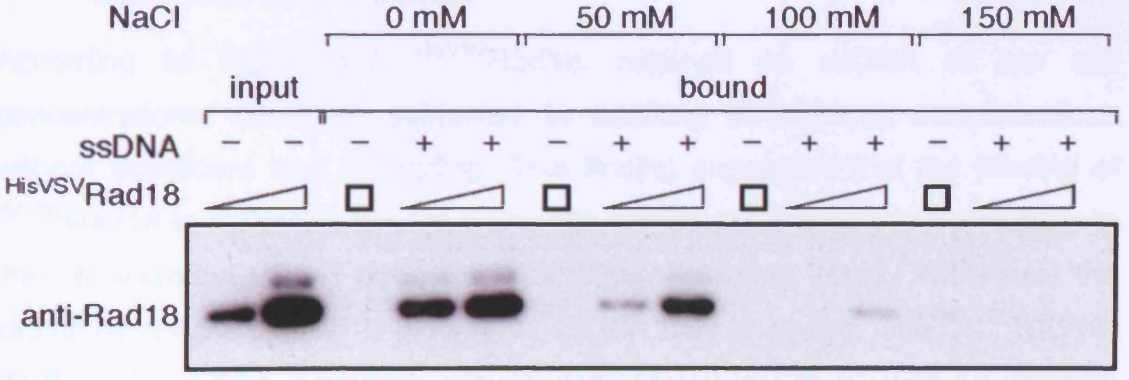

Figure 4.2 – Rad18 binding to ssDNA is stable even after stringent washing
The ^{HisVSV}Rad18-Rad6 complex (5 or 25 pmol) was incubated with a 75mer of mixed sequence (no. 870; ~ 5 pmol) at 4°C for 1 hour in PD Low-Salt Binding buffer supplemented with different NaCl concentrations (0, 50, 100, 150 and 250 mM NaCl). Then, the beads were washed 3 times with PD High-Salt Binding buffer and twice more with the same buffer with no BSA. After elution, the samples were subjected to SDS-PAGE followed by Western blotting. Rad18 was detected with anti-Rad18 antibody (polyclonal mouse 4 serum).

4.2.2 Rad18 Binds Directly to ssDNA

It was essential to establish that the binding of Rad18 to ssDNA was specific in our system. To this end, the retention of recombinant yeast Rad6, which was never reported to bind DNA on its own and does not contain any known DNA-binding motifs (Bailly *et al.*, 1994), was evaluated in parallel to that of the ^{HisVSV}Rad18-Rad6 complex. Their binding to ssDNA was tested at low salt concentrations with PD Low-Salt Binding buffer containing 15 mM KCl but no NaCl. As shown in Figure 4.3, ^{HisVsV}Rad18 was able to bind to an immobilized oligonucleotide, but did not bind to the DNA-free streptavidin beads. In contrast, binding of the recombinant Rad6 either to the DNA-free or to the ssDNA-bound streptavidin beads was not detected. Nevertheless, when Rad6 was present in a complex with ^{HisVSV}Rad18, it was retained on the ssDNA-bound beads, indicating that it was brought to the DNA via Rad18. Note that in Figure 4.3 the recombinant Rad6, purified from *E. coli*, is slightly larger than the Rad6, purified as a complex with ^{HisVSV}Rad18 from insect cells, due to a few additional residues that were left after its N-terminal tag was cleaved (see 2.12.4).

4.2.3 Kinetics of the interaction between the Rad18-Rad6 complex and ssDNA

According to Figure 4.2, ^{HisVSV}Rad18, retained on ssDNA at low salt concentrations, could be subjected to washing at high-salt concentrations without significant loss of binding. This finding suggested that the binding of ^{HisVSV}Rad18 to ssDNA at low ionic strength might confer an improved stability to their association during subsequent stringent washing steps. Therefore, the kinetic behaviour of Rad18 binding to ssDNA was analysed. The ^{HisVSV}Rad18-Rad6 complex was incubated with an immobilized oligonucleotide for different periods of time under conditions of low salt concentration, followed by washing steps with high-salt buffer. As demonstrated in Figure 4.4, a slight signal, corresponding to Rad18 binding, could be already detected after 5 minutes of incubation. However, at 30 minutes of incubation and onwards, the amount of DNA-retained Rad18 did not change significantly, suggesting a stable association of ^{HisVSV}Rad18 with ssDNA. According to the anti-Rad6 antibody Western blot, the binding pattern of Rad6 correlated with that of Rad18.

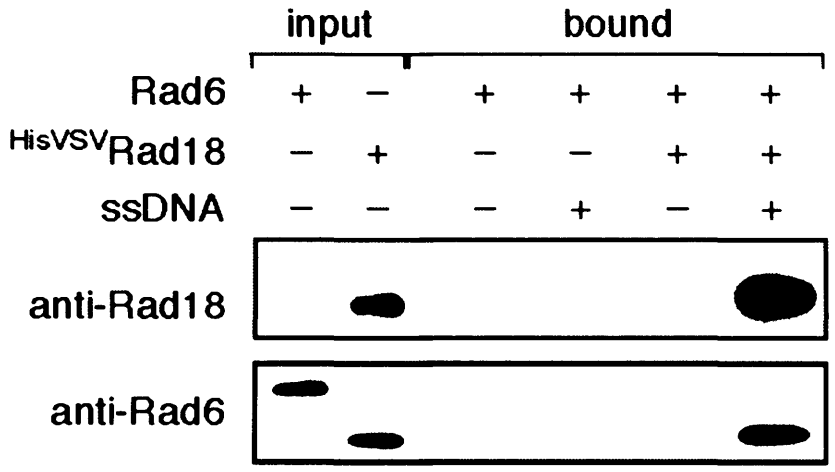

Figure 4.3 – Rad18 but not Rad6 binds directly to ssDNA
The ^{HisVSV}Rad18-Rad6 complex or the recombinant Rad6 protein shown in Figure 5.1 were used. Approximately 5 pmol of each protein were incubated with a 75mer oligonucleotide of mixed sequence (no. 870; ~ 5 pmol) at 4°C for 1 hour in PD Low-Salt Binding buffer. The beads were washed 3 times in PD High-Salt Binding buffer and twice with the same buffer with no BSA. After elution, the samples were subjected to SDS-PAGE followed by Western blotting. Rad18 was detected with anti-Rad18 antibody (polyclonal mouse 4 serum) and Rad6 was detected with anti-Rad6 antibody.

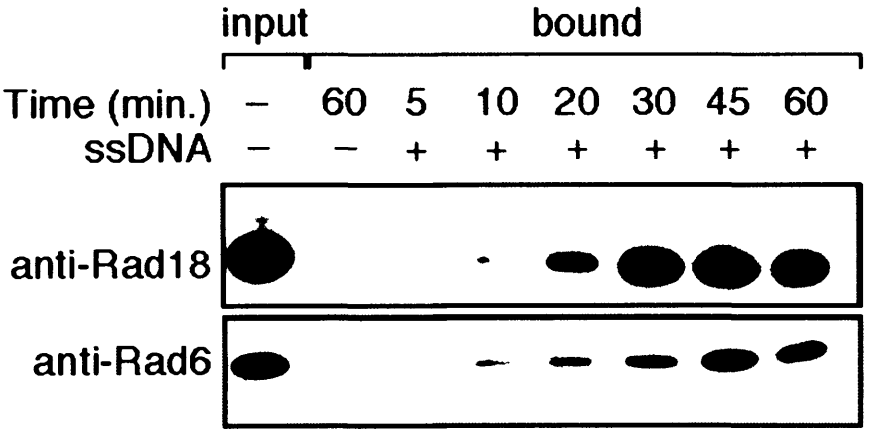

Figure 4.4 – Kinetics of the interaction between the Rad18-Rad6 complex and ssDNA
The ^{HisVSV}Rad18-Rad6 complex (5 pmol) was incubated with a 75mer oligonucleotide of mixed sequence (no. 870; ~ 5 pmol) at 4°C for different time points, as indicated above, in PD Low-Salt Binding buffer (15 mM KCl). The beads were washed 3 times in PD High-Salt Binding buffer (15 mM KCl and 250 mM NaCl) and twice with the same buffer with no BSA. After elution, the samples were subjected to SDS-PAGE followed by Western blotting. Rad18 was detected by anti-Rad18 antibody (polyclonal mouse 4 serum) and Rad6 was detected by anti-Rad6 antibody.

4.2.4 The Effect of Salt Type on Rad18's Binding to ssDNA

As shown in Figure 4.2, Rad18's binding to ssDNA was sensitive to NaCl concentration. However, not only salt concentration but also salt type can affect the binding of a protein to other proteins or to DNA. For instance, anion-specific effects could result from anions interacting at binding sites at the protein-water interface (Griep and McHenry, 1989) and interfere with the binding of Rad18 to ssDNA. Accordingly, in some cases, protein-DNA interactions were found to be less salt-sensitive to glutamate than to chloride (Paz-Elizur *et al.*, 1996). Following a study suggesting that glutamate is the major intracellular anion in *E. coli* (Richey *et al.*, 1987) and another suggesting that acetate-based buffers are preferred for DNA helicases' activity derived from yeast or human (Bachrati and Hickson, 2006), I decided to carry out DNA-binding experiments in buffers containing different salt types and concentrations.

^{HisVsV}Rad18-Rad6 was incubated with an immobilized oligonucleotide at various conditions as described in the figure legend below (Figure 4.5). Following one-hour incubation at 4°C, the beads were washed in parallel with a buffer containing 250 mM of the corresponding salt type. After elution, samples were subjected to SDS-PAGE and analysed by Western blotting. As shown in Figure 4.5A and Figure 4.5B, the affinity of Rad18 for ssDNA was reduced as salt concentration increased. However, for the glutamate salts as well as for the acetate salts this reduction was less pronounced at the intermediate salt concentration (100 mM).

As the experiment using potassium salts (Figure 4.5A), was done separately from the experiment using sodium salts (Figure 4.5B), the effect of all six salt types was tested in parallel using the same salt concentration (100 mM). As shown in Figure 4.5C, the positive effects of glutamate and acetate on the interactions between Rad18 and ssDNA, proposed by Figure 4.5A and Figure 4.5B, were confirmed. Apparently, a change in the cationic salt composition (sodium versus potassium) did not have a significant effect on these interactions.

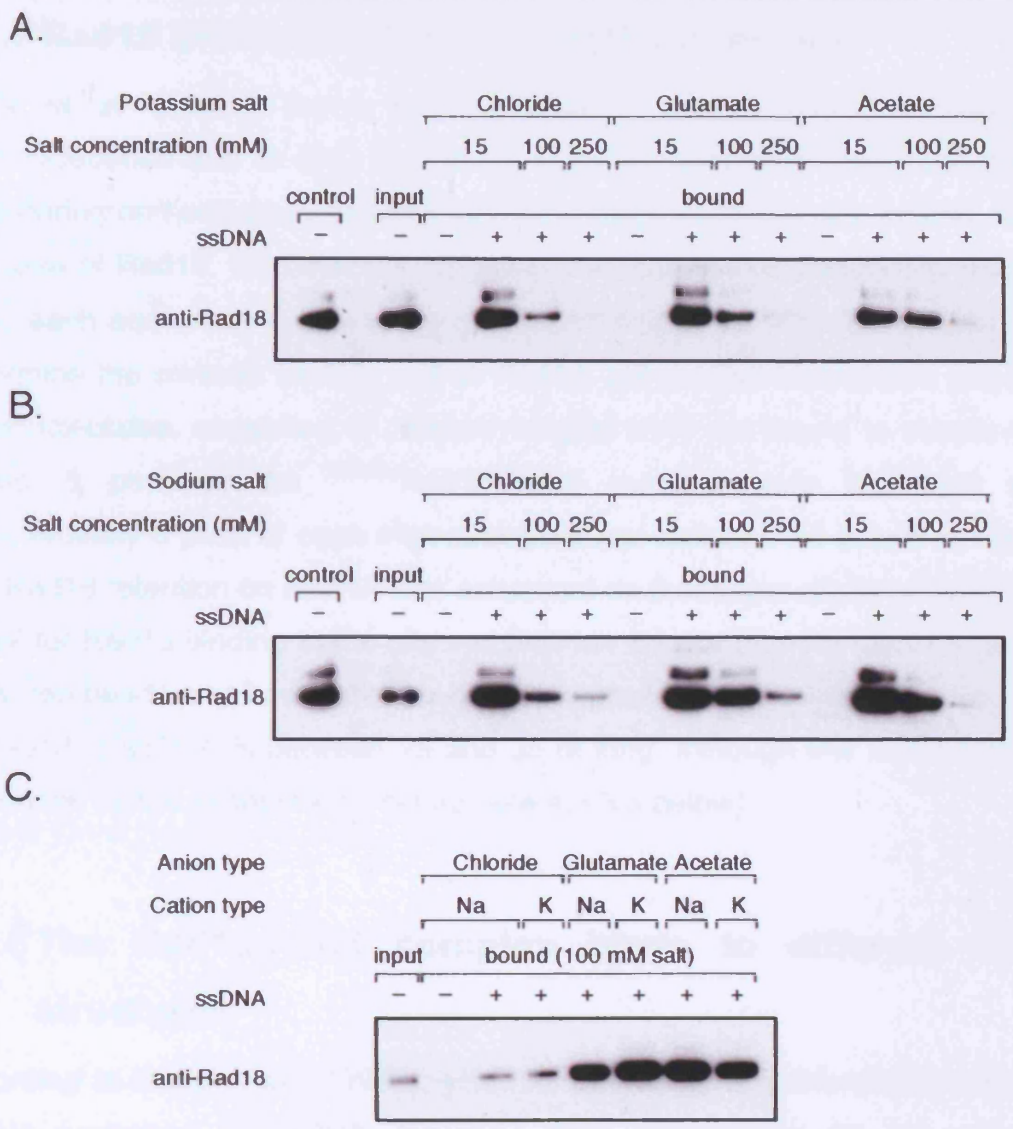

Figure 4.5 – Rad18 binding to ssDNA is less sensitive to glutamate or to acetate than to chloride anion

A. The ^{HisVSV}Rad18-Rad6 complex (5 pmol) was incubated with a 75mer oligonucleotide of mixed sequence (no. 870; ~ 5 pmol) at 4°C for 1 hour in PD Low-Salt Binding ("- KCl") buffer with different concentrations of potassium salts as indicated (15, 100 and 250 mM of potassium chloride, potassium glutamate and potassium acetate). Beads were then washed 3 times in PD Low-Salt Binding ("- KCl") buffer supplemented with 250 mM of the corresponding salt type and twice more in the same buffer with no BSA. The positive control sample was bound in PD Low-Salt Binding and was washed with PD High-Salt Binding buffer. After elution, the samples were subjected to SDS-PAGE followed by Western blotting. Rad18 was detected with anti-Rad18 antibody (polyclonal mouse 4 serum).

B. Same as in A., but instead of potassium salts, sodium salts were used for binding as indicated (15, 100 and 250 mM of sodium chloride, sodium glutamate and sodium acetate). For washing, PD Low-Salt Binding ("- KCl") buffer was supplemented with 250 mM of the corresponding salt type.

C. Same as in A., but instead of different salt concentrations, Rad18 was bound to the oligonucleotide in PD Low-Salt Binding ("- KCl") containing 100 mM of different salt types as indicated. The beads were washed with PD Low-Salt Binding ("- KCl") buffer that was supplemented with 250 mM of the corresponding salt type.

4.2.5 Rad18 Binds to Different Lengths of ssDNA

Bailly *et al.* (1997a) found that the yRad18 protein bound to poly(dT) oligonucleotides and to M13 ssDNA of a mixed nucleotide sequence. When considering non-sequence specific ssDNA-binding properties of a protein, as in the case of Rad18, the DNA can be viewed as a series of overlapping binding sites, each equivalent in size to the protein's binding site (Kim *et al.*, 1992). To determine the minimal binding site of Rad18, gel-purified biotinylated poly(dT) oligonucleotides, consisting of different lengths were pre-bound to streptavidin beads. 5 pmol of the ^{HisVSV}Rad18-Rad6 complex were incubated with approximately 5 pmol of each oligonucleotide per reaction. As shown in Figure 4.6, Rad18 retention on ssDNA was enhanced on the longer oligonucleotides. A signal for Rad18 binding to the oligonucleotides shorter than 35 bases or to the DNA-free beads was barely detected. This implies that the minimal binding site of Rad18 to ssDNA is between 25 and 35 nt long, although this result may be influenced by the experimental set up (see 4.3.3.3 below).

4.2.6 The Rad18-Rad6 complex binds to different DNA structures

According to Bailly *et al.* (1997a), yRad18 was found to preferentially bind to ssDNA compared to dsDNA. However, their experiments did not address whether Rad18 could bind to other DNA structures. In addition, PCNA, Rad18's substrate, is known to be required for processive replication and DNA repair events (Biswas *et al.*, 1995), which are all processes involving dynamic changes in the DNA structure. Moreover, PCNA ubiquitylation was shown to require replication or repair intermediates *in vivo* (Sarkar *et al.*, 2006; Davies *et al.*, 2008) and efficient Rad18-dependent PCNA ubiquitylation *in vitro* was obtained only when the PCNA was loaded on the DNA (Garg and Burgers, 2005). Thus, it is conceivable that Rad18 might encounter a variety of DNA structures *in vivo*. Therefore, it was important to assess the structure specificity of Rad18 binding to DNA. To this end, different DNA structures were prepared (Table 2-9) and immobilized on streptavidin beads. Two different amounts of the ^{HisVsV}Rad18-Rad6 complex were incubated with each DNA structure and the retention of Rad18 was analysed in PD Low-Salt Binding buffer or in the same

buffer supplemented with 100 mM NaCl. As shown in Figure 4.7, at both experimental conditions, Rad18 bound to ssDNA as expected. In addition, it bound to the branched DNA structures. At the low salt concentration, Rad18 retention to the 3'-Flap structure seemed somewhat better than its retention to the 5'-Flap structure or to the ssDNA. This small effect was reproducible. In addition, the signal obtained for Rad18 binding to the Splayed Duplex structure was comparable to that obtained for the ssDNA. In contrast, at 100 mM NaCl, the overall retention of Rad18 to any DNA structure seemed reduced and visualisation of a clear signal required longer exposure of the blot (compare the signal intensity of the input sample as well as the background signal for Rad18's retention to the DNA-free beads between the two experiments). At this salt concentration, Rad18 bound best to the Splayed Duplex structure, also in comparison to the ssDNA. What was apparent from both experiments was that the least preferred structure was the dsDNA. Surprisingly, despite the absence of ssDNA in the dsFork structure, Rad18 bound it better compared to the dsDNA structure (see Figure 4.7 – upper panel).

4.3 Discussion

4.3.1 Advantages and Disadvantage of the Experimental Methods

In order to characterise the binding properties of Rad18 to DNA, I used pull-down experiments with biotinylated oligonucleotides bound to streptavidin beads. Although this method enabled me to study different aspects of Rad18 interaction with DNA as will be discussed below, it had several disadvantages over other experimental methods, i.e. filter-binding assay or gel-shift assay. In contrast to the latter, where the binding molecules are analysed in solution, in pull-down experiments either the DNA or the protein has to be immobilized on beads, thus creating an artificial situation. In addition, as the protein is detected by Western blotting, this method is less sensitive by a few orders of magnitude compared to gel-shift assay or to filter-binding assay, in which the DNA is detected by radioactive labelling. Furthermore, due to the non-linear nature of the ECL reagent used to develop the Western blot, the results that were obtained by the pull-down experiments could not be considered quantitative.

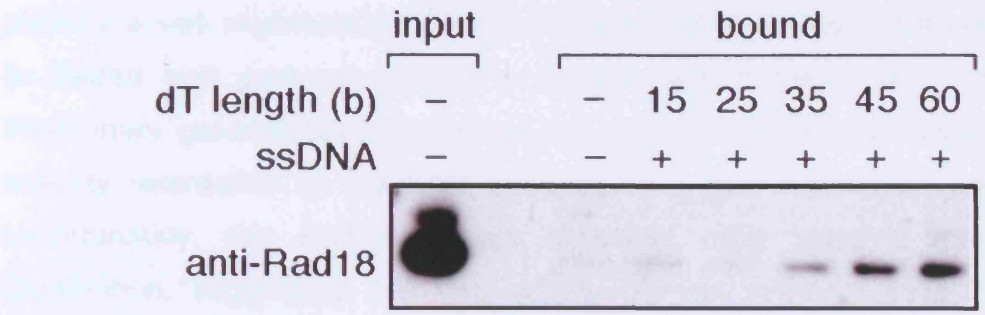

Figure 4.6 – The Rad18-Rad6 complex binds to different oligo dT lengths
The ^{HisVSV}Rad18-Rad6 complex (5 pmol) was incubated with poly(dT) oligonucleotides consisting of different lengths (15mer, 25mer, 35mer, 45mer and 60mer; oligos 1184, 1183, 1182, 1181 and 1180, respectively) at 4°C for 1 hour in PD Low-Salt Binding buffer. The beads were washed 3 times in PD High-Salt Binding buffer and twice more with the same buffer with no BSA. After elution, the samples were subjected to SDS-PAGE followed by Western blotting. Rad18 was detected with anti-Rad18 antibody (polyclonal mouse 4 serum).

Figure 4.7 – The Rad18-Rad6 complex binds to different DNA structures
The ^{HisVSV}Rad18-Rad6 complex (5 or 25 pmol) was incubated with approximately 5 pmol of each DNA structure (ssDNA, dsDNA, Splayed Duplex, 5'-Flap, 3'-Flap and dsFork) at 4°C for 1 hour in PD Low-Salt Binding buffer (low salt; 15 mM KCl) or with the same buffer supplemented with 100 mM NaCl (medium salt; 15 mM KCl + 100 mM NaCl). The beads were washed 3 times with PD High-Salt Binding buffer (15 mM KCl + 250 mM NaCl) and twice more with the same buffer with no BSA. After elution, the samples were subjected to SDS-PAGE followed by Western blotting. Rad18 was detected with anti-Rad18 antibody (polyclonal mouse 4 serum). Note that all of the DNA structures consist of a common 61mer oligonucleotide – XO1 (no. 1055).

Nevertheless, this method was chosen for the following reasons. Firstly, as the yeast ^{HisVSV}Rad18-Rad6 complex, isolated from insect cells, was only partially purified, it was important to determine that the ability to bind DNA was intrinsic to Rad18 and was not due to a contaminant in the protein preparation. Preliminary gel-shift experiments to test whether Rad18 was able to cause mobility retardation of the DNA resulted in a poor shift (data not shown). Unfortunately, this shift was also observed while using a mock-purified preparation, suggesting that this activity did not originate from the Rad18 protein. However, by performing pull-down experiments followed by Western blot analysis, a specific signal for Rad18 binding to the DNA was detected. Secondly, the pull-down method allowed the use of stringent washing steps to test the stability of the association between the Rad18 protein and the DNA. Lastly, this method had been successfully used in a number of studies (Zou and Elledge, 2003; Zou *et al.*, 2003).

Until now, the only published biochemical study regarding the DNA-binding properties of yeast Rad18 was based on the filter-binding assay (Bailly *et al.*, 1997a). Although the kinetic parameters for ssDNA-Rad18 interaction were not calculated, Bailly *et al.* (1997a) convincingly showed a preference for yRad18 binding to ssDNA over dsDNA. Recently, Notenboom *et al.* (2007) have confirmed a binding preference for ssDNA over dsDNA also for human Rad18 by gel shift assays. In addition, using surface plasmon resonance analysis they were able to show that hRad18's SAP domain but not the ZnF was sufficient for binding to both ssDNA and dsDNA, and calculate the corresponding apparent affinities. Surface plasmon resonance technique is a quantitative and sensitive method, allowing real-time interaction studies between an analyte and a surface-immobilized ligand, by measuring the change in the refractive index near the surface (Fivash *et al.*, 1998). Therefore, this method allowed Notenboom *et al.* (2007) to identify important residues in the extended loop of the SAP domain, which when mutated resulted in reduced affinities for DNA.

To summarise, using pull-down experiments to study the interaction of Rad18 and DNA, I observed qualitative changes in the affinity of Rad18 for the DNA under various experimental conditions (different incubation times – see Figure 4.4; different salt concentrations or salt types used in the binding buffer – see

Figure 4.2 and Figure 4.5). Furthermore, I was able to establish that the binding of Rad18 to the DNA was specific (Figure 4.3) and affected by the length of the ssDNA (Figure 4.6) or by the DNA structure (Figure 4.7). In most cases, when I analysed similar questions to those already addressed by Bailly *et al.* (1997a), similar results were obtained.

4.3.2 Experimental Conditions and Specificity of Binding

The buffer used in the biotinylated pull-down experiments contained the detergent NP-40 to avoid non-specific interactions between the proteins and the beads. In addition, the chelator EDTA was used to inhibit the contaminating nuclease activity observed in the ^{HisVSV}Rad18-Rad6 protein preparation. The binding reactions were performed at 4°C to ensure the stability of all the components during the binding.

As shown in Figure 4.3, Rad18 did not bind to the DNA-free beads. This supports the notion that the conditions used for the experiment resulted in a specific binding of Rad18 to the DNA. Moreover, Rad6 did not bind to the DNA on its own. Nonetheless, in the presence of Rad18, a significant percentage of Rad6 was pulled down, suggesting that when Rad6 is bound to Rad18 it can be brought to the DNA. This observation is consistent with previously published data (Bailly *et al.*, 1994; Bailly *et al.*, 1997a).

4.3.3 DNA-Binding Properties of Rad18

4.3.3.1 Binding Affinity

According to paragraph 4.2.1, the amount of Rad18 retained on the DNA was reduced with increased NaCl concentration, suggesting that the NaCl in the binding buffer reduced the affinity of Rad18 for ssDNA. This is consistent with Bailly *et al.* (1997a), in which Rad18 binding to the DNA was shown to be sensitive to increasing concentrations of salt. Noticeably, as shown in Figure 4.2, once Rad18 was bound to ssDNA at low salt concentration (15 mM KCl or 15 mM KCl + 50 mM NaCl) even repeated washing steps at high salt concentration (up to 250 mM NaCl) did not result in a complete dissociation of

Rad18 from the DNA, whereas in the binding reactions with higher salt concentrations (100 mM up to 250 mM), Rad18 binding to the DNA was no longer detected. These findings suggest that high NaCl concentrations can disrupt the association of Rad18 with DNA. However, once Rad18 binds to the DNA in low NaCl concentrations, it may undergo a conformational change that improves its resistance to the effects of NaCl.

Unfortunately, these results cannot directly predict the binding properties of Rad18 to DNA *in vivo*. It is plausible that yet unidentified post-translational modifications of Rad18 and / or interaction with other proteins could influence its affinity for ssDNA. In addition, local salt or protein concentrations might affect the binding of Rad18 to the DNA *in vivo*. Nonetheless, the ionic strength in yeast cells is most probably higher than 50 mM NaCl. Hence, Rad18 might not be able to bind DNA under physiological conditions.

When comparing the effect that different salt types had on Rad18 binding to ssDNA (Figure 4.5), both glutamate and acetate seemed to relax Rad18 sensitivity towards increasing salt concentrations in comparison to chloride. One explanation could be a differential effect that those anions have on the water molecules that mediate the hydrogen bonds between the protein and the DNA (Lilley, 1995). As mentioned in the introduction, the Hofmeister series is an empirical ranking of anions reflecting their effects on protein solubility and based on more recent studies, a similar ranking order of anions that enhance protein-DNA interactions was suggested to be: glutamate > fluoride > acetate > cloride > bromide = nitrate > iodide > hypochloride (Griep and McHenry, 1989). According to Figure 4.5, chloride ion seems to have a stronger disrupting effect on the interaction between Rad18 and ssDNA than glutamate or acetate. Consequently, it is likely that Rad18 binding to the DNA behaves according to the Hofmeister series.

4.3.3.2 Binding Kinetics

As observed in Figure 4.4, the binding of Rad18 to ssDNA at low salt concentrations resulted in their stable association towards subsequent high-salt washing. Although the high-salt washing steps took almost one hour, the

differences in the amount of bound Rad18 between the short low-salt incubation times and the longer low-salt incubation times were noticeable. This suggests that the salt-resistant binding of Rad18 to the DNA was not an immediate reaction but rather occurred gradually in a time scale of a few minutes. After 30 minutes of incubation, maximal signals of Rad18 binding to ssDNA were obtained, and there was no apparent change to retained levels of Rad18 in the later time points. A possible explanation could be that the ssDNA-bound Rad18 might undergo a slow conformational change that stabilises its binding to the ssDNA and reduces its dissociation rate. The results are consistent with this model as once this conformational change occurs, the stringent washing conditions do not lead to a significant loss of Rad18's binding. An additional experiment should have been performed to test if the binding of Rad18 to ssDNA is rescued by using low-salt instead of high-salt washing steps after the short low-salt incubation times. This result would have argued in favour of the proposed model.

In parallel to Rad18 binding, Rad6 was also retained on the DNA through its interaction with Rad18 and its binding kinetics correlated with those of Rad18.

Bailly *et al.* (1997a) performed the only published experiment addressing the binding kinetics of full-length yRad18 to the DNA. After 10 min incubation with radiolabelled ssDNA, an excess of cold ssDNA was added at indicated time points. Already after less then 2 min incubation, the relative binding was reduced to 20%, suggesting a relatively fast off-rate. Unfortunately, their result cannot be directly compared to the result from Figure 4.4, as the latter reflected a time course of salt-resistant DNA-protein association and not an assay for the off-rate of pre-bound Rad18-ssDNA complex.

4.3.3.3 Minimal Binding Site

Until now, the minimal binding site of the Rad18-Rad6 complex to the DNA has not been determined. Derived from Figure 4.6, it can be estimated that the minimal binding site required for binding of the Rad18-Rad6 complex to the ssDNA is between 25 and 35 nucleotides. The estimation was used in subsequent experiments, as will be discussed later in Chapter 6 (Figure 6.2).

Nevertheless, the minimal occluded site of proteins can vary between solution conditions and might depend on the approach used for analysis (Kumaran *et al.*, 2006). In our system, the ssDNA is attached on one end to streptavidin beads, which may cause sterical hindrance for the binding of proteins. Therefore, the observed minimal binding site of 25-35 nt may be an over-estimation of the actual one.

4.3.3.4 Structure Preference

Bailly *et al.* (1997a) and Notenboom *et al.* (2007) showed that yeast and human Rad18, respectively, have a preference for binding ssDNA over dsDNA. Consequently, my initial hypothesis was that the ssDNA would be the preferred structure in both tested salt conditions (Figure 4.7). In addition, if Rad18 could only bind to ssDNA, one should expect that the relative amount of bound Rad18 would correspond to the relative length of ssDNA region in a particular DNA structure. Although the amount of bound Rad18 on ssDNA and on the Splayed Duplex structure at the low salt concentration is comparable, Rad18 binds somewhat better to the 3'-Flap. Moreover, at the higher salt concentration, the DNA structural preference of Rad18 has slightly changed towards the Splayed Duplex, indicating that NaCl might influence the protein's conformation and consequently, its binding preferences to different DNA structures. Additionally, the salt may influence the DNA structure. According to these *in vitro* results, it seems that Rad18 can bind to DNA-branched structures. Consistently, Tsuji *et al.* (2008) have recently demonstrated that human Rad18 binds preferentially to forked DNA structures and to long ssDNA, suggesting that potentially Rad18 could recognise similar DNA intermediates resulting from replication fork stalling.

5 Results III: Interactions of the Rad18-Rad6 Complex and RPA

5.1 Introduction

Until recently, the up-stream signals that lead to the activation of the *RAD6* pathway by PCNA ubiquitylation were not clear. As mentioned before, it was presumed that the ssDNA-binding ability of Rad18 allowed it to directly recognise ssDNA stretches resulting from DNA damage sites, thus mediating DNA damage bypass (Bailly *et al.*, 1997a). However, the results presented in Chapter 4 suggest that under physiological conditions, yeast Rad18 is not able to bind ssDNA on its own. In parallel, recent findings in the laboratory provided additional clues regarding the signals required for PCNA ubiquitylation. Firstly, analysis of the cell-cycle dependence of PCNA ubiquitylation revealed that this modification occurs in S phase in response to DNA damage, but not in G1 or G2 arrested cells (Davies *et al.*, 2008, Figure 1A in Appendix). Subsequently, using a temperature-sensitive mutant of an essential kinase gene responsible for DNA replication initiation, *cdc7*^{ts}, active replication forks were shown to be required for PCNA ubiquitylation (Davies *et al.*, 2008, Figure 2 in Appendix). In addition, as over-expression of Rad18 relaxed the conditions required for PCNA modification (Davies *et al.*, 2008, Figure 1B in Appendix), it appears that under normal conditions, the E3 ligase is a limiting factor for PCNA ubiquitylation. Secondly, induction of PCNA modification correlated with treatment of DNA damaging agents that cause accumulation of ssDNA (Davies *et al.*, 2008, Figure 3 in Appendix). As ssDNA bound to RPA was suggested to be the signal for activation of the replication checkpoint (Zou and Elledge, 2003; Zou *et al.*, 2003), the possible contribution of RPA to PCNA ubiquitylation was studied. Interestingly, when Rfa1, the largest subunit of the RPA complex, was depleted to about 5% by the use of a heat-inducible degradation signal (Dohmen *et al.*, 1994), PCNA ubiquitylation was abolished. However, at the same time, the S phase dependent PCNA sumoylation seemed to be unaffected (Davies *et al.*, 2008, Figure 4E in Appendix). Taken together, these results suggested that upon DNA damage, PCNA is ubiquitylated on stalled replication forks and that RPA is required for the induction of this modification. As Rad18 was found to be

a limiting factor for PCNA ubiquitylation, RPA-bound ssDNA could be involved in the recruitment of Rad18 to stalled replication forks. To test this possibility, the interaction between Rad18 and RPA was studied. Co-immunoprecipitation experiments showed that RPA and Rad18 interacted *in vivo* with each other (Davies *et al.*, 2008, Figure 5G in Appendix). Furthermore, by two-hybrid analysis, Rad18 (but not Rad5) was found to interact with two subunits of the RPA complex, Rfa1 and Rfa2 (Davies *et al.*, 2008, Figure 5A in Appendix). In order to gain additional insights into the mechanism of the interaction between Rad18 and RPA, *in vitro* studies were carried out.

5.2 Results

5.2.1 Rad18 Interacts Directly with RPA

The recombinant yeast RPA complex was purified from *E. coli*, and as shown in Figure 5.1 (lane 3), it consists of three subunits: Rfa1, Rfa2 and Rfa3, with corresponding molecular weights of 69, 36 and 13 kDa, as expected. In order to test whether Rad18 and RPA interact physically with each other, RPA was covalently coupled to CH-sepharose beads. Subsequently, pull-down experiments with the ^{HisVSV}Rad18-Rad6 complex in the presence of a non-specific nuclease were performed. As shown in Figure 5.2, Rad18 was retained on the RPA- but not on the BSA-derivatised beads, suggesting that the two proteins interact physically with each other. To determine if Rad6 can bind to RPA directly or indirectly via its association with Rad18, the recombinant Rad6 protein and the ^{HisVSV}Rad18-Rad6 complex were assayed for interactions with RPA in a similar manner to that described above. ^{His}PCNA was used as a negative control since it was never reported to interact directly with RPA. As shown in Figure 5.1 (lanes 1 and 2), approximately 50 pmol of ^{HisVSV}Rad18-Rad6 complex had a comparable Coomassie staining to approximately 20 pmol of recombinant Rad6. 10% of these amounts were used as input for the experiment. As shown in Figure 5.3, Rad6 was able to interact with RPA either in the presence or in the absence of Rad18, suggesting that its interaction with RPA was direct. However, ^{His}PCNA did not bind to RPA, indicating that the experimental conditions allowed only specific interactions with RPA, as in the case of the ^{HisVSV}Rad18-Rad6 complex and the recombinant Rad6 protein.

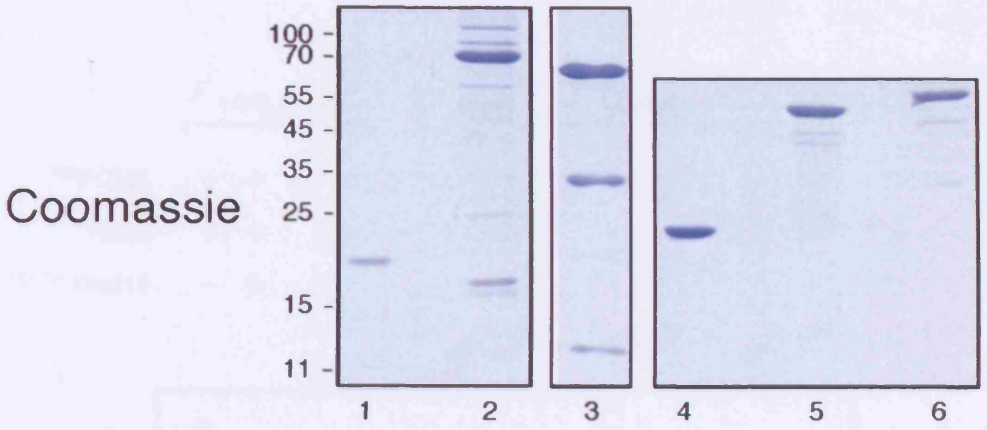

Figure 5.1 – Purified proteins used for interaction studies
The recombinant Rad6 protein (lane 1; 20 pmol) or the ^{HisVSV}Rad18-Rad6 complex (lane 2; 50 pmol) were analysed by SDS-PAGE followed by Coomassie staining to ensure comparable amounts of Rad6. Approximately 3 μg of RPA (lane 3), GST (lane 4), ^{GST}Rfa1 (182-421) (lane 5) or ^{GST}Rfa2 (lane 6) were visualised by Coomassie staining.

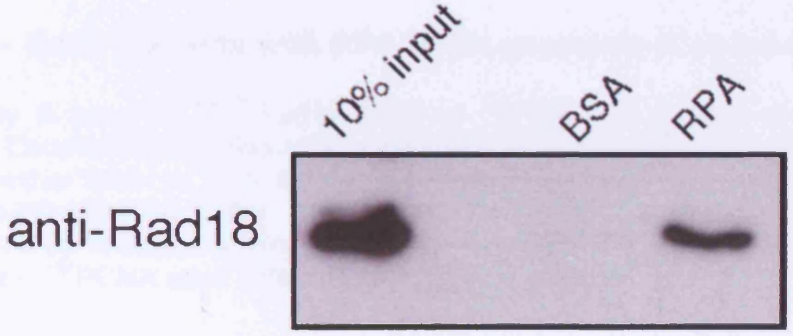

Figure 5.2 – ^{HisVSV}Rad18 and RPA interact directly with each other via protein-protein interactions.
The ^{HisVSV}Rad18-Rad6 complex (5 pmol) was incubated in Coupled-PD Binding buffer, supplemented with 2.5 u benzonase, at 4°C for 1 h with either BSA- or RPA-derivatised beads. The beads were washed 5 times with Coupled-PD Washing buffer. After elution, the samples were subjected to SDS-PAGE followed by Western blotting. Rad18 was detected with anti-Rad18 antibody (polyclonal mouse 4 serum).

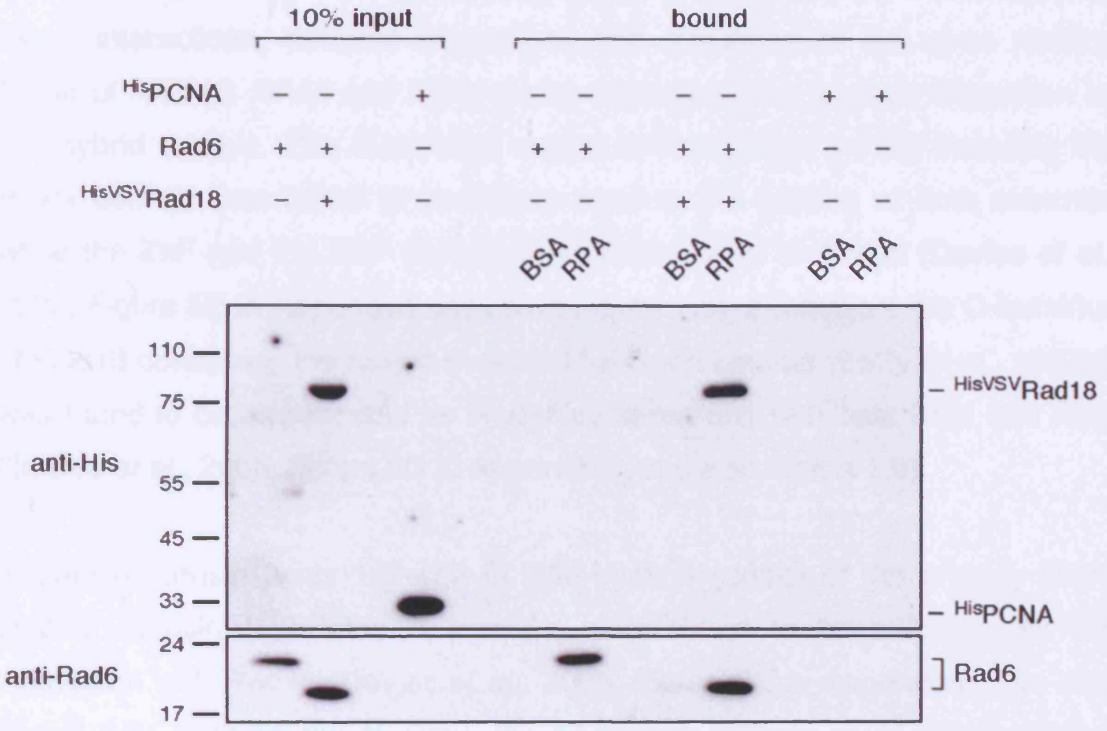

Figure 5.3 – Rad6 interacts with RPA in the presence or in the absence of Rad18

Approximately 5 pmol of ^{HisVSV}Rad18-Rad6 or ^{His}PCNA or 2 pmol of Rad6 were incubated in Coupled-PD Binding buffer, supplemented with 2.5 u benzonase, at 4°C for 1 h with either BSA- or RPA-derivatised beads. The beads were washed 5 times with Coupled-PD Washing buffer. After elution, the samples were subjected to SDS-PAGE followed by Western blotting. Rad6 was detected with anti-Rad6 antibody and ^{HisVSV}Rad18 and ^{His}PCNA were detected with anti-His antibody.

5.2.2 Mapping of Rad18-RPA Interaction

As mentioned before, Rad18 was shown to interact with Rfa1 and Rfa2 in the two-hybrid system (Davies *et al.*, 2008, Figure 5A in Appendix). To further map these interactions, different truncations and mutations of the open reading frame of *RAD18*, *RFA1* and *RFA2* genes were analysed for their interaction by two-hybrid assays. The N-terminal region of Rad18 (aa 1-192) including the RING domain was found to contribute most to the binding of both subunits, while the ZnF and the SAP domain were found to be irrelevant (Davies *et al.*, 2008, Figure 5D in Appendix); (see also Figure 1.8). In addition, the C-terminus of Rad18 containing the region essential for Rad6 binding (Bailly *et al.*, 1997b), was found to be dispensable for Rad18's interactions with both Rfa1 and Rfa2 (Davies *et al.*, 2008, Figure 5D in Appendix); (see also Figure 1.8).

In parallel, amino acids 167-452 of Rfa1, which consist of the primary DNA-binding domain (OB folds A and B), were found to be sufficient for the interaction with Rad18 (Davies *et al.*, 2008, Figure 5E in Appendix); (see also Figure 1.3). With regard to Rfa2, the interaction domain could not be further narrowed by two-hybrid due to auto-activation behaviour of its constructs in the assay.

In order to determine if Rfa2 or the DNA-binding domain of Rfa1 were able to directly interact with Rad18, *in vitro* pull-down assays were carried out.

^{GST}Rfa1 (182-421), the primary DNA-binding domain of yRfa1 (Gomes and Wold, 1996; Bochkarev *et al.*, 1997; Bochkarev *et al.*, 1999; Walther *et al.*, 1999; Park *et al.*, 2005), or ^{GST}Rfa2 were purified recombinantly from *E. coli* and visualised by Coomassie staining in Figure 5.1 lane 5 or lane 6, respectively. The interaction between the ^{HisVSV}Rad18-Rad6 complex and the ^{GST}Rfa1 (182-421) or the ^{GST}Rfa2 proteins was studied by pull-down experiments. As shown in Figure 5.4 and in Figure 5.5, the complex was able to bind to ^{GST}Rfa1 (182-421) or to ^{GST}Rfa2, respectively, but not to GST alone or to the protein-free glutathione sepharose beads.

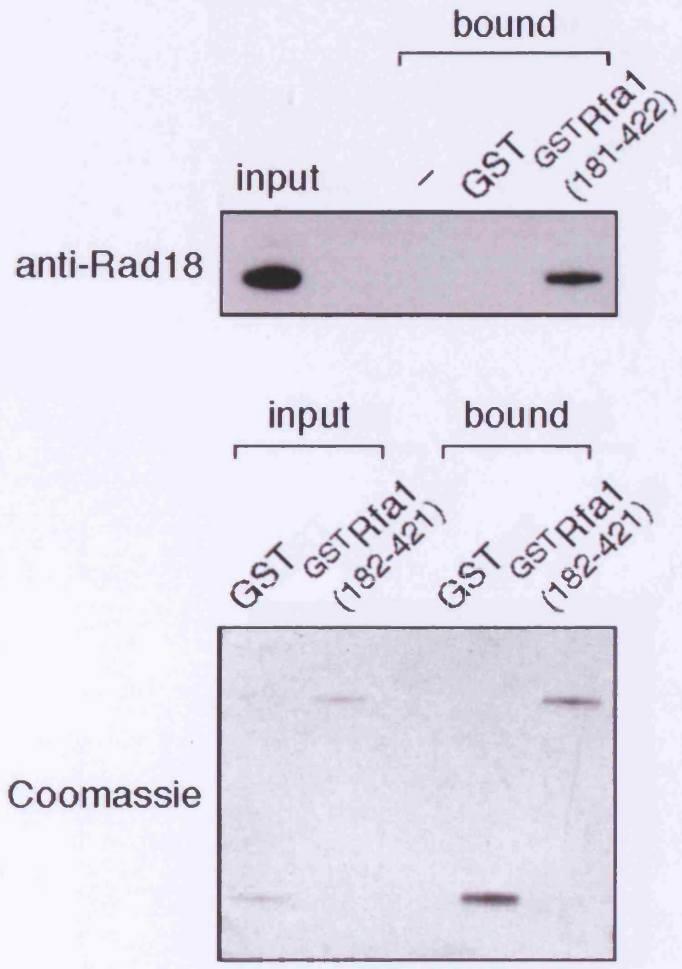

Figure 5.4 – ^{GST}Rfa1 (182-421) is sufficient for Rad18 interaction
Approximately 0.5 nmol of GST or ^{GST}Rfa1 (182-421) were pre-immobilized on glutathione sepharose in GST-PD Binding buffer for 30 min at 4°C. After a brief wash with GST-PD Binding buffer, 10 pmol of ^{HisVSV}Rad18-Rad6 were added in the same buffer containing 100 μg/mL BSA and incubated at 4°C for 1 h. Then, the beads were washed 3 times with 500 μL of GST-PD Binding buffer containing BSA and twice more with the same buffer without BSA. After elution, the samples were subjected to SDS-PAGE followed by Coomassie staining or Western blotting. Rad18 was detected with anti-Rad18 antibody (polyclonal mouse 4 serum).

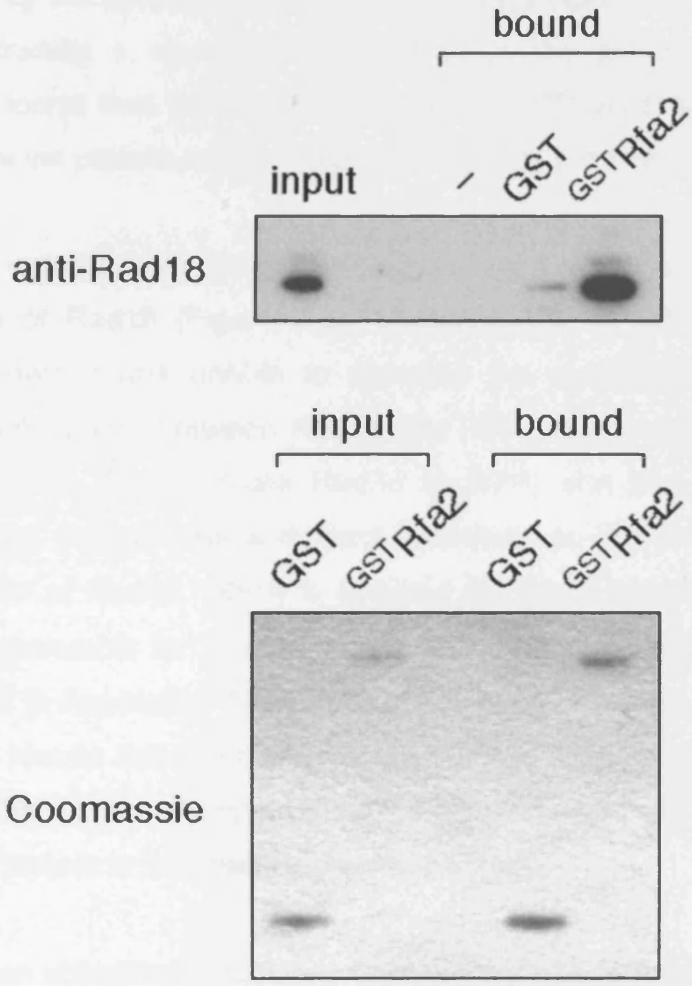

Figure 5.5 – ^{GST}Rfa2 is sufficient for Rad18 interaction
Approximately 0.5 nmol of GST or ^{GST}Rfa2 were pre-immobilized on glutathione sepharose in GST-PD Binding buffer for 30 min at 4°C. After a brief wash with GST-PD Binding buffer, 10 pmol ^{HisVSV}Rad18-Rad6 were added in the same buffer containing 100 μg/mL BSA and incubated at 4°C for 1 h. Then, the beads were washed 3 times with 500 μL of GST-PD Binding buffer containing BSA and twice more with the same buffer without BSA. After elution, the samples were subjected to SDS-PAGE followed by Coomassie staining or Western blotting. Rad18 was detected with anti-Rad18 antibody (polyclonal mouse 4 serum).

5.3 Discussion

As shown in Figure 5.2, the ^{HisVSV}Rad18-Rad6 complex and RPA interact physically with each other. This is in agreement with the results obtained by the two-hybrid and by the co-immunoprecipitation assays performed in Davies *et al.* (2008). By including a non-specific nuclease in the pull-down experiment (Figure 5.2), I found that the interaction between ^{HisVSV}Rad18-Rad6 complex and RPA occurs via protein-protein interactions and is not mediated by DNA.

Similarly, Rad6 was found to directly interact with RPA, either in the presence or in the absence of Rad18 (Figure 5.3). Unfortunately, as yRad18 cannot be purified on its own, I was unable to separate the contribution of the Rad6 protein on the interaction between Rad18 and RPA. In principle, these results cannot exclude that Rad6 recruits Rad18 to RPA, and that the interaction between the latter two proteins is indirect. However, as mentioned earlier, the C-terminal region of Rad18, which is required for Rad6 binding (Bailly *et al.*, 1997b), was dispensable for its interactions with Rfa1 and Rfa2 (Davies *et al.*, 2008, Figure 5D in Appendix). Therefore, this possibility seems unlikely. Taken together, these results indicate that both Rad18 and Rad6, separately or as a complex, are able to directly interact with RPA. However, the contribution of each individual protein to this interaction is still unknown.

Since Rad6 is an ubiquitin-conjugating enzyme that cooperates with additional ubiquitin ligases, Bre1 (Hwang *et al.*, 2003) and Ubr1 (Dohmen *et al.*, 1991), the significance of the interaction between Rad6 and RPA could extend beyond the DNA damage tolerance pathway. In principle, this interaction could have additional consequences, such as for gene transcription via modulation of histone H2B ubiquitylation or for protein degradation of the N-end rule substrates, but this has yet to be determined.

Due to the essential roles of PCNA and RPA during replication, it is plausible that they are in the proximity of each other. Nevertheless, up to date there is no published evidence regarding their physical interaction. Consequently, ^{His}PCNA was included as a negative control in the pull-down with RPA-derivatised beads. As ^{His}PCNA bound neither to the BSA- nor to the RPA-derivatised

beads, the identified interactions of RPA with either Rad18 or Rad6 in this experiment are likely to be specific.

By means of the two-hybrid analysis in Davies *et al.* (2008), the interactions between the Rad18 protein and the individual subunits of RPA were further mapped. Subsequently, pull-down assays with ^{GST}Rfa1 (182-421) verified the two-hybrid results and established that the DNA-binding domain of Rfa1 is sufficient for the interaction with Rad18 (Figure 5.4). Similarly, pull-down assays with ^{GST}Rfa2 were consistent with the two-hybrid results and determined that this subunit was sufficient for the interaction with Rad18 (Figure 5.5). In addition, these experiments revealed that both Rfa1 and Rfa2 subunits contribute independently to the interaction with Rad18. Accordingly, it is likely that Rad18's affinity for the RPA complex is greater than its affinities for each one of the individual subunits.

6 Results IV: Interactions of the Rad18-Rad6 Complex, RPA and ssDNA

6.1 Introduction

As described in Chapter 5, yeast Rad18 physically interacts with RPA. According to Chapter 4, and in agreement with previously published data (Bailly *et al.*, 1997a), yeast Rad18 has intrinsic ssDNA-binding activity. Therefore, I was interested to test how the addition of ssDNA affects the interaction between Rad18 and RPA. In addition, since ^{GST}Rfa1 (182-421), the primary DNA-binding domain of Rfa1, was found to be sufficient for direct interaction with ^{HisVSV}Rad18 (Figure 5.4), it was important to determine if this domain was able to bind to Rad18 and to ssDNA simultaneously. This would provide essential insights regarding the nature of the interaction between Rad18 and RPA.

6.2 Results

6.2.1.1 ssDNA Stimulates the Interaction between Rad18 and the DNA-Binding Domain of Rfa1

A simplified system was chosen to test the effects that ssDNA had on Rad18 interaction with the DNA-binding domain of Rfa1. I followed an experimental set-up that only allowed the ^{GST}Rfa1 (182-421) protein to directly interact with ssDNA. The DNA-binding domain of human RPA70 (181-422), had been crystallized with an eight nt long ssDNA (Bochkarev *et al.*, 1997); (see Figure 1.4). A simulation of the solution structure of the DNA-binding domain of yeast Rfa1 bound to ssDNA suggested a similar positioning of the oligonucleotide (Park *et al.*, 2005). As the minimal binding site required for Rad18-ssDNA interaction was estimated to be between 25 and 35 nucleotides (Figure 4.6), short oligo(dT) primers of 10, 16 or 35 bases were utilised.

First, the ability of the ^{GST}Rfa1 (182-421) protein to bind ssDNA in our system had to be verified. This was achieved by gel-shift assays comparing the mobility retardation of radiolabelled oligo(dT) oligonucleotides upon incubation with

different concentrations of ^{GST}Rfa1 (182-421). GST was used as a negative control, and the full RPA complex was used as a positive control. Approximately 0.5 pmol of radiolabelled 16mer or 35mer oligo(dT) primers were incubated with the proteins in GST-PD Binding buffer on ice for 20 min, subjected to native gel electrophoresis at 4°C and analysed by Western blot. As shown in Figure 6.1, even though ^{GST}Rfa1 (182-421) had higher affinity for the longer 35mer oligo(dT) than for the 16mer oligo(dT), increasing levels of this protein resulted in enhancement of complex formation for both of the tested oligonucleotides. In contrast, GST did not bind either of them while RPA was able to efficiently bind to the 35mer oligo(dT) but not to the shorter 16mer oligo(dT).

Subsequently, the effect of ssDNA on the interaction between ^{HisVSV}Rad18 and ^{GST}Rfa1 (182-421) was assessed. Oligo(dT) primers of 10, 16 or 35 bases were pre-incubated with ^{GST}Rfa1 (182-421) at an ssDNA:Rfa1 ratio of 1:1 or 5:1. ssDNA-bound ^{GST}Rfa1 (182-421) was immobilized on glutathione beads and used in pull-down experiments with ^{HisVSV}Rad18-Rad6. As shown in Figure 6.2, ssDNA pre-bound to ^{GST}Rfa1 (182-421) had a stimulatory effect on the retention of ^{HisVSV}Rad18, suggesting that the E3 has higher affinity for the ssDNA-bound conformation of Rfa1 than for the DNA-free form of Rfa1.

Since the ^{GST}Rfa2 protein was also found to be sufficient for direct interaction with ^{HisVSV}Rad18 (Figure 5.5), it might be important to examine the effect of ssDNA on the interaction between ^{HisVSV}Rad18 and ^{GST}Rfa2. An intrinsic but low affinity for ssDNA was demonstrated for yeast Rfa2 (Sibenaller *et al.*, 1998). In order to test the affinity of ^{GST}Rfa2 for ssDNA in our system, gel-shift experiment was carried out. As shown in Figure 6.3, ^{GST}Rfa2 was found to have a very low affinity for ssDNA compared to ^{GST}Rfa1 (182-421). Therefore, in the context of the full RPA complex, any effect that the ssDNA may have on the interactions between Rfa2 and Rad18 would likely be masked by the Rfa1 subunit. For this reason, the effect of ssDNA on the interaction between Rad18 and ^{GST}Rfa2 was not pursued. However, it may be worthwhile to investigate this effect in the future, as the binding of Rad18 to Rfa2 could result in a significant conformational change, and in turn affect Rad18's association with the ssDNA. Additionally, ssDNA might have a significant effect on the interaction between this subunit of RPA and Rad18.

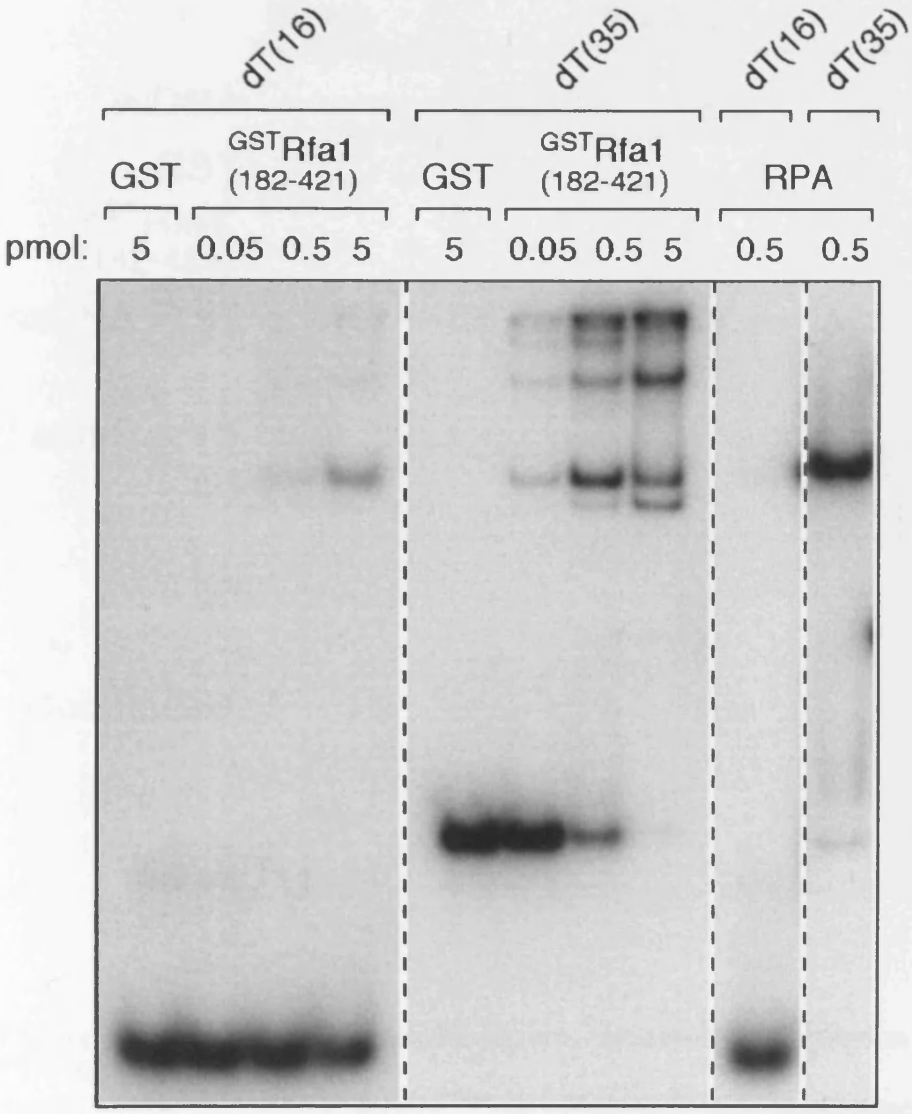

Figure 6.1 – ^{GST}Rfa1 (182-421) binds to short oligos with various affinities
Approximately 0.5 pmol of radiolabelled 16mer or 35mer oligo(dT) were incubated in GST-PD Binding buffer with GST, ^{GST}Rfa1 (182-421) or RPA, as indicated, for 20 min on ice. The samples were subjected to native gel electrophoresis at 4°C, the gel was dried and ^{32}P-labelled DNA was detected by autoradiography.

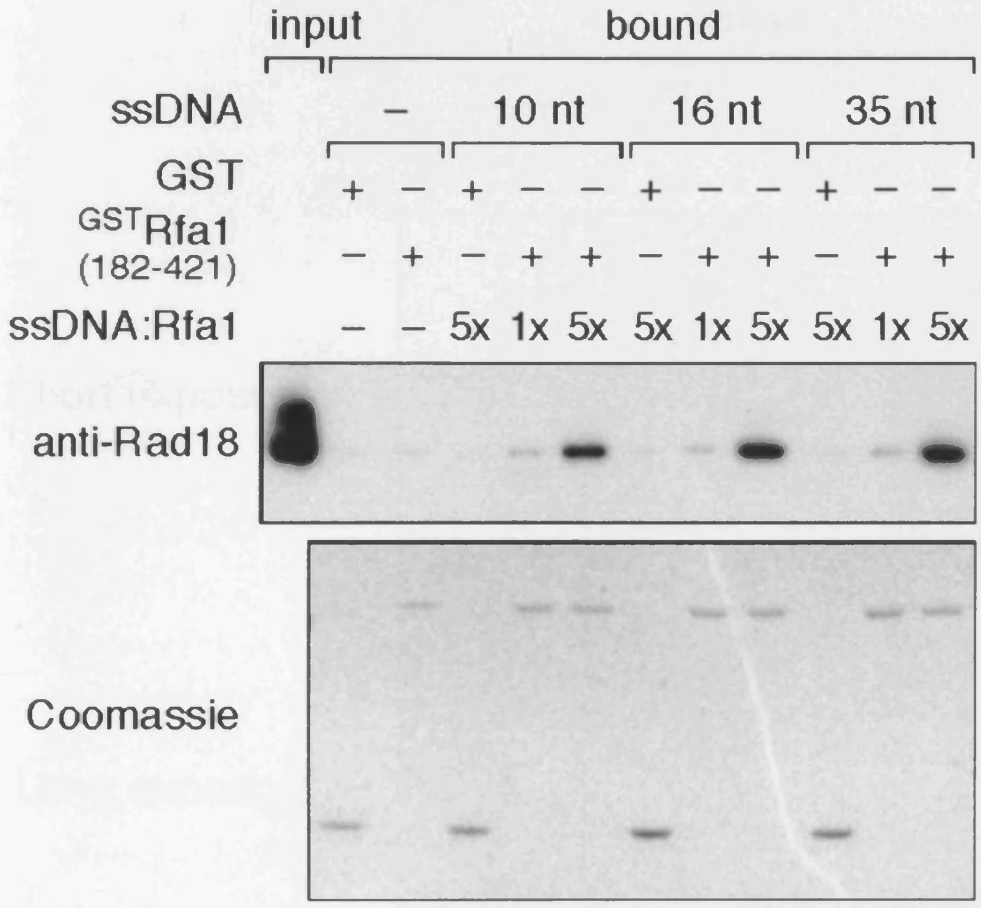

Figure 6.2 – ssDNA stimulates the interaction between ^{GST}Rfa1 and ^{HisVSV}Rad18

Approximately 0.5 nmol of GST or ^{GST}Rfa1 (182-421) were pre-incubated with oligo-dT of different lengths (10, 16 and 35 bases; oligo no. 1045, 1092 and 1094, respectively) at either ssDNA:Rfa1 ratio of 1:1 or 5:1 followed by incubation with glutathione sepharose beads with GST-PD Binding buffer. Subsequently, the beads were washed once with 500 µL GST-PD Binding buffer containing 100 µg/mL BSA and incubated with 10 pmol of the ^{HisVSV}Rad18-Rad6 complex in the same buffer at 4°C for 1 h. Then, the beads were washed 3 times with GST-PD Binding buffer containing BSA and twice more with the same buffer without BSA. After elution, the samples were subjected to SDS-PAGE followed by Coomassie staining or Western blotting. Rad18 was detected with anti-Rad18 antibody (polyclonal mouse 4 serum).

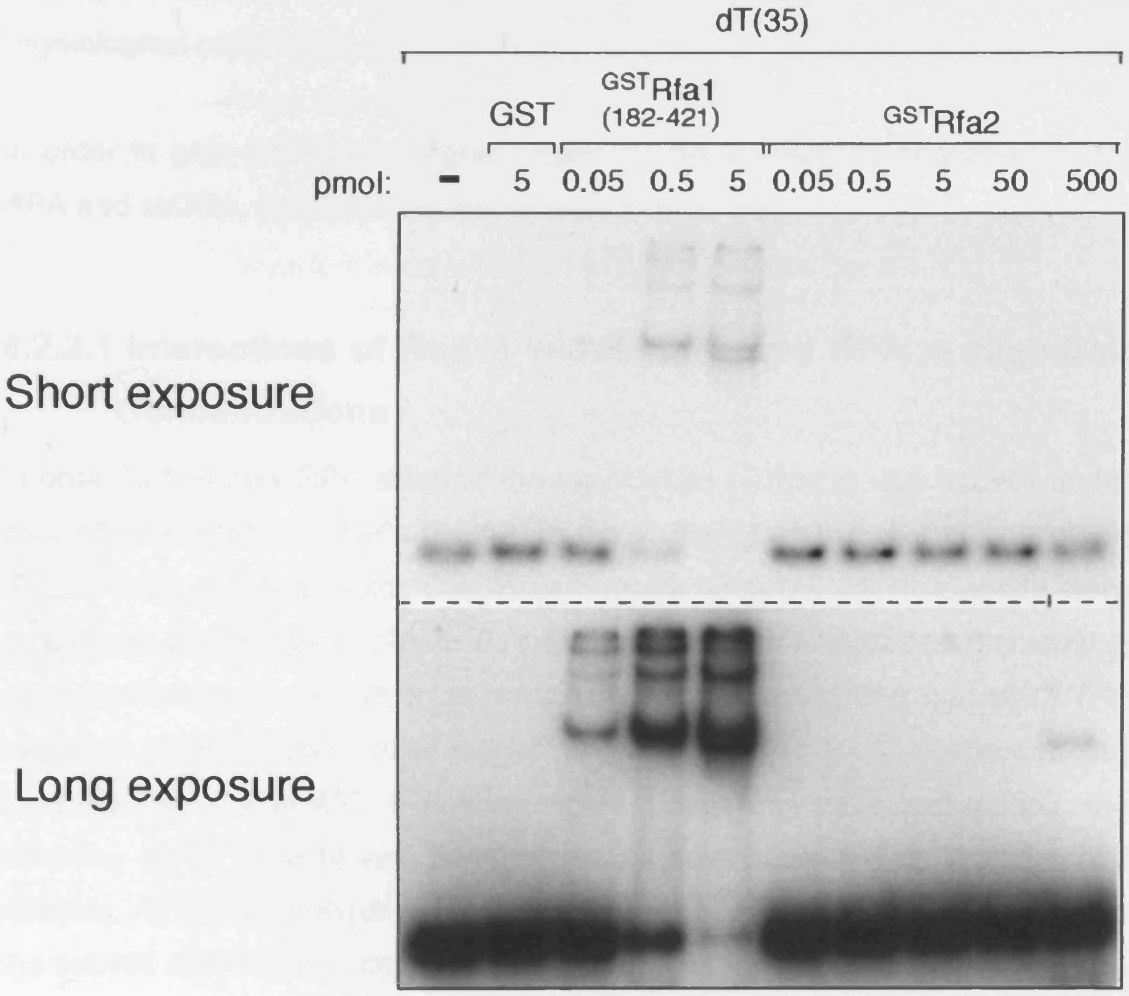

Figure 6.3 – ^{GST}Rfa2 has lower affinity for ssDNA than ^{GST}Rfa1 (182-421)
Approximately 0.5 pmol of radiolabelled 35mer oligo(dT) was incubated in GST-PD Binding buffer with GST, ^{GST}Rfa1 (182-421) or ^{GST}Rfa2, as indicated, for 30 min at 30°C. The samples were subjected to native gel electrophoresis at room temperature, the gel was dried and ^{32}P-labelled DNA was detected by autoradiography. Note that the short exposure corresponds to 4 h whereas the long exposure corresponds to 48 h.

6.2.2 Salt Concentration Defines Two Modes of Interaction

The results presented in Figure 6.2 led to the hypothesis that Rad18 could be recruited to RPA-coated ssDNA by means of their interaction. This model could also provide an explanation to the observation made in Chapter 4 regarding the inability of Rad18 to bind to ssDNA by itself at an ionic strength that resembles physiological conditions.

In order to gain additional insights regarding the interactions between Rad18, RPA and ssDNA, *in vitro* experiments were carried out.

6.2.2.1 Interactions of Rad18 with ssDNA and RPA at High Salt Concentrations

In order to test how RPA affected the association of Rad18 with ssDNA under conditions in which Rad18's binding to the ssDNA by itself was not observed (Figure 4.2), pull-down experiments with an immobilized oligonucleotide were performed. Either yeast RPA or *E. coli* SSB were pre-incubated at increasing concentrations with ssDNA in a binding buffer containing 250 mM NaCl (PD High-Salt Binding buffer). After a brief wash, ^{HisVSV}Rad18-Rad6 was added and incubated for 1 h at 4°C. Following high-salt washing steps and elution, the retention of ^{HisVSV}Rad18 and RPA on ssDNA was examined by Western blot analysis. As shown in Figure 6.4, in the absence of RPA, ^{HisVSV}Rad18 binding to the ssDNA could not be detected. In contrast, RPA binding to the ssDNA was independent of the presence of ^{HisVSV}Rad18, and increasing RPA levels in the input resulted in increasing levels of ssDNA-bound RPA. Consistent with the interaction described in Chapter 5, RPA recruited ^{HisVSV}Rad18 to the ssDNA, as increasing levels of ssDNA-bound RPA correlated with an enrichment of ^{HisVSV}Rad18 on the ssDNA. Importantly, this enrichment was not observed when SSB was used instead of RPA, suggesting a specific contribution of RPA to Rad18's association with ssDNA under these conditions.

6.2.2.2 Interactions of Rad18 with ssDNA and RPA at Low Salt Concentrations

In order to test how RPA affected Rad18 binding to ssDNA under conditions that were previously shown to allow the interaction between Rad18 and ssDNA (Figure 4.2), the experiment described in paragraph 6.2.2.1 was repeated with the only difference that during the incubation of the proteins with the ssDNA a binding buffer without NaCl was used (PD Low-Salt Binding buffer). As shown in Figure 6.5, under these experimental conditions, a significant level of ^{HisVSV}Rad18 was retained on the ssDNA in the absence of RPA. Similar to Figure 6.4, elevated levels of RPA in the input resulted in elevated levels of ssDNA-bound RPA.

Surprisingly, in contrast to the recruitment behaviour observed at high salt conditions, increasing levels of RPA on the ssDNA now reduced the levels of ssDNA-bound ^{HisVSV}Rad18. However, comparable amounts of SSB competed much more effectively with ^{HisVSV}Rad18 than RPA for ssDNA-binding. This indicates that, under the tested conditions, both RPA and ^{HisVSV}Rad18 probably share the space on the oligonucleotide (75 nt long), whereas increasing amounts of ssDNA-bound SSB prevent ^{HisVSV}Rad18 from binding to the ssDNA.

6.2.2.3 Interactions of Rad18 with ssDNA and RPA under a Range of Salt Concentrations

The results in Figure 6.4 and Figure 6.5, suggest two different modes of interaction between Rad18, RPA and ssDNA, depending on the ionic strength of the binding buffer. In order to assess the range of salt concentrations that corresponded to each interaction mode, the experiment described in paragraph 6.2.2.1 was performed in PD Low-Salt Binding buffer supplemented with different NaCl concentrations. As shown in Figure 6.6, under salt concentrations equivalent to or above 100 mM NaCl, RPA can efficiently recruit ^{HisVSV}Rad18 to the ssDNA. However, under salt concentrations equivalent to or below 50 mM NaCl, RPA and ^{HisVSV}Rad18 compete for ssDNA binding. Nevertheless, even in the latter experimental conditions, both proteins seem to be able to occupy the same stretch of ssDNA.

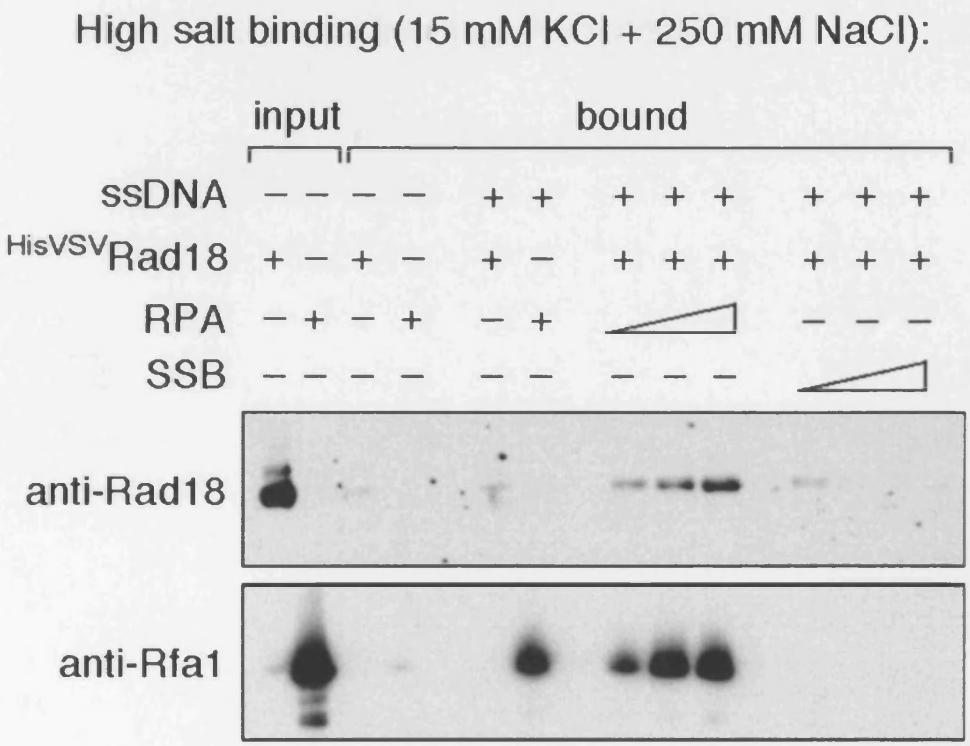

Figure 6.4 – RPA can recruit Rad18 to ssDNA *in vitro*
A 75mer oligonucleotide of mixed sequence (no. 870; ~ 5 pmol), immobilized on streptavidin beads, was incubated with RPA or SSB at increasing amounts (2.4, 8 or 24 pmol) at 4°C for 30 min in PD High-Salt Binding buffer. After a brief wash with the same buffer, the ^{HisVSV}Rad18-Rad6 complex (5 pmol) was added for 1 h incubation at 4°C. The beads were washed 3 times with PD High-Salt Binding buffer and twice with the same buffer with no BSA. After elution, the samples were subjected to SDS-PAGE followed by Western blotting. Rad18 was detected with anti-Rad18 antibody (polyclonal DH1 rabbit serum - see 2.11.1.2) and Rfa1 was detected with anti-Rfa1 antibody. Note that for the RPA blot, equal fractions of input and bound material were loaded. For the Rad18 blot, 1% of the input and 35% of the bound material were loaded.

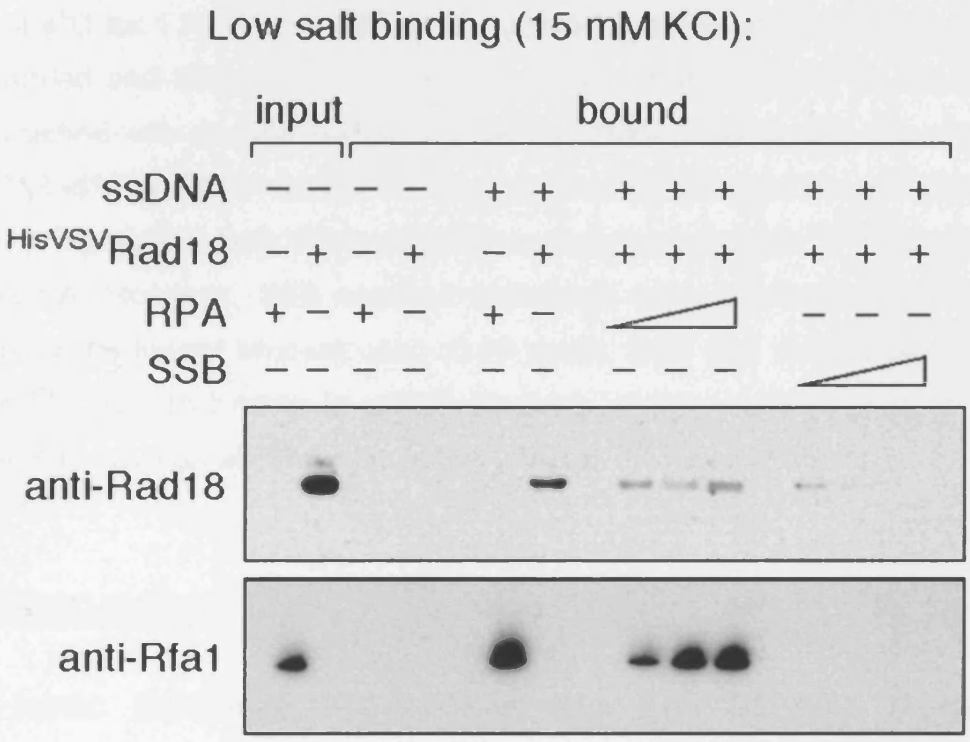

Figure 6.5 – Low salt concentration results in competition between Rad18 and RPA for binding to ssDNA

A 75mer oligonucleotide of mixed sequence (no. 870; ~ 5 pmol), immobilized on streptavidin beads, was incubated with RPA or SSB at increasing amounts (2.4, 8 or 24 pmol) at 4°C for 30 min in PD Low-Salt Binding buffer. After a brief wash, the ^{HisVSV}Rad18-Rad6 complex (5 pmol) was added for 1 h incubation with the same buffer at 4°C. The beads were washed 3 times with PD High-Salt Binding buffer and twice with the same buffer with no BSA. After elution, the samples were subjected to SDS-PAGE followed by Western blotting. Rad18 was detected with anti-Rad18 antibody (polyclonal DH1 rabbit serum - see 2.11.1.2) and Rfa1 was detected with anti-Rfa1 antibody. Note that for the RPA blot, equal fractions of input and bound material were loaded. For the Rad18 blot, 1% of the input and 35% of the bound material were loaded.

Next, I tested whether the competition observed under conditions of low ionic strength (Figure 6.5) was dependent on the order in which the proteins bound to the ssDNA. Therefore, a similar experiment to that shown in Figure 6.5 was carried out, but the order of addition of the proteins was reversed. At first, the ^{HisVSV}Rad18-Rad6 complex was incubated with ssDNA in binding buffer without NaCl at 4°C for 1 h. After a brief wash, increasing levels of either RPA or SSB were added and allowed to incubate for additional 30 min at 4°C. The beads were washed with a buffer containing 250 mM NaCl. After elution, the retention of ^{HisVSV}Rad18 and RPA on ssDNA was analysed by Western blot as before. As shown in Figure 6.7, both RPA and SSB were able to displace ^{HisVSV}Rad18 from the ssDNA. However, SSB seemed somewhat more efficient than RPA, as already at the lowest amount used (0.05 pmol), SSB was able to significantly reduce ^{HisVSV}Rad18 binding to ssDNA whereas, at that same amount, RPA did not seem to have an affect on the ssDNA-bound ^{HisVSV}Rad18 levels.

6.3 Discussion

6.3.1 Ionic Strength Modulates the Interactions between Rad18, RPA and ssDNA

6.3.1.1 ssDNA-Binding Properties of RPA and SSB

As mentioned in paragraph 1.3.2.4, alternative modes of RPA binding to ssDNA are believed to rise from differences in the number of its OB folds that contact the DNA (Philipova *et al.*, 1996) (see also Figure 1.3). Kumaran *et al.* (2006) found that the occluded site size required for yeast RPA binding was affected by salt concentration. At NaCl concentrations equivalent to or below 100 mM, the apparent occluded site was 18 – 20 nucleotides, at NaCl concentrations of 200 to 400 mM the length of this site increased to 21 – 23 nucleotides, and the maximal occluded site was 26 – 28 nucleotides in NaCl concentrations above 500 mM. Accordingly, in Figure 6.1, RPA was not able to bind to the short 16mer oligo(dT), but bound efficiently to the longer 35mer oligo(dT).

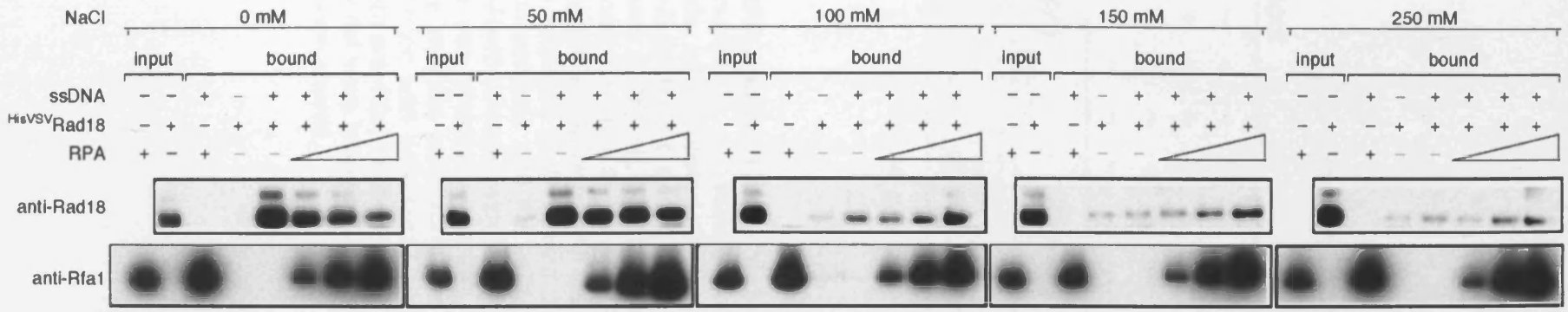

Figure 6.6 – Interactions of Rad18 with RPA and ssDNA under a range of salt concentrations

A 75mer oligonucleotide of mixed sequence (no. 870; ~ 5 pmol), immobilized on streptavidin beads, was incubated with RPA or SSB at increasing amounts (2.4, 8 or 24 pmol) at 4°C for 30 min in PD Low-Salt Binding buffer supplemented with different NaCl concentrations (0, 50, 100, 150 and 250 mM). After a brief wash, the ^{HisVSV}Rad18-Rad6 complex (5 pmol) was added for 1 h incubation at 4°C with the same buffer, keeping the ionic strength constant. The beads were then washed 3 times with PD High-Salt Binding buffer and twice with the same buffer with no BSA. After elution, the samples were subjected to SDS-PAGE followed by Western blotting. Rad18 was detected with anti-Rad18 antibody (polyclonal DH1 rabbit serum – see 2.11.1.2) and Rfa1 was detected with anti-Rfa1 antibody. Note that for the RPA blot, equal fractions of input and bound material were loaded. For the Rad18 blot, 1% of the input and 35% of the bound material were loaded.

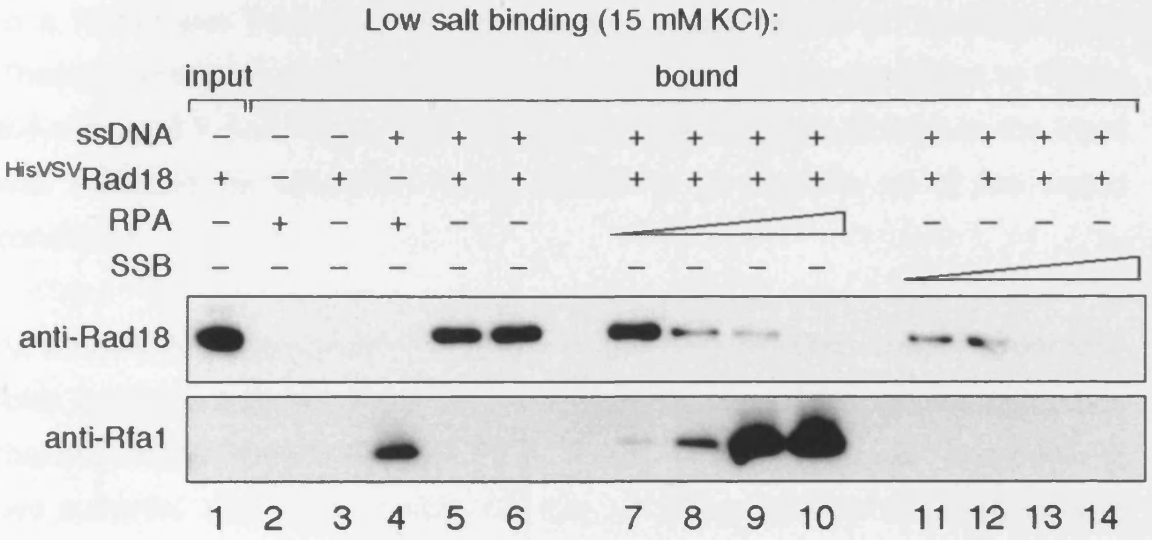

Figure 6.7 – RPA and SSB have higher affinity for ssDNA than Rad18
A 75mer oligonucleotide of mixed sequence (no. 870; ~ 5 pmol), immobilized on streptavidin beads, was incubated with the ^{HisVSV}Rad18-Rad6 complex (5 pmol) at 4°C for 1 h in PD Low-Salt Binding buffer. After a brief wash, RPA or SSB were added at increasing amounts (0.05, 0.5, 5 or 25 pmol) and the samples were allowed to incubate at 4°C for additional 30 min in the same buffer. The beads were washed 3 times with PD High-Salt Binding buffer and twice with the same buffer with no BSA. Note that in lane 5, the beads were subjected to the washing steps immediately after the incubation of the ^{HisVSV}Rad18-Rad6 complex with the ssDNA. In contrast, in lane 6, after pre-incubating the ^{HisVSV}Rad18-Rad6 complex with the ssDNA, PD Low-Salt Binding buffer was added and the sample was allowed to incubate for 30 min, before the beads were washed. After elution, the samples were subjected to SDS-PAGE followed by Western blotting. Rad18 was detected with anti-Rad18 antibody (polyclonal mouse 4 serum) and Rfa1 was detected with anti-Rfa1 antibody. Note that for the RPA blot, equal fractions of input and bound material were loaded. For the Rad18 blot, 1% of the input and 35% of the bound material were loaded.

The binding cooperativity can be affected by salt concentrations as well. Kumaran *et al.* (2006) found two modes of ssDNA-binding for yeast RPA, with RPA:ssDNA ratio of 1:1 or 2:1. At low salt concentration, both binding modes were detected whereas high salt concentration favoured the 1:1 binding mode. Taken these findings together, the expected number of RPA molecules to bind to a 75mer was 3 for the 1:1 binding mode and 6 for the 2:1 binding mode. These estimations were used for the experimental set-up described in Figure 6.4, Figure 6.5 and Figure 6.6. Correspondingly, 24 pmol of RPA in the input was sufficient for saturation of the ssDNA (~ 5 pmol) in all of the tested conditions.

As mentioned in paragraph 1.3.1, the *E. coli* SSB tetramer contains four OB-folds (one per subunit) and also has a complicated ssDNA-binding behaviour that depends on the solution conditions. It has two binding modes, one involving two subunits, with an occluded site size of 35 nucleotides and high binding cooperativity, and the other involving all four subunits, with an occluded site size of 65 nucleotides and low binding cooperativity (Lohman and Overman, 1985; Lohman and Ferrari, 1994).

Although the details of DNA-binding vary between RPA and SSB, (Philipova *et al.*, 1996) suggested that yeast RPA is more similar to bacterial SSB than thought previously. As Rad18 did not bind to the SSB-derivatised beads (see Figure 7.6 below) and considering the literature discussed above, SSB was chosen as a negative control in the studies elucidating the interaction between ssDNA, Rad18 and RPA.

6.3.1.2 RPA Recruits Rad18 to ssDNA at High Ionic Strength

According to Figure 6.4, RPA can efficiently recruit ^{HisVSV}Rad18 to ssDNA under conditions that do not allow the E3 to bind ssDNA by itself. Since SSB was not able to afford this effect, the recruitment was considered to be specific for RPA. Furthermore, the latter suggests that the recruitment does not arise from non-specific effects such as a change in the ssDNA conformation upon RPA or SSB binding. Rather, the specific recruitment of Rad18 to the ssDNA by RPA may be

mediated by protein-protein interactions. Alternatively, through these interactions RPA may stabilise the binding of Rad18 to ssDNA.

Although changes to the buffer conditions pose effects that are rather artificial, the results presented in Figure 6.6 indicate that under a range of 'physiological-like' salt concentrations, RPA is clearly needed for the recruitment of ^{HisVSV}Rad18 to the ssDNA. Importantly, these results are consistent with *in vivo* evidence, recently obtained in the laboratory, suggesting that the association of Rad18 with ssDNA correlates with that of RPA. Chromatin immunoprecipitation experiments from yeast cells, released from G1-arrest and treated with HU, revealed that Rad18 associates with replication forks near a replication origin (Davies *et al.*, 2008, Figure 6A in Appendix) similar to PCNA and RPA (Papouli *et al.*, 2005). Moreover, in *rad52* yeast cells, both Rfa1 and Rad18 are enriched next to an HO endonuclease-induced DSB (Davies *et al.*, 2008, Figure 6B and 6D in Appendix). These cells, deficient in homologous recombination and Rad51 filament formation, allow a prolonged binding by RPA to the resected DSB ends (Wang and Haber, 2004). This result suggests that Rad18 and RPA interact with each other on chromatin. Moreover, it excludes that the association of Rad18 with the DNA is mediated by PCNA (Davies *et al.*, 2008, Figure 6C in Appendix).

RPA is considered to be a modular protein that is able to interact with many proteins (Fanning *et al.*, 2006). Recruitment of proteins to ssDNA by RPA was proposed to occur via different mechanisms. On the one hand, RPA can engage in cooperative ssDNA-binding with other proteins. On the other hand, RPA can "trade places" on the ssDNA in a stepwise manner with another protein (Fanning *et al.*, 2006). The results presented in Figure 6.4 and in Figure 6.6 support the notion that, at high ionic stress, Rad18 and RPA could cooperatively bind to the ssDNA or that the binding of RPA would mediate the binding of Rad18. However, induced conformational changes of Rad18 upon RPA or ssDNA-binding have yet to be verified.

In the literature, there are additional reports for similar salt-sensitive behaviour of proteins that is overcome by interaction with another protein. For example, the catalytic subunit of the DNA-dependent protein kinase (DNA-PKcs), which is

a nuclear serine / threonine protein kinase, was found to bind dsDNA only at low NaCl concentration (10 mM) but not at higher salt concentrations (100 mM and 200 mM) (Hammarsten and Chu, 1998). However, in the presence of the non-specific DNA-end binding Ku protein, the interaction between DNA-PKcs and DNA was restored at high salt conditions, suggesting that Ku stabilises the binding of DNA-PKcs to DNA at physiological conditions (Hammarsten and Chu, 1998). Consequently, Smith and Jackson (1999) hypothesised that *in vivo*, Ku recruits DNA-PKcs to the DNA, facilitating the interaction between DNA-PK and DNA and thereby channelling the kinase activity to the appropriate substrates. Similarly, and in accordance with Davies *et al.* (2008), upon DNA damage, RPA might recruit Rad18 to stalled replication forks, facilitating PCNA ubiquitylation.

Precedence for the involvement of RPA in recruitment of DNA repair factors to ssDNA was shown for the human ATRIP-ATR and the yeast Ddc2-Mec1 complexes (Zou and Elledge, 2003; Zou *et al.*, 2003). This recruitment is important for the activation of the replication checkpoint (see 1.5.1). Although the circumstances for Rad18 and Ddc2-Mec1 recruitment are similar with regard to the cell-cycle phase and to the type of DNA damage inducing the response (see 1.5.2), the activation of the *RAD6* pathway and the replication checkpoint were found to be independent of each other (Davies *et al.*, 2008).

Taken together, the results presented in Chapter 6 and in Davies *et al.* (2008) support the hypothesis that *in vivo*, yeast Rad18 is recruited to RPA-coated ssDNA, and in the context of replication fork stalling, contributes to PCNA ubiquitylation. Thus, both Rad18 and RPA are important for the activation of the DNA damage tolerance pathway.

6.3.1.3 RPA Competes with Rad18 for ssDNA-Binding at Low Ionic Strength

Surprisingly, the results shown in Figure 6.5 and in Figure 6.6 suggest that the mode of interaction between ssDNA, Rad18 and RPA strongly depends on the ionic strength of the binding buffer. This phenomenon could be explained by

salt-dependent conformational changes of both proteins. As discussed above (6.3.1.1), RPA is known to have a complicated DNA-binding behaviour, which is affected by the buffer's ionic strength (Fanning *et al.*, 2006; Kumaran *et al.*, 2006). In addition, the results presented in Chapter 4 could be explained by salt-dependent conformational changes in Rad18 that modulate its ssDNA-binding ability. Therefore, it is probable that both proteins undergo conformational changes in response to different salt concentrations, which in turn modulate their interaction in the presence of DNA.

Apparently, at low ionic strength, Rad18 exhibits a detectable ssDNA-binding affinity by itself (Figure 4.2, Figure 6.5 and Figure 6.6). However, it does not appear to engage in cooperative binding with RPA. Instead, the two proteins compete for the same stretch of ssDNA. Under the same experimental conditions, the minimal length of DNA required for stable Rad18 binding was between 25 and 35 nucleotides (Figure 4.6), whereas the reported occluded binding site for RPA was between 18 and 20 nucleotides. Accordingly, RPA and Rad18 could share the space on the 75mer used in these experiments. However, since the reported occluded binding site for SSB was larger (65 nucleotides under similar salt concentration), Rad18 would not be able to occupy the space left after SSB binding.

SSB and RPA have very high affinities for ssDNA in the range of 10^{-9} – 10^{-10} M (Fanning *et al.*, 2006). Although the ssDNA-binding affinity of yeast Rad18 was never calculated, it can be assumed that it is significantly lower compared to that of RPA. Accordingly, at low ionic strength, both SSB and RPA compete with Rad18 for ssDNA-binding (Figure 6.7). However, SSB seems to compete more efficiently, suggesting that even under these conditions, weak or temporary interactions could still exist between Rad18 and RPA. Alternatively, the size difference in the occluded ssDNA-binding site for RPA and SSB could account for their somewhat different competition behaviours with Rad18.

6.3.2 Varying Affinities of RPA, ^{GST}Rfa1 (182-421) and ^{GST}Rfa2 for ssDNA

In order to verify the ssDNA-binding abilities of the individual subunits of RPA in our system, gel-shift assays were carried out. According to Figure 6.1, ^{GST}Rfa1 (182-421) was able to bind to both tested oligonucleotides, suggesting that the occluded site size for this construct can be shorter than 16 nucleotides. In addition, following incubation with the 35mer oligo(dT), there were four bands corresponding to four different ssDNA-^{GST}Rfa1 (182-421) complexes. These results are consistent with an occluded site size of eight nucleotides (Pfuetzner *et al.*, 1997), with protein:ssDNA ratio of 1:1, 2:1, 3:1 and 4:1. As expected, ^{GST}Rfa1 (182-421) exhibited significantly lower affinity for the shorter oligonucleotide than for the longer one (Fanning *et al.*, 2006).

When comparing the affinities of ^{GST}Rfa1 (182-421) and RPA for the 35mer oligo(dT), an apparent 10-fold reduction was observed for the Rfa1 DNA-binding domain. This is in agreement with Pfuetzner *et al.* (1997), suggesting that the GST tag does not significantly alter the ssDNA-binding properties of this domain. Consequently, ^{GST}Rfa1 (182-421) was further used to study how ssDNA effects its interaction with Rad18.

As shown in Figure 6.3 (longer exposure), ^{GST}Rfa2 was able to bind to the 35mer oligo(dT) at an apparent affinity that was less than 10000-fold compared to that of ^{GST}Rfa1 (182-421). According to Bastin-Shanower and Brill (2001), only a 100-fold reduction was observed between yeast Rfa2 and the DNA-binding domain of yeast Rfa1. Perhaps the GST tag fused to the Rfa2 subunit is responsible for the discrepancy between the results presented in Figure 6.3 and the published literature. Alternatively, differences in the experimental conditions, including the oligonucleotide length, the temperature or the buffer composition may account for this discrepancy. Due to the very low affinity observed for the ^{GST}Rfa2 construct for ssDNA in our system, studies regarding the effects of ssDNA on the interaction between Rad18 and ^{GST}Rfa2 were not pursued. Nonetheless, in order to gain a complete understanding of the network of interactions between Rad18, RPA and ssDNA, this should be an important aspect to explore in the future.

6.3.3 ssDNA Stimulates the Interaction between Rad18 and Rfa1 DNA-Binding Domain

Bochkareva *et al.* (2001) suggested that OB folds might participate in protein-protein interactions. Accordingly, ^{GST}Rfa1 (182-421) was found to be sufficient for Rad18's binding *in vitro* (Figure 5.4). As an OB domain can, in principle, bind to several types of molecules, it may have regulatory roles (Bochkareva *et al.*, 2001). The results presented in Figure 6.2 are in accordance with this notion. Pre-incubation of ^{GST}Rfa1 (182-421) with short oligonucleotides resulted in significant stimulation of ^{HisVSV}Rad18 binding, suggesting that ssDNA-bound ^{GST}Rfa1 (182-421) is a better binding partner for Rad18 than its ssDNA-free form.

According to Bochkareva *et al.* (2001), RPA undergoes a dramatic conformational change as a consequence of binding to ssDNA. The authors suggested that this conformational change could play a regulatory role for RPA-protein interaction via allosteric effects. For example, it could favour interactions with proteins that have higher affinity for DNA-bound RPA and disfavour interactions with proteins associating with DNA-free RPA. The results presented in Figure 6.2 indicate that conformational changes resulting from ^{GST}Rfa1 (182-421) binding to ssDNA favour the interactions between ^{GST}Rfa1 (182-421) and ^{HisVSV}Rad18. Furthermore, these results exclude a possibility of competition between ssDNA and Rad18 for ^{GST}Rfa1 (182-421) binding under these experimental conditions.

The oligonucleotides used in Figure 6.2 were too short to allow the binding of both proteins to the ssDNA. Although obtained from this simplified system, the results presented in Figure 6.2 can be applied to better understanding of principal characteristics of the interaction mechanism involving ssDNA, Rad18 and RPA. Consequently, this interaction might not require the DNA-binding ability of Rad18. However, further evidence has to be obtained to support this possibility (see Chapter 7 below).

7 Results V: Contribution of the SAP Domain to Rad18 Interactions and Activity

7.1 Introduction

The results presented in previous chapters (Chapters 4-6) as well as in Davies *et al.* (2008) suggest that Rad18 interacts physically with RPA, and that via their interaction Rad18 might be recruited to ssDNA under physiological conditions. However, these results do not address whether the interactions between Rad18, RPA and ssDNA are mediated solely by means of protein-protein interactions or whether the interaction of Rad18 with ssDNA is also required. Figure 7.1 below illustrates two possible models for the interactions between Rad18, RPA and ssDNA. Figure 7.1A represents a direct interaction between the Rad18-Rad6 complex and RPA, where the latter, in turn, physically interacts also with ssDNA. In this model, Rad18 does not contact the ssDNA directly. The stimulatory effect that ssDNA had on the interactions between Rad18 and ^{GST}RPA (182-421) (Figure 6.2) might offer an explanation of how the interaction of Rad18 with the ssDNA-bound RPA is favoured over the DNA-free form of RPA. Thus, *in vivo*, Rad18 would be recruited to chromatin-associated RPA with higher affinity than to the soluble RPA pool. Figure 7.1B represents an alternative model in which both RPA and Rad18 contact each other and the ssDNA simultaneously. In this scenario, the association of Rad18 with ssDNA could be stabilised by RPA under physiological conditions.

In order to test these two possible models, it was attempted to abolish Rad18's intrinsic ability to bind to ssDNA. If a mutant of Rad18 deficient in ssDNA-binding could still be recruited to the ssDNA by RPA, then the model in Figure 7.1A would provide a better explanation for the interactions within the complex. However, if the result were the opposite, and assuming that the DNA-independent interaction between this Rad18 mutant and RPA was unchanged, then the model in Figure 7.1B would best explain the interactions within the complex.

Although in the literature there were several suggestions for putative DNA-binding domains in yeast Rad18 (Bailly *et al.*, 1997b), until now there is no formal evidence to confirm their role in DNA-binding. In principle, both the ZnF and the SAP domain could participate in DNA-protein interactions, although yet unidentified domains could contribute as well. Indeed, both domains were suggested to be involved in the formation of human Rad18 foci in response to DNA damage (Nakajima *et al.*, 2006). However, the SAP domain was suggested to contribute to the localisation of Rad18 to stalled replication forks along with Polη, whereas the ZnF was found to be important for the formation of replication-independent damage-induced foci (Nakajima *et al.*, 2006).

Recently, in Notenboom *et al.* (2007), the different domains of human Rad18 were mapped and the SAP domain was found to be sufficient for both ssDNA and dsDNA-binding *in vitro*. In addition, the ZnF domain was not able to bind to DNA by itself, but instead was shown to bind to ubiquitin, indicating its possible role as an ubiquitin-binding domain (of type UBZ).

Although a discrepancy exists between these two publications regarding the role of hRad18's ZnF, both of them agree on the DNA-binding role of the SAP domain. Furthermore, important residues for ssDNA-binding that were identified within the SAP domain of hRad18 by Notenboom *et al.* (2007) are conserved in yeast, as shown by sequence alignment in Figure 7.1C. Therefore, the SAP domain was chosen as the best candidate to contribute to the ssDNA-binding activity of yeast Rad18.

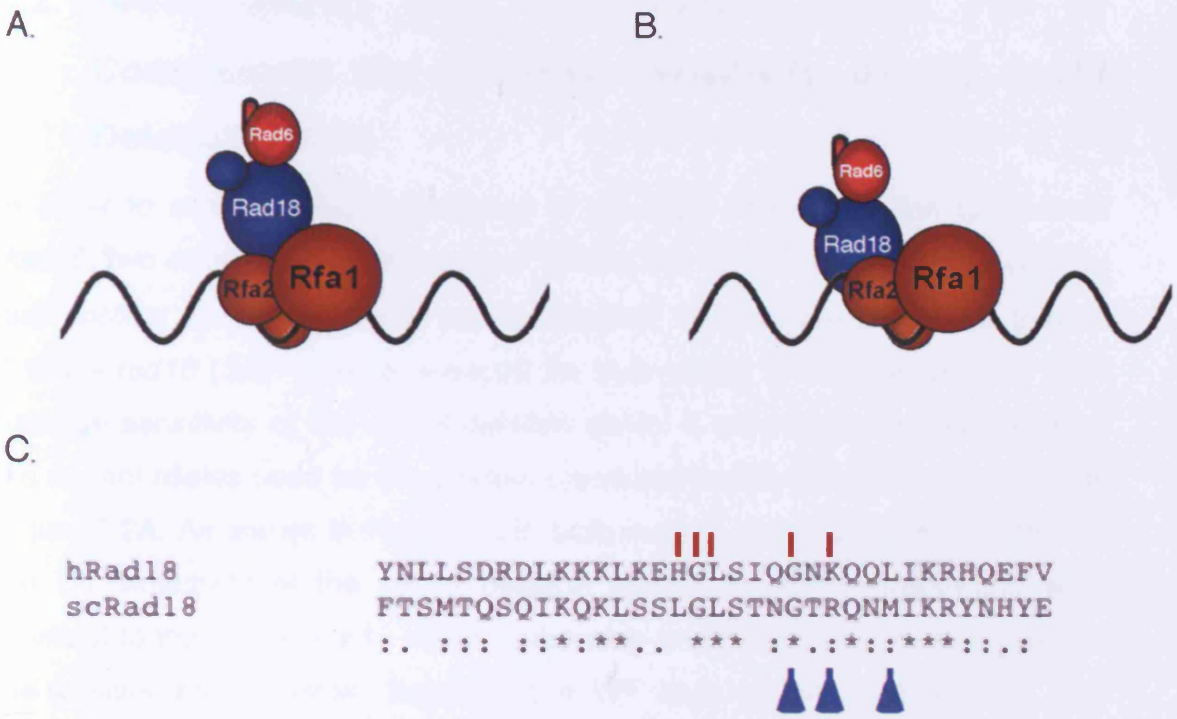

Figure 7.1 – Possible mechanisms for the interactions between Rad18, RPA and ssDNA

A. Protein-protein interactions between the Rad18-Rad6 complex and RPA are sufficient for mediating the interaction with ssDNA.

B. Protein-protein interactions between the Rad18-Rad6 complex and RPA, but also direct interaction between Rad18 and ssDNA are required for the stable association of the complex.

C. Sequence alignment of human and yeast Rad18's SAP domains. Important ssDNA-binding residues in human SAP domain according to Notenboom *et al.* (2007) are marked with red lines. Three residues in yeast SAP domain that were mutated to alanines for this thesis are marked with blue triangles (G299, R301 and M304).

7.2 Results

7.2.1 *rad18* (*SAP*Δ) and *rad18* (*SAP**) Alleles Fail to Complement the Damage Sensitivity of the *rad18* Deletion Strain

In order to establish the importance of the SAP domain for the function of Rad18, two *rad18* mutant alleles, one lacking the SAP domain – *rad18* (*SAP*Δ) and another harbouring three point mutations in conserved residues (Figure 7.1C) – *rad18* (*SAP**), were assayed for their ability to complement the DNA damage sensitivity of the *rad18* deletion strain. A schematic representation of the mutant alleles used for the studies presented in this chapter can be seen in Figure 7.2A. As shown in Figure 7.2B, both mutant alleles did not complement the UV sensitivity of the *rad18* deletion strain, and their sensitivities were identical to that of the *rad18* strain harbouring an empty plasmid. As expected, the positive control strain, harbouring a WT copy of the *RAD18* gene, was resistant to UV irradiation. Accordingly, in Figure 7.2C, both mutant alleles failed to complement the sensitivity of the *rad18* deletion for two other DNA damaging agents, 4NQO and MMS. Their defect was equivalent to that of the *rad18* deletion strain. In contrast, the positive control strain, harbouring a WT copy of the *RAD18* gene, was resistant to the different treatments, as expected.

One possible explanation for the inability of the mutant alleles to complement the deletion phenotype could be that the mutant proteins are unstable or are not produced. Figure 7.2D shows a comparison of Rad18 levels in total cell extracts derived from yeast strains used in Figure 7.2B and Figure 7.2C. Noticeably, the Rad18 levels in the *WT* yeast strain, used as a positive control, are higher than those of a *rad18* deletion strain complemented with a WT copy of the *RAD18* gene. However, the levels of the latter are similar to those of the Rad18 (SAP*) mutant. Unfortunately, the Rad18 (SAPΔ) could not be detected in this Western blot, as it was masked by one of the non-specific bands recognised by the antibody. Nevertheless, an immunoprecipitation experiment, performed with those strains, revealed that the levels of the Rad18 (SAPΔ) and the Rad18

(SAP*) proteins were somewhat reduced in comparison to the WT protein levels (Davies *et al.*, 2008, Figure 7D in Appendix).

To exclude that this reduction in the protein levels could account for the DNA damage sensitivity observed for the *rad18* (*SAP*Δ) and the *rad18* (*SAP**) mutants, the mutant alleles were over-expressed using the inducible *GAL1* promoter. As shown in Figure 7.3A, after induction of *RAD18* over-expression with galactose, the levels of the mutant proteins were comparable to that of the over-expressed Rad18 (WT) protein in total cell extracts. As expected, expression of the mutant alleles in a glucose-containing medium was repressed. As a positive control, a *WT* yeast strain, transformed with the *RAD18* gene under the *GAL1* promoter, was used. Thus, in this strain *RAD18* was expressed also in the glucose-containing medium. However, upon induction with galactose, there was a significant elevation in the protein levels.

Subsequently to ensuring equivalent protein levels (Figure 7.3A), these strains were analysed with respect to their DNA damage sensitivities by spot assays as before. As shown in Figure 7.3B, even when the mutant alleles were over-expressed, the DNA damage sensitivity to 4NQO or MMS was not rescued. As expected, the *WT* strain, transformed with a WT copy of the *RAD18* gene, was resistant to both tested drugs, on either the glucose- or the galactose-containing plates. Although the *RAD18* expression was significantly enhanced as a result of the induction with galactose, there was no change in the resistance of this strain. This suggests that a small amount of the Rad18 protein is sufficient for overcoming the DNA damage-induced sensitivity but also that its over-expression does not have a negative effect. In addition, the results suggest that the *rad18* deletion strain has a slight growth defect in comparison to the *WT* strain, which cannot be rescued by either one of the mutant alleles (Figure 7.3B – control plates).

Taken together, these results suggest that the SAP domain is essential for Rad18's function *in vivo*.

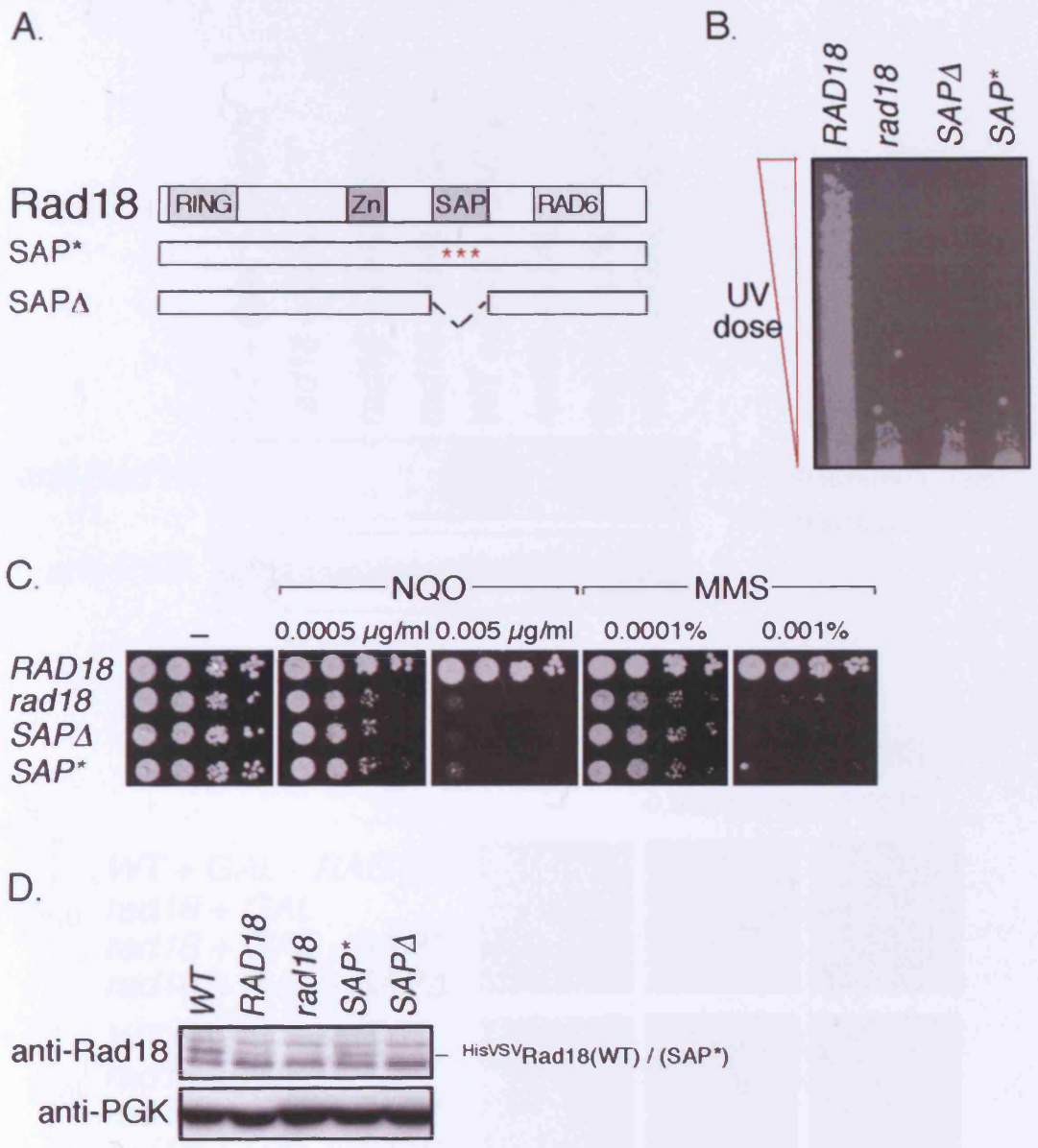

Figure 7.2 – *rad18* (*SAPΔ*) and *rad18* (*SAP) alleles cannot complement *rad18* sensitivity to DNA damage**

A. A schematic representation of two Rad18 mutant proteins: the *SAP** construct harbours three amino acid substitutions (G299A/R301A/M304A), whereas in the *SAPΔ* construct the entire SAP domain, amino acids 279 to 312, is deleted.

B. A UV sensitivity assay was performed with *rad18* strain complemented with *RAD18 WT*, empty plasmid, *SAPΔ* or *SAP** constructs.

C. Spot assays for 4NQO and MMS sensitivity were performed on *rad18* deletion strain, complemented by the indicated *RAD18* constructs as in B.

D. Western blot analysis of total cell extracts derived from yeast strains used in B and in C. The *WT* strain was included as a positive control for Rad18 protein levels. Rad18 was detected with anti-Rad18 antibody (DH1 rabbit polyclonal serum – see 2.11.1.2). Note that a non-specific band, recognised by the antibody, is masking the signal for Rad18 (SAPΔ). PGK was detected by anti-PGK antibody as a loading control.

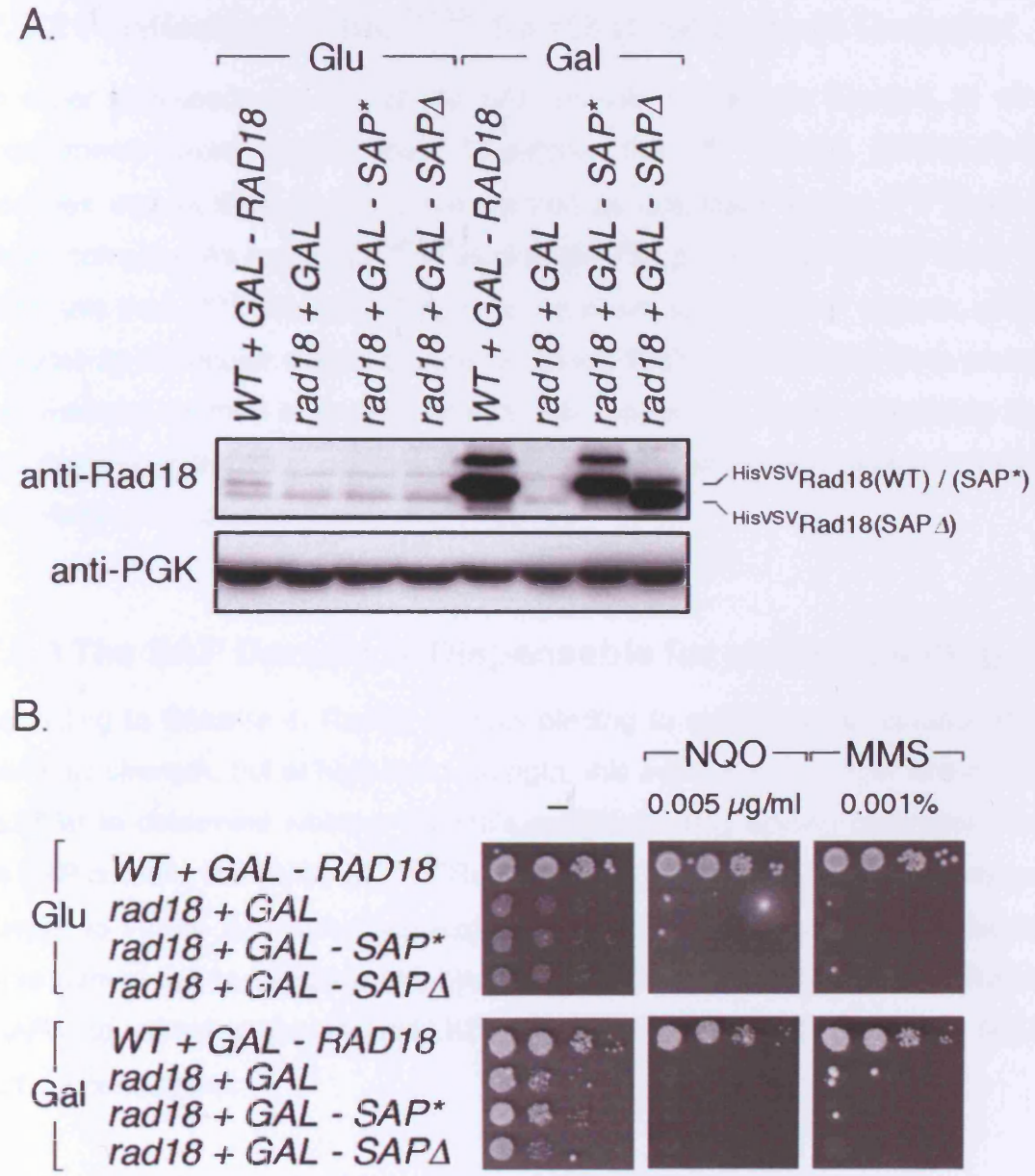

Figure 7.3 – Over-expression of *RAD18* mutant alleles does not rescue *rad18* sensitivity to DNA damage

A. Western blot analysis of total cell extracts derived from yeast strains grown in medium containing either glucose (Glu) or galactose (Gal). The *rad18* deletion strain was complemented with an empty plasmid or with *SAPΔ* or *SAP** constructs under control of the *GAL1* promoter. The *WT* strain transformed with the *GAL-RAD18* construct was used as a positive control. Rad18 was detected with anti-Rad18 antibody (DH1 rabbit polyclonal serum – see 2.11.1.2) and PGK was detected by anti-PGK antibody as a loading control.

B. Spot assays for 4NQO and MMS sensitivity were performed on the *rad18* deletion strain, complemented by the indicated *RAD18* constructs as in A. The *WT* strain transformed with *GAL-RAD18* construct was used as a positive control. Cells were grown on plates containing either glucose (Glu) or galactose (Gal) with the respective drugs, as indicated.

7.2.2 Purification of the ^{HisVSV}Rad18 (SAPΔ)-Rad6 Complex

In order to dissect the role of the SAP domain in Rad18's function, *in vitro* experiments were carried out. Therefore, the ^{HisVSV}Rad18 (SAPΔ)-Rad6 complex was purified by the same method as described for the ^{HisVSV}Rad18-Rad6 complex. As expected, ^{HisVSV}Rad18 (SAPΔ) protein ran slightly lower on SDS gels than ^{HisVSV}Rad18 (WT) due to the absence of the SAP domain, which reduces its molecular weight by approximately 4 kDa (Figure 7.4). Both protein preparations seemed to contain comparable amounts of Rad6, suggesting that the deletion of the SAP domain did not affect the interaction between Rad18 and Rad6, as expected (Bailly *et al.*, 1997b).

7.2.3 The SAP Domain is Dispensable for ssDNA-Binding

According to Chapter 4, Rad18 exhibits binding to ssDNA under conditions of low ionic strength, but at high ionic strength, this activity is no longer detectable. In order to determine whether Rad18's ssDNA-binding activity originates from its SAP domain, the ability of ^{HisVSV}Rad18 (SAPΔ) to bind ssDNA was analysed. Similar to Figure 4.2, pull-down experiments with immobilized oligonucleotide were carried out to compare the binding of ^{HisVSV}Rad18 (WT) and ^{HisVSV}Rad18 (SAPΔ) to ssDNA at low (15 mM KCl) and high (15 mM KCl + 150 mM NaCl) salt concentrations.

As shown in Figure 7.5, at low salt concentration, both proteins were retained on the ssDNA. This surprising result suggests that ^{HisVSV}Rad18 (SAPΔ) still contains an intrinsic ability to bind to ssDNA. When comparing the Western blot signal of the input samples, it is apparent that more ^{HisVSV}Rad18 (SAPΔ) was used than WT protein in this experiment. Hence, it is difficult to assess if there is a difference between the affinities of the WT and the mutant protein for ssDNA. As expected, neither of the proteins seemed to be able to bind to the ssDNA at high salt concentration.

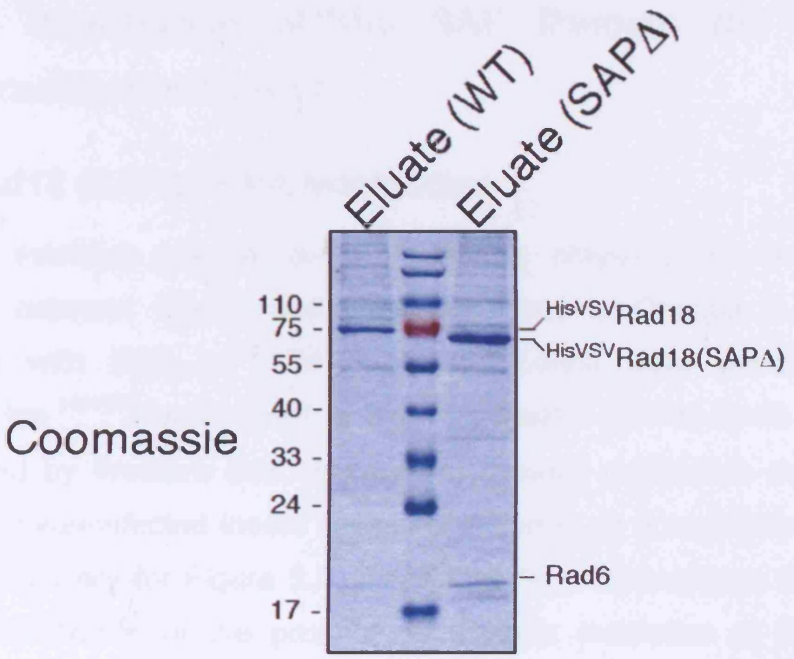

Figure 7.4 – Purified ^{HisVSV}Rad18 (SAPΔ)-Rad6 complex
Comparison of protein preparations from baculovirus-infected Sf9 insect cells. ^{HisVSV}Rad18-Rad6 and ^{HisVSV}Rad18 (SAPΔ)-Rad6, approximately 0.5 μg and 1 μg, respectively, were loaded and analysed by Coomassie staining.

Figure 7.5 – ^{HisVSV}Rad18 (SAPΔ) can still bind to ssDNA at low ionic strength
Approximately 5 and 10 pmol of ^{HisVSV}Rad18-Rad6 and ^{HisVSV}Rad18 (SAPΔ)-Rad6 complexes were incubated with a 75mer of mixed sequence (no. 870; ~ 5 pmol) at 4°C for 1 hour in PD Low-Salt Binding buffer supplemented with different NaCl concentrations (0 and 150 mM NaCl). Then, the beads were washed 3 times with PD High-Salt Binding buffer and twice more with the same buffer with no BSA. After elution, the samples were subjected to SDS-PAGE followed by Western blotting. Rad18 was detected with anti-Rad18 antibody (polyclonal mouse 4 serum).

7.2.4 The Importance of the SAP Domain for Rad18's Interactions with RPA

7.2.4.1 Rad18 (SAPΔ)-RPA Interaction

In order to establish whether the SAP domain played a role in the direct interactions between Rad18 and RPA described in Chapter 5, pull-down experiments with SSB- or RPA-derivatised beads were performed. The retention of the ^{HisVSV}Rad18-Rad6 or the ^{HisVSV}Rad18 (SAPΔ)-Rad6 complexes was analysed by Western blot. In addition, a mock purification derived from *RAD6* baculovirus-infected insect cells was included as a negative control. As described previously for Figure 5.2, a non-specific endonuclease was present during the incubation of the proteins to exclude mediation of DNA in the interactions. As shown in Figure 7.6A, the amount of ^{HisVSV}Rad18 (SAPΔ) that was able to bind to the RPA-derivatised beads was significantly reduced compared to ^{HisVSV}Rad18, suggesting a possible role for the SAP domain in the protein-protein interactions between Rad18 and RPA.

7.2.4.2 Rad18 (SAPΔ)-Rfa1 DNA-Binding Domain Interaction

In order to test the interaction between ^{HisVSV}Rad18 (SAPΔ) and the DNA-binding domain of Rfa1, either GST or ^{GST}Rfa1 (182-421) were immobilized on glutathione sepharose beads and incubated with either ^{HisVSV}Rad18-Rad6 or ^{HisVSV}Rad18 (SAPΔ)-Rad6. As shown in Figure 7.6B, both WT and mutant proteins bound to ^{GST}Rfa1 (182-421) at comparable amounts, suggesting that the deletion of the SAP domain does not significantly alter the binding properties of Rad18 to the DNA-binding domain of Rfa1. Furthermore, this conclusion is in agreement with Figure 7.8A, showing that both *rad18* (*SAPΔ*) and *rad18* (*SAP**) constructs retained the ability to interact with different constructs of *RFA1* in the two-hybrid system with a similar pattern to that of *RAD18* (*WT*) (see middle panel (-HLW)). In the same experiment, the *rad18* (1-192) construct, used as positive control, gave the strongest interaction signals (see right panel (-AHLW)), as expected, and its interaction pattern was consistent with previously published data for the *rad18* (1-248) construct (Davies *et al.*, 2008, Figure 5E).

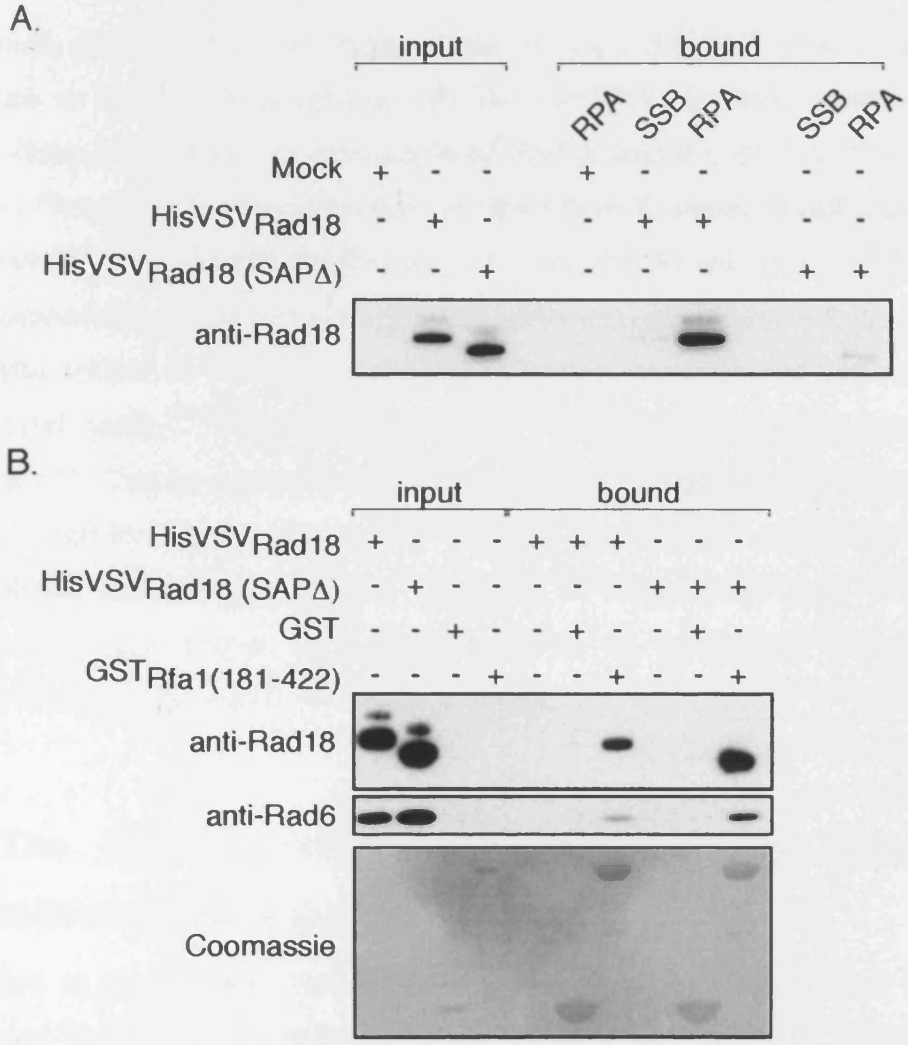

Figure 7.6 – ^{HisVSV}Rad18 (SAPΔ) can still bind to Rfa1 via its DNA-binding domain but not to the RPA complex

A. A mock purification, ^{HisVSV}Rad18-Rad6 or ^{HisVSV}Rad18 (SAPΔ)-Rad6 (~ 5 pmol) were incubated in Coupled-PD Binding buffer, supplemented with 2.5 u benzonase, at 4°C for 1 h with either SSB- or RPA-derivatised beads. The beads were washed 5 times with Coupled-PD Washing buffer. After elution, the samples were subjected to SDS-PAGE followed by Western blotting. Rad18 was detected with anti-Rad18 antibody (polyclonal mouse 4 serum). 5% of the input and 35% of the bound material were loaded.

B. Approximately 0.5 nmol of GST or ^{GST}Rfa1 (182-421) were pre-immobilized on glutathione sepharose in GST-PD Binding buffer for 1 h at 4°C. After a brief wash with GST-PD Binding buffer, ^{HisVSV}Rad18-Rad6 or ^{HisVSV}Rad18 (SAPΔ)-Rad6 (~ 10 pmol) were added in the same buffer containing 100 μg/mL BSA and incubated at 4°C for 1.5 h. Then, the beads were washed 3 times with 500 μL of GST-PD Binding buffer containing BSA and twice more with the same buffer without BSA. After elution, the samples were subjected to SDS-PAGE followed by Coomassie staining or Western blotting. Rad18 was detected with anti-Rad18 antibody (polyclonal mouse 4 serum) and Rad6 was detected with anti-Rad6 antibody. Note that for the Rad18 and the Rad6 blots 1% input and 35% of the bound material were loaded. For the Coomassie staining, equal fractions of input and bound material were loaded.

7.2.5 ^{HisVSV}Rad18 (SAPΔ) is Recruited to ssDNA by RPA

The results presented above suggest that although the SAP domain seems to contribute to Rad18's interactions with the full RPA complex, deletion of this domain does not disrupt the interaction of Rad18 with the DNA-binding domain of Rfa1. Therefore, it was important to determine if, under conditions of high ionic strength, ^{HisVSV}Rad18 (SAPΔ) was still recruited to ssDNA by RPA. Similar to the experiment presented in Figure 6.4, RPA was pre-incubated at increasing levels with ssDNA in PD High-Salt Binding buffer, consisting of 250 mM NaCl. After a brief wash, ^{HisVSV}Rad18-Rad6 or ^{HisVSV}Rad18 (SAPΔ)-Rad6 were added for 1 h at 4°C. The beads were washed with PD High-Salt Binding buffer, eluted and examined for the retention of ^{HisVSV}Rad18 and RPA on ssDNA by Western blot analysis. According to Figure 7.7, both ^{HisVSV}Rad18 WT and ^{HisVSV}Rad18 (SAPΔ) were recruited to the ssDNA by RPA, as increasing levels of RPA resulted in enhanced retention of both proteins.

7.2.6 The SAP Domain Contributes to the Interaction between Rad18 and PCNA

In addition to its putative role in DNA-binding or in the interactions between Rad18 and RPA, the SAP domain of Rad18 could be involved in other protein-protein interactions, which are essential for Rad18's function. I decided to test two of these interactions, the self-association of Rad18 and the interaction of the E3 with its substrate, PCNA, by two-hybrid approach. Consequently, *rad18* (*SAPΔ*), *rad18* (*SAP**), a *rad18* (1-192) truncation and *RAD18* (*WT*) constructs were analysed with respect to their interactions with different constructs of *RAD18* and *POL30*.

As shown in Figure 7.8B – middle panel (-HLW), the dimerisation of Rad18 was preserved even for the mutant alleles, indicating that the SAP domain is not required for Rad18's interactions with itself. These results are in agreement with Ulrich and Jentsch (2000) that implicated the N-terminus of Rad18, which lacks the SAP domain, in its self-association. As expected, *rad18* (1-192) showed the strongest signals for the interaction with itself (see right panel (-AHLW) and Helle Ulrich – unpublished results).

In addition, *POL30* showed fairly weak but detectable signals for the interaction with itself, consistent with the fact that PCNA forms a trimer *in vivo* (see middle panel (-HLW)). Interestingly, the interaction of both *rad18* mutant alleles with *POL30* seemed to be significantly reduced compared to the *RAD18* (*WT*) and the *rad18* (1-192) constructs (see middle panel (-HLW)). This result could imply that the SAP domain plays a regulatory role in Rad18's interaction with its substrate, PCNA.

7.2.7 The Catalytic Activity of the ^{HisVSV}Rad18 (SAPΔ)-Rad6 Complex

Lack of interaction between Rad18 (SAPΔ) and PCNA might affect Rad18's catalytic activity. In order to test this, *in vitro* PCNA ubiquitylation assays with ^{HisVSV}Rad18-Rad6 and ^{HisVSV}Rad18 (SAPΔ)-Rad6 were carried out. Based on the procedure described in paragraph 2.14.1, increasing amounts of a mock purification, ^{HisVSV}Rad18-Rad6 or ^{HisVSV}Rad18 (SAPΔ)-Rad6 were added to a reaction mixture containing E1, ubiquitin, ^{His}PCNA and ATP. After incubation of 2 h at 30°C, the samples were analysed by Western blot.

As shown in Figure 7.9 (upper panel), the auto-ubiquitylation activities of WT and mutant proteins were comparable, suggesting that the SAP domain is dispensable for the ubiquitin ligase activity per se. However, PCNA modification was significantly reduced in the reaction with the ^{HisVSV}Rad18 (SAPΔ)-Rad6 complex compared to that of the ^{HisVSV}Rad18-Rad6 complex (Figure 7.9 – lower panels). This result is consistent with the contribution of the SAP domain to the interaction between Rad18 and PCNA, suggested from Figure 7.8.

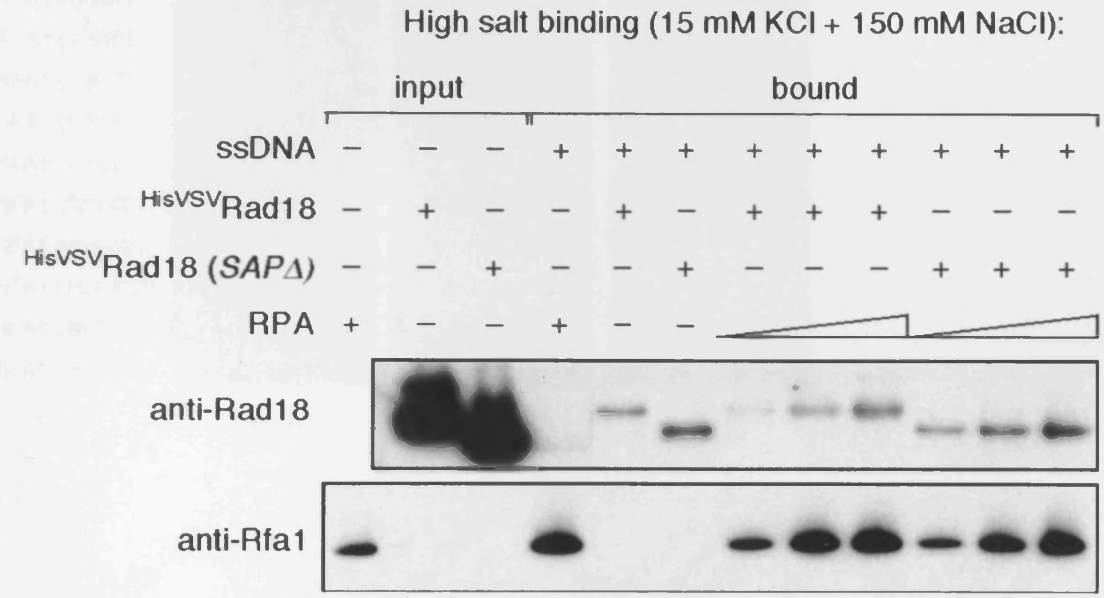

Figure 7.7 - ^{HisVSV}Rad18 (SAPΔ) is recruited to ssDNA by RPA
A 75mer oligonucleotide of mixed sequence (no. 870; ~ 5 pmol), immobilized on streptavidin beads, was incubated with RPA at increasing amounts (2.4, 8 or 24 pmol) at 4°C for 30 min in PD High-Salt Binding buffer. After a brief wash with the same buffer, The ^{HisVSV}Rad18-Rad6 and the ^{HisVSV}Rad18 (SAPΔ)-Rad6 complexes (10 pmol each) were added at 4°C for 1 h incubation. The beads were washed 3 times in PD High-Salt Binding buffer and twice with the same buffer with no BSA. After elution, the samples were subjected to SDS-PAGE followed by Western blotting. Rad18 was detected with anti-Rad18 antibody (polyclonal DH1 rabbit serum - see 2.11.1.2) and Rfa1 was detected with anti-Rfa1 antibody. Note that for the RPA blot, equal fractions of input and bound material were loaded. For the Rad18 blot, 1% of the input and 35% of the bound material were loaded.

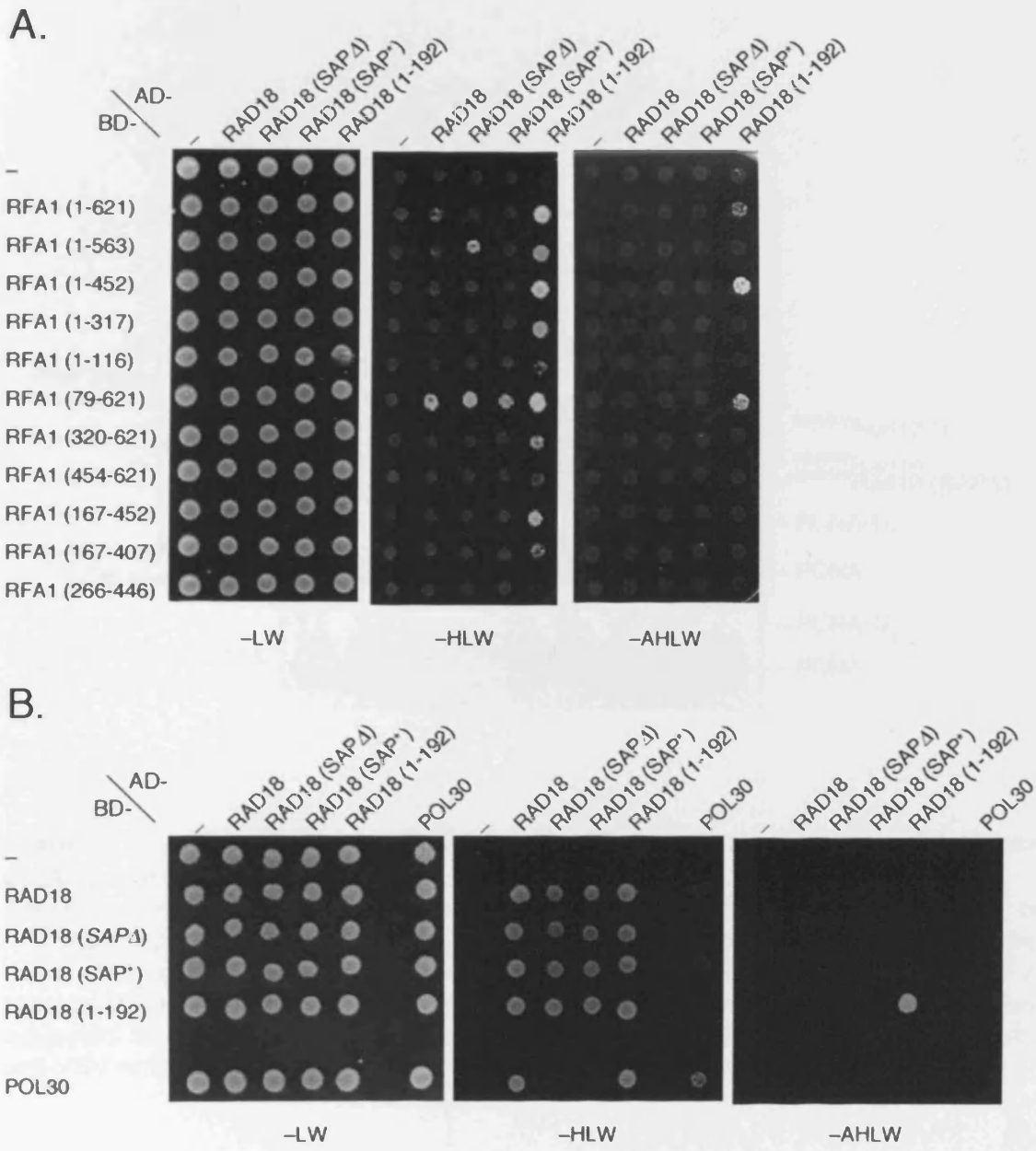

Figure 7.8 – Protein-protein interactions between Rad18 SAP mutant proteins, Rfa1 and PCNA

A. The open reading frames of *RFA1* and its truncations were expressed as fusions to the Gal4 DNA-binding domain (BD), whereas the open reading frames of the *RAD18* constructs were expressed as fusions to the Gal4 activation domain (AD). The presence of the constructs was confirmed by growth on selective medium lacking leucine and tryptophane (-LW). Positive interactions were scored by growth on plates lacking histidine (-HLW) and stronger interactions on plates lacking histidine and adenine (-AHLW) in addition to leucine and tryptophane.

B. The open reading frames of *RAD18* and *POL30* constructs were expressed as fusions to the Gal4 activation (AD) and DNA-binding domains (BD). The experiment was performed as in A.

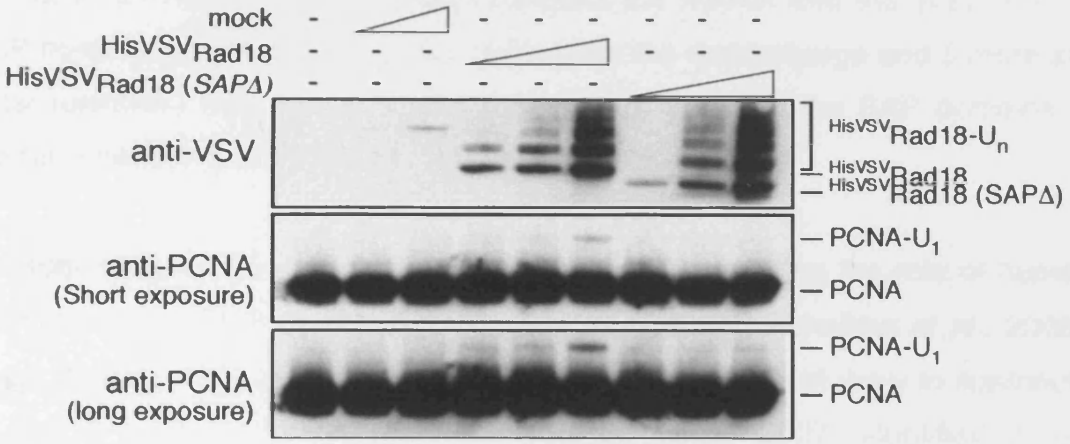

Figure 7.9 – The ^{HisVSV}Rad18 (SAPΔ)-Rad6 complex retains its E3 ligase activity but cannot ubiquitylate PCNA

Either buffer or increasing amounts of mock purification, ^{HisVSV}Rad18-Rad6 or ^{HisVSV}Rad18 (SAPΔ)-Rad6 (2.4, 8 or 24 pmol) were added to a reaction mix containing 112.5 nM yeast E1, 65 μM ubiquitin and 3 μM ^{His}PCNA. The proteins were incubated in Ubiquitylation buffer at 30°C for 2 h. Then, the reaction was stopped, the samples were subjected to SDS-PAGE and analysed by Western blotting. Rad18 was detected by anti-VSV antibody and PCNA was detected by anti-PCNA antibody (polyclonal).

7.3 Discussion

7.3.1 Comparison between the hRad18 and the yRad18 SAP Domains

The SAP domain is a 35 amino acid domain, predicted to have a helix-extended loop-helix structure, and is believed to be involved in DNA-binding (Aravind and Koonin, 2000). According to the alignment shown in Figure 7.1C, 11 out of 35 residues are identical between the human and the yeast Rad18 SAP domains, additional 14 amino acids have the same charge and 5 more are polar residues. Thus, with respect to homology between the SAP domains of the two species, there is a 31% identity and 86% similarity.

Consequently, and in line with the published data regarding the role of human SAP domain in DNA-binding (Notenboom *et al.*, 2007; Nakajima *et al.*, 2006), yeast Rad18's SAP domain was chosen as the domain most likely to contribute to Rad18 ssDNA-binding ability. Notenboom *et al.* (2007) identified a few residues in hRad18, which are important for hRad18's binding to ssDNA, located in the predicted loop region of its SAP domain. Therefore, two of these conserved residues were mutated to alanine (G279 and R301). In addition, a third residue (M304) was mutated based on the consensus sequence of the SAP domain among different proteins (see Figure 1.2). In parallel, the entire domain (amino acids 279 – 312) was deleted (Figure 7.2A).

7.3.2 The SAP Domain is Essential for Rad18's Activity *In vivo*

According to Figure 7.2, neither the *rad18 (SAPΔ)* nor the *rad18 (SAP*)* allele rescued the sensitivity of a *rad18* deletion strain to UV irradiation (B) or to other DNA damaging agents, 4NQO and MMS (C). According to Davies *et al.* (2008) the levels of the mutant proteins seemed to be somewhat reduced in comparison to that of the WT protein. To exclude that the difference in the protein levels was responsible for the DNA damage sensitivity of the SAP mutant strains, the *WT* and the mutant *rad18* alleles were over-expressed under control of the *GAL1* promoter. Indeed, as shown in Figure 7.3, both

mutant alleles failed to complement the sensitivity of the *rad18* deletion strain to MMS or 4NQO, even though the protein levels were significantly enhanced upon induction with galactose. Consequently, I can conclude that the SAP domain of Rad18 is required for protection from DNA damage *in vivo*. This conclusion is in accordance with Davies *et al.* (2008), in which PCNA ubiquitylation in response to MMS treatment was shown to be impaired in both *rad18 (SAPΔ)* and *rad18 (SAP*)* mutants.

7.3.3 Dissecting the Role of the SAP Domain *In vitro*

7.3.3.1 ssDNA-Rad18 (SAPΔ) Interactions

Notenboom *et al.* (2007) found that the SAP domain of hRad18 was sufficient to bind to ssDNA *in vitro*, and that it bound to a 40mer oligo(dT) with an apparent affinity of 1.1 μM. However, since they did not analyse the DNA-binding of the SAP domain mutant in the context of the full-length protein, it is not clear from their results if the SAP domain is the only domain necessary for hRad18 interactions with DNA. A recent publication by Tsuji *et al.* (2008) complemented these findings by showing that the SAP domain of hRad18 was crucial for its DNA-binding activity, as a deletion of this domain impaired the efficient binding of hRad18 to ssDNA as well as to forked-DNA structures. Taken together, the evidence presented in these two publications indicates that the SAP domain of human Rad18 is both necessary and sufficient for its ability to bind to DNA *in vitro*.

According to Figure 7.5, yeast ^{HisVSV}Rad18 (SAPΔ) still retains the ability to bind to ssDNA at low ionic strength *in vitro*. Moreover, preliminary experiments with different DNA structures suggest that ^{HisVSV}Rad18 (SAPΔ) binds to DNA with similar structural preferences to that of the WT protein (data not shown). Due to the homology between the SAP domains of the human and the yeast Rad18 protein, discussed in paragraph 7.3.1, these results were unexpected. Nevertheless, since the experimental method was not quantitative as discussed in 4.3.1, I cannot exclude that the deletion of the SAP domain resulted in a reduction of Rad18's affinity for ssDNA. But even if the SAP domain of yeast Rad18 could potentially contribute to its interactions with ssDNA, the results

presented in Figure 7.5 indicate that, most likely, there are additional domains involved in the ssDNA-binding activity of yeast Rad18.

The ZnF of Rad18 was suggested as a putative DNA-binding domain (Bailly *et al.*, 1997b). According to Nakajima *et al.* (2006), the ZnF of human Rad18 was important for its localisation to replication-independent damage-induced foci *in vivo*. In contrast, Notenboom *et al.* (2007) could not detect binding of the human GST-ZnF construct to ssDNA or to dsDNA but rather suggested a role in ubiquitin binding. Consistent with this notion, an MBP-fused construct of ZnF from human Rad18 was shown to bind to K48-linked-poly-ubiquitin chains *in vitro* (Bish and Myers, 2007). Thus, further analysis is required to determine if the SAP domain of yeast Rad18 is at all involved in DNA-binding and if the ZnF or alternative yet unidentified domains are important for this activity.

7.3.3.2 Rad18 (SAPΔ)-RPA Interactions

The ^{HisVSV}Rad18 (SAPΔ) protein binds to the DNA-binding domain of Rfa1 with a similar affinity to that of the WT protein (Figure 7.6B). This *in vitro* result was expected, as it is in agreement with the two-hybrid results in Davies *et al.* (2008) demonstrating that the SAP domain is dispensable for Rad18's interaction with Rfa1. In addition, it is consistent with the two-hybrid results presented in Figure 7.8A.

However, as shown in Figure 7.6A, the ability of the ^{HisVSV}Rad18 (SAPΔ) protein to bind to the RPA complex is significantly reduced compared to the WT protein. In principle, it is possible that the deficiency of this Rad18 mutant to bind to RPA originates from a defect in binding to Rfa2. However, this possibility is unlikely, since a *rad18* (1-192) construct, which completely lacks the SAP domain, was sufficient for Rfa2 binding (Davies *et al.*, 2008, Figure 5D in Appendix). An alternative explanation could be that the SAP domain of Rad18 mediates its interaction with the full RPA complex via a surface that is formed between two or three RPA subunits. Thus, the absence of the SAP domain only affects the interaction of Rad18 with the full RPA complex, but not with its individual subunits. In another scenario, the absence of the SAP domain may

have an indirect effect causing a conformational change in the Rad18 protein, which in turn results in the inhibition of its interaction with the RPA complex.

7.3.3.3 ssDNA-Rad18 (SAPΔ)-RPA Interactions

Although Figure 7.6 presents conflicting results regarding the importance of the SAP domain in the interaction between Rad18 and RPA, Figure 7.5 suggests that this domain is not essential for the interaction between Rad18 and ssDNA. As shown in Figure 7.7, ^{HisVSV}Rad18 (SAPΔ) can be recruited to ssDNA by RPA at high salt concentrations, similar to the WT protein. This result is consistent with the notion that ^{HisVSV}Rad18 (SAPΔ) can still bind to the DNA-binding domain of Rfa1 but contradicts the reduced binding observed for ^{HisVSV}Rad18 (SAPΔ) and RPA in the absence of DNA. A possible explanation to solve this discrepancy is that Rad18 could have higher affinity for ssDNA-bound RPA, and that this enhanced affinity would compensate for the effect observed in Figure 7.6A. This hypothesis is supported by the stimulation of the interactions between ^{HisVSV}Rad18 and ^{GST}Rfa1 (182-421) in the presence of short oligonucleotides (Figure 6.2).

Unfortunately, due to the remaining ssDNA-binding ability of ^{HisVSV}Rad18 (SAPΔ), I was not able to determine whether the association between Rad18 and ssDNA is essential for its recruitment to the DNA by RPA, as was initially planned.

7.3.3.4 Rad18 (SAPΔ)-PCNA Interactions

As shown in Figure 7.8, the interactions of the *rad18* (SAPΔ) and the *rad18* (SAP*) constructs with the *RFA1* and the *RAD18* constructs in the two-hybrid assay seemed unaffected, but the interaction with the *POL30* construct was significantly reduced compared to that of the WT Rad18 protein. This was rather a surprise, as the N-terminus of *RAD18* (1-192), lacking the SAP domain, was sufficient for the interaction with *POL30*. Accordingly, the SAP domain might have a regulatory effect specific for PCNA binding. For example, the mutation or the deletion of this domain could result in conformational changes that do not

affect Rad18's interactions with Rfa1 or with itself, but cause an alteration in Rad18's interactions with PCNA.

7.3.3.5 The Catalytic Activity of Rad18 (SAPΔ)

As shown in Figure 7.9 (upper panel – anti-VSV antibody blot), ^{HisVSV}Rad18 (SAPΔ) is proficient in its auto-ubiquitylation at similar levels to those observed for the WT protein. As the auto-ubiquitylation activity is often regarded as a hallmark for the catalytic activity of E3 enzymes, this result indicates that the ubiquitin ligase activity per se is not impaired in the mutant. Furthermore, the interaction with Rad6, the E2 ubiquitin-conjugating partner of Rad18, seems to be intact (Figure 7.4). The latter supports the notion that mechanistically, the ubiquitin conjugation ability of ^{HisVSV}Rad18 (SAPΔ)-Rad6 complex is comparable to that of ^{HisVSV}Rad18-Rad6 complex.

The fact that the SAP domain is not important for Rad18's auto-ubiquitylation is consistent with additional observations for other E3s containing SAP domains. For example, the SAP domain of the E3 SUMO ligase, Siz1, was found to be dispensable for Cdc3 sumoylation *in vitro* (Takahashi and Kikuchi, 2005). In addition, recently obtained results in the Ulrich laboratory indicate that the SAP domain of Siz1 is involved in dsDNA-binding and is not absolutely required for PCNA sumoylation (Parker *et al.*, *in revision*).

Nevertheless, according to Figure 7.9 (lower panels – anti-PCNA antibody blots), it appears that the ^{HisVSV}Rad18 (SAPΔ)-Rad6 complex is significantly impaired in PCNA ubiquitylation as compared to the ^{HisVSV}Rad18-Rad6 complex. Although the experimental conditions used here represent only basal levels of PCNA modification by the Rad18-Rad6 complex (Garg and Burgers, 2005; Haracska *et al.*, 2006; Davies *et al.*, 2008), they could, in principle, reflect a real effect. In the future, it will be important to study the affects of the SAP domain on the catalytic activity of Rad18 in a system that allows the loading of PCNA on the DNA prior to ubiquitylation.

Consistently, yeast *rad18* SAP mutants were found to be deficient in MMS-induced PCNA ubiquitylation (Davies *et al.*, 2008, Figure 7D in Appendix). A possible explanation for this result as well as for the result obtained in Figure 7.9 could be that a deletion of the SAP domain induces a conformational change in Rad18. This change, in turn, reduces Rad18's ability to bind to PCNA (see Figure 7.8B), and consequently reduces Rad18's ability to efficiently modify the clamp.

Recently published data by Tsuji *et al.* (2008) suggested a role for the SAP domain of human Rad18 in PCNA ubiquitylation *in vivo*. However, they did not address the possibility that this effect is caused by a direct reduction of PCNA – hRad18 interactions. Instead, they focus on the possibility that mutations in the SAP domain of the E3 impair its DNA-binding ability, consequently leading to the deficiency in PCNA modification. In theory, both possibilities may contribute together to the disruption of hRad18's catalytic activity.

To summarise the results presented in this chapter, I have provided compelling evidence, both *in vivo* and *in vitro*, for the essential role of the SAP domain of yeast Rad18 in the DNA damage tolerance pathway.

7.3.3.6 Additional Putative Roles of the SAP Domain

As the SAP domain seems to be essential for yeast Rad18 function *in vivo*, it is tempting to speculate on possible additional roles for it, taking into account the literature regarding the role of this domain in other proteins.

7.3.3.6.1 Regulation of Localisation by the SAP Domain

The N-terminal SAP domain of the E3 SUMO ligase, Siz1, seems to play a role in its localisation to the nucleus throughout the cell cycle (Takahashi and Kikuchi, 2005; Reindle *et al.*, 2006). Furthermore, Siz1's SAP domain consists of an acceptor site for auto-sumoylation of the E3 *in vitro*, and Takahashi and Kikuchi (2005) postulated that this auto-modification facilitates the dissociation of Siz1 from chromatin, and in turn affects its cellular localisation. However, no formal evidence was provided for this, and the SAP domain could either

contribute to the nuclear import or to nuclear retention of Siz1 (Reindle *et al.*, 2006). Furthermore, an overlap of the SAP domain with the nuclear localisation signal was not excluded.

As ^{HisVSV}Rad18 (SAPΔ) and ^{HisVSV}Rad18 auto-ubiquitylate with similar levels, it is unlikely that Rad18's SAP domain harbours a site for its auto-modification. In addition, Rad6-mediated auto-ubiquitylation was suggested to regulate hRad18's localisation and protein levels (Miyase *et al.*, 2005). This required the self-association of hRad18, independent of the SAP domain. Consistent with Ulrich and Jentsch (2000) and with the results obtained by two-hybrid analysis (Figure 7.8B), the SAP domain of yeast Rad18 is not involved in its self-association. Thus, the localisation of either hRad18 or yRad18 proteins is unlikely to be mediated by their SAP domain.

7.3.3.6.2 Regulation of Substrate Selectivity

A SAP deletion mutant of Siz1 failed to sumolyate a few of its known targets, but was proficient in sumoylation of others (Reindle *et al.*, 2006). Consequently, the authors suggested a role of the SAP domain in substrate selectivity, influenced either by protein-protein interactions or by DNA-protein interactions. Parker *et al.* (*in revision*) suggested an attractive mechanism for the regulation of PCNA sumoylation by Siz1, in which the association of the clamp with the DNA leads to its modification. But in this specific case, even though the SAP domain of Siz1 is required for dsDNA-binding, it was found to be dispensable for PCNA sumoylation.

In contrast, PIAS1, a member of the PIAS family, requires its SAP domain for two important functions. On one hand, the SAP domain mediates PIAS1 binding to AT-rich DNA. On the other hand, this domain is specifically involved in PIAS1 binding to its sumoylation substrate, p53 (Okubo *et al.*, 2004). In their study, Notenboom *et al.* (2007) suggested that the manner in which hRad18 and PIAS1 bind to DNA is conserved. Accordingly, it is plausible that hRad18's SAP domain plays a dual role in Rad18 function, mediating both DNA-binding and PCNA recognition.

The function of yet another E3 SUMO ligase protein, PIASxα, is regulated via its SAP domain, independently of the protein's sumoylation activity. This protein was shown to employ a co-repression activity towards a transcription factor of the EST family, Fli1. This repression, which involves the re-localisation of the latter to nuclear bodies, was dependent on the proteins' physical interactions via the EST domain of Fli1 and the SAP domain of PIASxα (van den Akker *et al.*, 2005).

In agreement with Figure 7.8B and with Figure 7.9, the deletion or the mutation of the SAP domain of yeast Rad18 result in the disruption of its interaction with PCNA. However, this effect may not be direct. The deletion or the mutation of the SAP domain might confer conformational changes to Rad18, and alter its interactions with the clamp or with other proteins.

8 Discussion and Outlook

The purpose of this thesis was to gain insights into the biochemical functions of the Rad18 protein from *S. cerevisiae* and to broaden our understanding regarding its role mediating the DNA damage tolerance pathway. The characterisation of the DNA-binding activity of the recombinant yeast Rad18-Rad6 complex in this work led to the finding that Rad18 is able to bind to other DNA structures, in addition to its reported ability to bind to ssDNA. This *in vitro* activity was recapitulated for human Rad18 in a recent publication (Tsuji *et al.*, 2008). Furthermore, this work shows that the intrinsic DNA-binding ability of yeast Rad18 is dependent on the ionic strength of the buffer, in agreement with Bailly *et al.* (1997a). Interestingly, the binding of yRad18 to ssDNA at low ionic strength confers a stable association of the E3 ligase with the DNA for subsequent high ionic strength conditions. This novel observation suggests a complex salt-dependent behaviour of yRad18, which probably involves several conformations of this protein. Importantly, this work demonstrates that yRad18 is unable to bind to ssDNA under physiological-like conditions and argues against the widespread speculation that Rad18 recognises ssDNA *in vivo* by itself. Moreover, this work provides compelling evidence for the physical interaction between the yeast Rad18-Rad6 complex and RPA and for the stimulation of their association by ssDNA. Strikingly, at physiological-like ionic strength, RPA recruits the Rad18-Rad6 complex to ssDNA. This finding, supported by additional data obtained in the Ulrich lab by my colleagues and published in Davies *et al.* (2008), suggests that RPA-coated ssDNA recruits Rad18 to sites of DNA damage, thus providing the up-stream signal for the activation of the DNA damage tolerance pathway and for PCNA ubiquitylation. Finally, this work shows that the SAP domain of yRad18 is essential for its *in vivo* function. Furthermore, the gathered evidence suggests that mutation or deletion of this domain impairs the interaction of Rad18 with its substrate, PCNA, and thereby prevents the ubiquitylation of the clamp. These findings are consistent with the observations made *in vivo* (Davies *et al.*, 2008).

8.1 The Catalytic Activity of Rad18

The recombinant yeast ^{HisVSV}Rad18-Rad6 complex was partially purified from baculovirus-infected insect cells. Its catalytic activity was verified with regard to the auto-ubiquitylation of Rad18, a self-modification activity characteristic for many E3 ligases (Lorick *et al.*, 1999). Furthermore, its ability to mono-ubiquitylate PCNA *in vitro* was confirmed. Although PCNA mono-ubiquitylation reaction was performed under conditions, which allowed only basal levels of modification (Garg and Burgers, 2005), the specificity for lysine 164 was demonstrated. Taken together, the results presented in Chapter 3 suggest that the purified complex is functional and folded properly.

The purification method, which involved the fractionation of the insect cells to cytoplasm and nuclei, revealed interesting differences between the cytoplasm-derived ^{HisVSV}Rad18-Rad6 complex and the nuclei-derived one. The former was post-translationally modified, whereas the latter was not (Figure 3.4A). Furthermore, the former had enhanced E3 ligase activity for itself and for PCNA (Figure 3.5 and data not shown). The results presented in Figure 3.5 show that the cytoplasm-derived yeast ^{HisVSV}Rad18-Rad6 is mono-ubiquitylated in the insect cells. This finding recapitulates the observations made for the mammalian Rad18 by Miyase *et al.* (2005).

Indication that yRad18 mono-ubiquitylation is a physiologically relevant modification and not an artefact of the expression system was obtained by pull-down experiments from yeast cells over-expressing ^{His}ubiquitin. Several lines of evidence argue in favour of the hypothesis that the role of Rad18's modification in yeast may be different than that reported for the mammalian Rad18. First, Miyase *et al.* (2005) concluded that the mono-ubiquitylated form of mammalian Rad18 protein, which was predominantly found in the cytoplasm, reflects a regulatory mechanism and that Rad6-dependent poly-ubiquitylation of Rad18 led to its subsequent degradation. In yeast cells, although Rad6 seems to contribute somewhat to Rad18 ubiquitylation, it may not be the only E2 enzyme involved in this modification. This result is in contrast to the observations made by Miyase *et al.* (2005) for mammalian Rad18. Furthermore, the levels of the

yeast Rad18 protein in the yeast strains over-expressing ^{His}ubiquitin were not reduced in comparison to those with normal ubiquitin levels, suggesting that this modification does not lead to the degradation of yRad18. Second, Notenboom *et al.* (2007) have identified four different mono-ubiquitylation sites in murine Rad18 by mass spectrometry. Even though these sites are conserved in human Rad18, they are not conserved in yeast. Hence, the function of this modification may not be conserved either.

In order to determine the role of Rad18 ubiquitylation in yeast, a further characterisation of this modification is required. First, it is important to study the timing of this modification and the localisation of modified Rad18. Preliminary data suggests that this modification is constitutive and does not require induction by specific conditions, such as DNA damage. Although Rad18 protein levels do not seem to significantly fluctuate during the cell cycle (unpublished data – Davies and Ulrich), it is predominantly active during S phase (Davies *et al.*, 2008). It would be important to establish whether the levels of the modification changed instead. Second, identification of the ubiquitylation sites on yRad18 could provide essential tools for mutational analysis, potentially leading to the elucidation of a physiological role for this modification. Third, determining which type of poly-ubiquitin chains are conjugated to Rad18 can provide important clues regarding the consequences of this modification.

Perhaps Rad18 ubiquitylation results from non-specific ubiquitin ligase activity of its catalytic domain. Alternatively, it may serve as a regulatory mechanism for its function. As E3 ligases provide the specificity to the ubiquitylation process, their regulation can determine when and where their substrates are modified (Pickart, 2001). In the literature, there are examples for different covalent modifications of E3s that contribute to their function, such as sumoylation and phosphorylation (Pickart, 2001). In some cases, mono-ubiquitylation of the E3 is required prior to the conjugation of the substrate. This coupled-mono-ubiquitylation mechanism was suggested for substrates that contain ubiquitin-binding domains, but may also apply to substrates that do not contain them (Woelk *et al.*, 2006). As previously mentioned, mono-ubiquitylated Rad18, derived from the cytoplasm of insect cells, was more efficient than unmodified

Rad18, derived from the nuclei, with regard to both auto-ubiquitylation and mono-ubiquitylation of PCNA. This can be explained either by direct or indirect effects of the conjugated ubiquitin on Rad18. A direct effect would be a mechanistic pre-requisite for subsequent PCNA ubiquitylation. The conjugation of the first ubiquitin on Rad18 might be an intermediate rate-limiting step prior to the modification of the clamp. An indirect effect would be inducing a conformational change that enhances the association of Rad18 with PCNA or makes it a better E3 ligase by positioning the players involved in the correct conformation for the catalytic activity. Although these speculations are exciting, I cannot exclude that the results presented in Figure 3.5 are dependent on the expression system used or on the protein preparation, as discussed before in paragraph 3.2.5.3.

Nevertheless, it is clear that a restriction of Rad18 activity is essential for the cell, as the DNA tolerance pathway should act only when needed (Ulrich, 2005). Davies *et al.* (2008) provided evidence that this is achieved by maintenance of low levels of the yRad18 protein, as over-expression of Rad18 relaxes the requirement for PCNA ubiquitylation. The results presented in this thesis and in Davies *et al.* (2008) implicate RPA in the recruitment of Rad18 to the sites of DNA damage, thus providing another level of regulation on its activity.

8.2 Interactions between Rad18 and DNA

The results presented in Chapter 4 of this thesis demonstrate that the yeast Rad18 protein harbours an intrinsic DNA-binding ability. This activity is highly sensitive to salt concentrations (Figure 4.1 and Figure 4.2), in agreement with Bailly *et al.* (1997a). In addition, the results presented in Figure 4.5 suggest that Rad18 binding to ssDNA is affected by different anions in correlation with the Hofmeister series (Griep and McHenry, 1989). Taken together, the evidence in Chapter 4 indicate that the interaction between Rad18 and ssDNA is mediated by a network of hydrogen and electrostatic bonds that are sensitive to the ionic strength of the buffer.

The results presented in Figure 4.7 are consistent with the notion that Rad18 binds to ssDNA preferentially over dsDNA (Bailly *et al.*, 1997a; Notenboom *et al.*, 2007). However, in both ionic strength conditions that were tested, Rad18 was able to bind to other DNA structures with ssDNA regions but also to dsFork-DNA, containing no unpaired bases. According to Figure 4.6, Rad18 binds better to longer ssDNA oligonucleotides than to shorter ones. These results are consistent with Tsuji *et al.* (2008) regarding the structural binding preference of human Rad18. Furthermore, these results may suggest that *in vivo*, Rad18 binds to replication intermediates or to stalled replication forks.

The result in Figure 4.3 indicates that the Rad6 protein is not able to bind to ssDNA by itself, but can be brought to the ssDNA via its interaction with Rad18. This observation supports earlier findings by Bailly *et al.* (1994).

The experimental method that was used to study the interaction between Rad18 and DNA revealed a complex behaviour, which is dependent on the salt concentration in the buffer. As mentioned earlier, Rad18 readily binds to ssDNA at low salt concentrations. However, if the incubation of this protein and the ssDNA occurs at high salt concentrations instead, then a reduced or no binding is observed. Interestingly, if the binding partners are incubated at low salt concentrations first, but then exposed to high salt washes, then their association seems to become salt-resistant. This is a slow effect, as shown in Figure 4.4. A hypothesis that could explain these observations would be that at low salt concentrations, Rad18 binds to the ssDNA with low affinity. Following this binding, a slow conformational change occurs, possibly involving the Rad18-Rad6 complex, the ssDNA or both. As a consequence, the Rad18 protein associates with the ssDNA in a high affinity mode, which is stable to high salt washes. However, if the Rad18-Rad6 complex is incubated at high salt concentrations in its DNA-free form, it may have a different conformation that prevents it from binding to the ssDNA in the first place. Additional experiments involving different incubation periods and washes with different salt concentrations may shed additional light on the timing and the mechanism of these conformational changes.

As the binding of the Rad18-Rad6 complex to the ssDNA was not detected under physiological-like ionic strength conditions (Figure 4.2), these results question the ability of yeast Rad18 to bind to ssDNA by itself *in vivo*. This behaviour of yeast Rad18 may be different than that reported for the human Rad18 protein (Notenboom *et al.*, 2007; Tsuji *et al.*, 2008). Consistently, the domain responsible for the intrinsic ssDNA-binding ability of Rad18 may not be conserved among species (see Chapter 7).

8.3 Interactions between Rad18 and RPA

The results presented in Chapter 5, together with additional evidence published in Davies *et al.* (2008) indicate that the Rad18-Rad6 complex and RPA interact physically with each other. This interaction probably occurs via direct contacts of the E3 with two subunits of the RPA complex, Rfa2 and the DNA-binding domain of Rfa1 (Figure 5.4 and Figure 5.5). The N-terminal region of Rad18 (amino acids 1-192), including a functional RING domain, was shown to be sufficient for the interaction with both RPA subunits (Davies *et al.*, 2008, Figure 5D and 5E in Appendix). Furthermore, Rad6 appears to contribute to the direct interaction with RPA (Figure 5.3). These interactions proved to be specific, as under the same reaction conditions, PCNA did not bind to RPA (Figure 5.3).

RPA is a modular protein that often makes more than one contact with its binding partners (Ball *et al.*, 2007). The interactions of RPA with other proteins predominantly involve Rfa1, Rfa2 or both (Wold, 1997). For instance, XPA was reported to bind both Rfa1 and Rfa2 (Matsuda *et al.*, 1995). Similarly, Rad51 and Rad52 bind to RPA via these two subunits (Jackson *et al.*, 2002; Stauffer and Chazin, 2004). Furthermore, the ssDNA-binding site of human RPA70 is directly involved in the interactions with human XPA, Rad52 or Rad51 (Jackson *et al.*, 2002; Daughdrill *et al.*, 2003; Stauffer and Chazin, 2004). Therefore, the molecular mechanism by which RPA interacts with Rad18 may correspond to the way it interacts with other proteins. The interactions of RPA with various binding partners via the same subunits and domains may play an important regulatory role. For example, a particular DNA repair pathway may be preferred at a particular time by competition between binding partners of RPA from

different repair pathways. Alternatively, the interactions of RPA with proteins from the same DNA repair pathway may be regulated in a sequential mode by a 'hand-off' mechanism (Fanning *et al.*, 2006); (see also 1.3.2.5).

Apparently, the N-terminal part of yRad18, which contributes to most of its interactions with its known binding partners (unpublished data and Ulrich and Jentsch, 2000), is also responsible for its interactions with RPA (Davies *et al.*, 2008). A closer look into the two-hybrid results presented in Davies *et al.* (2008) suggests complex interaction behaviour of Rad18 toward RPA. First, the *rad18* (83-248) construct is sufficient for the interaction with Rfa2, but is deficient in Rfa1 binding, suggesting that the two RPA subunits bind to different regions within the N-terminal part of Rad18. Second, the C-terminus of Rad18 seems to play an inhibitory role for Rad18's binding to both RPA subunits, as C-terminal truncations of Rad18 give enhanced interaction signals compared to the full-length protein. Since the C-terminus of Rad18 contains an acidic region (Bailly *et al.*, 1997b), it may participate in binding to RPA in the absence of ssDNA, mimicking its charge. This binding mechanism was suggested for the Rad51 protein (Stauffer and Chazin, 2004). However, in the presence of ssDNA and as a result of ssDNA-induced conformational changes, this region would be displaced from RPA allowing the N-terminal region of Rad18 to cooperatively bind to RPA and to ssDNA with higher affinities. This speculative mechanism can be tested by competition experiments with the C-terminal or the N-terminal truncation constructs of Rad18 for binding to RPA, ssDNA or both.

8.4 Interactions between Rad18, RPA and ssDNA

The results presented in Chapter 6 indicate that RPA can associate with the Rad18-Rad6 complex on ssDNA *in vitro*. This conclusion is consistent with the *in vivo* observations made by Davies *et al.* (2008) and is supported mainly by two important findings obtained in this thesis. The first finding is that the interaction between the DNA-binding domain of Rfa1 and the ^{HisVSV}Rad18-Rad6 complex is stimulated by ssDNA (Figure 6.2). Upon binding to ssDNA, the DNA-binding domain of Rfa1 was reported to undergo significant conformational changes, resulting in different accessibilities of side-chain residues within that

region (Bochkareva *et al.*, 2001). Thus, additional or alternative residues of Rfa1 may contact the Rad18-Rad6 complex and enhance the formation and the stability of the quaternary ssDNA-RPA-Rad18-Rad6 complex. Therefore, the DNA-binding domain of Rfa1 may be considered a better binding partner for the Rad18-Rad6 complex in the presence of ssDNA. Hence, *in vivo* ssDNA-bound RPA may be preferred over ssDNA-free RPA by the Rad18-Rad6 complex through Rfa1, providing a regulatory mechanism for directing it to ssDNA-bound RPA (see Figure 8.1A). Interestingly, short oligonucleotides, to which the Rad18-Rad6 complex was not able to bind, promote its association with RPA in a similar manner to longer oligonucleotides. This suggests that under the tested conditions, the direct contact between ssDNA and the Rad18-Rad6 complex is not necessary for the association of the quaternary complex. However, additional studies are needed to dissect the network of interactions within this complex (see Chapter 7). As mentioned in paragraph 6.2.1.1, it would be interesting to determine the effects of ssDNA on the interaction between Rfa2 and Rad18-Rad6.

The second and most important finding in this thesis is that under physiological-like salt concentrations, RPA recruits the ^{HisVSV}Rad18-Rad6 complex to ssDNA (Figure 6.4 and Figure 6.5). This behaviour was specific for RPA, as bacterial SSB failed to recruit the Rad18-Rad6 complex under the same conditions. Thus, under conditions in which the binding of the Rad18-Rad6 complex to ssDNA cannot be detected (Figure 4.2), RPA enables the binding of this complex to ssDNA (Figure 6.4 and Figure 6.5). Figure 8.1C illustrates how increasing amounts of RPA, pre-bound on ssDNA, enhance the binding of the Rad18-Rad6 complex to ssDNA. A similar recruitment effect was observed for the Mec1-Ddc2 complex or for the Rad17 protein (Zou and Elledge, 2003; Zou *et al.*, 2003). The recruitment of the Rad18-Rad6 complex to ssDNA by RPA may be mediated solely by protein-protein interactions (Figure 7.1A). Alternatively, RPA may stabilise the interactions between the Rad18-Rad6 complex and the ssDNA (Figure 7.1B). Examples for both mechanisms can be found in the literature. For instance, the interaction between Rad52 and RPA stimulates their interactions with ssDNA (Jackson *et al.*, 2002). Using a Rad52 mutant lacking the ability to bind to ssDNA, the authors found that the enhanced

binding of the RPA-Rad52 complex to ssDNA is mediated through the protein-protein interactions between Rad52 and the Rfa2 subunit. An example for the second mechanism was reported for RPA and XPA. Their complex was reported to have an enhanced recognition of damaged DNA in comparison to the individual proteins (He *et al.*, 1995). This effect was interpreted as the stabilisation of XPA binding to DNA lesions by RPA (Wang *et al.*, 2000). As the *RAD6* and the NER pathways are likely to deal with similar lesions on the DNA but at different timing (see 1.4.2) it would be interesting to test the behaviour of RPA and the Rad18-Rad6 complex on damaged DNA as well.

According to Davies *et al.* (2008) RPA specifically contributes to PCNA ubiquitylation but not to PCNA sumoylation, as depletion of the Rfa1 subunits abolishes only the former modification in response to DNA damage. In addition, the association of the Rad18 protein with chromatin correlates with that of RPA. Taken together, the results presented in this thesis and in Davies *et al.* (2008) argue in favour of a model in which RPA plays an important role in the initiation of the DNA damage tolerance pathway. As a result of DNA lesions, which cause the uncoupling of the helicase movement from that of the replicative DNA polymerases, ssDNA regions are exposed in the vicinity of stalled replication forks (Byun *et al.*, 2005); (see Figure 8.2A). These ssDNA stretches are covered by RPA (Figure 8.2B) and serve as a signal to recruit the Mec1-Ddc2 complex and activate the replication checkpoint response (Zou and Elledge, 2003; Zou *et al.*, 2003). In a parallel but independent manner (Davies *et al.*, 2008), the Rad18-Rad6 complex is recruited to stalled replication forks (Figure 8.2C). Consequently, PCNA is modified (Figure 8.2D) and activates the DNA damage tolerance pathway (Figure 8.2E). The mono-ubiquitylation of PCNA appears to be a rate-limiting step for subsequent poly-ubiquitylation by Rad5 and the Mms2-Ubc13 hetero-dimer (Parker and Ulrich – unpublished results). Therefore, it is still not clear how the choice is made between the error-free and the error-prone branches of the DNA damage tolerance pathway.

Figure 8.1 – The interactions between Rad18-Rad6, RPA and DNA

A. The Rad18-Rad6 complex interacts with RPA. The interactions are mediated by a direct contact between the E3 and two of the RPA subunits, Rfa2 and the DNA binding domain of Rfa1. Rad6 seems to contribute as well to the physical interaction with RPA. Rad18-Rad6 can interact with either DNA-free RPA or DNA-bound RPA. The latter is hypothesised to be preferred over the former, as the binding of Rad18-Rad6 and the DNA binding domain of Rfa1 is stimulated in the presence of oligonucleotides.
B. At low salt concentrations, the Rad18-Rad6 complex can bind to ssDNA on its own, via direct interactions between Rad18 and the DNA (1). When low amounts of RPA are pre-bound to ssDNA, both proteins can share the space on the DNA (2). However, increasing levels of RPA compete with the E3 for the binding to ssDNA (3).
C. At physiological-like or high salt concentrations, the Rad18-Rad6 complex cannot bind to ssDNA on its own (1). Increasing amounts of RPA, pre-bound to ssDNA, enhance the binding of the E3 on the ssDNA (2 + 3), suggesting that *in vivo*, Rad18-Rad6 may be recruited to stalled replication forks by RPA.

A.

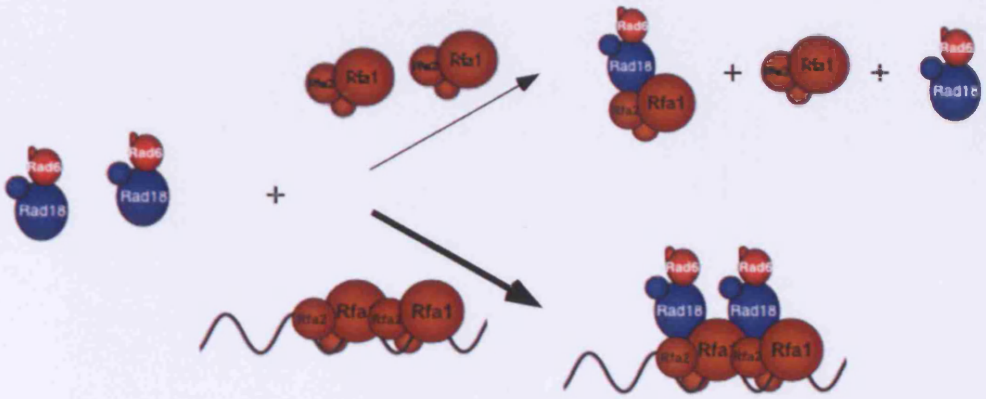

B. Low salt

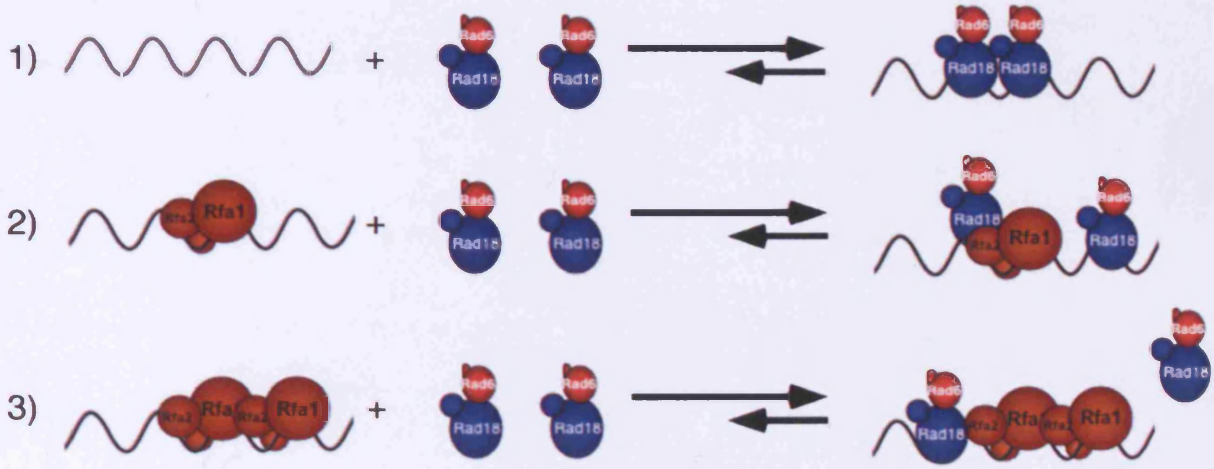

C. 'Physiological-like' or high salt

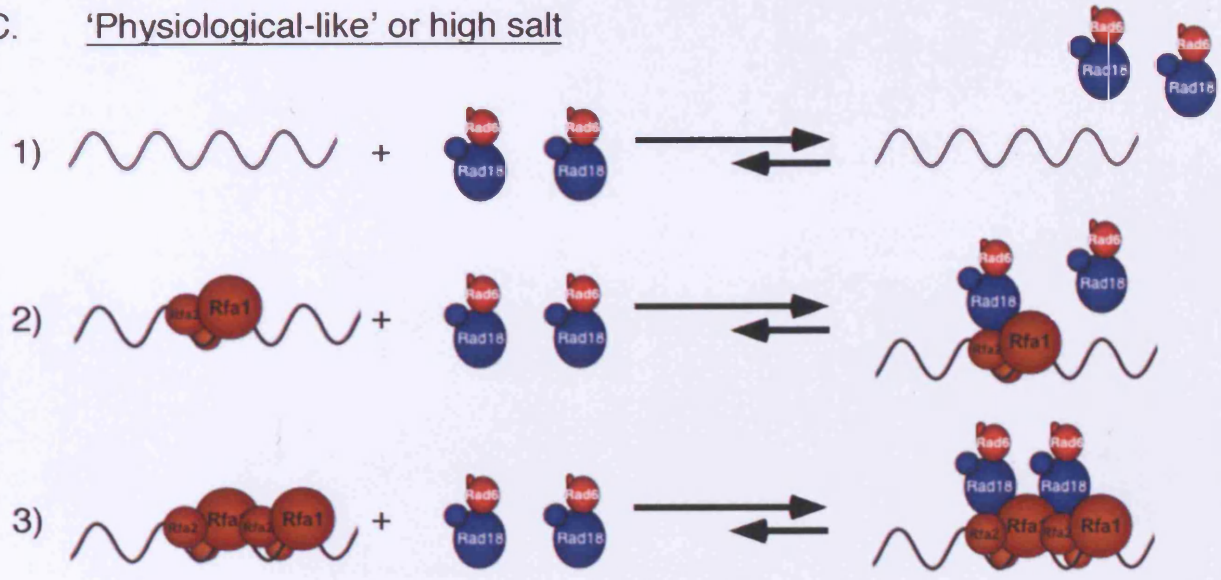

Figure 8.2– Model for the activation of the DNA damage tolerance pathway through Rad18-Rad6 recruitment by RPA

As a result of DNA lesions, which cause the uncoupling of the helicase movement from that of the replicative DNA polymerases, ssDNA regions are exposed in the vicinity of stalled replication forks (A). RPA quickly binds to these ssDNA stretches (B) and recruits the Rad18-Rad6 complex (C). Consequently, PCNA is mono-ubiquitylated (D) and the DNA damage tolerance pathways are activated (E). The replicative DNA polymerase can be replaced by TLS polymerases that may be recruited to the replication fork by mono-ubiquitylated PCNA, activating translesion synthesis (TLS) for lesion bypass (E – left panel). Alternatively, Rad18 may recruit the Rad5-Ubc13-Mms2 complex to the stalled fork. Hence, PCNA can be poly-ubiquitylated leading to the activation of the damage avoidance (DA) pathway (E – right panel).

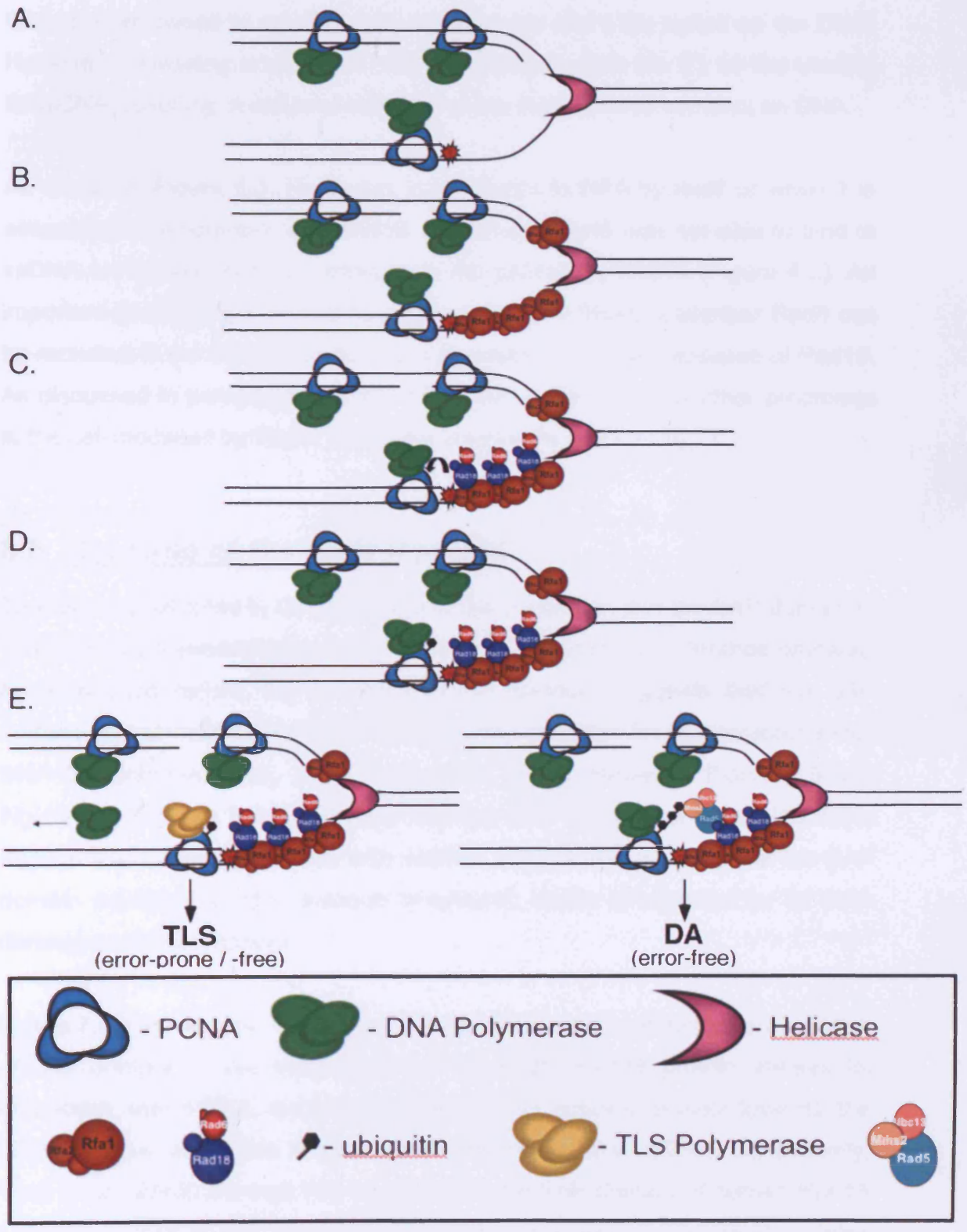
A.
B.
C.
D.
E.
TLS
(error-prone / -free)
DA
(error-free)
- PCNA
- DNA Polymerase
- Helicase
Rfa1
Rad18
- ubiquitin
- TLS Polymerase
Rad5

Interestingly, the ability of RPA to recruit Rad18-Rad6 to ssDNA depends on the ionic strength of the buffer. As illustrated in Figure 8.1B, at low salt concentrations, the complex can bind to ssDNA by itself. When low levels of RPA are pre-bound to ssDNA, both proteins can share the space on the DNA. However, increasing amounts of RPA can compete with the E3 for the binding to ssDNA, resulting in reduced retention of the Rad18-Rad6 complex on DNA.

As shown in Figure 5.3, Rad6 can bind directly to RPA by itself or when it is associated in a complex with Rad18. In contrast, Rad6 was not able to bind to ssDNA on its own, but was brought to the ssDNA by Rad18 (Figure 4.3). An important question that should be addressed in the future is whether Rad6 can be recruited to the ssDNA via its interaction with RPA, in the absence of Rad18. As discussed in paragraph 5.3, this may have implications for other processes in the cell mediated by Rad6, which are independent of Rad18.

8.5 The Role of the SAP Domain

The results presented in Chapter 7 led to the conclusion that the SAP domain of yeast Rad18 is essential for its activity in the DNA damage tolerance pathway. As mentioned before, the evidence in the literature suggests that the SAP domain of mammalian Rad18 is sufficient and necessary for its interactions with DNA (Notenboom *et al.*, 2007; Tsuji *et al.*, 2008). However, Figure 7.5 and Figure 7.7 support the hypothesis that the SAP domain of yeast Rad18 is dispensable for its interactions with ssDNA. Thus, it is most likely that the SAP domain mediates another function of yRad18, which is essential for its DNA damage protection activity.

Figure 7.8B and Figure 7.9 support the hypothesis that a mutation or a deletion of this domain in the context of the full-length Rad18 protein impairs its interaction with PCNA, and thereby disrupts its catalytic activity towards the clamp. These results are in agreement with Davies *et al.* (2008). Consistently, Tsuji *et al.* (2008) showed that mutations in the SAP domain of human Rad18 failed to support PCNA mono-ubiquitylation *in vivo* and *in vitro*. Most proteins that interact with PCNA contain the PIP motif (Moldovan *et al.*, 2007) but this

domain is missing from Rad18. Notenboom *et al.* (2007) found by gel filtration analysis that the N-terminal part of Rad18 (aa 16-366) was sufficient for PCNA binding. This region contains the RING, the ZnF and the SAP domains. Notenboom *et al.* (2007) were not able to localise the binding of PCNA to any of these domains, suggesting that the interactions with PCNA are mediated through more than one of these domains or that a yet unidentified domain for PCNA binding exists in this region. Their results are consistent with Figure 7.8B in which an N-terminal construct of yRad18 that lacks the SAP and the ZnF domains is sufficient for PCNA binding. Taken together, the evidence for both yeast and human Rad18 supports the hypothesis that the SAP domain does not interact directly with PCNA. Nevertheless, a mutation or a deletion of the SAP in the context of the full-length protein might alter its structure in the vicinity of the residues mediating the interaction between the clamp and the E3 and therefore disrupt their association. Possibly, this structure-function relationship of the SAP domain can also account for the impaired interactions between Rad18 (SAPΔ) and RPA, observed in Figure 7.6A. However, in order to confirm the results obtained by the two-hybrid analysis (Figure 7.8B), additional experiments have to be performed. Co-immunoprecipitation assays with both PCNA and Rad18 from *rad18 SAP* mutants should be used as an alternative method to show whether Rad18's SAP domain is important for their interaction *in vivo*. Furthermore, *in vitro* interaction assays with purified proteins could determine if a mutation or a deletion of the SAP domain results in impairment of Rad18's binding to PCNA. Moreover, testing if the SAP domain is sufficient for direct interaction with PCNA would be equally important. However, the latter is unlikely, as a *rad18* (1-192) truncation that lacks the SAP domain interacted with PCNA in the two-hybrid system (Figure 7.8B and Helle Ulrich –unpublished results).

Apart from RPA, the novel interactor of Rad18 presented in this thesis, there are additional known binding partners of yeast Rad18, such as Rad5 (Ulrich and Jentsch, 2000) and Ubc9 (Hoege *et al.*, 2002). Thus, it would be interesting to test if a deletion or a mutation in Rad18's SAP domain could affect its interactions with those proteins. This should address whether the SAP domain

regulates Rad18-PCNA interactions specifically, or if its importance extends to additional protein-protein interactions of Rad18.

Taken these results together, the Rad18 (SAPΔ)-Rad6 complex may still be recruited to ssDNA stretches at stalled replication forks by RPA (Figure 7.7). Although it then may be in the vicinity of PCNA, Figure 7.8B supports the hypothesis that its interaction with the clamp is compromised. Consistently, and in agreement with Figure 7.9, this mutant may no longer be able to mono-ubiquitylated PCNA at stalled replication forks. Thus, this mutant is deficient in the activation of DNA damage tolerance either via the error-prone or the error-free sub-pathways. Both Figure 7.2 and Figure 7.3 support this conclusion as well as Davies *et al.* (2008).

8.6 Outlook

The results presented in this thesis and in Davies *et al.* (2008) suggest that the up-stream signals that activate the DNA damage tolerance pathway involve the recruitment of the Rad18-Rad6 complex to stalled replication forks by RPA. Hence, in response to replication fork stalling and as a consequence of the exposure of ssDNA regions bound by RPA, PCNA mono-ubiquitylation is facilitated.

The Ulrich lab is very interested in the molecular mechanisms involved in PCNA ubiquitylation. Therefore, it would be important to understand the significance of the results presented in this thesis in the context of the reconstituted PCNA ubiquitylation reaction when the clamp is loaded onto DNA. Recently, my colleague was able to establish the system for the reconstitution of DNA-dependent mono- and poly-ubiquitylation of PCNA *in vitro* (Parker and Ulrich – unpublished results). When different salt concentrations were applied to the reaction for PCNA mono-ubiquitylation, high salt concentrations resulted in lower modification efficiency compared to low salt concentrations. This result is consistent with the notion that high salt concentrations disrupt the interactions between Rad18 and ssDNA, and thereby reduce the catalytic activity of the E3

towards the clamp. However, the effects of the salt concentration on PCNA loading cannot be excluded.

The recruitment of the Rad18-Rad6 complex to ssDNA by RPA may have stimulatory effects on the ubiquitylation of PCNA. Alternatively, it may only enable the E2-E3 complex to localise to sites of stalled replication forks at the right time. In the latter case, the interaction of RPA with the Rad18-Rad6 complex would be separate from its catalytic activity. Analogously, although the ATRIP-ATR complex is recruited to ssDNA by RPA, the addition of either RPA or ssDNA-bound RPA failed to stimulate its kinase activity (Ball *et al.*, 2007).

Preliminary experiments to test the effect of RPA on PCNA modification at high salt concentrations were performed with PCNA loaded onto a circular viron ssDNA annealed with several oligonucleotides. Interestingly, PCNA mono-ubiquitylation levels were abolished in the absence of RPA and restored in its presence (Parker and Ulrich – unpublished results). However, this effect turned out to be independent of RPA as it was reproduced when bacterial SSB was used instead. Thus, it appears that at high salt concentrations, the loading of PCNA on the DNA may be compromised, and either RPA or SSB can rescue the binding of the clamp to DNA. However, additional experiments with PCNA loaded onto different DNA structures might reveal an RPA-dependent stimulation of the ubiquitylation reaction.

Additional factors could affect the reconstituted PCNA ubiquitylation reaction that should be taken into consideration. RPA and RFC, the clamp loader, are known to interact with each other (Yuzhakov *et al.*, 1999). Through their association, the loading of PCNA onto an ssDNA-dsDNA junction is facilitated and stabilised. Furthermore, one of the subunits of the human RFC complex, Rfc2, was shown to be ubiquitylated by hRad18 in response to DNA damage (Tomida *et al.*, 2008). Interestingly, hRPA was reported to have an inhibitory effect on this modification. Future studies should reveal the interplay between the modifications of the clamp and the clamp loader and additional aspects of the regulation of Rad18 activity by RPA.

9 References

Aboussekhra, A., Biggerstaff, M., Shivji, M. K., Vilpo, J. A., Moncollin, V., Podust, V. N., Protic, M., Hubscher, U., Egly, J. M. and Wood, R. D. (1995). "Mammalian DNA nucleotide excision repair reconstituted with purified protein components." Cell **80**(6): 859-68.

Abramova, N. A., Russell, J., Botchan, M. and Li, R. (1997). "Interaction between replication protein A and p53 is disrupted after UV damage in a DNA repair-dependent manner." Proc Natl Acad Sci U S A **94**(14): 7186-91.

Adachi, Y. and Laemmli, U. K. (1992). "Identification of nuclear pre-replication centers poised for DNA synthesis in *Xenopus* egg extracts: immunolocalization study of replication protein A." J Cell Biol **119**(1): 1-15.

Aguilera, A. and Gomez-Gonzalez, B. (2008). "Genome instability: a mechanistic view of its causes and consequences." Nat Rev Genet **9**(3): 204-17.

Alani, E., Thresher, R., Griffith, J. D. and Kolodner, R. D. (1992). "Characterization of DNA-binding and strand-exchange stimulation properties of y-RPA, a yeast single-strand-DNA-binding protein." J Mol Biol **227**(1): 54-71.

Andreassen, P. R., Ho, G. P. and D'Andrea, A. D. (2006). "DNA damage responses and their many interactions with the replication fork." Carcinogenesis **27**(5): 883-92.

Aravind, L. and Koonin, E. V. (2000). "SAP - a putative DNA-binding motif involved in chromosomal organization." Trends Biochem Sci **25**(3): 112-4.

Ashley, C., Pastushok, L., McKenna, S., Ellison, M. J. and Xiao, W. (2002). "Roles of mouse *UBC13* in DNA postreplication repair and Lys63-linked ubiquitination." Gene **285**(1-2): 183-91.

Atanassov, B., Gospodinov, A., Stoimenov, I., Mladenov, E., Russev, G., Tsaneva, I. and Anachkova, B. (2005). "Repair of DNA interstrand crosslinks may take place at the nuclear matrix." J Cell Biochem **96**(1): 126-36.

Bachrati, C. Z. and Hickson, I. D. (2006). "Analysis of the DNA unwinding activity of RecQ family helicases." Methods Enzymol **409**: 86-100.

Bailly, V., Lamb, J., Sung, P., Prakash, S. and Prakash, L. (1994). "Specific complex formation between yeast RAD6 and RAD18 proteins: a potential

mechanism for targeting RAD6 ubiquitin-conjugating activity to DNA damage sites." Genes Dev **8**(7): 811-20.

Bailly, V., Lauder, S., Prakash, S. and Prakash, L. (1997a). "Yeast DNA repair proteins Rad6 and Rad18 form a heterodimer that has ubiquitin conjugating, DNA binding, and ATP hydrolytic activities." J Biol Chem **272**(37): 23360-5.

Bailly, V., Prakash, S. and Prakash, L. (1997b). "Domains required for dimerization of yeast Rad6 ubiquitin-conjugating enzyme and Rad18 DNA binding protein." Mol Cell Biol **17**(8): 4536-43.

Baker, T. A. and Bell, S. P. (1998). "Polymerases and the replisome: machines within machines." Cell **92**(3): 295-305.

Ball, H. L., Ehrhardt, M. R., Mordes, D. A., Glick, G. G., Chazin, W. J. and Cortez, D. (2007). "Function of a conserved checkpoint recruitment domain in ATRIP proteins." Mol Cell Biol **27**(9): 3367-77.

Barzel, A. and Kupiec, M. (2008). "Finding a match: how do homologous sequences get together for recombination?" Nat Rev Genet **9**(1): 27-37.

Bastin-Shanower, S. A. and Brill, S. J. (2001). "Functional analysis of the four DNA binding domains of replication protein A. The role of RPA2 in ssDNA binding." J Biol Chem **276**(39): 36446-53.

Bentley, N. J., Holtzman, D. A., Flaggs, G., Keegan, K. S., DeMaggio, A., Ford, J. C., Hoekstra, M. and Carr, A. M. (1996). "The *Schizosaccharomyces pombe rad3* checkpoint gene." Embo J **15**(23): 6641-51.

Bienko, M., Green, C. M., Crosetto, N., Rudolf, F., Zapart, G., Coull, B., Kannouche, P., Wider, G., Peter, M., Lehmann, A. R., Hofmann, K. and Dikic, I. (2005). "Ubiquitin-binding domains in Y-family polymerases regulate translesion synthesis." Science **310**(5755): 1821-4.

Bish, R. A. and Myers, M. P. (2007). "Werner helicase-interacting protein 1 binds polyubiquitin via its zinc finger domain." J Biol Chem **282**(32): 23184-93.

Biswas, E. E., Chen, P. H. and Biswas, S. B. (1995). "Overexpression and rapid purification of biologically active yeast proliferating cell nuclear antigen." Protein Expr Purif **6**(6): 763-70.

Blackwell, L. J. and Borowiec, J. A. (1994). "Human replication protein A binds single-stranded DNA in two distinct complexes." Mol Cell Biol **14**(6): 3993-4001.

Blackwell, L. J., Borowiec, J. A. and Masrangelo, I. A. (1996). "Single-stranded-DNA binding alters human replication protein A structure and facilitates interaction with DNA-dependent protein kinase." Mol Cell Biol **16**(9): 4798-807.

Blastyak, A., Pinter, L., Unk, I., Prakash, L., Prakash, S. and Haracska, L. (2007). "Yeast Rad5 protein required for postreplication repair has a DNA helicase activity specific for replication fork regression." Mol Cell **28**(1): 167-75.

Bochkarev, A. and Bochkareva, E. (2004). "From RPA to BRCA2: lessons from single-stranded DNA binding by the OB-fold." Curr Opin Struct Biol **14**(1): 36-42.

Bochkarev, A., Bochkareva, E., Frappier, L. and Edwards, A. M. (1999). "The crystal structure of the complex of replication protein A subunits RPA32 and RPA14 reveals a mechanism for single-stranded DNA binding." Embo J **18**(16): 4498-504.

Bochkarev, A., Pfuetzner, R. A., Edwards, A. M. and Frappier, L. (1997). "Structure of the single-stranded-DNA-binding domain of replication protein A bound to DNA." Nature **385**(6612): 176-81.

Bochkareva, E., Belegu, V., Korolev, S. and Bochkarev, A. (2001). "Structure of the major single-stranded DNA-binding domain of replication protein A suggests a dynamic mechanism for DNA binding." Embo J **20**(3): 612-8.

Bradford, M. M. (1976). "A rapid and sensitive method for the quantitation of microgram quantities of protein utilizing the principle of protein-dye binding." Anal Biochem **72**: 248-54.

Branzei, D. and Foiani, M. (2005). "The DNA damage response during DNA replication." Curr Opin Cell Biol **17**(6): 568-75.

Branzei, D. and Foiani, M. (2007). "Interplay of replication checkpoints and repair proteins at stalled replication forks." DNA Repair (Amst) **6**(7): 994-1003.

Branzei, D. and Foiani, M. (2008). "Regulation of DNA repair throughout the cell cycle." Nat Rev Mol Cell Biol **9**(4): 297-308.

Braun, K. A., Lao, Y., He, Z., Ingles, C. J. and Wold, M. S. (1997). "Role of protein-protein interactions in the function of replication protein A (RPA): RPA modulates the activity of DNA polymerase alpha by multiple mechanisms." Biochemistry **36**(28): 8443-54.

Brill, S. J. and Bastin-Shanower, S. (1998). "Identification and characterization of the fourth single-stranded-DNA binding domain of replication protein A." Mol Cell Biol **18**(12): 7225-34.

Brill, S. J. and Stillman, B. (1989). "Yeast replication factor-A functions in the unwinding of the SV40 origin of DNA replication." Nature **342**(6245): 92-5.

Brill, S. J. and Stillman, B. (1991). "Replication factor-A from *Saccharomyces cerevisiae* is encoded by three essential genes coordinately expressed at S phase." Genes Dev **5**(9): 1589-600.

Broomfield, S., Chow, B. L. and Xiao, W. (1998). "*MMS2*, encoding a ubiquitin-conjugating-enzyme-like protein, is a member of the yeast error-free postreplication repair pathway." Proc Natl Acad Sci U S A **95**(10): 5678-83.

Broomfield, S., Hryciw, T. and Xiao, W. (2001). "DNA postreplication repair and mutagenesis in *Saccharomyces cerevisiae*." Mutat Res **486**(3): 167-84.

Brusky, J., Zhu, Y. and Xiao, W. (2000). "*UBC13*, a DNA-damage-inducible gene, is a member of the error-free postreplication repair pathway in *Saccharomyces cerevisiae*." Curr Genet **37**(3): 168-74.

Bujalowski, W., Overman, L. B. and Lohman, T. M. (1988). "Binding mode transitions of *Escherichia coli* single strand binding protein-single-stranded DNA complexes. Cation, anion, pH, and binding density effects." J Biol Chem **263**(10): 4629-40.

Byun, T. S., Pacek, M., Yee, M. C., Walter, J. C. and Cimprich, K. A. (2005). "Functional uncoupling of MCM helicase and DNA polymerase activities activates the ATR-dependent checkpoint." Genes Dev **19**(9): 1040-52.

Cai, J., Uhlmann, F., Gibbs, E., Flores-Rozas, H., Lee, C. G., Phillips, B., Finkelstein, J., Yao, N., O'Donnell, M. and Hurwitz, J. (1996). "Reconstitution of human replication factor C from its five subunits in baculovirus-infected insect cells." Proc Natl Acad Sci U S A **93**(23): 12896-901.

Cassier-Chauvat, C. and Fabre, F. (1991). "A similar defect in UV-induced mutagenesis conferred by the *rad6* and *rad18* mutations of *Saccharomyces cerevisiae*." Mutat Res **254**(3): 247-53.

Chanet, R., Magana-Schwencke, N. and Fabre, F. (1988). "Potential DNA-binding domains in the *RAD18* gene product of *Saccharomyces cerevisiae*." Gene **74**(2): 543-7.

Chen, S., Davies, A. A., Sagan, D. and Ulrich, H. D. (2005). "The RING finger ATPase Rad5p of *Saccharomyces cerevisiae* contributes to DNA double-strand break repair in a ubiquitin-independent manner." Nucleic Acids Res **33**(18): 5878-86.

Cimprich, K. A. (2007). "Probing ATR activation with model DNA templates." Cell Cycle **6**(19): 2348-54.

Cox, B. S. and Parry, J. M. (1968). "The isolation, genetics and survival characteristics of ultraviolet light-sensitive mutants in yeast." Mutat Res **6**(1): 37-55.

Craven, R. J., Greenwell, P. W., Dominska, M. and Petes, T. D. (2002). "Regulation of genome stability by *TEL1* and *MEC1*, yeast homologs of the mammalian *ATM* and *ATR* genes." Genetics **161**(2): 493-507.

Daughdrill, G. W., Buchko, G. W., Botuyan, M. V., Arrowsmith, C., Wold, M. S., Kennedy, M. A. and Lowry, D. F. (2003). "Chemical shift changes provide evidence for overlapping single-stranded DNA- and XPA-binding sites on the 70 kDa subunit of human replication protein A." Nucleic Acids Res **31**(14): 4176-83.

Davies, A. A., Friedberg, E. C., Tomkinson, A. E., Wood, R. D. and West, S. C. (1995). "Role of the Rad1 and Rad10 proteins in nucleotide excision repair and recombination." J Biol Chem **270**(42): 24638-41.

Davies, A. A., Huttner, D., Daigaku, Y., Chen, S. and Ulrich, H. D. (2008). "Activation of ubiquitin-dependent DNA damage bypass is mediated by replication protein a." Mol Cell **29**(5): 625-36.

de Lima-Bessa, K. M., Armelini, M. G., Chigancas, V., Jacysyn, J. F., Amarante-Mendes, G. P., Sarasin, A. and Menck, C. F. (2008). "CPDs and 6-4PPs play different roles in UV-induced cell death in normal and NER-deficient human cells." DNA Repair (Amst) **7**(2): 303-12.

Devany, M., Kappes, F., Chen, K. M., Markovitz, D. M. and Matsuo, H. (2008). "Solution NMR structure of the N-terminal domain of the human DEK protein." Protein Sci **17**(2): 205-15.

Dickerson, R. E. and Chiu, T. K. (1997). "Helix bending as a factor in protein/DNA recognition." Biopolymers **44**(4): 361-403.

Dohmen, R. J., Madura, K., Bartel, B. and Varshavsky, A. (1991). "The N-end rule is mediated by the UBC2(RAD6) ubiquitin-conjugating enzyme." Proc Natl Acad Sci U S A **88**(16): 7351-5.

Dohmen, R. J., Wu, P. and Varshavsky, A. (1994). "Heat-inducible degron: a method for constructing temperature-sensitive mutants." Science **263**(5151): 1273-6.

Dornreiter, I., Erdile, L. F., Gilbert, I. U., von Winkler, D., Kelly, T. J. and Fanning, E. (1992). "Interaction of DNA polymerase alpha-primase with cellular replication protein A and SV40 T antigen." Embo J **11**(2): 769-76.

Dutta, A., Ruppert, J. M., Aster, J. C. and Winchester, E. (1993). "Inhibition of DNA replication factor RPA by p53." Nature **365**(6441): 79-82.

Dzantiev, L., Constantin, N., Genschel, J., Iyer, R. R., Burgers, P. M. and Modrich, P. (2004). "A defined human system that supports bidirectional mismatch-provoked excision." Mol Cell **15**(1): 31-41.

Fabre, F., Magana-Schwencke, N. and Chanet, R. (1989). "Isolation of the *RAD18* gene of *Saccharomyces cerevisiae* and construction of *rad18* deletion mutants." Mol Gen Genet **215**(3): 425-30.

Fairman, M. P. and Stillman, B. (1988). "Cellular factors required for multiple stages of SV40 DNA replication *in vitro*." Embo J **7**(4): 1211-8.

Fan, J., Matsumoto, Y. and Wilson, D. M., 3rd (2006). "Nucleotide sequence and DNA secondary structure, as well as replication protein A, modulate the single-stranded abasic endonuclease activity of APE1." J Biol Chem **281**(7): 3889-98.

Fan, J. and Wilson, D. M., 3rd (2005). "Protein-protein interactions and posttranslational modifications in mammalian base excision repair." Free Radic Biol Med **38**(9): 1121-38.

Fanning, E., Klimovich, V. and Nager, A. R. (2006). "A dynamic model for replication protein A (RPA) function in DNA processing pathways." Nucleic Acids Res **34**(15): 4126-37.

Finley, D., Ozkaynak, E. and Varshavsky, A. (1987). "The yeast polyubiquitin gene is essential for resistance to high temperatures, starvation, and other stresses." Cell **48**(6): 1035-46.

Firmenich, A. A., Elias-Arnanz, M. and Berg, P. (1995). "A novel allele of *Saccharomyces cerevisiae RFA1* that is deficient in recombination and repair and suppressible by *RAD52*." Mol Cell Biol **15**(3): 1620-31.

Fivash, M., Towler, E. M. and Fisher, R. J. (1998). "BIAcore for macromolecular interaction." Curr Opin Biotechnol **9**(1): 97-101.

Fortini, P., Pascucci, B., Parlanti, E., D'Errico, M., Simonelli, V. and Dogliotti, E. (2003). "The base excision repair: mechanisms and its relevance for cancer susceptibility." Biochimie **85**(11): 1053-71.

Franko, J., Ashley, C. and Xiao, W. (2001). "Molecular cloning and functional characterization of two murine cDNAs which encode Ubc variants involved in DNA repair and mutagenesis." Biochim Biophys Acta **1519**(1-2): 70-7.

Friedberg, E. C. (2003). "DNA damage and repair." Nature **421**(6921): 436-40.

Friedberg, E. C., Walker, G. C. and Siede, W., Eds. (1995). DNA repair and mutagenesis. Washington, DC, American society for microbiology.

Fu, Y., Zhu, Y., Zhang, K., Yeung, M., Durocher, D. and Xiao, W. (2008). "Rad6-Rad18 mediates a eukaryotic SOS response by ubiquitinating the 9-1-1 checkpoint clamp." Cell **133**(4): 601-11.

Gamsjaeger, R., Liew, C. K., Loughlin, F. E., Crossley, M. and Mackay, J. P. (2007). "Sticky fingers: zinc-fingers as protein-recognition motifs." Trends Biochem Sci **32**(2): 63-70.

Garg, P. and Burgers, P. M. (2005). "Ubiquitinated proliferating cell nuclear antigen activates translesion DNA polymerases eta and REV1." Proc Natl Acad Sci U S A **102**(51): 18361-6.

Geiss-Friedlander, R. and Melchior, F. (2007). "Concepts in sumoylation: a decade on." Nat Rev Mol Cell Biol **8**(12): 947-56.

Gohring, F., Schwab, B. L., Nicotera, P., Leist, M. and Fackelmayer, F. O. (1997). "The novel SAR-binding domain of scaffold attachment factor A (SAF-A) is a target in apoptotic nuclear breakdown." Embo J **16**(24): 7361-71.

Gomes, X. V. and Wold, M. S. (1996). "Functional domains of the 70-kilodalton subunit of human replication protein A." Biochemistry **35**(32): 10558-68.

Goosen, N. and Moolenaar, G. F. (2008). "Repair of UV damage in bacteria." DNA Repair (Amst) **7**(3): 353-79.

Griep, M. A. and McHenry, C. S. (1989). "Glutamate overcomes the salt inhibition of DNA polymerase III holoenzyme." J Biol Chem **264**(19): 11294-301.

Guo, C., Sonoda, E., Tang, T. S., Parker, J. L., Bielen, A. B., Takeda, S., Ulrich, H. D. and Friedberg, E. C. (2006a). "REV1 protein interacts with PCNA: significance of the REV1 BRCT domain *in vitro* and *in vivo*." Mol Cell **23**(2): 265-71.

Guo, C., Tang, T. S., Bienko, M., Dikic, I. and Friedberg, E. C. (2008). "Requirements for the interaction of mouse Polkappa with ubiquitin and its biological significance." J Biol Chem **283**(8): 4658-64.

Guo, C., Tang, T. S., Bienko, M., Parker, J. L., Bielen, A. B., Sonoda, E., Takeda, S., Ulrich, H. D., Dikic, I. and Friedberg, E. C. (2006a). "Ubiquitin-binding motifs in REV1 protein are required for its role in the tolerance of DNA damage." Mol Cell Biol **26**(23): 8892-900.

Guo, S., Zhang, Y., Yuan, F., Gao, Y., Gu, L., Wong, I. and Li, G. M. (2006b). "Regulation of replication protein A functions in DNA mismatch repair by phosphorylation." J Biol Chem **281**(31): 21607-16.

Habraken, Y., Sung, P., Prakash, L. and Prakash, S. (1995). "Structure-specific nuclease activity in yeast nucleotide excision repair protein Rad2." J Biol Chem **270**(50): 30194-8.

Hakem, R. (2008). "DNA-damage repair; the good, the bad, and the ugly." Embo J **27**(4): 589-605.

Hammarsten, O. and Chu, G. (1998). "DNA-dependent protein kinase: DNA binding and activation in the absence of Ku." Proc Natl Acad Sci U S A **95**(2): 525-30.

Haracska, L., Unk, I., Prakash, L. and Prakash, S. (2006). "Ubiquitylation of yeast proliferating cell nuclear antigen and its implications for translesion DNA synthesis." Proc Natl Acad Sci U S A **103**(17): 6477-82.

Harfe, B. D. and Jinks-Robertson, S. (2000). "DNA mismatch repair and genetic instability." Annu Rev Genet **34**: 359-399.

Harper, J. W. and Elledge, S. J. (2007). "The DNA damage response: ten years after." Mol Cell **28**(5): 739-45.

Harper, J. W. and Schulman, B. A. (2006). "Structural complexity in ubiquitin recognition." Cell **124**(6): 1133-6.

Hays, S. L., Firmenich, A. A., Massey, P., Banerjee, R. and Berg, P. (1998). "Studies of the interaction between Rad52 protein and the yeast single-stranded DNA binding protein RPA." Mol Cell Biol **18**(7): 4400-6.

He, Z., Brinton, B. T., Greenblatt, J., Hassell, J. A. and Ingles, C. J. (1993). "The transactivator proteins VP16 and GAL4 bind replication factor A." Cell **73**(6): 1223-32.

He, Z., Henricksen, L. A., Wold, M. S. and Ingles, C. J. (1995). "RPA involvement in the damage-recognition and incision steps of nucleotide excision repair." Nature **374**(6522): 566-9.

Henricksen, L. A., Umbricht, C. B. and Wold, M. S. (1994). "Recombinant replication protein A: expression, complex formation, and functional characterization." J Biol Chem **269**(15): 11121-32.

Heyer, W. D., Rao, M. R., Erdile, L. F., Kelly, T. J. and Kolodner, R. D. (1990). "An essential *Saccharomyces cerevisiae* single-stranded DNA binding protein is homologous to the large subunit of human RP-A." Embo J **9**(7): 2321-9.

Hoege, C., Pfander, B., Moldovan, G. L., Pyrowolakis, G. and Jentsch, S. (2002). "*RAD6*-dependent DNA repair is linked to modification of PCNA by ubiquitin and SUMO." Nature **419**(6903): 135-41.

Hoeijmakers, J. H. (2001). "Genome maintenance mechanisms for preventing cancer." Nature **411**(6835): 366-74.

Hofmann, R. M. and Pickart, C. M. (1999). "Noncanonical *MMS2*-encoded ubiquitin-conjugating enzyme functions in assembly of novel polyubiquitin chains for DNA repair." Cell **96**(5): 645-53.

Hoppe, T. (2005). "Multiubiquitylation by E4 enzymes: 'one size' doesn't fit all." Trends Biochem Sci **30**(4): 183-7.

Huang, T. T., Nijman, S. M., Mirchandani, K. D., Galardy, P. J., Cohn, M. A., Haas, W., Gygi, S. P., Ploegh, H. L., Bernards, R. and D'Andrea, A. D. (2006). "Regulation of monoubiquitinated PCNA by DUB autocleavage." Nat Cell Biol **8**(4): 339-47.

Hwang, W. W., Venkatasubrahmanyam, S., Ianculescu, A. G., Tong, A., Boone, C. and Madhani, H. D. (2003). "A conserved RING finger protein required for histone H2B monoubiquitination and cell size control." Mol Cell **11**(1): 261-6.

Iyer, L. M., Babu, M. M. and Aravind, L. (2006). "The HIRAN domain and recruitment of chromatin remodeling and repair activities to damaged DNA." Cell Cycle **5**(7): 775-82.

Jackson, A. L. and Loeb, L. A. (2001). "The contribution of endogenous sources of DNA damage to the multiple mutations in cancer." Mutat Res **477**(1-2): 7-21.

Jackson, D., Dhar, K., Wahl, J. K., Wold, M. S. and Borgstahl, G. E. (2002). "Analysis of the human replication protein A:Rad52 complex: evidence for crosstalk between RPA32, RPA70, Rad52 and DNA." J Mol Biol **321**(1): 133-48.

James, P., Halladay, J. and Craig, E. A. (1996). "Genomic libraries and a host strain designed for highly efficient two-hybrid selection in yeast." Genetics **144**(4): 1425-36.

Jentsch, S., McGrath, J. P. and Varshavsky, A. (1987). "The yeast DNA repair gene *RAD6* encodes a ubiquitin-conjugating enzyme." Nature **329**(6135): 131-4.

Johnson, R. E., Henderson, S. T., Petes, T. D., Prakash, S., Bankmann, M. and Prakash, L. (1992). "*Saccharomyces cerevisiae RAD5*-encoded DNA repair protein contains DNA helicase and zinc-binding sequence motifs and affects the stability of simple repetitive sequences in the genome." Mol Cell Biol **12**(9): 3807-18.

Johnson, R. E., Prakash, S. and Prakash, L. (1994). "Yeast DNA repair protein RAD5 that promotes instability of simple repetitive sequences is a DNA-dependent ATPase." J Biol Chem **269**(45): 28259-62.

Johnson, R. E., Prakash, S. and Prakash, L. (1999). "Efficient bypass of a thymine-thymine dimer by yeast DNA polymerase, Poleta." Science **283**(5404): 1001-4.

Jones, J. S., Weber, S. and Prakash, L. (1988). "The *Saccharomyces cerevisiae RAD18* gene encodes a protein that contains potential zinc finger domains for nucleic acid binding and a putative nucleotide binding sequence." Nucleic Acids Res **16**(14B): 7119-31.

Kakar, S., Watson, N. B. and McGregor, W. G. (2008). "RAD18 signals DNA polymerase IOTA to stalled replication forks in cells entering S-phase with DNA damage." Adv Exp Med Biol **614**: 137-43.

Kannouche, P. L., Wing, J. and Lehmann, A. R. (2004). "Interaction of human DNA polymerase eta with monoubiquitinated PCNA: a possible mechanism for the polymerase switch in response to DNA damage." Mol Cell **14**(4): 491-500.

Kim, C., Snyder, R. O. and Wold, M. S. (1992). "Binding properties of replication protein A from human and yeast cells." Mol Cell Biol **12**(7): 3050-9.

Kim, R., Sandler, S. J., Goldman, S., Yokota, H., Clark, A. J. and Kim, S.-H. (1998). "Overexpression of archaeal proteins in *Escherichia coli*." Biotech Letters **20**(3): 207-10.

Kipp, M., Gohring, F., Ostendorp, T., van Drunen, C. M., van Driel, R., Przybylski, M. and Fackelmayer, F. O. (2000). "SAF-Box, a conserved protein domain that specifically recognizes scaffold attachment region DNA." Mol Cell Biol **20**(20): 7480-9.

Koken, M. H., Reynolds, P., Jaspers-Dekker, I., Prakash, L., Prakash, S., Bootsma, D. and Hoeijmakers, J. H. (1991). "Structural and functional conservation of two human homologs of the yeast DNA repair gene *RAD6*." Proc Natl Acad Sci U S A **88**(20): 8865-9.

Krauss, G., Sindermann, H., Schomburg, U. and Maass, G. (1981). "*Escherichia coli* single-strand deoxyribonucleic acid binding protein: stability, specificity, and kinetics of complexes with oligonucleotides and deoxyribonucleic acid." Biochemistry **20**(18): 5346-52.

Krejci, L., Van Komen, S., Li, Y., Villemain, J., Reddy, M. S., Klein, H., Ellenberger, T. and Sung, P. (2003). "DNA helicase Srs2 disrupts the Rad51 presynaptic filament." Nature **423**(6937): 305-9.

Krishna, S. S., Majumdar, I. and Grishin, N. V. (2003). "Structural classification of zinc fingers: survey and summary." Nucleic Acids Res **31**(2): 532-50.

Kumaran, S., Kozlov, A. G. and Lohman, T. M. (2006). "*Saccharomyces cerevisiae* replication protein A binds to single-stranded DNA in multiple salt-dependent modes." Biochemistry **45**(39): 11958-73.

Kunkel, T. A. and Erie, D. A. (2005). "DNA mismatch repair." Annu Rev Biochem **74**: 681-710.

Kur, J., Olszewski, M., Dlugolecka, A. and Filipkowski, P. (2005). "Single-stranded DNA-binding proteins (SSBs) -- sources and applications in molecular biology." Acta Biochim Pol **52**(3): 569-74.

Kurz, E. U. and Lees-Miller, S. P. (2004). "DNA damage-induced activation of *ATM* and *ATM*-dependent signaling pathways." DNA Repair (Amst) **3**(8-9): 889-900.

Laemmli, U. K. (1970). "Cleavage of structural proteins during the assembly of the head of *bacteriophage T4*." Nature **227**(5259): 680-5.

Lambert, S. and Carr, A. M. (2005). "Checkpoint responses to replication fork barriers." Biochimie **87**(7): 591-602.

Lambert, S., Froget, B. and Carr, A. M. (2007). "Arrested replication fork processing: interplay between checkpoints and recombination." DNA Repair (Amst) **6**(7): 1042-61.

Lao, Y., Gomes, X. V., Ren, Y., Taylor, J. S. and Wold, M. S. (2000). "Replication protein A interactions with DNA. III. Molecular basis of recognition of damaged DNA." Biochemistry **39**(5): 850-9.

Lao, Y., Lee, C. G. and Wold, M. S. (1999). "Replication protein A interactions with DNA. 2. Characterization of double-stranded DNA-binding/helix-destabilization activities and the role of the zinc-finger domain in DNA interactions." Biochemistry **38**(13): 3974-84.

Lawley, P. D., Lethbridge, J. H., Edwards, P. A. and Shooter, K. V. (1969). "Inactivation of *bacteriophage T7* by mono- and difunctional sulphur mustards in relation to cross-linking and depurination of bacteriophage DNA." J Mol Biol **39**(1): 181-98.

Lawrence, C. W. (2007). "Following the *RAD6* pathway." DNA Repair (Amst) **6**(5): 676-86.

Lawrence, C. W. and Christensen, R. (1976). "UV mutagenesis in radiation-sensitive strains of yeast." Genetics **82**(2): 207-32.

Leach, C. A. and Michael, W. M. (2005). "Ubiquitin/SUMO modification of PCNA promotes replication fork progression in *Xenopus laevis* egg extracts." J Cell Biol **171**(6): 947-54.

Lehman, J. A., Hoelz, D. J. and Turchi, J. J. (2008). "DNA-Dependent Conformational Changes in the Ku Heterodimer." Biochemistry **47**(15): 4359-68.

Lehmann, A. R. (2006a). "New functions for Y family polymerases." Mol Cell **24**(4): 493-5.

Lehmann, A. R. (2006b). "Translesion synthesis in mammalian cells." Exp Cell Res **312**(14): 2673-6.

Lehmann, A. R. and Fuchs, R. P. (2006). "Gaps and forks in DNA replication: Rediscovering old models." DNA Repair (Amst) **5**(12): 1495-8.

Leirmo, S., Harrison, C., Cayley, D. S., Burgess, R. R. and Record, M. T., Jr. (1987). "Replacement of potassium chloride by potassium glutamate dramatically enhances protein-DNA interactions in vitro." Biochemistry **26**(8): 2095-101.

Li, G. M. (2008). "Mechanisms and functions of DNA mismatch repair." Cell Res **18**(1): 85-98.

Li, R. and Botchan, M. R. (1993). "The acidic transcriptional activation domains of VP16 and p53 bind the cellular replication protein A and stimulate *in vitro BPV-1* DNA replication." Cell **73**(6): 1207-21.

Lilley, D. M. J. (1995). DNA-Protein: Structural Interactions. Oxford New York Tokyo, Oxford University Press.

Lin, Y. L., Chen, C., Keshav, K. F., Winchester, E. and Dutta, A. (1996). "Dissection of functional domains of the human DNA replication protein complex replication protein A." J Biol Chem **271**(29): 17190-8.

Lohman, T. M. and Ferrari, M. E. (1994). "*Escherichia coli* single-stranded DNA-binding protein: multiple DNA-binding modes and cooperativities." Annu Rev Biochem **63**: 527-70.

Lohman, T. M. and Overman, L. B. (1985). "Two binding modes in *Escherichia coli* single strand binding protein-single stranded DNA complexes. Modulation by NaCl concentration." J Biol Chem **260**(6): 3594-603.

Lohman, T. M., Overman, L. B. and Datta, S. (1986). "Salt-dependent changes in the DNA binding co-operativity of *Escherichia coli* single strand binding protein." J Mol Biol **187**(4): 603-15.

Longhese, M. P., Plevani, P. and Lucchini, G. (1994). "Replication factor A is required *in vivo* for DNA replication, repair, and recombination." Mol Cell Biol **14**(12): 7884-90.

Loo, Y. M. and Melendy, T. (2004). "Recruitment of replication protein A by the papillomavirus E1 protein and modulation by single-stranded DNA." J Virol **78**(4): 1605-15.

Lopes, M., Cotta-Ramusino, C., Pellicioli, A., Liberi, G., Plevani, P., Muzi-Falconi, M., Newlon, C. S. and Foiani, M. (2001). "The DNA replication checkpoint response stabilizes stalled replication forks." Nature **412**(6846): 557-61.

Lopes, M., Foiani, M. and Sogo, J. M. (2006). "Multiple mechanisms control chromosome integrity after replication fork uncoupling and restart at irreparable UV lesions." Mol Cell **21**(1): 15-27.

Lorick, K. L., Jensen, J. P., Fang, S., Ong, A. M., Hatakeyama, S. and Weissman, A. M. (1999). "RING fingers mediate ubiquitin-conjugating

enzyme (E2)-dependent ubiquitination." Proc Natl Acad Sci U S A **96**(20): 11364-9.

Luckow, V. A., Lee, S. C., Barry, G. F. and Olins, P. O. (1993). "Efficient generation of infectious recombinant baculoviruses by site-specific transposon-mediated insertion of foreign genes into a baculovirus genome propagated in Escherichia coli." J Virol **67**(8): 4566-79.

Ludlum, D. B., Warner, R. C. and Wahba, A. J. (1964). "Alkylation of Synthetic Polynucleotides." Science **145**: 397-9.

Mackay, J. P. and Crossley, M. (1998). "Zinc fingers are sticking together." Trends Biochem Sci **23**(1): 1-4.

Mackereth, C. D., Arrowsmith, C. H., Edwards, A. M. and McIntosh, L. P. (2000). "Zinc-bundle structure of the essential RNA polymerase subunit RPB10 from *Methanobacterium thermoautotrophicum*." Proc Natl Acad Sci U S A **97**(12): 6316-21.

Matsuda, T., Saijo, M., Kuraoka, I., Kobayashi, T., Nakatsu, Y., Nagai, A., Enjoji, T., Masutani, C., Sugasawa, K., Hanaoka, F. and et al. (1995). "DNA repair protein XPA binds replication protein A (RPA)." J Biol Chem **270**(8): 4152-7.

Matsunaga, T., Park, C. H., Bessho, T., Mu, D. and Sancar, A. (1996). "Replication protein A confers structure-specific endonuclease activities to the XPF-ERCC1 and XPG subunits of human DNA repair excision nuclease." J Biol Chem **271**(19): 11047-50.

McEachern, M. J. and Haber, J. E. (2006). "Break-induced replication and recombinational telomere elongation in yeast." Annu Rev Biochem **75**: 111-35.

McGlynn, P. and Lloyd, R. G. (2002). "Recombinational repair and restart of damaged replication forks." Nat Rev Mol Cell Biol **3**(11): 859-70.

McHugh, P. J., Sones, W. R. and Hartley, J. A. (2000). "Repair of intermediate structures produced at DNA interstrand cross-links in *Saccharomyces cerevisiae*." Mol Cell Biol **20**(10): 3425-33.

McHugh, P. J., Spanswick, V. J. and Hartley, J. A. (2001). "Repair of DNA interstrand crosslinks: molecular mechanisms and clinical relevance." Lancet Oncol **2**(8): 483-90.

McIlwraith, M. J. and West, S. C. (2008). "DNA repair synthesis facilitates RAD52-mediated second-end capture during DSB repair." Mol Cell **29**(4): 510-6.

McKenna, S., Spyracopoulos, L., Moraes, T., Pastushok, L., Ptak, C., Xiao, W. and Ellison, M. J. (2001). "Noncovalent interaction between ubiquitin and

the human DNA repair protein Mms2 is required for Ubc13-mediated polyubiquitination." J Biol Chem **276**(43): 40120-6.

Miller, J., McLachlan, A. D. and Klug, A. (1985). "Repetitive zinc-binding domains in the protein transcription factor IIIA from *Xenopus* oocytes." Embo J **4**(6): 1609-14.

Miyase, S., Tateishi, S., Watanabe, K., Tomita, K., Suzuki, K., Inoue, H. and Yamaizumi, M. (2005). "Differential regulation of Rad18 through Rad6-dependent mono- and polyubiquitination." J Biol Chem **280**(1): 515-24.

Mladenov, E., Anachkova, B. and Tsaneva, I. (2006). "Sub-nuclear localization of Rad51 in response to DNA damage." Genes Cells **11**(5): 513-24.

Moldovan, G. L., Pfander, B. and Jentsch, S. (2007). "PCNA, the maestro of the replication fork." Cell **129**(4): 665-79.

Motegi, A., Sood, R., Moinova, H., Markowitz, S. D., Liu, P. P. and Myung, K. (2006). "Human SHPRH suppresses genomic instability through proliferating cell nuclear antigen polyubiquitination." J Cell Biol **175**(5): 703-8.

Murzin, A. G. (1993). "OB(oligonucleotide/oligosaccharide binding)-fold: common structural and functional solution for non-homologous sequences." Embo J **12**(3): 861-7.

Muzi-Falconi, M., Liberi, G., Lucca, C. and Foiani, M. (2003). "Mechanisms controlling the integrity of replicating chromosomes in budding yeast." Cell Cycle **2**(6): 564-7.

Nakajima, S., Lan, L., Kanno, S., Usami, N., Kobayashi, K., Mori, M., Shiomi, T. and Yasui, A. (2006). "Replication-dependent and -independent responses of RAD18 to DNA damage in human cells." J Biol Chem **281**(45): 34687-95.

Nelson, J. R., Lawrence, C. W. and Hinkle, D. C. (1996). "Deoxycytidyl transferase activity of yeast REV1 protein." Nature **382**(6593): 729-31.

Notenboom, V., Hibbert, R. G., van Rossum-Fikkert, S. E., Olsen, J. V., Mann, M. and Sixma, T. K. (2007). "Functional characterization of Rad18 domains for Rad6, ubiquitin, DNA binding and PCNA modification." Nucleic Acids Res **35**(17): 5819-30.

Ogi, T., Shinkai, Y., Tanaka, K. and Ohmori, H. (2002). "Polkappa protects mammalian cells against the lethal and mutagenic effects of *benzo[a]pyrene*." Proc Natl Acad Sci U S A **99**(24): 15548-53.

Ohmori, H., Friedberg, E. C., Fuchs, R. P., Goodman, M. F., Hanaoka, F., Hinkle, D., Kunkel, T. A., Lawrence, C. W., Livneh, Z., Nohmi, T., Prakash, L., Prakash, S., Todo, T., Walker, G. C., Wang, Z. and

Woodgate, R. (2001). "The Y-family of DNA polymerases." Mol Cell **8**(1): 7-8.

Okubo, S., Hara, F., Tsuchida, Y., Shimotakahara, S., Suzuki, S., Hatanaka, H., Yokoyama, S., Tanaka, H., Yasuda, H. and Shindo, H. (2004). "NMR structure of the N-terminal domain of SUMO ligase PIAS1 and its interaction with tumor suppressor p53 and A/T-rich DNA oligomers." J Biol Chem **279**(30): 31455-61.

Ong, T., Matter, B. E. and de Serres, F. J. (1975). "Genetic characterization of *adenine-3* mutants induced by 4-nitroquinoline 1-oxide and 4-hydroxyaminoquinoline 1-oxide in *Neurospora crassa*." Cancer Res **35**(2): 291-5.

Overman, L. B., Bujalowski, W. and Lohman, T. M. (1988). "Equilibrium binding of *Escherichia coli* single-strand binding protein to single-stranded nucleic acids in the (SSB)65 binding mode. Cation and anion effects and polynucleotide specificity." Biochemistry **27**(1): 456-71.

Pages, V. and Fuchs, R. P. (2002). "How DNA lesions are turned into mutations within cells?" Oncogene **21**(58): 8957-66.

Palvimo, J. J. (2007). "PIAS proteins as regulators of small ubiquitin-related modifier (SUMO) modifications and transcription." Biochem Soc Trans **35**(Pt 6): 1405-8.

Papouli, E., Chen, S., Davies, A. A., Huttner, D., Krejci, L., Sung, P. and Ulrich, H. D. (2005). "Crosstalk between SUMO and ubiquitin on PCNA is mediated by recruitment of the helicase Srs2p." Mol Cell **19**(1): 123-33.

Park, C. H., Bessho, T., Matsunaga, T. and Sancar, A. (1995). "Purification and characterization of the XPF-ERCC1 complex of human DNA repair excision nuclease." J Biol Chem **270**(39): 22657-60.

Park, C. J., Lee, J. H. and Choi, B. S. (2005). "Solution structure of the DNA-binding domain of RPA from *Saccharomyces cerevisiae* and its interaction with single-stranded DNA and SV40 T antigen." Nucleic Acids Res **33**(13): 4172-81.

Parker, J. L., Bielen, A. B., Dikic, I. and Ulrich, H. D. (2007). "Contributions of ubiquitin- and PCNA-binding domains to the activity of Polymerase eta in *Saccharomyces cerevisiae*." Nucleic Acids Res **35**(3): 881-9.

Parker, J. L., Bucceri, A., Davies, A. A., Heidrich, K., Windecker, H. and Ulrich, H. D. (*in revision*). "SUMO modification of PCNA is regulated by DNA." EMBO J.

Parrilla-Castellar, E. R., Arlander, S. J. and Karnitz, L. (2004). "Dial 9-1-1 for DNA damage: the Rad9-Hus1-Rad1 (9-1-1) clamp complex." DNA Repair (Amst) **3**(8-9): 1009-14.

Passmore, L. A. and Barford, D. (2004). "Getting into position: the catalytic mechanisms of protein ubiquitylation." Biochem J **379**(Pt 3): 513-25.

Paz-Elizur, T., Takeshita, M., Goodman, M., O'Donnell, M. and Livneh, Z. (1996). "Mechanism of translesion DNA synthesis by DNA polymerase II. Comparison to DNA polymerases I and III core." J Biol Chem **271**(40): 24662-9.

Petrini, J. H. and Stracker, T. H. (2003). "The cellular response to DNA double-strand breaks: defining the sensors and mediators." Trends Cell Biol **13**(9): 458-62.

Pfander, B., Moldovan, G. L., Sacher, M., Hoege, C. and Jentsch, S. (2005). "SUMO-modified PCNA recruits Srs2 to prevent recombination during S phase." Nature **436**(7049): 428-33.

Pfuetzner, R. A., Bochkarev, A., Frappier, L. and Edwards, A. M. (1997). "Replication protein A. Characterization and crystallization of the DNA binding domain." J Biol Chem **272**(1): 430-4.

Philipova, D., Mullen, J. R., Maniar, H. S., Lu, J., Gu, C. and Brill, S. J. (1996). "A hierarchy of SSB protomers in replication protein A." Genes Dev **10**(17): 2222-33.

Pickart, C. M. (2001). "Mechanisms underlying ubiquitination." Annu Rev Biochem **70**: 503-33.

Pickart, C. M. and Fushman, D. (2004). "Polyubiquitin chains: polymeric protein signals." Curr Opin Chem Biol **8**(6): 610-6.

Prakash, L. (1975). "The effect of genes controlling radiation sensitivity on chemical mutagenesis in yeast." Basic Life Sci **5A**: 393-5.

Prakash, S., Johnson, R. E. and Prakash, L. (2005). "Eukaryotic translesion synthesis DNA polymerases: specificity of structure and function." Annu Rev Biochem **74**: 317-53.

Prakash, S. and Prakash, L. (2000). "Nucleotide excision repair in yeast." Mutat Res **451**(1-2): 13-24.

Puig, O., Caspary, F., Rigaut, G., Rutz, B., Bouveret, E., Bragado-Nilsson, E., Wilm, M. and Seraphin, B. (2001). "The tandem affinity purification (TAP) method: a general procedure of protein complex purification." Methods **24**(3): 218-29.

Ramilo, C., Gu, L., Guo, S., Zhang, X., Patrick, S. M., Turchi, J. J. and Li, G. M. (2002). "Partial reconstitution of human DNA mismatch repair *in vitro*: characterization of the role of human replication protein A." Mol Cell Biol **22**(7): 2037-46.

Record, M. T., Jr., Anderson, C. F., Mills, P., Mossing, M. and Roe, J. H. (1985). "Ions as regulators of protein-nucleic acid interactions *in vitro* and *in vivo*." Adv Biophys **20**: 109-35.

Reindle, A., Belichenko, I., Bylebyl, G. R., Chen, X. L., Gandhi, N. and Johnson, E. S. (2006). "Multiple domains in Siz SUMO ligases contribute to substrate selectivity." J Cell Sci **119**(Pt 22): 4749-57.

Richey, B., Cayley, D. S., Mossing, M. C., Kolka, C., Anderson, C. F., Farrar, T. C. and Record, M. T., Jr. (1987). "Variability of the intracellular ionic environment of *Escherichia coli*. Differences between *in vitro* and *in vivo* effects of ion concentrations on protein-DNA interactions and gene expression." J Biol Chem **262**(15): 7157-64.

Rocha, W. and Verreault, A. (2008). "Clothing up DNA for all seasons: Histone chaperones and nucleosome assembly pathways." FEBS Lett.

Rubin, G. M., Yandell, M. D., Wortman, J. R., Gabor Miklos, G. L., Nelson, C. R., Hariharan, I. K., Fortini, M. E., Li, P. W., Apweiler, R., Fleischmann, W., Cherry, J. M., Henikoff, S., Skupski, M. P., Misra, S., Ashburner, M., Birney, E., Boguski, M. S., Brody, T., Brokstein, P., Celniker, S. E., Chervitz, S. A., Coates, D., Cravchik, A., Gabrielian, A., Galle, R. F., Gelbart, W. M., George, R. A., Goldstein, L. S., Gong, F., Guan, P., Harris, N. L., Hay, B. A., Hoskins, R. A., Li, J., Li, Z., Hynes, R. O., Jones, S. J., Kuehl, P. M., Lemaitre, B., Littleton, J. T., Morrison, D. K., Mungall, C., O'Farrell, P. H., Pickeral, O. K., Shue, C., Vosshall, L. B., Zhang, J., Zhao, Q., Zheng, X. H. and Lewis, S. (2000). "Comparative genomics of the eukaryotes." Science **287**(5461): 2204-15.

Rupp, W. D. and Howard-Flanders, P. (1968). "Discontinuities in the DNA synthesized in an excision-defective strain of *Escherichia coli* following ultraviolet irradiation." J Mol Biol **31**(2): 291-304.

Sahara, S., Aoto, M., Eguchi, Y., Imamoto, N., Yoneda, Y. and Tsujimoto, Y. (1999). "Acinus is a caspase-3-activated protein required for apoptotic chromatin condensation." Nature **401**(6749): 168-73.

Sakamoto, S., Nishikawa, K., Heo, S. J., Goto, M., Furuichi, Y. and Shimamoto, A. (2001). "Werner helicase relocates into nuclear foci in response to DNA damaging agents and co-localizes with RPA and Rad51." Genes Cells **6**(5): 421-30.

Sambrook, J., Fritsch, E. F. and Maniatis, T. (1989). Molecular cloning: A laboratory manual. Cold Spring Harbor, New York, Cold Spring Harbor Laboratory Press.

Sarkar, S., Davies, A. A., Ulrich, H. D. and McHugh, P. J. (2006). "DNA interstrand crosslink repair during G1 involves nucleotide excision repair and DNA polymerase zeta." Embo J **25**(6): 1285-94.

Sedgwick, B., Bates, P. A., Paik, J., Jacobs, S. C. and Lindahl, T. (2007). "Repair of alkylated DNA: recent advances." DNA Repair (Amst) **6**(4): 429-42.

Seeman, N. C., Rosenberg, J. M. and Rich, A. (1976). "Sequence-specific recognition of double helical nucleic acids by proteins." Proc Natl Acad Sci U S A **73**(3): 804-8.

Setlow, J. K. (1966). "Photoreactivation." Radiat Res: Suppl 6:141+.

Shechter, D., Costanzo, V. and Gautier, J. (2004). "Regulation of DNA replication by ATR: signaling in response to DNA intermediates." DNA Repair (Amst) **3**(8-9): 901-8.

Sibenaller, Z. A., Sorensen, B. R. and Wold, M. S. (1998). "The 32- and 14-kilodalton subunits of replication protein A are responsible for species-specific interactions with single-stranded DNA." Biochemistry **37**(36): 12496-506.

Smith, G. C. and Jackson, S. P. (1999). "The DNA-dependent protein kinase." Genes Dev **13**(8): 916-34.

Smith, J., Zou, H. and Rothstein, R. (2000). "Characterization of genetic interactions with *RFA1*: the role of RPA in DNA replication and telomere maintenance." Biochimie **82**(1): 71-8.

Sogo, J. M., Lopes, M. and Foiani, M. (2002). "Fork reversal and ssDNA accumulation at stalled replication forks owing to checkpoint defects." Science **297**(5581): 599-602.

Stauffer, M. E. and Chazin, W. J. (2004). "Physical interaction between replication protein A and Rad51 promotes exchange on single-stranded DNA." J Biol Chem **279**(24): 25638-45.

Stelter, P. and Ulrich, H. D. (2003). "Control of spontaneous and damage-induced mutagenesis by SUMO and ubiquitin conjugation." Nature **425**(6954): 188-91.

Stigger, E., Drissi, R. and Lee, S. H. (1998). "Functional analysis of human replication protein A in nucleotide excision repair." J Biol Chem **273**(15): 9337-43.

Sugiyama, T., New, J. H. and Kowalczykowski, S. C. (1998). "DNA annealing by RAD52 protein is stimulated by specific interaction with the complex of replication protein A and single-stranded DNA." Proc Natl Acad Sci U S A **95**(11): 6049-54.

Sugiyama, T., Zaitseva, E. M. and Kowalczykowski, S. C. (1997). "A single-stranded DNA-binding protein is needed for efficient presynaptic complex formation by the *Saccharomyces cerevisiae* Rad51 protein." J Biol Chem **272**(12): 7940-5.

Sung, P., Guzder, S. N., Prakash, L. and Prakash, S. (1996). "Reconstitution of TFIIH and requirement of its DNA helicase subunits, Rad3 and Rad25, in the incision step of nucleotide excision repair." J Biol Chem **271**(18): 10821-6.

Sung, P., Prakash, S. and Prakash, L. (1990). "Mutation of cysteine-88 in the *Saccharomyces cerevisiae* RAD6 protein abolishes its ubiquitin-conjugating activity and its various biological functions." Proc Natl Acad Sci U S A **87**(7): 2695-9.

Takahashi, Y. and Kikuchi, Y. (2005). "Yeast PIAS-type Ull1/Siz1 is composed of SUMO ligase and regulatory domains." J Biol Chem **280**(43): 35822-8.

Tanaka, T. and Nasmyth, K. (1998). "Association of RPA with chromosomal replication origins requires an Mcm protein, and is regulated by Rad53, and cyclin- and Dbf4-dependent kinases." Embo J **17**(17): 5182-91.

Tateishi, S., Sakuraba, Y., Masuyama, S., Inoue, H. and Yamaizumi, M. (2000). "Dysfunction of human Rad18 results in defective postreplication repair and hypersensitivity to multiple mutagens." Proc Natl Acad Sci U S A **97**(14): 7927-32.

Tercero, J. A. and Diffley, J. F. (2001). "Regulation of DNA replication fork progression through damaged DNA by the Mec1/Rad53 checkpoint." Nature **412**(6846): 553-7.

Theobald, D. L., Mitton-Fry, R. M. and Wuttke, D. S. (2003). "Nucleic acid recognition by OB-fold proteins." Annu Rev Biophys Biomol Struct **32**: 115-33.

Tibbetts, R. S., Brumbaugh, K. M., Williams, J. M., Sarkaria, J. N., Cliby, W. A., Shieh, S. Y., Taya, Y., Prives, C. and Abraham, R. T. (1999). "A role for ATR in the DNA damage-induced phosphorylation of p53." Genes Dev **13**(2): 152-7.

Tomida, J., Masuda, Y., Hiroaki, H., Ishikawa, T., Song, I., Tsurimoto, T., Tateishi, S., Shiomi, T., Kamei, Y., Kim, J., Kamiya, K., Vaziri, C., Ohmori, H. and Todo, T. (2008). "DNA damage-induced ubiquitylation of RFC2 subunit of replication factor C complex." J Biol Chem **283**(14): 9071-9.

Torres-Ramos, C. A., Prakash, S. and Prakash, L. (2002). "Requirement of *RAD5* and *MMS2* for postreplication repair of UV-damaged DNA in *Saccharomyces cerevisiae*." Mol Cell Biol **22**(7): 2419-26.

Tsuji, Y., Watanabe, K., Araki, K., Shinohara, M., Yamagata, Y., Tsurimoto, T., Hanaoka, F., Yamamura, K., Yamaizumi, M. and Tateishi, S. (2008). "Recognition of forked and single-stranded DNA structures by human RAD18 complexed with RAD6B protein triggers its recruitment to stalled replication forks." Genes Cells **13**(4): 343-54.

Ulrich, H. D. (2001). "The *srs2* suppressor of UV sensitivity acts specifically on the *RAD5*- and *MMS2*-dependent branch of the *RAD6* pathway." Nucleic Acids Res **29**(17): 3487-94.

Ulrich, H. D. (2002). "Natural substrates of the proteasome and their recognition by the ubiquitin system." Curr Top Microbiol Immunol **268**: 137-74.

Ulrich, H. D. (2003). "Protein-protein interactions within an E2-RING finger complex. Implications for ubiquitin-dependent DNA damage repair." J Biol Chem **278**(9): 7051-8.

Ulrich, H. D. (2004). "How to activate a damage-tolerant polymerase: consequences of PCNA modifications by ubiquitin and SUMO." Cell Cycle **3**(1): 15-8.

Ulrich, H. D. (2005). "The *RAD6* pathway: control of DNA damage bypass and mutagenesis by ubiquitin and SUMO." Chembiochem **6**(10): 1735-43.

Ulrich, H. D. (2005b). "Mutual interactions between the SUMO and ubiquitin systems: a plea of no contest." Trends Cell Biol **15**(10): 525-32.

Ulrich, H. D. (2007). "Conservation of DNA damage tolerance pathways from yeast to humans." Biochem Soc Trans **35**(Pt 5): 1334-7.

Ulrich, H. D. and Jentsch, S. (2000). "Two RING finger proteins mediate cooperation between ubiquitin-conjugating enzymes in DNA repair." Embo J **19**(13): 3388-97.

Ulrich, H. D., Patten, P. A., Yang, P. L., Romesberg, F. E. and Schultz, P. G. (1995). "Expression studies of catalytic antibodies." Proc Natl Acad Sci U S A **92**(25): 11907-11.

Unk, I., Hajdu, I., Fatyol, K., Hurwitz, J., Yoon, J. H., Prakash, L., Prakash, S. and Haracska, L. (2008). "Human HLTF functions as a ubiquitin ligase for proliferating cell nuclear antigen polyubiquitination." Proc Natl Acad Sci U S A **105**(10): 3768-73.

van den Akker, E., Ano, S., Shih, H. M., Wang, L. C., Pironin, M., Palvimo, J. J., Kotaja, N., Kirsh, O., Dejean, A. and Ghysdael, J. (2005). "FLI-1 functionally interacts with PIASxalpha, a member of the PIAS E3 SUMO ligase family." J Biol Chem **280**(45): 38035-46.

van Hoffen, A., Venema, J., Meschini, R., van Zeeland, A. A. and Mullenders, L. H. (1995). "Transcription-coupled repair removes both cyclobutane pyrimidine dimers and 6-4 photoproducts with equal efficiency and in a sequential way from transcribed DNA in xeroderma pigmentosum group C fibroblasts." EMBO J **14**(2): 360-7.

VanDemark, A. P., Blanksma, M., Ferris, E., Heroux, A., Hill, C. P. and Formosa, T. (2006). "The structure of the yFACT Pob3-M domain, its

interaction with the DNA replication factor RPA, and a potential role in nucleosome deposition." Mol Cell **22**(3): 363-74.

Varadan, R., Assfalg, M., Haririnia, A., Raasi, S., Pickart, C. and Fushman, D. (2004). "Solution conformation of Lys63-linked di-ubiquitin chain provides clues to functional diversity of polyubiquitin signaling." J Biol Chem **279**(8): 7055-63.

Veatch, W. and Okada, S. (1969). "Radiation-induced breaks of DNA in cultured mammalian cells." Biophys J **9**(3): 330-46.

Viadiu, H. and Aggarwal, A. K. (1998). "The role of metals in catalysis by the restriction endonuclease *BamHI*." Nat Struct Biol **5**(10): 910-6.

Walker, J. R., Corpina, R. A. and Goldberg, J. (2001). "Structure of the Ku heterodimer bound to DNA and its implications for double-strand break repair." Nature **412**(6847): 607-14.

Walther, A. P., Gomes, X. V., Lao, Y., Lee, C. G. and Wold, M. S. (1999). "Replication protein A interactions with DNA. 1. Functions of the DNA-binding and zinc-finger domains of the 70-kDa subunit." Biochemistry **38**(13): 3963-73.

Wang, M., Mahrenholz, A. and Lee, S. H. (2000). "RPA stabilizes the XPA-damaged DNA complex through protein-protein interaction." Biochemistry **39**(21): 6433-9.

Wang, W. (2007). "Emergence of a DNA-damage response network consisting of *Fanconi anaemia* and BRCA proteins." Nat Rev Genet **8**(10): 735-48.

Wang, X. and Haber, J. E. (2004). "Role of *Saccharomyces* single-stranded DNA-binding protein RPA in the strand invasion step of double-strand break repair." PLoS Biol **2**(1): E21.

Ward, I. M., Minn, K. and Chen, J. (2004). "UV-induced *ataxia-telangiectasia-mutated and Rad3-related* (*ATR*) activation requires replication stress." J Biol Chem **279**(11): 9677-80.

Washington, M. T., Johnson, R. E., Prakash, S. and Prakash, L. (2000). "Accuracy of thymine-thymine dimer bypass by *Saccharomyces cerevisiae* DNA polymerase eta." Proc Natl Acad Sci U S A **97**(7): 3094-9.

Watanabe, K., Tateishi, S., Kawasuji, M., Tsurimoto, T., Inoue, H. and Yamaizumi, M. (2004). "Rad18 guides poleta to replication stalling sites through physical interaction and PCNA monoubiquitination." Embo J **23**(19): 3886-96.

Weiner, J. H., Bertsch, L. L. and Kornberg, A. (1975). "The deoxyribonucleic acid unwinding protein of *Escherichia coli*. Properties and functions in replication." J Biol Chem **250**(6): 1972-80.

Wilson, D. M., 3rd and Bohr, V. A. (2007). "The mechanics of base excision repair, and its relationship to aging and disease." DNA Repair (Amst) **6**(4): 544-59.

Windecker, H. and Ulrich, H. D. (2008). "Architecture and assembly of poly-SUMO chains on PCNA in *Saccharomyces cerevisiae*." J Mol Biol **376**(1): 221-31.

Woelk, T., Oldrini, B., Maspero, E., Confalonieri, S., Cavallaro, E., Di Fiore, P. P. and Polo, S. (2006). "Molecular mechanisms of coupled monoubiquitination." Nat Cell Biol **8**(11): 1246-54.

Wold, M. S. (1997). "Replication protein A: a heterotrimeric, single-stranded DNA-binding protein required for eukaryotic DNA metabolism." Annu Rev Biochem **66**: 61-92.

Wold, M. S. and Kelly, T. (1988). "Purification and characterization of replication protein A, a cellular protein required for *in vitro* replication of simian virus 40 DNA." Proc Natl Acad Sci U S A **85**(8): 2523-7.

Wood, A., Garg, P. and Burgers, P. M. (2007). "A ubiquitin-binding motif in the translesion DNA polymerase Rev1 mediates its essential functional interaction with ubiquitinated proliferating cell nuclear antigen in response to DNA damage." J Biol Chem **282**(28): 20256-63.

Xin, H., Lin, W., Sumanasekera, W., Zhang, Y., Wu, X. and Wang, Z. (2000). "The human *RAD18* gene product interacts with *HHR6A* and *HHR6B*." Nucleic Acids Res **28**(14): 2847-54.

Yang, W. and Woodgate, R. (2007). "What a difference a decade makes: insights into translesion DNA synthesis." Proc Natl Acad Sci U S A **104**(40): 15591-8.

Yuzhakov, A., Kelman, Z., Hurwitz, J. and O'Donnell, M. (1999). "Multiple competition reactions for RPA order the assembly of the DNA polymerase delta holoenzyme." EMBO J **18**(21): 6189-99.

Zhang, D., Frappier, L., Gibbs, E., Hurwitz, J. and O'Donnell, M. (1998). "Human RPA (hSSB) interacts with EBNA1, the latent origin binding protein of Epstein-Barr virus." Nucleic Acids Res **26**(2): 631-7.

Zhang, H. and Lawrence, C. W. (2005a). "The error-free component of the *RAD6/RAD18* DNA damage tolerance pathway of budding yeast employs sister-strand recombination." Proc Natl Acad Sci U S A **102**(44): 15954-9.

Zhang, Y., Yuan, F., Presnell, S. R., Tian, K., Gao, Y., Tomkinson, A. E., Gu, L. and Li, G. M. (2005b). "Reconstitution of 5'-directed human mismatch repair in a purified system." Cell **122**(5): 693-705.

Zou, L. and Elledge, S. J. (2003). "Sensing DNA damage through ATRIP recognition of RPA-ssDNA complexes." Science **300**(5625): 1542-8.

Zou, L., Liu, D. and Elledge, S. J. (2003). "Replication protein A-mediated recruitment and activation of Rad17 complexes." Proc Natl Acad Sci U S A **100**(24): 13827-32.

10 Appendix

Table 10-1

No. oHU	Name	Sequence	Length (nt)	Features and Use
55	RAD6 up	CCGGATCCTGCAGTCAGTC TGCTTCGTCGTC	31	Antisense Amplification of ORF
57	RAD18 up	CCGGATCCTGCAGTTAATT GTTACCGGGTGG	31	Antisense Amplification of ORF
72	Rad18 promoter up	GACCTGCAGGATCCGAGTA GTAAAAATGGCCTTTTC	36	Antisense Amplification of promoter
73	RAD18 promoter down	CCGAATTCCTCACCGAAAA CTAATTATTC	29	Antisense Amplification of promoter
168	RAD18 C48S down	CATTTTCAAGCTTGTGTATT AGAACACATTTGAAT	35	Sense Mutagenesis of ORF C48S (RING finger)
169	RAD18 C48S up	AATACACAAGCTTGAAAATG TATGGCCACAAG	32	Antisense Mutagenesis of ORF C48S (RING finger)
170	RAD18 GAA down	GGGGCAGCGAGCTCATATA GGAAATTACTTGAA	33	Sense Mutagenesis of ORF G365A/K366A/S367 A (ATPase)
171	RAD18 GAA up	TGAGCTCGCTGCCCCATTA CTCTTCATTATC	31	Antisense Mutagenesis of ORF G365A/K366A/S367 A (ATPase)
179	RAD18-AA(110/111) down	GTCCCTGAGAATGcGGcAGT ACCAGGTCCTG	31	Sense Mutagenesis of ORF E110/111A
180	RAD18-AA(110/111) up	CAGGACCTGGTACTgCCgCA TTCTCAGGGAC	31	Antisense Mutagenesis of ORF E110/111A
181	RAD18-AAA(136-138) down	GTGTAAATGCCGCTGcTGcT GcCTTGCAAATTGTTGCAAC	40	Sense Mutagenesis of ORF D136/137/138A
182	RAD18-AAA(136-138) up	GTTGCAACAATTTGCAAGgC AgCAgCAGCGGCATTTACAC	40	Antisense Mutagenesis of ORF D136/137/138A
183	RAD18-AA(151/152) down	GCAACAAGTGAAAGAAAAC TTGCCgcAgcATCCATGACTG ATATATTACC	50	Sense Mutagenesis of ORF K151A/R152A
184	RAD18-AA(151/152) up	GGTAATATATCAGTCATGGA TgcTgcGGCAAGTTTTCTTTC ACTTGTTGC	50	Antisense Mutagenesis of ORF K151A/R152A
185	RAD18-AAA(178-180) down	GTTCAGAAGTGAACGTATCg cGgcAgcATCAAAGCCAAATG AACAAATGGCCC	53	Sense Mutagenesis of ORF K178/179/180A
186	RAD18-AAA(178-180) up	GGGCCATTTGTTCATTTGGC TTTGATgcTgcCgcGATACGT TCACTTCTGAAC	53	Antisense Mutagenesis of ORF K178/179/180A
187	RAD18-S(190) down	GAACAAATGGCCCAGaGCC CCATATGTCAAC	31	Sense Mutagenesis of ORF C190S (Zinc finger)

188	RAD18-S(190) up	GTTGACATATGGGGCtCTGG GCCATTTGTTC	31	Antisense Mutagenesis of ORF C190S (Zinc finger)
189	RAD18-AA(208/209) down	CCTTGAAAAAACACATTTGG cTGcATGCCTAACTTTACAAT CAC	44	Sense Mutagenesis of ORF D208A/E209A
190	RAD18-AA(208/209) up	GTGATTGTAAAGTTAGGCAT gCAgCCAAATGTGTTTTTTCA AGG	44	Antisense Mutagenesis of ORF D208A/E209A
536	RAD18 down (pET)	ACTAGGATCCGCACCAAAT AACCACTGCAAG	31	Sense Amplification of ORF
537	RAD18 up (pET)	GTGTGGTACCTTAATTGTTA CCGGGTGGGT	30	Antisense Amplification of ORF
538	RAD6 down (pET)	ACTAGGATCCAATGTCCACA CCAGCTAGAAG	31	Sense Amplification of ORF
539	RAD6 up (pET)	GTGTGGTACCTCAGTCTGC TTCGTCGTCG	29	Antisense Amplification of ORF
543	PhoA linker I	GGTATCTAGAGGTTGAGGT GATTCCATGGATCCATTCTG CAGCTAGAGGTTGAGGTGA TTTTATGG	66	Linker for pUC-PhoA-Duet
544	PhoA linker II	TGCCAAGCTTACTCGAGGG TACCATGCATTGGGAGATCT GCCATAAAATCACCTCAACC TCT	62	Linker for pUC-PhoA-Duet
545	PhoA seq	CGAGACTTATAGTCGCTTTG TT	22	Sense Amplification of promoter
724	pFastBacHTc down	AGCATCAAGATCTCATGTCG TACTACCATCA	31	Sense Sequencing
794	[Phi]X-174-1	ATTTTCTCATTTTCCGCCAG CAGTCCAC	28	Antisense [Phi]X-174 ssDNA DNA-binding assays
795	[Phi]X-174-2	TCAACAGGAGCAGGAAAGC GAGGGTATC	28	Antisense [Phi]X-174 ssDNA DNA-binding assays
796	[Phi]X-174-3	CACGACGCAATGGAGAAAG ACGGAGAGC	28	Antisense [Phi]X-174 ssDNA DNA-binding assays
797	[Phi]X-174-4	GCCCAGAGATTAGAGCGCA TGACAAGTA	28	Antisense [Phi]X-174 ssDNA DNA-binding assays
798	[Phi]X-174-5	GCTTCGGCGTTATAACCTCA CACTCAATCTTTT	33	Antisense [Phi]X-174 ssDNA DNA-binding assays
799	[Phi]X-174-6	CGCCAGCAATAGCACCAAA CATAAATCACCTCACT	35	Antisense [Phi]X-174 ssDNA DNA-binding assays
800	[Phi]X-174-7	TCAAATCCGGCGTCAACCA TACCAGCAGAG	30	Antisense [Phi]X-174 ssDNA DNA-binding assays
801	[Phi]X-174-8	GAAAAATATCAACCACACCA GAAGCAGCATCAGT	34	Antisense [Phi]X-174 ssDNA DNA-binding assays
802	[Phi]X-174-9	CGAACTCAACGCCCTGCAT ACGAAAAGA	28	Antisense [Phi]X-174 ssDNA DNA-binding assays
803	[Phi]X-174-10	CGTGAAAAAGCGTCCTGCG TGTAGCGAACT	30	Antisense [Phi]X-174 ssDNA DNA-binding assays

834	ssDNA-bio	TTGTAAAACGACGGCCAGT GAATTCATCATCAATAATAT ACCTTATTTTGGCAGGCGG TGTTAATACTGACCGCC[Bio TEG-Q]	75	3'-biotinylated DNA-binding assays
835	dsDNA	GGCGGTCAGTATTAACACC GCCTGCCAAAATAAGGTATA TTATTGATGATGAATTCACT GGCCGTCGTTTTACAA	75	Reverse complement to oHU834 DNA-binding assays
844	XO1c	GGGTGAACCTGCAGGTGGG CAAAGATGTCCTAGCAAGG CACTGGTAGAATTCGGCAG CGTC	61	Reverse complement to XO1 (oHU1055) DNA-binding assays (Table 2-9)
847	XO4	ATCGATAGTCGGATCCTCTA GACAGCTCCATGTAGCAAG GCACTGGTAGAATTCGGCA GCGT	62	Splayed arm with XO1 (oHU1055) DNA-binding assays (Table 2-9)
848	XO2.1/2	TGGGTGAACCTGCAGGTGG GCAAAGATGTCC	31	DNA-binding assays (Table 2-9)
849	XO3.1/2	CATGGAGCTGTCTAGAGGA TCCGACTATCGA	31	DNA-binding assays (Table 2-9)
870	ssDNA-bio II	ATGGATTAGATAGACGAAGT TGTCAAGAGCTCTGCTGCT GGTAACACCGTATGCTAGT ACACTGCGTTTATGTAT[BioT EG-Q]	75	3'-biotinylated DNA-binding assays (Weak secondary structure; Sequence based on *PGK1*)
871	dsDNA II	ATACATAAACGCAGTGTACT AGCATACGGTGTTACCAGC AGCAGAGCTCTTGACAACTT CGTCTATCTAATCCAT	75	Reverse complement to oHU870 DNA-binding assays
881	RAD18 SAPΔ up	CCAAAGCATAAAATTGATCT TCGGCAATCT	30	Antisense Mutagenesis of ORF (279-312)Δ (SAP domain)
882	RAD18 SAPΔ down	GAAGATCAATTTTATGCTTT GGAATTCTAATTTTTG	36	Sense Mutagenesis of ORF (279-312)Δ (SAP domain)
883	RAD18 SAP* up	CgcGTTTTGCgcAGTAgCATT AGTTGACAGTCCCAAC	37	Antisense Mutagenesis of ORF G299A/R301A/M304 A (SAP domain)
884	RAD18 SAP* down	GcTACTgcGCAAAACgcGATT AAAAGATACAATCACTAC	39	Sense Mutagenesis of ORF G299A/R301A/M304 A (SAP domain)
885	pFastBacHTc down new	AGCATCAAGATCTCATGTCG TACTACCATCACCA	34	Sense Amplification of tag
886	RAD6 C88S up	AATATCCAAAgAAATTTCAC CATTTGCATAGAC	33	Antisense Mutagenesis of ORF C88S
887	RAD6 C88S down	TGGTGAAATTTcTTTGGATA TTTTGCAGAACAG	33	Sense Mutagenesis of ORF C88S
906	ssDNA-bio III	CGCCAGCAATAGCACCAAA CATAAATCACCTCACT[BioTE G-Q]	35	3'-biotinylated Identical to oHU799 DNA-binding assays

907	dsDNA III	AGTGAGGTGATTTATGTTTG GTGCTATTGCTGGCG	35	Reverse complement to oHU906 DNA-binding assays
1045	dT 10mer	TTTTTTTTTT	10	DNA-binding assays
1055	XO1	[BiodT]ACGCTGCCGAATTCT ACCAGTGCCTTGCTAGGAC ATCTTTGCCCACCTGCAGG TTCACCC	61	5'-biotinylated DNA-binding assays (Table 2-9)
1092	dT 16mer	TTTTTTTTTTTTTTTT	16	DNA-binding assays
1093	dT 25mer	TTTTTTTTTTTTTTTTTTTTT TTT	25	DNA-binding assays
1094	dT 35mer	TTTTTTTTTTTTTTTTTTTTT TTTTTTTTTTTT	35	DNA-binding assays
1095	dT 75mer	TTTTTTTTTTTTTTTTTTTTT TTTTTTTTTTTTTTTTTTTTT TTTTTTTTTTTTTTTTTTTTT TTTTTTTTT	75	DNA-binding assays
1177	36mer-5' biotin	[BiodT]ACGCTGCCGAATTCT ACCAGTG CCTTGCTAGGACA	36	5'-biotinylated Based on XO1 3'-Flap of 5 nucleotides with oHU847 & oHU849 DNA-binding assays
1178	46mer-5' biotin	[BiodT]ACGCTGCCGAATTCT ACCAGTGCCTTGCTAGGAC ATCTTTGCCCA	46	5'-biotinylated Based on XO1 3'-Flap of 15 nucleotides with oHU847 & oHU849 DNA-binding assays
1179	76mer-5' biotin	[BiodT]ACGCTGCCGAATTCT ACCAGTGCCTTGCTAGGAC ATCTTTGCCCACCTGCAGG TTCACCCTTTTTTTTTTTTT T	76	5'-biotinylated Based on XO1 3'-Flap of 45 nucleotides with oHU847 & oHU849 DNA-binding assays
1180	dT 60mer 3' biotin	TTTTTTTTTTTTTTTTTTTTT TTTTTTTTTTTTTTTTTTTTT TTTTTTTTTTTTTT[BioTEG -Q]	60	3'-biotinylated DNA-binding assays
1181	dT 45mer 3' biotin	TTTTTTTTTTTTTTTTTTTTT TTTTTTTTTTTTTTTTTTTTT T[BioTEG-Q]	45	3'-biotinylated DNA-binding assays
1182	dT 35mer 3' biotin	TTTTTTTTTTTTTTTTTTTTT TTTTTTTTTTTT[BioTEG-Q]	35	3'-biotinylated DNA-binding assays
1183	dT 25mer 3' biotin	TTTTTTTTTTTTTTTTTTTTT TTT[BioTEG-Q]	25	3'-biotinylated DNA-binding assays
1184	dT 15mer 3' biotin	TTTTTTTTTTTTTT[BioTEG-Q]	15	3'-biotinylated DNA-binding assays
-	M13 reverse	CAGGAAACAGCTATGAC	17	Sequencing

Table 10-1: The sequences of all the oligonucleotides that were used.

Published work presented in this thesis:

Davies, A. A., Huttner, D., Daigaku, Y., Chen, S. and Ulrich, H. D. (2008). "Activation of ubiquitin-dependent DNA damage bypass is mediated by replication protein a." Mol Cell **29**(5): 625-36.

This manuscript is attached below.

This author performed / was involved in:

- Purification of the proteins used in the manuscript
- Pull-down assays with ^{GST}Rfa1 (182-421), ^{GST}Rfa2 and Rad18
- Gel-shift assays with ^{GST}Rfa1 (182-421), ^{GST}Rfa2 and ssDNA
- Biochemical analysis of the interactions between Rad18-Rad6, RPA and ssDNA
- Sensitivity spot assay of the *rad18* SAP mutation and deletion strains
- Manuscript revision
- Experimental suggestions

Work contributed to not presented in this thesis:

Papouli, E., Chen, S., Davies, A. A., Huttner, D., Krejci, L., Sung, P. and Ulrich, H. D. (2005). "Crosstalk between SUMO and ubiquitin on PCNA is mediated by recruitment of the helicase Srs2p." Mol Cell **19**(1): 123-33.

This author performed / was involved in:

- Co-immunoprecipitation experiments between PCNA and Srs2
- Pull-down assays with sumoylated PCNA and Srs2
- Experimental suggestions

Molecular Cell
Article

Activation of Ubiquitin-Dependent DNA Damage Bypass Is Mediated by Replication Protein A

Adelina A. Davies,[1] Diana Huttner,[1] Yasukazu Daigaku,[1] Shuhua Chen,[1,2] and Helle D. Ulrich[1,*]
[1]Cancer Research UK London Research Institute, Clare Hall Laboratories, Blanche Lane, South Mimms EN6 3LD, UK
[2]Present address: Institute for Neurophysiology, University of Cologne, Robert Koch Strasse, Cologne D-50931, Germany.
*Correspondence: helle.ulrich@cancer.org.uk
DOI 10.1016/j.molcel.2007.12.016

SUMMARY

Replicative DNA damage bypass, mediated by the ubiquitylation of the sliding clamp protein PCNA, facilitates the survival of a cell in the presence of genotoxic agents, but it can also promote genomic instability by damage-induced mutagenesis. We show here that PCNA ubiquitylation in budding yeast is activated independently of the replication-dependent S phase checkpoint but by similar conditions involving the accumulation of single-stranded DNA at stalled replication intermediates. The ssDNA-binding replication protein A (RPA), an essential complex involved in most DNA transactions, is required for damage-induced PCNA ubiquitylation. We found that RPA directly interacts with the ubiquitin ligase responsible for the modification of PCNA, Rad18, both in yeast and in mammalian cells. Association of the ligase with chromatin is detected where RPA is most abundant, and purified RPA can recruit Rad18 to ssDNA in vitro. Our results therefore implicate the RPA complex in the activation of DNA damage tolerance.

INTRODUCTION

DNA damage tolerance enables a cell to resolve replication problems such as damage-induced fork stalling (Lawrence, 1994; Lehmann, 2002; Ulrich, 2005). Replicative bypass of DNA lesions occurs via translesion synthesis (TLS) by specialized damage-tolerant DNA polymerases or by an error-free damage avoidance pathway that makes use of the information of the newly synthesized sister chromatid (Lawrence, 1994). Both pathways are activated by posttranslational modification of the replicative sliding clamp, proliferating cell nuclear antigen (PCNA) (Hoege et al., 2002; Kannouche et al., 2004; Stelter and Ulrich, 2003; Watanabe et al., 2004). In response to DNA damage, monoubiquitylation of PCNA at a conserved lysine, K164, activates the damage-tolerant polymerases for TLS, whereas polyubiquitylation is required for error-free damage avoidance. Independent of DNA damage, budding yeast PCNA is also modified during S phase by the ubiquitin-like protein SUMO (Papouli et al., 2005; Pfander et al., 2005). PCNA monoubiquitylation involves the ubiquitin-conjugating enzyme (E2) Rad6 and its cognate ubiquitin ligase (E3), Rad18. A second E2-E3 pair, the heterodimeric E2 Ubc13-Mms2 with the E3 Rad5, is responsible for polyubiquitylation. Although it promotes resistance to genotoxic agents, TLS is a potentially mutagenic process that endangers the cell's genomic stability. At the same time, failure to reactivate stalled replication forks may lead to genome instability by inducing DNA double-strand breaks (DSBs) and gross chromosomal aberrations (Branzei and Foiani, 2005). Stringent control over DNA damage bypass is therefore essential, but the upstream signals that activate PCNA modification in vivo are not well defined.

One of the important regulatory mechanisms responsible for the sensing of DNA damage and replication stress is the replication-dependent S phase checkpoint, a surveillance system that inhibits the firing of late-replication origins, prevents cell-cycle progression to mitosis, and is important for the stabilization of stalled replication forks (Branzei and Foiani, 2005; Nyberg et al., 2002). The ATR-ATRIP kinase complex and the PCNA-like 9-1-1 checkpoint clamp, responsible for initiating the checkpoint signaling cascade during S phase, are activated by replication fork stalling. Their recruitment to stretches of single-stranded (ss)DNA is mediated by interactions of ATRIP and the 9-1-1-specific clamp loader with the ssDNA-binding RPA complex (Zou and Elledge, 2003; Zou et al., 2003).

Our analysis of the mechanisms that control the activity of the *RAD6* pathway in budding yeast now reveals striking parallels to the replication checkpoint response: although the two systems operate independently, they are activated in a similar fashion by stalled replication intermediates that involve an accumulation of ssDNA. We show that yeast and human Rad18, like ATRIP and the 9-1-1 clamp loader, directly interact with the RPA complex. In vivo, the abundance of Rad18 on DNA mirrors that of RPA even in the absence of its physiological target, PCNA, and depletion of RPA prevents damage-induced PCNA ubiquitylation in S phase. In vitro, the RPA complex can recruit the ubiquitin ligase to ssDNA. These results suggest an effective activation mechanism for ubiquitin-dependent damage bypass.

RESULTS

Replication Forks Are Required for PCNA Ubiquitylation

In order to characterize the conditions required for PCNA ubiquitylation in *S. cerevisiae*, we examined possible contributions of the DNA damage checkpoint and cell-cycle regulation. We found that, in budding yeast, as in *X. laevis* egg extracts and in *S. pombe* (Chang et al., 2006; Frampton et al., 2006), ubiquitin-dependent DNA damage tolerance and checkpoint signaling operate independently (see Figure S1 available online). Given the importance

SPECIAL NOTE

THIS ITEM IS BOUND IN SUCH A MANNER AND WHILE EVERY EFFORT HAS BEEN MADE TO REPRODUCE THE CENTRES, FORCE WOULD RESULT IN DAMAGE

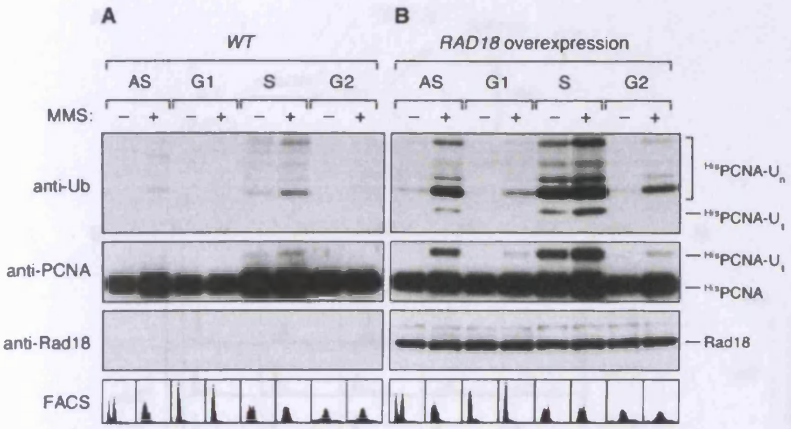

Figure 1. Effects of the Cell Cycle and *RAD18* Overexpression on PCNA Ubiquitylation

(A) Cell-cycle dependence of PCNA modification. Cells arrested in G1, S, and G2 phase were treated with 0.02% MMS for 90 min where indicated, and modifications of ^{His}PCNA, isolated under denaturing conditions, were detected by western blot. DNA contents were monitored by flow cytometry (FACS). Asynchronous cells (AS) were processed in parallel.

(B) Effects of *RAD18* overexpression on PCNA modification throughout the cell cycle. Cells were treated and analyzed as in (A). Note that, in this panel, monoubiquitylated PCNA is abundant enough to be detected by the anti-ubiquitin antibody, which recognizes this form very poorly (Hoege et al., 2002). Rad18 was detected in total cell extracts.

of ubiquitylated PCNA for replicative lesion bypass, the modification is expected to be most relevant during S phase. In fact, consistent with our previous findings (Papouli et al., 2005) and with the situation in mammalian cells (Kannouche et al., 2004), arrest in S phase with hydroxyurea (HU), which causes replication fork stalling by nucleotide depletion without directly damaging DNA, is sufficient to trigger PCNA modification (Figure 1A). In contrast, ubiquitylated PCNA was not detected in G1- or G2-arrested cells even after treatment with DNA-damaging agents. This indicates that, even in asynchronous populations, all detectable PCNA ubiquitylation arises from S phase cells.

The absence of ubiquitylated PCNA outside of S phase could be due to the lack of replication forks. Alternatively, the physiological state of the cell, defined by the activities of cyclin-dependent kinases, could control PCNA modification. In order to directly examine the need for DNA replication, we made use of a temperature-sensitive mutant of an essential kinase gene responsible for DNA replication initiation, *cdc7*^{ts} (Figure 2) (Hartwell, 1973). At the permissive temperature, *cdc7*^{ts} cells undergo regular cycles of DNA replication and cell division, whereas upon release from G1 arrest at the restrictive temperature, the mutant enters the cell cycle without initiating DNA replication (Figure 2B). Degradation of the CDK inhibitor Sic1 at the beginning of S phase and later on the accumulation of the mitotic cyclin Clb2 proceeds normally in *cdc7*^{ts} cells (Figure 2C), indicating that the physiological state under these conditions resembles a passage through the cell cycle. Following the scheme outlined in Figure 2A, we asked whether DNA damage would trigger PCNA modification in the mutant. We found that *WT* cells underwent PCNA ubiquitylation normally at 24°C and 37°C, but in *cdc7*^{ts} the modification was visible only at the permissive temperature (Figure 2D). In order to exclude the possibility that the kinase activity of Cdc7 itself was needed for the modification, we examined a strain in which the requirement for *CDC7* is bypassed by a mutation in *MCM5*, encoding a subunit of the replicative helicase (Hardy et al., 1997). In the context of this allele, *bob1*, deletion of *CDC7* did not abolish PCNA ubiquitylation, implying that the Cdc7 kinase itself is dispensable for modification of the clamp (Figure 2E). This suggests that PCNA needs to be engaged in replication for efficient ubiquitylation in vivo.

Not All Types of DNA Damage Induce PCNA Ubiquitylation

We next asked what types of lesions would induce PCNA modification during DNA replication. In addition to UV radiation and methyl methane sulfonate (MMS), which induce ubiquitylation in all species examined so far, agents that cause bulky adducts such as 4-nitroquinoline oxide (NQO) and also the oxidizing agent hydrogen peroxide (H_2O_2) were found to be active (Figure 3A). As observed in *S. pombe* (Frampton et al., 2006), PCNA was also ubiquitylated after treatment with ionizing radiation (IR) (Figure 3A), despite our previous finding that PCNA ubiquitylation site mutants are not particularly sensitive to IR, and DSBs induced by an endonuclease do not cause PCNA modification (Chen et al., 2005). Moreover, mammalian cells do not ubiquitylate PCNA after IR treatment (Kannouche et al., 2004). A possible explanation for the IR-induced modification of *S. cerevisiae* and *S. pombe* PCNA may therefore be base damage associated with the high doses of radiation used in the yeast system rather than DSBs per se.

To further explore this hypothesis, we analyzed the response to chemicals that cause DSBs by different mechanisms. Bleomycin, which acts independently of the cell-cycle phase, did not trigger PCNA modification (Figure 3A), although it affected viability (Figure 3B). Camptothecin (CPT), a topoisomerase I inhibitor, induces covalent adducts of the enzyme to DNA, which are converted to DSBs in S phase through collisions with replication forks (Liu et al., 2000). Despite its S phase-specific action, CPT treatment did not result in PCNA ubiquitylation (Figure 3A). In order to exclude the possibility that the drug had simply no effect at the concentrations used in this experiment, we examined PCNA modifications in a *rad52* mutant, which is highly sensitive to CPT (Figure 3C). Again, we did not observe PCNA ubiquitylation in response to CPT in *rad52*, whereas its reaction to MMS was comparable to that of *WT* cells (Figure 3D). Likewise, CPT induces PCNA modifications very modestly in *S. pombe* when compared to HU or UV (Frampton et al., 2006), and the drug is also a poor inducer of the replication checkpoint in budding yeast (Redon et al., 2003) (Figure 3E).

Replication fork stalling by treatment with HU or adduct-forming agents like MMS results in an inhibition of DNA polymerases

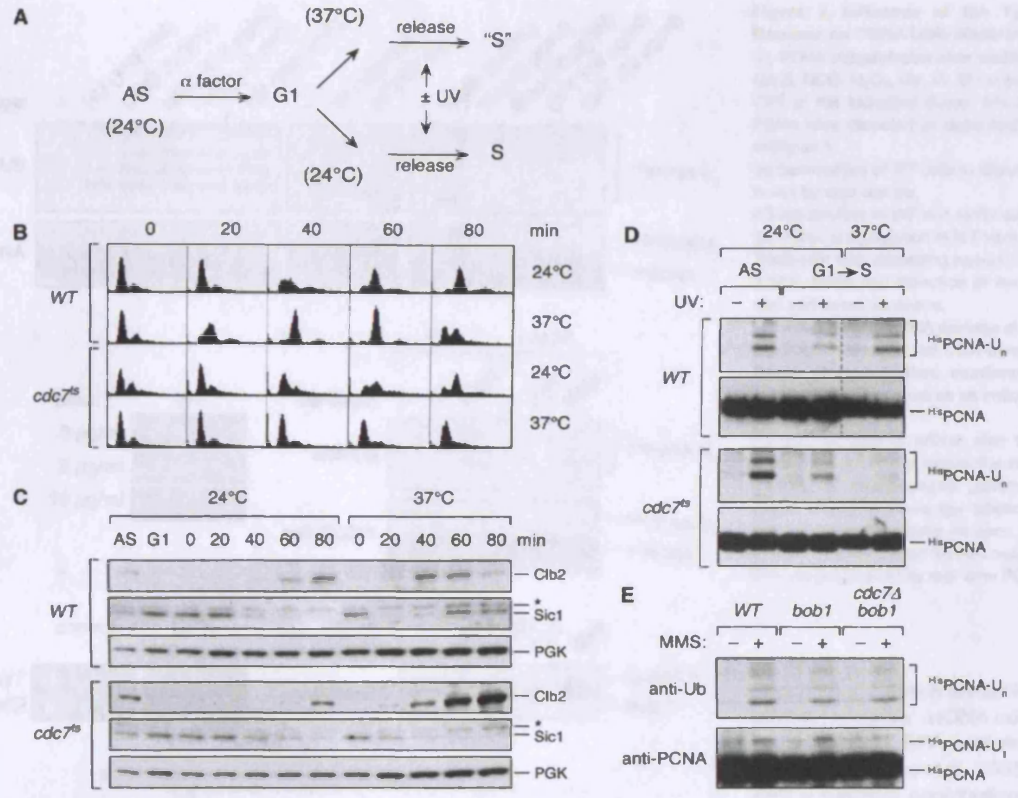

Figure 2. Active Replication Forks Are Required for PCNA Ubiquitylation

(A) Experimental strategy to prevent the formation of replication forks in the *cdc7*^{ts} mutant.

(B) FACS profiles of *WT* and *cdc7*^{ts} cells subjected to the treatment outlined in (A).

(C) Progression through the cell cycle in *WT* and *cdc7*^{ts} cells as monitored by Clb2 and Sic1 levels. Note that at 37°C *WT* cells have completed mitosis and re-entered G1 phase at 80 min, whereas *cdc7*^{ts} mutants accumulate in G2/M with abnormally high Clb2 and low Sic1 levels. The asterisk indicates a band cross-reactive to the Sic1 antibody. Detection of phosphoglycerate kinase (PGK) served as a loading control.

(D) Damage-induced PCNA ubiquitylation in *WT* and *cdc7*^{ts} cells after treatment as outlined in (A). S phase samples in *cdc7*^{ts} cells and in *WT* at 24°C were taken 40 min after release, whereas the S phase sample in the *WT* at 37°C was taken after 25 min due to the faster cell-cycle progression at this temperature (see [B] and [C]).

(E) *CDC7* is dispensable for PCNA ubiquitylation. Damage-induced PCNA modification was examined in asynchronous cultures of isogenic WT, *bob1*, and *bob1 cdc7Δ* cells.

and an accumulation of ssDNA due to the continuing movement of the replicative helicase (Branzei and Foiani, 2005). In contrast, collision of the replication machinery with CPT-induced topoisomerase adducts and DSB formation is expected to affect the entire replicon and should therefore not initially involve an accumulation of ssDNA. In support of this model, radioactive labeling of nondenatured total DNA by random priming was significantly enhanced after MMS or HU, but not after CPT treatment (Figure 3F). This even applied to the checkpoint-defective *rad53* mutant, which is known to accumulate ssDNA in response to replication stress (Sogo et al., 2002). In *rad52* cells, the difference was less pronounced, but we cannot rule out a replication-independent effect of the mutation—for example, on formation or resection of DSBs—that would have no consequences for PCNA modification. Thus, PCNA ubiquitylation correlates well with elevated levels of ssDNA during replication.

Overexpression of RAD18 Relaxes the Conditions for PCNA Modification

Given that the ubiquitin ligases, Rad18 and Rad5, are ssDNA-binding proteins, they might directly recognize a blocked fork by associating with the stretches of ssDNA adjacent to the stalled polymerase-PCNA complex. If these enzymes are limiting factors in transmitting the signal for modification, changes in their abundance should affect the extent of modification. We therefore analyzed the consequences of overexpressing *RAD18*, encoding the E3 responsible for PCNA monoubiquitylation. Figure 1B shows that overexpression of *RAD18* caused significantly increased levels of ubiquitylated PCNA. In asynchronous populations, *RAD18* overexpression resulted in constitutive modification of PCNA even in undamaged cells, suggesting that fork stalling was no longer required. Likewise, the modification was no longer restricted to S phase, as ubiquitylated PCNA now

SPECIAL NOTE

THIS ITEM IS BOUND IN SUCH A MANNER AND WHILE EVERY EFFORT HAS BEEN MADE TO REPRODUCE THE CENTRES, FORCE WOULD RESULT IN DAMAGE

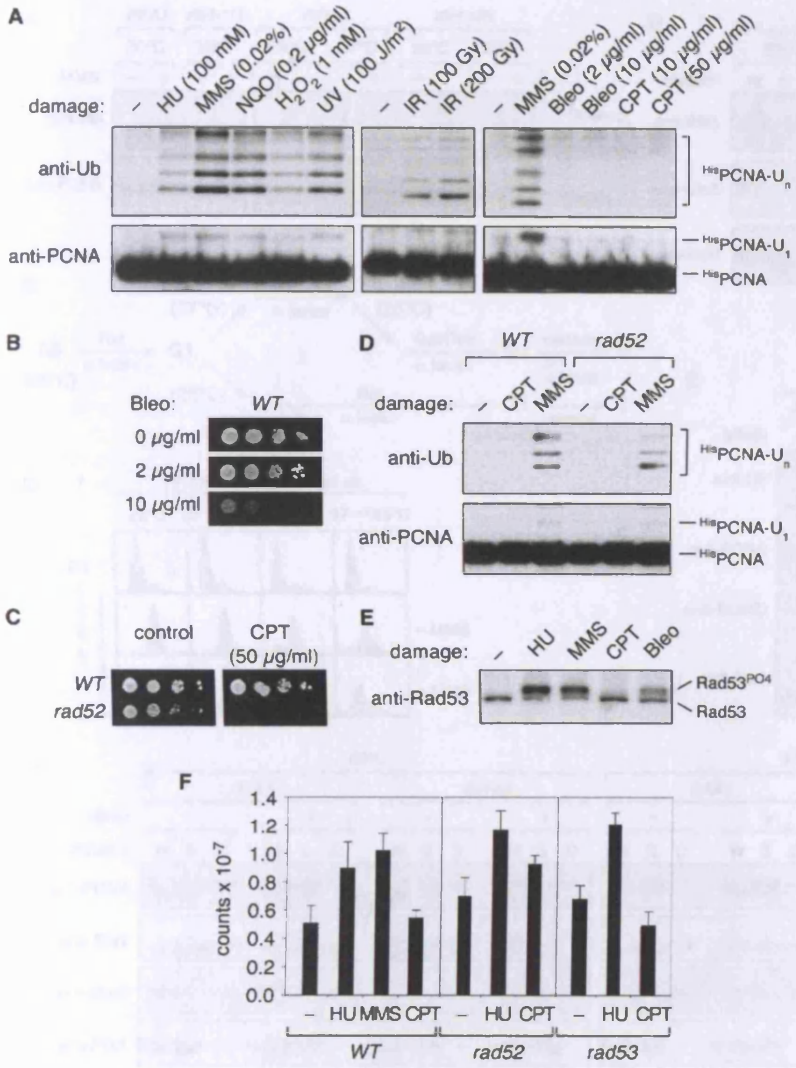

Figure 3. Influence of the Type of DNA Damage on PCNA Ubiquitylation

(A) PCNA ubiquitylation after treatment with HU, MMS, NQO, H_2O_2, UV, IR, Bleomycin (Bleo), and CPT at the indicated doses. Modified forms of PCNA were detected as described in the legend to Figure 1.

(B) Sensitivities of *WT* cells to Bleomycin as monitored by spot assays.

(C) Sensitivities of *WT* and *rad52* cells to CPT.

(D) PCNA ubiquitylation in *WT* versus *rad52* cells. Treatment with damaging agents (50 μg/ml CPT, 0.02% MMS) and detection of the modifications was performed as above.

(E) Induction of the DNA damage checkpoint after treatment with selected DNA-damaging agents. Rad53 phosphorylation, monitored by western blot analysis, was used as an indicator of checkpoint activation.

(F) Quantification of ssDNA after treatment with MMS, HU, or CPT by radioactive random-primed labeling of nondenatured genomic DNA. The graph shows the average labeling efficiencies with standard deviations (in cpm) from triplicate experiments, corrected for the amount of template DNA as determined by real-time PCR.

appeared in G1- and G2-arrested cells. Outside of S phase, however, DNA damage was still a prerequisite for the reaction. Taken together, elevated levels of Rad18 afforded PCNA ubiquitylation whenever the clamp was detectable in association with chromatin (Figure S2), strongly suggesting that the modification takes place on DNA. Consistent with this notion, loading of PCNA onto DNA was shown to be required for efficient modification in vitro (Garg and Burgers, 2005).

RPA Is Required for Ubiquitylation of PCNA

Our findings suggest that PCNA ubiquitylation is induced by the recruitment of Rad18 to regions of ssDNA exposed by the uncoupling of helicase movement from DNA synthesis, analogous to the way in which stalled forks are believed to activate the replication checkpoint (Branzei and Foiani, 2005). Considering that the factor responsible for recruitment of the ATR kinase complex and the 9-1-1 clamp loader is not naked ssDNA but rather ssDNA coated by the ssDNA-binding RPA complex (Zou and Elledge, 2003; Zou et al., 2003), we examined a possible contribution of RPA to PCNA ubiquitylation.

The *rfa1-t11* mutant (K45E), defective in homologous recombination and recruitment of checkpoint factors (Umezu et al., 1998; Zou and Elledge, 2003; Zou et al., 2003), was competent in damage-induced PCNA ubiquitylation (Figure 4A). Likewise, a temperature-sensitive mutant, *rfa1-t33* (S373P), which is unable to mediate DNA replication at the restrictive temperature (Umezu et al., 1998), ubiquitylated PCNA normally. This indicates that the replicative function of RPA is not required for PCNA modification. However, even at the restrictive temperature, the mutant protein was found in association with DNA (Figure 4B), which leaves the possibility that it was still able to promote the recruitment or activation of Rad18. A panel of *rfa2* and *rfa3* mutants defective in various aspects of DNA replication and repair (Maniar et al., 1997) had relatively minor effects on PCNA ubiquitylation (Figure S3). We therefore examined the consequences of depleting Rfa1 by means of a heat-inducible degradation signal (Dohmen et al., 1994). Following the procedure outlined in Figure 4C, we induced degradation of the $Rfa1^{td}$ protein in G1-arrested cells. The *rfa1-td* mutant engaged in DNA replication (Figure 4D) with less than 5% of the $Rfa1^{td}$ protein remaining, but damage-induced PCNA ubiquitylation was almost completely abolished (Figure 4E). In contrast, S phase-associated sumoylation of PCNA, which likewise depends

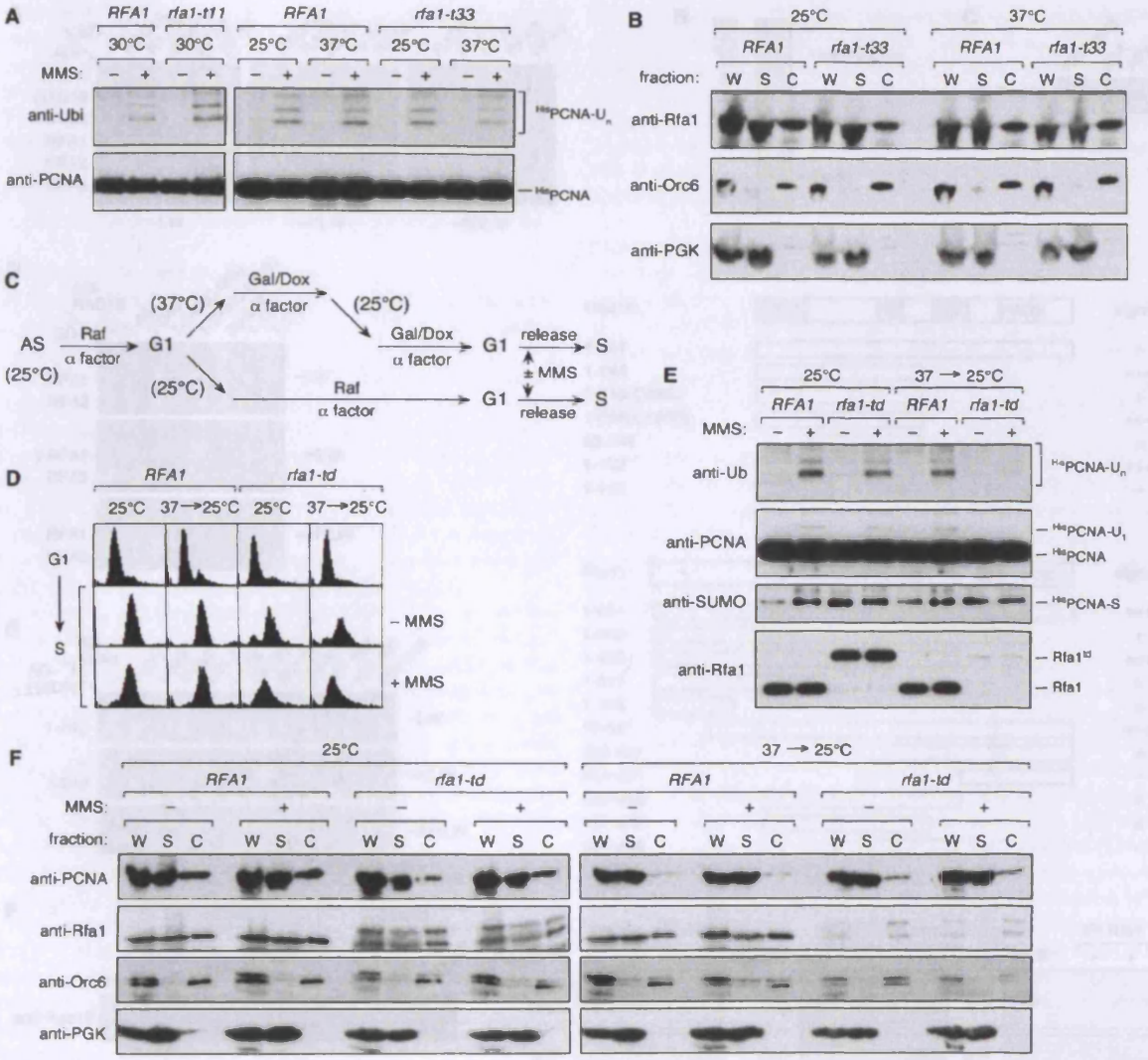

Figure 4. RPA Is Required for PCNA Ubiquitylation

(A) PCNA is ubiquitylated normally in the *rfa1-t11* and *rfa1-t33* mutants. MMS-induced PCNA ubiquitylation was detected as described in the legend to Figure 1 in *WT* (*RFA1*) and two *rfa1* mutants.

(B) DNA association of the mutant protein encoded by *rfa1-t33* is indistinguishable from the *WT* protein at 25°C and 37°C. Whole-cell extracts (W) were fractionated by centrifugation into soluble (S) and chromatin-associated (C) material. Proteins were detected by western blot. The distributions of the chromatin-associated Orc6 protein and soluble PGK served as controls for the quality of fractionation.

(C) Experimental strategy to deplete Rfa1^{td} from yeast cells. In the *rfa1-td* strain, the construct encoding the heat-labile Rfa1^{td} protein is controlled by a doxycycline (Dox)-repressible promoter, and *UBR1*, encoding the E3 responsible for degradation of Rfa1^{td}, is induced by galactose (Gal). Rfa1^{td} remains stable at 25°C in raffinose (Raf) medium. Temperature effects were excluded by returning the cells to 25°C without allowing resynthesis of Rfa1^{td} before releasing them into S phase.

(D) DNA replication proceeds after depletion of the Rfa1^{td} protein. FACS samples were taken before and 50 min after release from G1 arrest following the scheme shown in (C).

(E) Loss of damage-induced PCNA ubiquitylation after depletion of the Rfa1^{td} protein. ^{His}PCNA and its modified forms were detected as in Figure 1. Rfa1 was detected in total cell extracts.

(F) Chromatin association of PCNA in *RFA1* and *rfa1-td*. Chromatin-binding assays were performed as described in (B). Note that the Rfa1^{td} protein remaining after depletion is entirely associated with chromatin. The degron tag is partially cleaved from the protein during extract preparation.

SPECIAL NOTE

THIS ITEM IS BOUND IN SUCH A MANNER AND WHILE EVERY EFFORT HAS BEEN MADE TO REPRODUCE THE CENTRES, FORCE WOULD RESULT IN DAMAGE

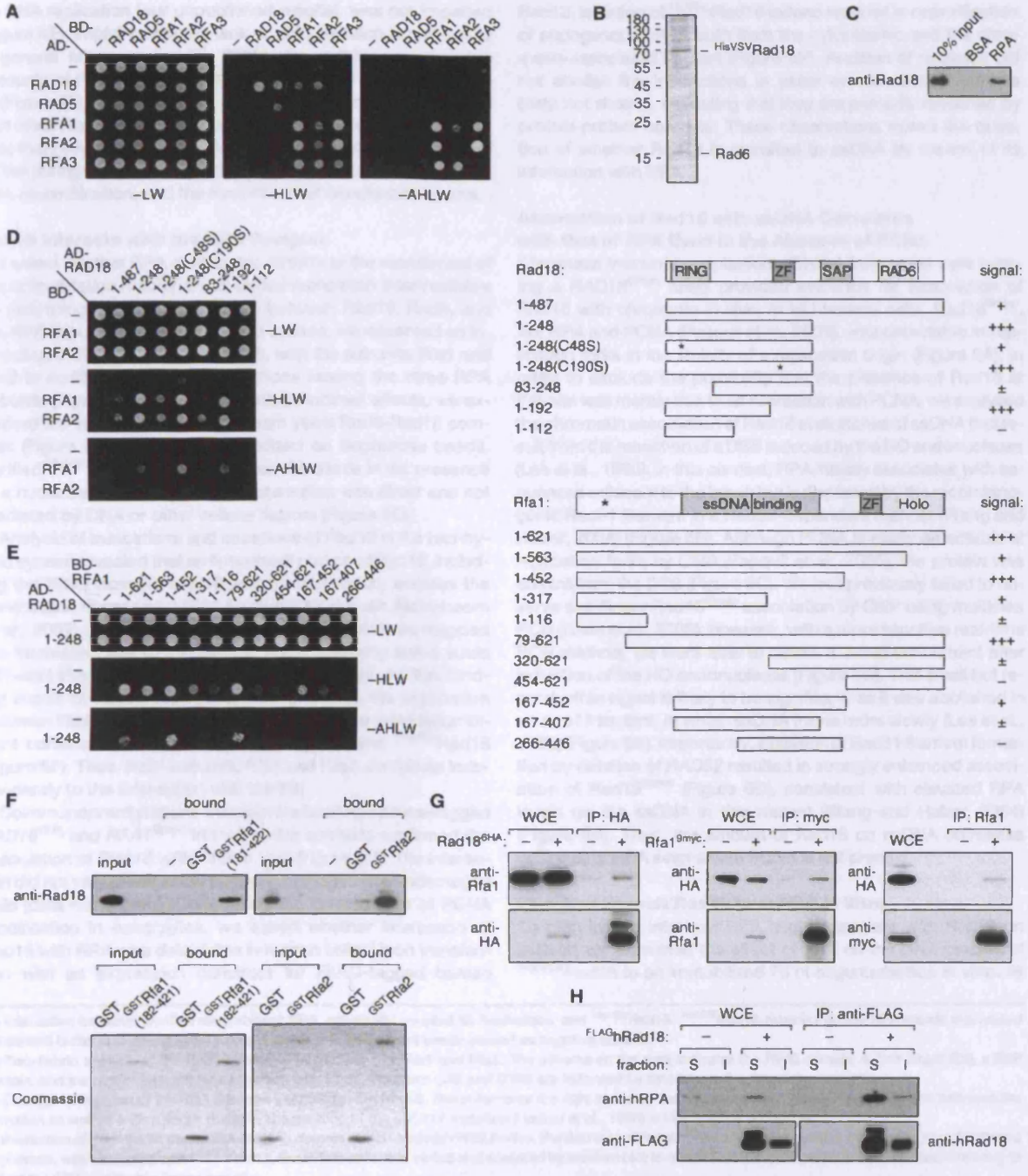

Figure 5. Interaction of Rad18 with the RPA Complex

(A) Protein-protein interactions between Rad18, Rad5, and the RPA subunits Rfa1, Rfa2, and Rfa3 in the yeast two-hybrid system. The open reading frames were expressed as fusions to the Gal4 activation (AD) and DNA-binding domains (BD), and the presence of the constructs was confirmed by growth on selective medium (-LW). Positive interactions were scored by growth on plates lacking histidine (-HLW) and stronger interactions on plates lacking histidine and adenine (-AHLW). Interactions between Rad18 and Rad5 (Ulrich and Jentsch, 2000) and between the individual RPA subunits are shown as internal controls.

(B) Coomassie-stained gel of recombinant ^{HisVSV}Rad18 isolated in complex with untagged Rad6 from baculovirus-infected insect cells.

on DNA replication (our unpublished results), was not impaired (Figure 4E), implying that the lack of ubiquitylation is not due to a general failure to modify PCNA. In addition, comparable amounts of PCNA were chromatin-associated in *WT* and *rfa1-td* (Figure 4F), suggesting that replication forks remain largely intact when Rfa1 levels are seriously reduced. These findings indicate that RPA is required for damage-dependent ubiquitylation of PCNA during S phase, independent of its function in DNA replication, recombination, and the recruitment of checkpoint factors.

Rad18 Interacts with the RPA Complex

We asked whether RPA contributes directly to the recruitment of the ubiquitylation machinery to stalled replication intermediates by examining possible interactions between Rad18, Rad5, and the RPA subunits. In the two-hybrid system, we observed an interaction of Rad18, but not of Rad5, with the subunits Rfa1 and Rfa2 in addition to mutual interactions among the three RPA subunits (Figure 5A). In order to exclude indirect effects, we examined the interaction of recombinant yeast Rad6-Rad18 complex (Figure 5B) with RPA immobilized on Sepharose beads. Purified ^{HisVSV}Rad18 was retained on the beads in the presence of a nuclease, indicating that the interaction was direct and not mediated by DNA or other cellular factors (Figure 5C).

Analysis of truncations and mutations of Rad18 in the two-hybrid system revealed that an N-terminal portion of Rad18, including the RING domain, is sufficient for interaction, whereas the central Zinc finger and a DNA-binding SAP domain (Notenboom et al., 2007) are irrelevant (Figure 5D). Within Rfa1, we mapped the interaction site to the central region spanning amino acids 167–452 (Figure 5E), which comprises the primary ssDNA-binding motifs of RPA. This interaction, as well as the association between Rad18 and Rfa2, was confirmed in vitro using recombinant constructs ^{GST}Rfa1(182–421), ^{GST}Rfa2, and ^{HisVSV}Rad18 (Figure 5F). Thus, both subunits, Rfa1 and Rfa2, contribute independently to the interaction with the E3.

Coimmunoprecipitations from strains bearing epitope-tagged *RAD18*^{6HA} and *RFA1*^{9myc} in their native contexts confirmed the association of Rad18 with RPA in vivo (Figure 5G). The interaction did not vary measurably between damaged and undamaged cells (data not shown). Considering the conservation of PCNA modification in eukaryotes, we asked whether interaction of Rad18 with RPA was detectable in human cells. Upon transfection with an expression construct for FLAG-tagged human Rad18, isolation of ^{FLAG}hRad18 indeed resulted in copurification of endogenous hRPA both from the cytoplasmic and the chromatin-associated fraction (Figure 5H). Addition of nuclease did not abolish the interactions in yeast or mammalian extracts (data not shown), indicating that they are primarily mediated by protein-protein contacts. These observations raised the question of whether Rad18 is recruited to ssDNA by means of its interaction with RPA.

Association of Rad18 with ssDNA Correlates with that of RPA Even in the Absence of PCNA

Chromatin immunoprecipitations (ChIPs) from yeast cells bearing a *RAD18*^{9myc} allele provided evidence for association of Rad18 with chromatin in vivo. In HU-treated cells, Rad18^{9myc}, like RPA and PCNA (Papouli et al., 2005), was detectable at replication forks in the vicinity of a replication origin (Figure 6A). In order to exclude the possibility that the presence of Rad18 at this site was merely due to its interaction with PCNA, we analyzed the chromatin association of Rad18 at stretches of ssDNA that result from the resection of a DSB induced by the HO endonuclease (Lee et al., 1998). In this context, RPA initially associates with sequences adjacent to the break but is displaced by the recombinogenic Rad51 filament in a Rad52-dependent manner (Wang and Haber, 2004) (Figure 6B). Although PCNA is easily detectable at replication forks by ChIP (Papouli et al., 2005), the protein was absent from the DSB (Figure 6C). We had previously failed to observe significant Rad18^{9myc} association by ChIP using multiplex PCR (Chen et al., 2005); however, with a more sensitive real-time PCR method, we were able to detect a 2-fold enrichment after induction of the HO endonuclease (Figure 6D). This small but reproducible signal is likely to be significant, as it was abolished in an *mre11* mutant, in which ssDNA forms more slowly (Lee et al., 1998) (Figure S4). Importantly, inhibition of Rad51 filament formation by deletion of *RAD52* resulted in strongly enhanced association of Rad18^{9myc} (Figure 6D), consistent with elevated RPA levels on the ssDNA in this mutant (Wang and Haber, 2004) (Figure 6B). Thus, the amount of Rad18 on ssDNA correlates with that of RPA even where PCNA is not present.

RPA Can Recruit Rad18 to ssDNA In Vitro

To gain insight into how RPA might associate with Rad18 on ssDNA, we examined the effect of RPA on the DNA binding of ^{HisVSV}Rad18 to an immobilized 75 nt oligonucleotide in vitro. At

(C) Interaction between purified recombinant RPA, covalently coupled to Sepharose, and ^{HisVSV}Rad18. ^{HisVSV}Rad18 retained on the RPA beads was eluted in Laemmli buffer and detected by western blotting. BSA-coupled beads served as negative control.

(D) Two-hybrid analysis of the Rad18 domains interacting with Rfa1 and Rfa2. The scheme on the right indicates the RING domain, a Zinc finger (ZF), a SAP domain, and the region relevant for interaction with Rad6. Positions C48 and C190 are indicated by asterisks in the respective mutants.

(E) Two-hybrid analysis of the Rfa1 domains interacting with Rad18. The scheme on the right indicates the regions relevant for ssDNA binding and holocomplex formation as well as a Zinc finger domain. The position of the *rfa1-t11* mutation (Umezu et al., 1998) is indicated by an asterisk.

(F) Interaction of Rad18 with the ssDNA-binding domain of Rfa1 and with Rfa2 in vitro. Purified recombinant ^{GST}Rfa1(182–421) or Rfa2, immobilized on glutathione Sepharose, was incubated with ^{HisVSV}Rad18. Bound material was eluted and analyzed by western blot to detect Rad18 (upper panel) or by Coomassie staining to detect the GST constructs (lower panel).

(G) In vivo interaction of Rad18 with RPA was analyzed by coimmunoprecipitation of yeast Rad18^{6HA} and Rfa1^{9myc} by using the indicated antibodies. Strains expressing untagged *RAD18* or *RFA1* served as negative controls for precipitation of Rad18^{6HA} and Rfa1^{9myc}, respectively. In the anti-Rfa1 precipitation, antibody was omitted as a negative control. Bands of higher molecular weight in anti-HA precipitates represent ubiquitylated Rad18^{6HA}.

(H) Interaction between hRad18 and hRPA in cultured human cells. Immunoprecipitations (anti-FLAG) were performed from extracts derived from HEK293T cells transiently transfected with an expression construct for ^{FLAG}hRad18. Cells transfected with the empty vector served as negative control. Extracts were partitioned into detergent-soluble (S) and -insoluble (I) material. Note that ^{FLAG}hRad18 is monoubiquitylated in the soluble fraction, which includes the cytoplasmic material, but not in the chromatin-associated fraction.

SPECIAL NOTE

THIS ITEM IS BOUND IN SUCH A MANNER AND WHILE EVERY EFFORT HAS BEEN MADE TO REPRODUCE THE CENTRES, FORCE WOULD RESULT IN DAMAGE

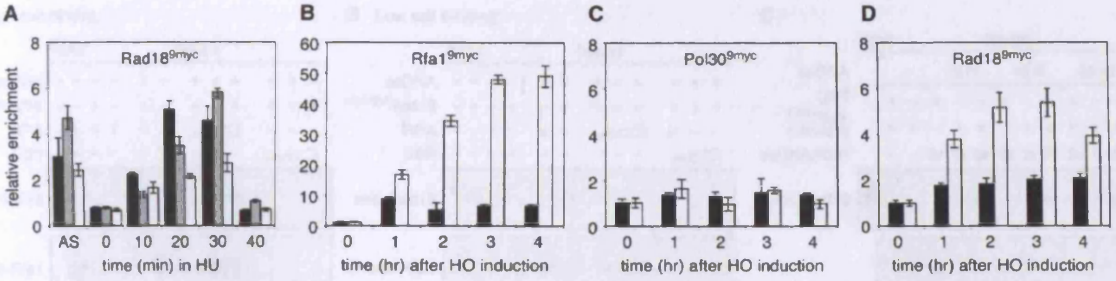

Figure 6. In Vivo Association of Rad18 with ssDNA

(A) Association of Rad18^{9myc} with a replication fork in HU-treated cells detected by ChIP after release from G1 arrest. Rad18^{9myc} was precipitated (anti-myc) from formaldehyde-crosslinked cells at the indicated times, and associated DNA was quantified by real-time PCNA using primers specific for an early-firing origin, ARS607 (black); a sequence 4 kbp removed from ARS607 (gray); and a late-firing origin, ARS501 (white). AS, asynchronous cells. Error bars in all panels represent combined standard deviations from three independent amplifications.

(B) Rfa1^{9myc} is detectable by ChIP at sequences adjacent to an HO-induced DSB. Enrichment of sequences adjacent to the HO site (*MAT*) relative to those at an unrelated locus (*ACT1*) in immunoprecipitates (anti-myc) from crosslinked cells was followed over the indicated time using real-time PCR as in (A). ChIP assays were performed in *WT* (black) and *rad52* mutants (white).

(C) PCNA (Pol30^{9myc}) is not detectable by ChIP at the site of an HO-induced DSB in *WT* (black) or *rad52* (white) cells.

(D) Association of Rad18^{9myc} next to a DSB, analyzed as above in *WT* (black) and *rad52* (white) cells.

250 mM sodium chloride, binding of ^{HisVSV}Rad18 by itself was undetectable, but increasing levels of RPA afforded a robust and RPA-specific enrichment of the E3 in the bound material, indicating that RPA recruits ^{HisVSV}Rad18 to ssDNA (Figure 7A). Similar results were obtained at 150 mM NaCl (data not shown). Surprisingly, under low-salt conditions, ^{HisVSV}Rad18 alone associated with the oligonucleotide, and RPA now caused a reduction in the amount of bound ^{HisVSV}Rad18 (Figure 7B). However, comparable quantities of the bacterial ssDNA-binding protein, SSB, competed much more effectively with ^{HisVSV}Rad18 than RPA, indicating that, even at low ionic strength, RPA and the E3 can occupy a common stretch of DNA.

In order to assess in a simplified system whether RPA can simultaneously interact with ssDNA and Rad18, we examined the interaction of the E3 with ^{GST}Rfa1(182–421) in the presence of short oligonucleotides with no measurable affinity for Rad18 (data not shown) and varying affinities for Rfa1 (Fanning et al., 2006) (Figure S5). We found that ssDNA prebound to Rfa1 enhanced retention of Rad18, suggesting that Rfa1 in its DNA-bound conformation interacts with Rad18 better than free in solution (Figure 7C). An interaction of RPA with Rad18 not involving DNA binding of Rad18 itself thus appears possible. Yet, the Rad18 SAP domain, responsible for DNA binding of the human protein (Notenboom et al., 2007), was previously shown to be involved in the assembly of the E3 at replication foci (Nakajima et al., 2006). Inactivation of this domain in yeast Rad18 abolished its function in vivo, as judged by PCNA modification and DNA damage sensitivity (Figures 7C and 7D), despite the ability of the mutants to autoubiquitylate in vitro (data not shown). Hence, DNA binding by Rad18 itself also appears to be important for its activity toward PCNA.

DISCUSSION

RPA has been implicated in virtually all eukaryotic DNA transactions (Fanning et al., 2006; Zou et al., 2006). Its stabilizing effect on ssDNA is essential for replication, recombination, and nucleotide excision repair, but the complex engages in DNA metabolism even more directly by means of protein-protein interactions, for example with DNA polymerase α/primase or the recombination protein Rad52. During S phase, RPA-coated ssDNA signals replication stress by recruiting the PCNA-like 9-1-1 clamp and the ATR/ATRIP checkpoint kinase complex to sites where polymerase stalling has resulted in exposure of extended stretches of ssDNA (Zou and Elledge, 2003; Zou et al., 2003). Our findings now point to an even more general role of RPA in dealing with replication problems that appears to be conserved from yeast to mammals.

RPA Contributes Independently to Damage Signaling and Damage Bypass

Loss of PCNA ubiquitylation upon depletion of Rfa1 implicates RPA in the activation of the *RAD6* pathway, suggesting that the complex is responsible not only for the sensing of damaged DNA and the stabilization of stalled forks but also for initiating the steps necessary to overcome the damage that caused the arrest. Our results indicate that the requirements of RPA for replication and recombination are genetically and physically separable from its role in DNA damage bypass.

Identification of RPA-covered ssDNA as an upstream signal for the *RAD6* pathway explains a large body of circumstantial evidence defining the conditions that induce PCNA ubiquitylation. Although experiments with synchronized cells suggest that DNA damage causes PCNA ubiquitylation primarily during S phase, the cell-cycle stage itself is irrelevant for the modification: on one hand, a replication initiation defect abolishes PCNA ubiquitylation under conditions that physiologically resemble S phase. On the other hand, the reaction can be triggered in G1 by stalled replication intermediates resulting from the processing of DNA interstrand crosslinks (Sarkar et al., 2006). Hence, stalled replication intermediates appear to be both necessary and sufficient for activation of PCNA ubiquitylation.

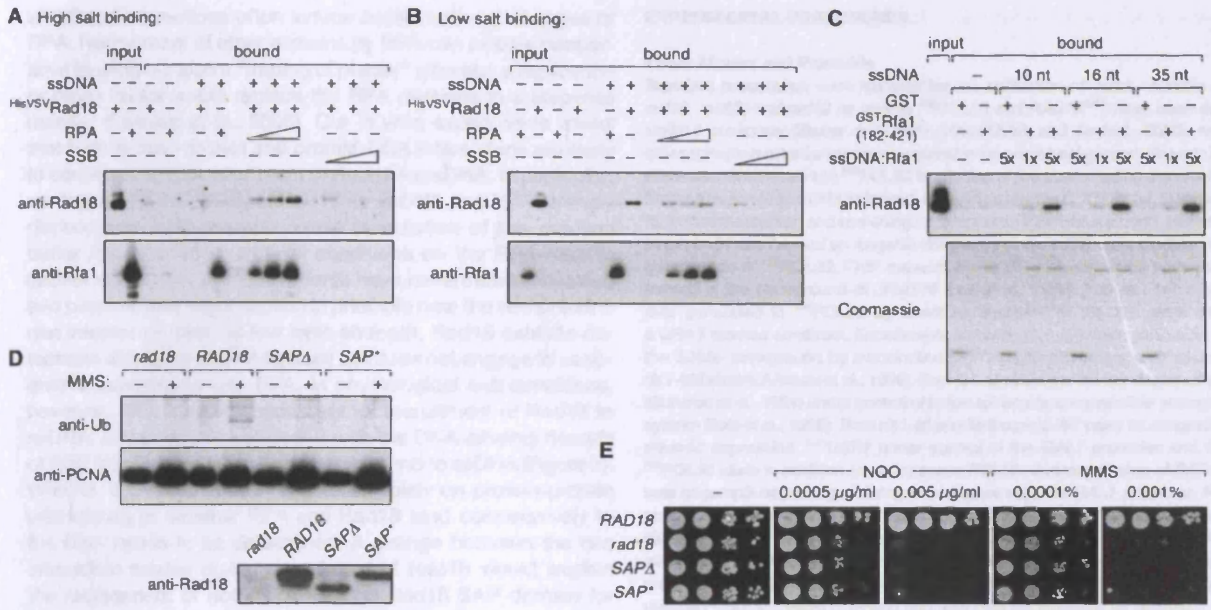

Figure 7. Effects of DNA on the Interaction between Rad18 and RPA

(A) Recruitment of ^{HisVSV}Rad18 to RPA-coated ssDNA under high-salt conditions. A 75 nt 5′-biotinylated oligonucleotide was immobilized on streptavidin agarose and preincubated with increasing amounts of purified yeast RPA, and retention of ^{HisVSV}Rad18 was analyzed by western blotting. RPA and ^{HisVSV}Rad18 were allowed to bind in a buffer containing 15 mM KCl and 250 mM NaCl.

(B) DNA binding of ^{HisVSV}Rad18 under low-salt conditions. The experiment was performed exactly as in (A), except that the proteins were allowed to bind to the ssDNA at 15 mM KCl.

(C) Preincubation of short oligonucleotides with ^{GST}Rfa1(182–421) at a ratio of 1:1 or 5:1 enhances interaction with Rad18. Pull-down assays were performed as described in the legend to Figure 5F.

(D) Deletion (Δ) or mutation (*) of the Rad18 SAP domain impairs PCNA ubiquitylation in vivo. The *rad18* deletion mutant was complemented by the indicated alleles, and PCNA modifications were analyzed as in Figure 1. Presence of the mutant proteins was verified by immunoprecipitation and western blot (lower panel).

(E) The Rad18 SAP domain is required for protection from DNA damage in vivo. Spot assays for NQO and MMS sensitivity were performed on a *rad18* deletion mutant complemented by the indicated *RAD18* constructs.

A need for ssDNA at the sites of stalled replication intermediates is implied by our inability to detect PCNA modification in response to DSB-inducing agents that do not cause base damage. Even CPT, which induces strand breaks in a replication-dependent manner and stalls replication forks, did not result in PCNA ubiquitylation, consistent with our finding that this drug does not cause accumulation of ssDNA. By similar reasoning, uncoupling between polymerase and helicase has been suggested to activate damage bypass in *X. laevis* egg extracts (Chang et al., 2006).

Elevated levels of Rad18 can overcome the requirement for fork stalling and promote ubiquitylation of PCNA whenever the clamp is associated with DNA (Figure 1B). This suggests that the E3 is rate limiting for the reaction, and higher concentrations will drive ubiquitylation at shorter or more transient stretches of ssDNA during undisturbed replication. Constitutive modification of PCNA, as observed in *S. pombe* and in *X. laevis* egg extracts (Frampton et al., 2006; Leach and Michael, 2005), might therefore be caused by a higher expression level or a lower activation threshold of Rad18 in these systems. A higher incidence of spontaneous fork stalling or intrinsic damage might have the same effect.

Finally, a placement of RPA-covered ssDNA upstream of PCNA ubiquitylation explains the similarities between the signals for modification of the clamp and those that elicit the replication-dependent S phase checkpoint (Branzei and Foiani, 2005). Given that the domains required for the recruitment of the checkpoint factors and for interaction with Rad18 are distinct, the two pathways—damage sensing and damage bypass—appear to originate independently from a common structure. Intriguingly, a reduction in PCNA ubiquitylation has been reported in mammalian cells upon siRNA-mediated downregulation of ATR (Bi et al., 2006). Hence, while damage tolerance is clearly independent of checkpoint function in *S. cerevisiae* (Figure S1), *S. pombe*, and *X. laevis* (Chang et al., 2006; Frampton et al., 2006), an indirect contribution of the kinase in the mammalian system remains possible.

Interactions of RPA and Rad18 on ssDNA

RPA is well known for a complicated DNA-binding behavior that involves several distinct binding modes and varies considerably with ionic strength (Fanning et al., 2006). Interactions with other cellular factors may involve either one or multiple of its subunits,

SPECIAL NOTE

THIS ITEM IS BOUND IN SUCH A MANNER AND WHILE EVERY EFFORT HAS BEEN MADE TO REPRODUCE THE CENTRES, FORCE WOULD RESULT IN DAMAGE

and these interactions often induce conformational changes of RPA. Recruitment of other proteins by RPA can involve cooperative binding but also a "trading of places" whereby a replication or repair factor would replace the RPA domains in a stepwise manner (Fanning et al., 2006). Our in vitro experiments reveal that both protein-protein and protein-DNA interactions are likely to contribute to the recruitment of Rad18 to ssDNA. In particular, we found that the affinity of Rad18 for ssDNA and RPA strongly depends on ionic strength. While modulation of the reaction buffer imposes rather artificial conditions on the RPA-Rad18-ssDNA interaction, our experiments have nevertheless revealed two patterns that might explain in principle how the two proteins can interact on DNA: at low ionic strength, Rad18 exhibits detectable affinity for ssDNA by itself but does not engage in cooperative interactions with RPA. In physiological salt conditions, however, RPA is clearly necessary for recruitment of Rad18 to ssDNA, and interaction of Rad18 with the DNA-binding domain of Rfa1 is enhanced when the latter is bound to ssDNA (Figure 7). Whether the association in vivo relies solely on protein-protein interactions or whether RPA and Rad18 bind cooperatively to the DNA needs to be determined. A change between the two interaction modes during recruitment of Rad18 would explain the requirement of both RPA and the Rad18 SAP domain for PCNA ubiquitylation. However, the SAP domain may also have other functions in addition to DNA binding.

Implications of the Rad18-RPA Interaction for Rad18 Function

The physical interactions between RPA and Rad18, detectable in yeast and mammalian cells, suggest that RPA recruits Rad18 to ssDNA by direct association. In the context of a stalled replication fork, it is likely that additional cellular factors will also influence the behavior of Rad18. For example, interaction of the E3 with its target, PCNA, might affect its DNA-binding properties. Alternatively, Rad18 might undergo a conformational change upon DNA binding that would in turn modulate its interactions with PCNA, RPA, or Rad5. Notably, C-terminal truncations of Rad18 excluding the DNA-binding SAP domain consistently exhibit stronger interaction signals than the full-length protein in two-hybrid assays (Figure 5D) (Ulrich and Jentsch, 2000), possibly indicating an inhibitory function of the C-terminal domain that might be relieved by DNA binding. Further biochemical studies and isolation of selectively interaction-deficient mutants of both Rad18 and RPA will be necessary to define the molecular mechanism by which RPA targets Rad18 to its sites of action. However, the presence of Rad18 at ssDNA in vivo correlates with that of RPA even in the absence of its ubiquitylation target, PCNA. Association of the E3 with HO-induced DSBs might therefore suggest additional, PCNA-independent functions. Consistent with this notion, yeast *rad18*, but not ubiquitylation-deficient PCNA mutants, are highly sensitive to IR (Chen et al., 2005; Friedl et al., 2001), and the phenotypes of vertebrate *rad18*$^{-/-}$ cells have implicated the E3 in the repair of DNA-strand breaks and recombination (Shiomi et al., 2007; Szuts et al., 2006). However, the relevant ubiquitylation targets as well as possible contributions of the RPA complex to these alternative functions remain to be identified.

EXPERIMENTAL PROCEDURES

Yeast Strains and Plasmids

Standard procedures were followed for the cultivation of yeast. Mutants in *rad18*, *rad53*, and *rad52* as well as ^{His}*POL30* and *RAD18*^{6HA} have been described previously (Stelter and Ulrich, 2003; Ulrich and Jentsch, 2000), and other epitope-marked alleles were created in the same background. The *cdc7*^{ts} allele was transferred into ^{His}*POL30* by cloning of the open reading frame with flanking regions into a *URA3* plasmid, integration into the *CDC7* locus, selection for loss of the marker, and screening for temperature-sensitive growth. Mutants *bob1*, *bob1 cdc7Δ*, and an isogenic *WT* (Hardy et al., 1997) were modified by introduction of ^{His}*POL30*. ChIP experiments at HO-induced DSBs were performed in the background of JKM179 (Lee et al., 1998). The *rfa1-t11* strain was generated in ^{His}*POL30* by direct replacement of the *WT* allele with a *URA3*-marked construct. Experiments involving *rfa1-t33* were performed in the S288c background by introduction of ^{His}*POL30* into isogenic *RFA1* and *rfa1-t33* strains (Umezu et al., 1998). The *rfa1-td* strain carries the degron allele (Dohmen et al., 1994) under control of a dual tetracycline-repressible promoter system (Belli et al., 1998). Both *rfa1-td* and its isogenic *WT* carry an integrative plasmid expressing ^{myc}*UBR1* under control of the *GAL1* promoter and the ^{His}*POL30* allele in addition to endogenous *POL30*. Overexpression of *RAD18* was accomplished using an integrative vector with the *GAL1* promoter. For complementation of *rad18* with *WT*, *SAPΔ* (amino acids 279–312), or *SAP** (G299A, R301A, M304A), we used integrative vectors carrying the respective alleles under control of the *RAD18* promoter. Strains with a *bar1* deletion were used for experiments involving G1 synchronization, except for those used in Figure 4. Details of strains and plasmids are available on request.

Antibodies

Rabbit polyclonal antibodies were obtained from S. Brill (Rfa1), J. Diffley (Sic1, Rad53, Orc6), or S. West (hRPA); purchased from Santa Cruz Biotechnology (Clb2, myc, HA) or Abcam (hRad18); or generated for our lab (PCNA, Rad18); monoclonals were from Molecular Probes (PGK), Sigma (FLAG), Cell Signaling Technology (ubiquitin, P4D1) or Cancer Research UK (myc, 9E10; HA, 12CA5).

Detection of PCNA Modifications

Strains bearing the ^{His}*POL30* allele were subjected to the desired treatment and processed for isolation of ^{His}PCNA by Ni-NTA pull-downs under denaturing conditions followed by detection of PCNA and ubiquitin as described previously (Hoege et al., 2002; Stelter and Ulrich, 2003). Responses to DNA damage were analyzed by treatment with HU, MMS, NQO, Bleo, CPT, or H_2O_2 in liquid YPD medium for 90 min. For UV irradiation, exponentially growing cultures were plated onto solid YPD medium, irradiated at 254 nm (UV Stratalinker 2400, Stratagene), resuspended in fresh medium, and incubated for 40 min prior to analysis. Treatment with IR was performed with a ^{137}Cs γ source in liquid YPD. Cell-cycle arrests in G1, S, and G2 were achieved by treatment with α factor (10 ng/ml), HU (100 mM), or nocodazole (15 μg/ml), respectively, and monitored by propidium iodide staining and flow cytometry.

Induction of Rfa1^{td} Degradation

Cells were pregrown in raffinose medium at 25°C and blocked in G1 with 5 μg/ml α factor for 3 hr. After exchange into galactose medium with 100 μg/ml doxycyclin and α factor and incubation for 1 hr, the temperature was raised to 37°C, and incubation was continued for 2 hr. After returning the cultures to 25°C and addition of more α factor (2 μg/ml), cells were incubated for another 2 hr before being released into S phase by washing in galactose/doxycyclin medium. Control cultures were blocked in G1 and kept in raffinose medium at 25°C for 3 hr before release in raffinose medium. Damage was induced after release by addition of 0.02% MMS for 90 min.

Analysis of DNA Damage Sensitivities and Checkpoint Activation

Sensitivities to Bleo, CPT, NQO, and MMS were analyzed by spot assays on YPD plates containing the indicated concentrations of damaging agents as described previously (Stelter and Ulrich, 2003). Strains were spotted onto the plates in 10-fold serial dilutions. Phosphorylation of Rad53 was followed by preparation of total cell extracts under denaturing conditions and western blotting.

Analysis of Protein-Protein Interactions in the Two-Hybrid System

Protein-protein interactions were monitored in the reporter strain PJ69-4A as described previously (Ulrich and Jentsch, 2000) by using constructs based on fusions to the Gal4 activation and DNA-binding domains. Constructs for full-length *RAD18* and *RAD5* have been described (Ulrich and Jentsch, 2000). Mutations C48S and C190S were introduced by PCR. The *RFA1*, *RFA2*, and *RFA3* open reading frames were amplified by PCR from genomic DNA. Truncations were generated using appropriate internal restriction sites.

Immunoprecipitations in Yeast

Total cell extracts were prepared from yeast strains expressing *RFA1*^{9myc} and/or *RAD18*^{6HA} by lysis with zirconium/silica beads in 50 mM Tris-HCl (pH 7.5), 250 mM KCl, 20% glycerol, 1% NP40, 2 mM DTT, and protease inhibitors. Immunoprecipitations were performed from ~6×10^8 cells (~4 mg total protein) by incubation with 3–5 μg antibody for 2 hr, addition of 20 μl Protein G agarose (Roche), and further incubation for 1 hr followed by washing five times with lysis buffer and once with the same buffer containing no detergent.

Immunoprecipitations in Mammalian Cell Culture

HEK293T cells were transiently transfected with a construct encoding FLAG-tagged human Rad18 (Mulder et al., 2002). After 3 days, cell extracts were prepared from one 90 mm plate per immunoprecipitation in 50 mM Tris-HCl (pH 7.5), 25 mM NaCl, 1.05 mM sucrose, 3 mM $MgCl_2$, 1 mM EGTA, 0.5% NP40, and protease inhibitors. Soluble material was recovered by centrifugation at 2000 rpm for 5 min. The pellet was washed twice with lysis buffer and extracted with 50 mM Tris-HCl (pH 7.5), 125 mM NaCl, 1 mM EDTA, 0.5% NP40, and protease inhibitors for 30 min on ice to yield the detergent-insoluble chromatin fraction. Both extracts were centrifuged at 13,000 rpm for 15 min, and the lysates were precleared with Protein G agarose for 1 hr. Immunoprecipitations were performed with 20 μl anti-FLAG agarose (Sigma) for 3 hr. The beads were washed four times with 50 mM Tris-HCl (pH 7.5), 200 mM NaCl, 1% NP40, and protease inhibitors and twice with the same buffer without NP40.

Chromatin Immunoprecipitations

ChIP assays at replication forks were performed as described previously (Papouli et al., 2005). A full description of the assay conditions for ChIP at HO-induced DSBs (Chen et al., 2005) is available in the Supplemental Data.

Chromatin-Binding Assays

Fractionation of total cell extracts prepared by spheroplast lysis into soluble and chromatin-bound fractions was achieved by centrifugation through a sucrose cushion essentially as described (Liang and Stillman, 1997).

Quantification of ssDNA

After the desired treatment of exponential cultures, genomic DNA was isolated from ~5×10^7 cells with the DNeasy Blood & Tissue Kit (QIAGEN) according to the manufacturer's instructions. Klenow enzyme (0.5 U) with 0.5 μl hexanucleotide mix (Roche), 7.5 μCi ^{32}P-dCTP, and 5 mM each of cold dATP, dGTP, and dTTP were used in 5 μl random-primed labeling reactions on 100 ng of nondenatured DNA for 16 hr at room temperature (RT). Unincorporated nucleotides were removed by two steps of ammonium acetate precipitation. Aliquots of 2 μl spotted in duplicate on nitrocellulose were quantified by phosphorimaging. A correction factor for the exact amount of input DNA was determined by real-time PCR quantification of the template with primers specific for the *PAC2* gene (5′-AATAACGAATTGAGCTATGACACCAA-3′ and 5′-AGCTTACTCATATCGATTTCATACGACTT-3′). Standard deviations were calculated from triplicate measurements.

Protein Preparations

Bacterial SSB was from Promega. Yeast RPA was purified from *E. coli* as described (Sibenaller et al., 1998). The expression constructs for ^{GST}Rfa1(181–422) and ^{GST}Rfa2 were generated in pGEX-4T-3 (GE Healthcare); the proteins were produced in *E. coli* and purified by affinity chromatography on glutathione Sepharose. Expression constructs for yeast ^{HisVSV}Rad18 and untagged Rad6 were generated in the vector pFastBAC (Invitrogen). The proteins were produced in Sf9 insect cells and purified as a complex from cytoplasmic extracts on Ni-NTA agarose. Thus, Rad6 was present in all experiments involving ^{HisVSV}Rad18. Protein concentrations were determined by comparison to a BSA standard.

Analysis of Protein-Protein Interactions In Vitro

Interaction of ^{HisVSV}Rad18 with RPA in the absence of DNA was examined by covalent coupling of yeast RPA to activated CH Sepharose 4B (at 2.5 μg/ml) and monitoring retention of ^{HisVSV}Rad18 in 50 mM Tris-HCl (pH 7.5), 100 mM NaCl, 5 mM $MgCl_2$, 0.05% Triton X-100, and 2.5 U benzonase (Novagen). Beads (20 μl) were incubated with ~2 pmol ^{HisVSV}Rad18 for 2 hr at 4°C and washed five times with the same buffer containing 250 mM NaCl. BSA-derivatized beads served as negative control. Bound material was eluted with Laemmli buffer and analyzed by western blotting.

Interaction of Rad18 with ^{GST}Rfa1(182–421) or ^{GST}Rfa2 was assayed by immobilizing 0.5 nmol fusion protein on glutathione Sepharose for 30 min at 4°C, followed by a brief wash in a buffer containing 50 mM Tris-HCl (pH 7.5), 50 mM NaCl, 1 mM EDTA, and 0.05% Triton X-100. ^{HisVSV}Rad18 (10 pmol) was added in the same buffer containing 100 μg/ml BSA and incubated for 60 min at 4°C. Beads were washed five times in buffer without BSA, and bound material was eluted as above and analyzed by western blotting and Coomassie blue staining. Where indicated, GST or ^{GST}Rfa1(182–421) was incubated with a 1× or 5× molar excess of oligo-dT (10, 16, or 35 nt) for 45 min before binding to the beads.

Binding of ^{HisVSV}Rad18 to RPA-covered ssDNA was examined by immobilizing a 75 nt, 5′-biotinylated oligonucleotide of mixed sequence on streptavidin agarose (Pierce) in phosphate-buffered saline (PBS) with 1 mM EDTA for 1 hr at RT. After washing three times in PBS with 1 mM EDTA and three times in binding buffer (25 mM HEPES-NaOH [pH 7.5], 15 mM KCl, 1 mM EDTA, 0.05% Triton X-100, 0.5 mM DTT, 100 μg/ml BSA, supplemented with 150 or 250 mM NaCl for high-salt conditions), 15 μl beads per reaction (~5 pmol of the oligonucleotide) were incubated with increasing amounts of purified yeast RPA or bacterial SSB (2.4, 8, and 24 pmol) for 30 min at 4°C. Beads were washed once, and ~5 pmol ^{HisVSV}Rad18 was added. Incubation was continued for 1 hr at 4°C, and the beads were washed three times with high-salt binding buffer and twice with the same buffer containing no BSA. Bound material was eluted as above and detected by western blotting. For RPA blots, equal fractions of input and bound material were loaded. For Rad18 blots, 1% of the input and 35% of the bound material were loaded.

SUPPLEMENTAL DATA

Supplemental Data include Supplemental Experimental Procedures and five figures and can be found with this article online at http://www.molecule.org/cgi/content/full/29/5/625/DC1/.

ACKNOWLEDGMENTS

We thank T. Sixma for helpful discussions and communication of unpublished results; C. Zierhut and J. Diffley for the gift of and advice on the *rfa1-td* strain; and S. Brill, J. Diffley, R. Kolodner, L. Mulder, R. Sclafani, S. West, and M. Wold for generous gifts of reagents. This work was funded by Cancer Research UK, the German Ministry for Education and Research (BMBF), the EMBO Young Investigator Programme and a predoctoral fellowship from the Boehringer Ingelheim Foundation (to D.H.).

Received: July 28, 2007
Revised: October 25, 2007
Accepted: December 21, 2007
Published: March 13, 2008

REFERENCES

Belli, G., Gari, E., Piedrafita, L., Aldea, M., and Herrero, E. (1998). An activator/repressor dual system allows tight tetracycline-regulated gene expression in budding yeast. Nucleic Acids Res. *26*, 942–947.

Bi, X., Barkley, L.R., Slater, D.M., Tateishi, S., Yamaizumi, M., Ohmori, H., and Vaziri, C. (2006). Rad18 regulates DNA polymerase κ and is required for recovery from S-phase checkpoint-mediated arrest. Mol. Cell. Biol. *26*, 3527–3540.

SPECIAL NOTE

THIS ITEM IS BOUND IN SUCH A MANNER AND WHILE EVERY EFFORT HAS BEEN MADE TO REPRODUCE THE CENTRES, FORCE WOULD RESULT IN DAMAGE

Branzei, D., and Foiani, M. (2005). The DNA damage response during DNA replication. Curr. Opin. Cell Biol. *17*, 568–575.

Chang, D.J., Lupardus, P.J., and Cimprich, K.A. (2006). Monoubiquitination of proliferating cell nuclear antigen induced by stalled replication requires uncoupling of DNA polymerase and mini-chromosome maintenance helicase activities. J. Biol. Chem. *281*, 32081–32088.

Chen, S., Davies, A.A., Sagan, D., and Ulrich, H.D. (2005). The RING finger ATPase Rad5p of *Saccharomyces cerevisiae* contributes to DNA double-strand break repair in a ubiquitin-independent manner. Nucleic Acids Res. *33*, 5878–5886.

Dohmen, R.J., Wu, P., and Varshavsky, A. (1994). Heat-inducible degron: a method for constructing temperature-sensitive mutants. Science *263*, 1273–1276.

Fanning, E., Klimovich, V., and Nager, A.R. (2006). A dynamic model for replication protein A (RPA) function in DNA processing pathways. Nucleic Acids Res. *34*, 4126–4137.

Frampton, J., Irmisch, A., Green, C.M., Neiss, A., Trickey, M., Ulrich, H.D., Furuya, K., Watts, F.Z., Carr, A.M., and Lehmann, A.R. (2006). Postreplication repair and PCNA modification in *Schizosaccharomyces pombe*. Mol. Biol. Cell *17*, 2976–2985.

Friedl, A.A., Liefshitz, B., Steinlauf, R., and Kupiec, M. (2001). Deletion of the *SRS2* gene suppresses elevated recombination and DNA damage sensitivity in *rad5* and *rad18* mutants of *Saccharomyces cerevisiae*. Mutat. Res. *486*, 137–146.

Garg, P., and Burgers, P.M. (2005). Ubiquitinated proliferating cell nuclear antigen activates translesion DNA polymerases η and REV1. Proc. Natl. Acad. Sci. USA *102*, 18361–18366.

Hardy, C.F., Dryga, O., Seematter, S., Pahl, P.M., and Sclafani, R.A. (1997). *mcm5/cdc46-bob1* bypasses the requirement for the S phase activator Cdc7p. Proc. Natl. Acad. Sci. USA *94*, 3151–3155.

Hartwell, L.H. (1973). Three additional genes required for deoxyribonucleic acid synthesis in *Saccharomyces cerevisiae*. J. Bacteriol. *115*, 966–974.

Hoege, C., Pfander, B., Moldovan, G.L., Pyrowolakis, G., and Jentsch, S. (2002). *RAD6*-dependent DNA repair is linked to modification of PCNA by ubiquitin and SUMO. Nature *419*, 135–141.

Kannouche, P.L., Wing, J., and Lehmann, A.R. (2004). Interaction of human DNA polymerase η with monoubiquitinated PCNA: a possible mechanism for the polymerase switch in response to DNA damage. Mol. Cell *14*, 491–500.

Lawrence, C. (1994). The *RAD6* DNA repair pathway in *Saccharomyces cerevisiae*: what does it do, and how does it do it? Bioessays *16*, 253–258.

Leach, C.A., and Michael, W.M. (2005). Ubiquitin/SUMO modification of PCNA promotes replication fork progression in *Xenopus laevis* egg extracts. J. Cell Biol. *171*, 947–954.

Lee, S.E., Moore, J.K., Holmes, A., Umezu, K., Kolodner, R.D., and Haber, J.E. (1998). *Saccharomyces* Ku70, Mre11/Rad50 and RPA proteins regulate adaptation to G2/M arrest after DNA damage. Cell *94*, 399–409.

Lehmann, A.R. (2002). Replication of damaged DNA in mammalian cells: new solutions to an old problem. Mutat. Res. *509*, 23–34.

Liang, C., and Stillman, B. (1997). Persistent initiation of DNA replication and chromatin-bound MCM proteins during the cell cycle in cdc6 mutants. Genes Dev. *11*, 3375–3386.

Liu, L.F., Desai, S.D., Li, T.K., Mao, Y., Sun, M., and Sim, S.P. (2000). Mechanism of action of camptothecin. Ann. N Y Acad. Sci. *922*, 1–10.

Maniar, H.S., Wilson, R., and Brill, S.J. (1997). Roles of replication protein-A subunits 2 and 3 in DNA replication fork movement in *Saccharomyces cerevisiae*. Genetics *145*, 891–902.

Mulder, L.C., Chakrabarti, L.A., and Muesing, M.A. (2002). Interaction of HIV-1 integrase with DNA repair protein hRad18. J. Biol. Chem. *277*, 27489–27493.

Nakajima, S., Lan, L., Kanno, S., Usami, N., Kobayashi, K., Mori, M., Shiomi, T., and Yasui, A. (2006). Replication-dependent and -independent responses of RAD18 to DNA damage in human cells. J. Biol. Chem. *281*, 34687–34695.

Notenboom, V., Hibbert, R.G., van Rossum-Fikkert, S.E., Olsen, J.V., Mann, M., and Sixma, T.K. (2007). Functional characterization of Rad18 domains for Rad6, ubiquitin, DNA binding and PCNA modification. Nucleic Acids Res. *35*, 5819–5830.

Nyberg, K.A., Michelson, R.J., Putnam, C.W., and Weinert, T.A. (2002). Toward maintaining the genome: DNA damage and replication checkpoints. Annu. Rev. Genet. *36*, 617–656.

Papouli, E., Chen, S., Davies, A.A., Huttner, D., Krejci, L., Sung, P., and Ulrich, H.D. (2005). Crosstalk between SUMO and ubiquitin on PCNA is mediated by recruitment of the helicase Srs2p. Mol. Cell *19*, 123–133.

Pfander, B., Moldovan, G.L., Sacher, M., Hoege, C., and Jentsch, S. (2005). SUMO-modified PCNA recruits Srs2 to prevent recombination during S phase. Nature *436*, 428–433.

Redon, C., Pilch, D.R., Rogakou, E.P., Orr, A.H., Lowndes, N.F., and Bonner, W.M. (2003). Yeast histone 2A serine 129 is essential for the efficient repair of checkpoint-blind DNA damage. EMBO Rep. *4*, 678–684.

Sarkar, S., Davies, A.A., Ulrich, H.D., and McHugh, P.J. (2006). DNA interstrand crosslink repair during G1 involves nucleotide excision repair and DNA polymerase ζ. EMBO J. *25*, 1285–1294.

Shiomi, N., Mori, M., Tsuji, H., Imai, T., Inoue, H., Tateishi, S., Yamaizumi, M., and Shiomi, T. (2007). Human RAD18 is involved in S phase-specific single-strand break repair without PCNA monoubiquitination. Nucleic Acids Res. *35*, e9. 10.1093/nar/gkl979.

Sibenaller, Z.A., Sorensen, B.R., and Wold, M.S. (1998). The 32- and 14-kilodalton subunits of replication protein A are responsible for species-specific interactions with single-stranded DNA. Biochemistry *37*, 12496–12506.

Sogo, J.M., Lopes, M., and Foiani, M. (2002). Fork reversal and ssDNA accumulation at stalled replication forks owing to checkpoint defects. Science *297*, 599–602.

Stelter, P., and Ulrich, H.D. (2003). Control of spontaneous and damage-induced mutagenesis by SUMO and ubiquitin conjugation. Nature *425*, 188–191.

Szuts, D., Simpson, L.J., Kabani, S., Yamazoe, M., and Sale, J.E. (2006). Role for RAD18 in homologous recombination in DT40 cells. Mol. Cell. Biol. *26*, 8032–8041.

Ulrich, H.D. (2005). The *RAD6* pathway: control of DNA damage bypass and mutagenesis by ubiquitin and SUMO. ChemBioChem *6*, 1735–1743.

Ulrich, H.D., and Jentsch, S. (2000). Two RING finger proteins mediate cooperation between ubiquitin-conjugating enzymes in DNA repair. EMBO J. *19*, 3388–3397.

Umezu, K., Sugawara, N., Chen, C., Haber, J.E., and Kolodner, R.D. (1998). Genetic analysis of yeast RPA1 reveals its multiple functions in DNA metabolism. Genetics *148*, 989–1005.

Wang, X., and Haber, J.E. (2004). Role of *Saccharomyces* single-stranded DNA-binding protein RPA in the strand invasion step of double-strand break repair. PLoS Biol. *2*, E21. 10.1371/journal.pbio.0020021.

Watanabe, K., Tateishi, S., Kawasuji, M., Tsurimoto, T., Inoue, H., and Yamaizumi, M. (2004). Rad18 guides polη to replication stalling sites through physical interaction and PCNA monoubiquitination. EMBO J. *23*, 3886–3896.

Zou, L., and Elledge, S.J. (2003). Sensing DNA damage through ATRIP recognition of RPA-ssDNA complexes. Science *300*, 1542–1548.

Zou, L., Liu, D., and Elledge, S.J. (2003). Replication protein A-mediated recruitment and activation of Rad17 complexes. Proc. Natl. Acad. Sci. USA *100*, 13827–13832.

Zou, Y., Liu, Y., Wu, X., and Shell, S.M. (2006). Functions of human replication protein A (RPA): from DNA replication to DNA damage and stress responses. J. Cell. Physiol. *208*, 267–273.